AIR SYSTEM WINTER FIELD STUDY IN THE AOSERP STUDY AREA, FEBRUARY 1977

by

F. FANAKI, R. MICKLE, M. LUSIS, J. KOVALICK, J. MARKES,
F. FROUDE, J. ARNOLD, A. GALLANT, S. MELNICHUK,
D. BRYMER, A. GAUDENZI, A. MOSER, and D. BAGG

Fisheries and Environment Canada
Atmospheric Environment Service

for

ALBERTA OIL SANDS ENVIRONMENTAL
RESEARCH PROGRAM

Projects ME 1.5.2 and ME 3.5.1

April 1979

TABLE OF CONTENTS

TABLE OF CONTENTS (CONCLUDED)

LIST OF TABLES

LIST OF FIGURES

LIST OF FIGURES (CONTINUED)

LIST OF FIGURES (CONTINUED)

LIST OF FIGURES (CONTINUED)

LIST OF FIGURES (CONTINUED)

LIST OF FIGURES (CONCLUDED)

ABSTRACT

The second in a series of Atmospheric Environment Service field studies in the Athabasca Oil Sands area was carried out during 3-13 February 1977. The objectives of the study were the same as those of the March 1976 study, namely to obtain information on the meteorology of the area and/or the dispersal and behaviour of the Great Canadian Oil Sands (GCOS) plume. In addition, the study was extended to determine the rate of SO_2 oxidation of the GCOS plume and to determine its constituents. As a consequence, the AES experimental program consisted of wind, temperature, and humidity measurements as a function of height using balloon-borne minisondes and radiosondes tracked by theodolities and a tethersonde-borne instrument; photography of the GCOS plume; and aircraft sampling of SO_2, sulphate, and sulphuric acid in the GCOS plume downwind to about 30 km from the stack.

For the majority of the experiments, surface inversion conditions were observed. The meteorological structure at Lower Syncrude Site and at Syncrude Mine Site is discussed. Typically, with a cross-valley flow, the wind at the lower site was decoupled from the winds aloft, with the lower level flow aligning with the valley walls. The wind at the upper site showed a similar shifting of the surface winds to align along the valley direction. These results suggest that during stable conditions, the flow through the surface inversion is strongly influenced by the broad basin of the Athabasca River.

Two acoustic sounders were employed at different locations to examine the temperature structure of the atmospheric boundary layer. The formation and breakup of the inversion layers over the Athabasca Oil Sands area were recorded by the sounders and are discussed in this report.

Comparison of the sounder records with the sonde profiles gave good agreement. This suggests that the sounder may be used successfully to measure inversion heights at the Athabasca Oil Sands area. In such an application, at least one minisonde station should be used with the acoustic system, for calibration purposes.

This assessment of the predictive capability of plume rise formulas showed that the Holland and the Briggs formulas appear to predict plume use better than the other formulas tested. For two cases selected for analysis of plume behaviour, comparisons are made between the observed dispersion coefficients and some theoretical models for different stability classes. The TVA method of O_2 appears to predict the observed plume dispersion coefficients better than the Pasquell-Gifford model. The reverse is true for σ_y.

SO_2 oxidation rates were found to be low. Within the experimental scatter of the data, the rate as measured was essentially zero, in spite of the fact that the particulate loading in the plume was relatively high and that a mathematical model of heterogeneous oxidation suggests that appreciable rates should have been measured on certain occasions.

ACKNOWLEDGEMENTS

The authors would like to express their thanks to Mr. M. Strosher (Alberta Environment) and Mr. W.L. Cary (GCOS) for kindly supplying us with the GCOS emission data. Thanks are due to Mr. R. Angle, Mr. M. Strosher, Dr. H.E. Turner, and Mr. A. Mann, who reviewed the first draft of this report. Sincere appreciation is also expressed to the AOSERP staff, especially Mr. D. Hädler and Mr. A. Mann, who assisted us during our field study and provided us with a comfortable home during our stay at the camp.

The authors gratefully acknowledge the interest in and support of this work by the AES Region staff, in particular Messrs. W. Schmitke and V. Nespliak, in setting up some of the field equipment and the operation of the minisonde system.

Research projects ME 1.5.2 and ME 3.5.1 were founded by the Alberta Oil Sands Environmental Research Program, a joint Alberta-Canada research program established to fund, direct, and co-ordinate environmental research in the Athabasca Oil Sands area of northeastern Alberta.

1. INTRODUCTION

The intensive field study of March 1976 in the Alberta Oil Sands Environmental Research Program (AOSERP) study area (Figure 1) yielded interesting results concerning the meteorology and deposition and disperal of pollutants in the area (Fanaki 1978). It was felt, however, that a further field study was needed for winter conditions to add statistical significance to the data obtained in March 1976.

The following report describes in detail the second in a series of Atmospheric Environment Service (AES) winter field studies that were carried out during the period 3-13 February 1977.

The objectives of the study were the same as those of the March 1976 study:

1. To obtain detailed information in space and time on wind flow, temperature, and the thermal turbulent structure of the atmospheric boundary layer in that area; and
2. To obtain information on the rise of the Great Canadian Oil Sands (GCOS) plumes, their behaviour, and dispersal, as a function of meteorological conditions and downwind distance.

In addition, measurements of dispersion coefficients by means of turbulence measurements and plume sampling were made. Furthermore, the study was extended to include measurements of the rate of SO_2 oxidation in the GCOS plumes as a function of plume age.

As a consequence, the AES experimental program consisted of wind, temperature, and humidity measurements as a function of height using balloon-borne minisondes and radiosondes tracked by theodolites and a tethersonde-borne instrument; photography of the GCOS plume; and aircraft sampling of SO_2, sulphate, and sulphuric acid in the GCOS plume to about 30 km downwind from the source.

The measurements were supported by stack sampling made by GCOS. Figure 2 gives an overall view of the concurrent activities during the 10-day study.

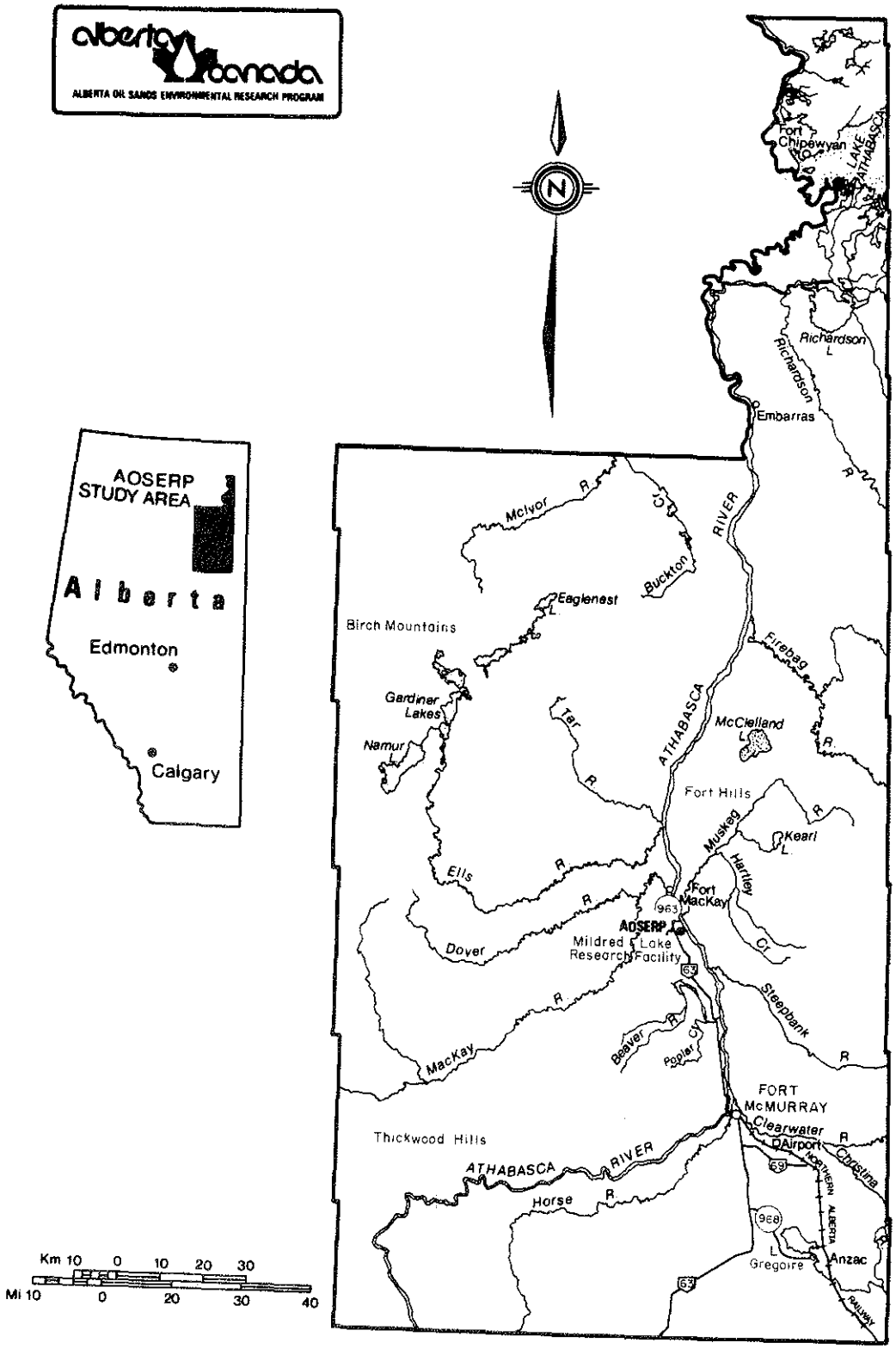

Figure 1. AOSERP study area.

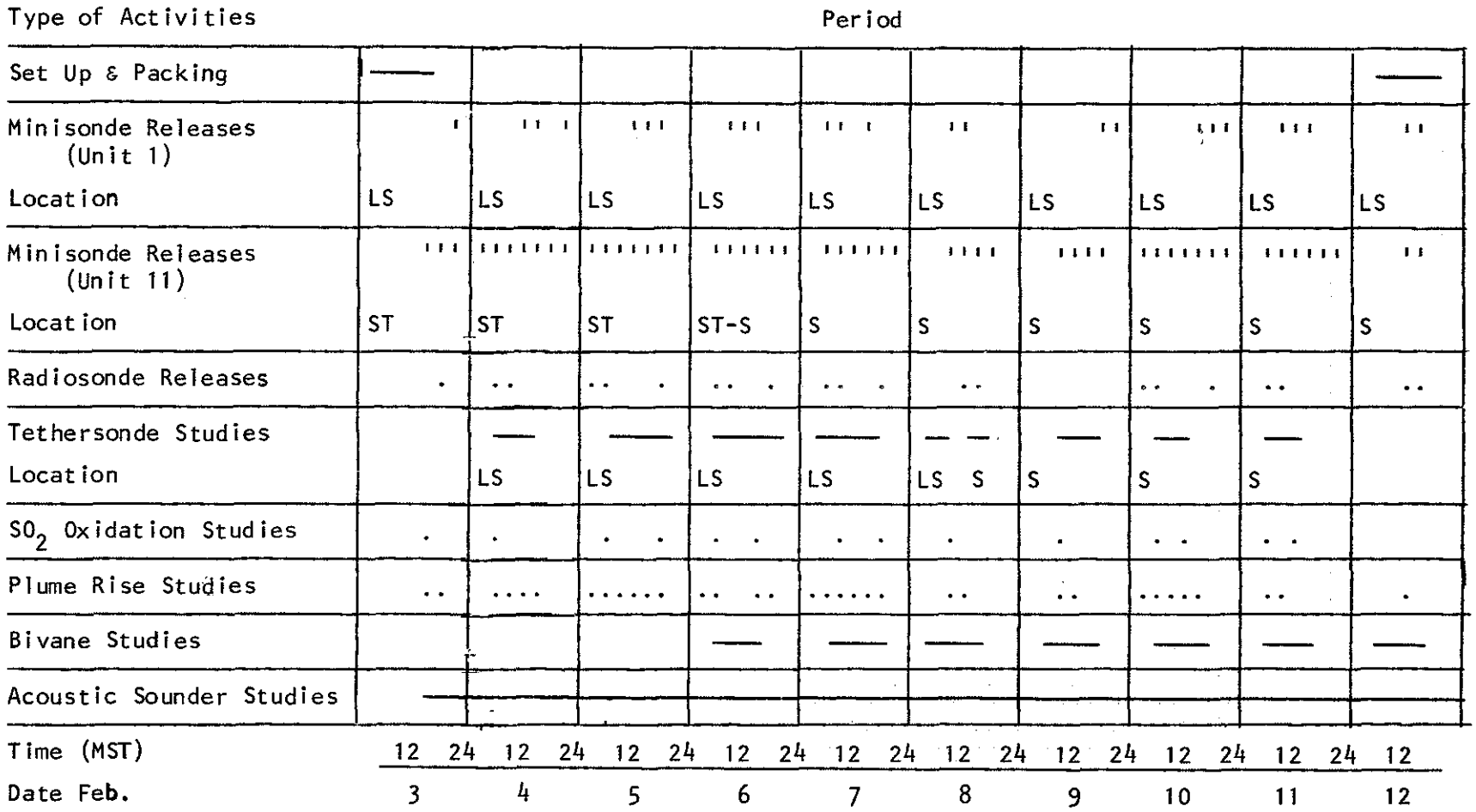

Figure 2. AES activities in the oil sands area for the period 3-12 February 1977. (LS = Lower Syncrude; S = Syncrude; ST = Supertest Hill)

The temperature during the study period was about 15°C above normal; however, in spite of this warm spell, the program was successful, and the scope of the observations was larger than that of the first study.

2. EXPERIMENTAL SITE AND SOURCE DESCRIPTION

The AOSERP general study area comprises 28 600 km^2 (Figure 1). The project study area centres on the GCOS and Syncrude plants, approximately 40 km north of Fort McMurray. Both plants lie west of the Athabasca River. Figure 3 shows the plants' locations. At the time of writing (March 1978), only the GCOS plant was in operation, while the Syncrude plant was under construction.

The topography around the Athabasca River in that area is slightly variable, ranging from undulating to rolling land. The Athabasca River flows through the study area from south to north. The river valley has an elevation of about 230 m mean sea level (MSL) and a width of about 1 km at the GCOS plant. The valley's slope rises gradually to an elevation of about 400 m at 25 km to the east and, for the same distance to the west, to an elevation of 520 m. The GCOS plant is located within the valley, while Syncrude is about 5 km west of the GCOS plant.

Currently, the major sources of air pollution are the Power Plant Stack (A), the Refinery Flare Stack (B), and the Incinerator Stack (C), all at GCOS. Their physical characteristics and relative location were described previously (Fanaki 1978).

Emission parameters of Stack A for the period of observation are given in Table 1.

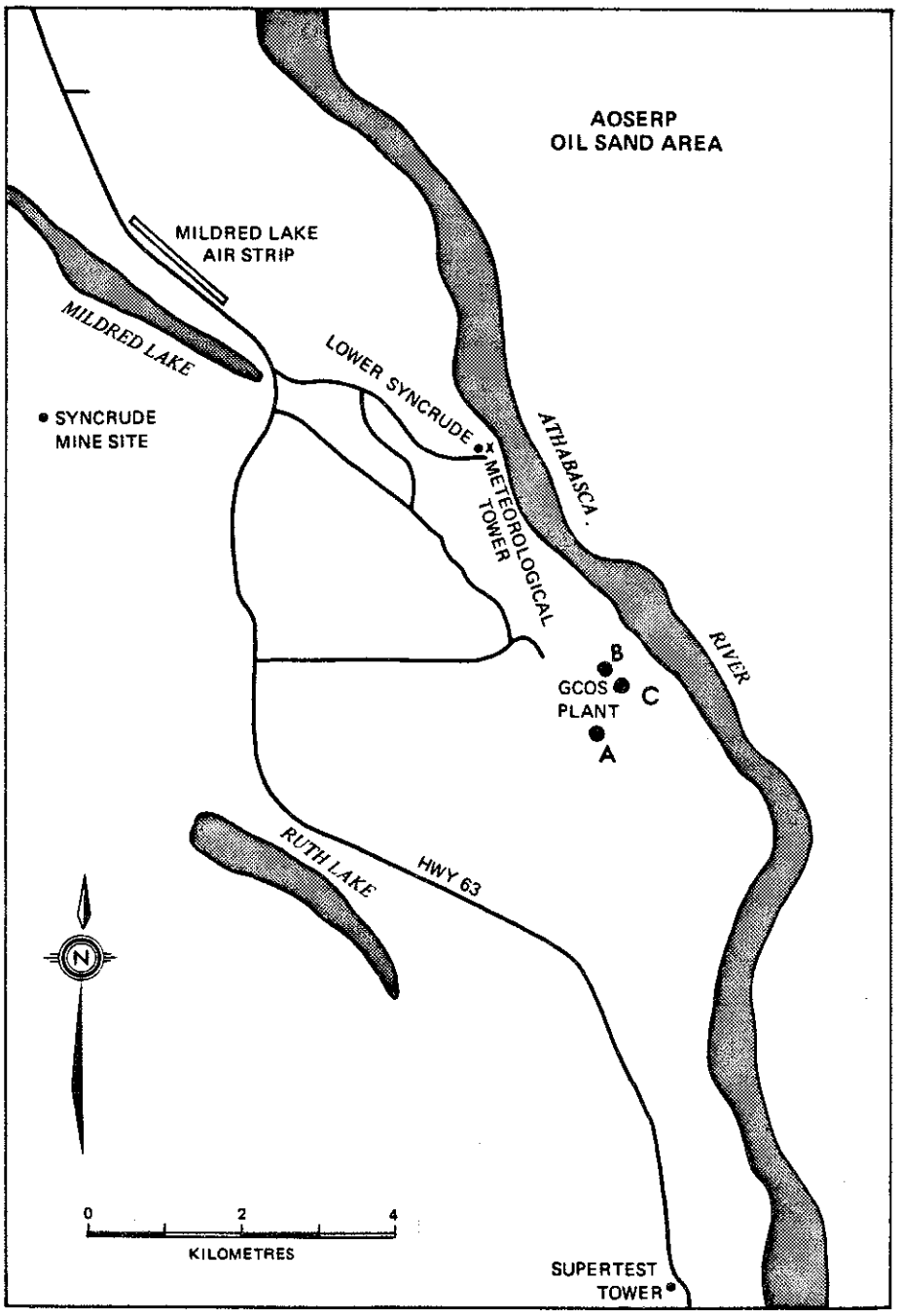

Figure 3. Map of the oil sands area showing the locations of the GCOS plant, Syncrude mine site, and the meteorological tower at Lower Syncrude.

Table 1. Power plant stack emission data for February 1977[a].

Date	Time	SO_2 Emissions ($kg.s^{-1}$)	Effluent ($m^3.s^{-1}$)	Exit Velocity ($m.s^{-1}$)	Gas Temperature (^oC)
3 Feb/77	1100	2.85	467	20.1	285
	1200	2.96	433	19.5	-
	1300	2.99	474	20.5	288
	1400	2.71	461	19.1	274
	1500	2.64	484	-	-
	1600	2.96	453	19.8	271
	1700	2.90	467	-	-
4 Feb/77	0600	1.91	469	-	-
	0700	2.96	464	-	-
	0800	2.90	431	19.8	282
	0900	2.87	431	19.7	285
	1000	2.73	469	18.2	274
	1100	2.70	461	18.2	274
	1200	2.79	461	-	-
	1300			19.8	285
	1400			19.5	285
	1600			19.5	290
5 Feb/77	0600	2.73	-	-	-
	0700	2.75	-	-	-
	0800	2.59	112	17.4	271
	0900	2.66	428	18.1	279
	1000	2.79	447	18.9	279
	1100	2.79	447	18.9	279
	1200	2.79	-	-	-
	1300	2.90	482	-	279
	1400	2.92	465	-	274
	1500	2.85	-	-	-
	1600	2.83	445	18.9	274

continued ...

Table 1. Continued.

Date	Time	SO_2 Emissions ($kg \cdot s^{-1}$)	Effluent ($m^3 \cdot s^{-1}$)	Exit Velocity ($m \cdot s^{-1}$)	Gas Temperature (^oC)
6 Feb/77	0600	2.78	-	-	-
	0700	2.64	-	-	-
	0800	2.69	419	17.1	271
	0900	2.78	438	18.5	274
	1000	2.72	431	18.2	274
	1100	2.66	412	17.4	268
	1200	2.66	-	-	-
	1300	2.69	423	17.9	271
	1400	2.79	440	18.6	274
	1500	2.78	-	-	-
	1600	2.70	426	18.0	274
	1700	2.75	-	-	-
	1800	2.73	-	-	-
7 Feb/77	0600	2.89	-	-	-
	0700	2.74	-	-	-
	0800	2.81	447	18.9	282
	0900	2.85	457	19.3	279
	1000	2.95	479	20.3	290
	1100	2.98	479	20.3	282
	1200	2.92	-	-	-
	1300	2.84	443	18.7	268
	1400	2.84	450	19.1	271
	1500	2.93	-	-	-
	1600	2.72	428	18.1	268
	1700	2.87	-	-	-
8 Feb/77	0600	2.16	-	-	-
	0700	2.14	-	-	-
	0800	2.40	374	15.8	287
	0900	2.30	358	15.1	282
	1000	2.35	371	15.6	289

continued.....

Table 1. Continued.

Date	Time	SO_2 Emissions ($kg \cdot s^{-1}$)	Effluent Rate ($m^3 \cdot s^{-1}$)	Exit Velocity ($m \cdot s^{-1}$)	Gas Temperature (^oC)
8 Feb/77	1100	2.18	346	14.6	295
	1200	2.19	-	-	-
	1300	-	360	15.2	283
	1400	-	358	15.1	284
	1600	-	341	14.4	281
9 Feb/77	0600	2.38	-	-	-
	0700	2.30	-	-	-
	0800	2.24	346	14.6	292
	0900	2.19	346	14.6	289
	1000	2.24	355	15.0	292
	1100	2.23	349	14.8	286
	1200	2.15	-	-	-
	1300	-	361	15.2	289
	1400	-	378	16.0	293
	1600	-	370	15.6	292
10 Feb/77	0600	2.36	-	-	-
	0700	3.33	-	-	-
	0800	2.32	361	15.3	290
	0900	2.35	373	15.8	293
	1000	2.29	361	15.2	289
	1100	2.36	381	16.1	290
	1200	2.32	-	-	-
	1300	2.33	369	15.6	290
	1400	2.40	382	16.2	289
	1500	2.32	-	-	-
	1600	2.32	376	15.9	293
	1700	2.36	-	-	-
	1800	2.40	-	-	-

continued ...

Table 1. Concluded.

Date	Time	SO_2 Emissions ($kg.s^{-1}$)	Effluent Rate ($m^3.s^{-1}$)	Exit Velocity ($m.s^{-1}$)	Gas Temperature (^oC)
11 Feb/77	0600	2.43	-	-	-
	0700	2.38	-	-	-
	0800	2.30		15.6	294
	0900	2.33		15.8	297
	1000	2.29		15.3	295
	1100	2.27		15.1	290
	1200	2.30	-	-	-
	1300	2.33		16.1	298
	1400	2.36		16.2	300
	1500	2.23	-	-	-
	1600	2.35	-	15.8	297
	1700	2.29	-	-	-
	1800	2.27	-	-	-
12 Feb/77	0800			14.3	281
	0900			14.9	283
	1000			14.7	282
	1100			14.7	278

[a] Data from which calculations were made were obtained from Alberta Environment.

3. METEOROLOGICAL CONDITIONS

3.1 SYNOPTIC CONDITIONS

A day-by-day description of the weather for the period of the study is given in Appendix 8.1. For each of these days, the regional synoptic weather pattern at 1100 Mountain Standard Time (MST) (1800Z) is shown in Figures 65 to 74.

3.2 PROFILES OF TEMPERATURE AND WIND

Measurements of the variation of meteorological properties in the vertical direction are very informative. They reflect the effect of small-scale surface roughness, large-scale terrain features, surface heat flux, and the mean properties of the geostrophic flow. Such measurements, along with air pollution measurements, can be used to validate numerical model calculations. When used in conjunction with longer-term climatological measurements, they allow an estimate of the air pollution potential for that period to be ascertained.

For this study, four types of soundings are made using minisondes, radiosondes, a tethersonde system, and a bivane. In addition, an acoustic sounder was used to examine the temperature structure of the atmospheric boundary layer of that area.

3.2.1 Minisonde and Radiosonde Measurements

At the project study area, three sites were established from which the minisonde (M/S) soundings could be made. One site was located at the Lower Syncrude and the other two sites were located at the Syncrude Mine Site and the Supertest Tower Site, respectively (Figure 3). A photograph of the M/S before release at the Syncrude Mine Site is shown in Figure 4.

Each site consisted of three baselines, staked, and measured. Prior to a sounding, a baseline approximately perpendicular to the wind was chosen, and a theodolie was set up at each end. A helium-filled balloon was then launched, carrying an M/S

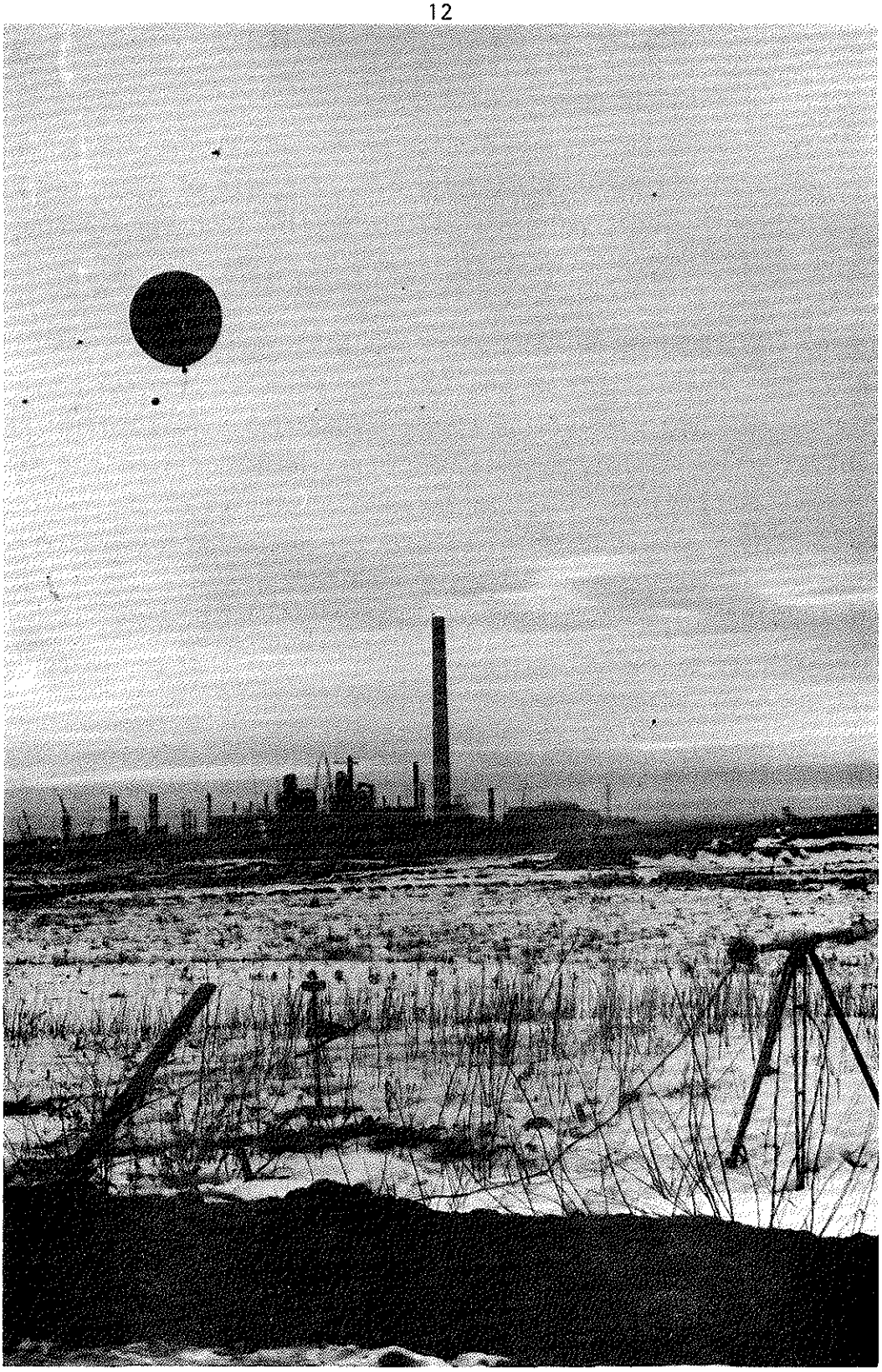

Figure 4. Minisonde balloon is ready for release at the Syncrude Mine Site.

or a radiosonde. The M/S provided the height temperature resolution required for this study, while the radiosonde provided dew point measurements required for the SO_2 oxidation and acoustic sounder studies. The M/S balloon was tracked by the two theodolites, which took simultaneous readings of its position every 30 s. These data permitted the calculation of position and velocity, from which the profiles of wind speed, wind direction, and temperature were drawn.

Because of the heterogeneity of the region, M/S's were always launched simultaneously from two different sites to define horizontal variations in the wind patterns. Because height information for the radiosonde was available through pressure-temperature calculations, wind measurements were derived from a single theodolite.

Mobile teams were dispatched daily to two sites before dawn. A daily schedule of quasi-simultaneous six soundings from both sites during the day was attempted. A list of the sounding locations and the time of releases is given in Figure 2.

Tables of temperature, wind speed, and wind direction versus height as measured by the M/S and the radiosonde were made and are compiled in a separate file (see Descriptive Summary). The figures display a set of graphs describing wind speed, wind direction, and atmospheric temperatures as a function of height above MSL. A sample of these data is shown in Figure 5.

3.2.2 Bivane Measurements

Measurements of the fluctuations of the absolute value of the wind vector and its fluctuations in both azimuth and elevation angles were made at the Lower Syncrude site using a Gill Anemometer bicane. The bivane was mounted at the top of the permanent 150 m meteorological tower located on relatively level ground at the Athabasca River valley (Figure 3). The valley is broken by the Athabasca River, which flows from south to north and is about 300 m across at the tower location. The east bank of the river rises relatively rapidly to a height of about 60 m and is covered with trees, averaging 10 m in height. The west bank of the river rises

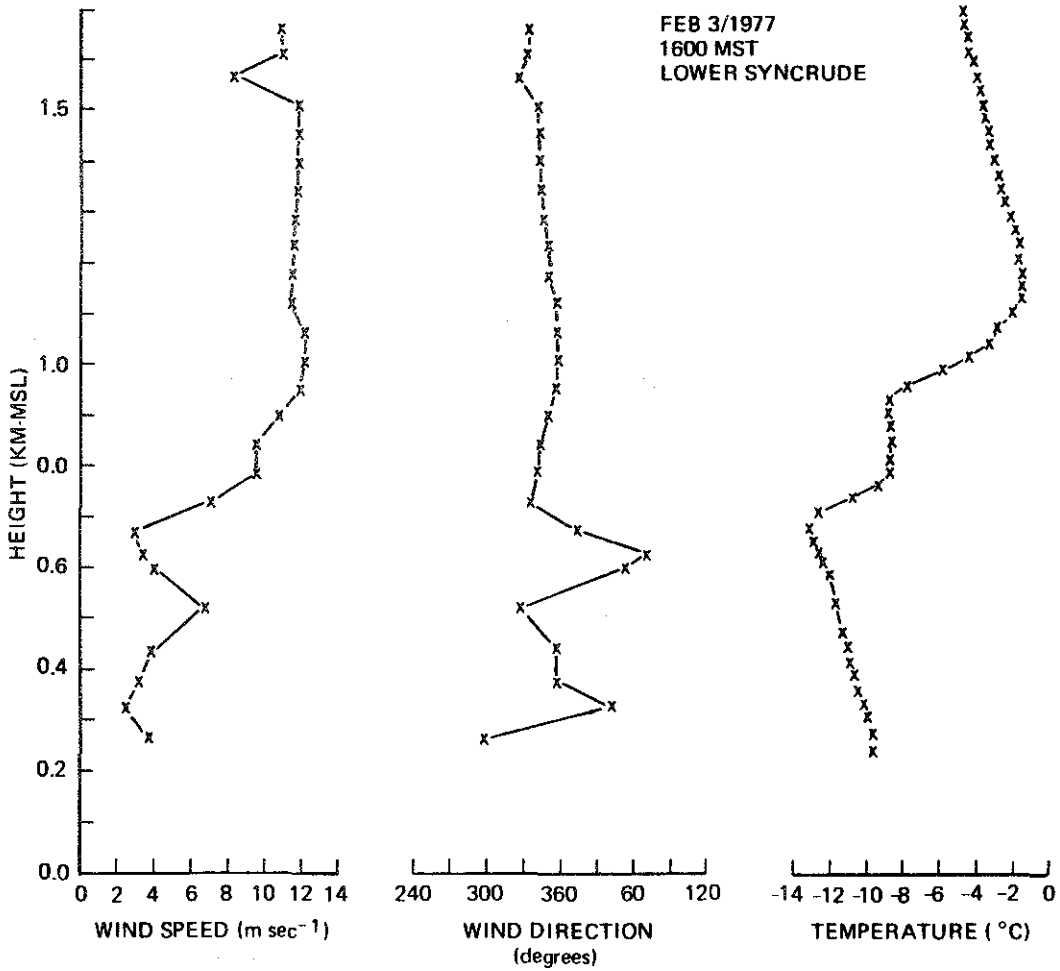

Figure 5. Profiles of wind speed, wind direction, and atmospheric temperature obtained by the minisondes.

gradually for a distance of 1.5 km and then sharply to 30 m in height. North and west of the tower, at a distance of about 100 m, the land is covered with trees, mostly spruce and poplar, averaging 15 m in height. The area south of the tower is relatively clear; the nearest buildings are 800 m due south of the tower. The buildings' heights vary from a few metres to tens of metres.

The bivane data were recored on a three-channel chart recorder, which was installed in the tower shelter. A continuous record of wind speed and direction fluctuations was made.

Due to the malfunction of the bivane's equipment, only the last few days of the data were obtained. The first few days were spent in adjusting the bivane. Although it was desirable to obtain observations for a longer period, it is felt that the data obtained are sufficient to drawn the conclusions described below.

The data collected represent 20 h of observations. A sample of the recorded data is shown in Figure 6. The data were divided into 30 min segments. Nonoverlapping 4 s smoothed values of elevation (θ) and azimuth (ϕ) angle were scaled by hand. The travel time of the plume, during this study, usually exceeded 20 s; the standard deviations of azimuth (σ_ϕ) and elevation (σ_θ) were obtained by using 5 s mean values.

Gifford (1960) and Munn (1964) have indicated that wind direction variances should be computed from running rather than end-to-end means. The bivane readings were then grouped by overlapping pairs, fives, tens, and twenties to yield standard deviations for presmoothing times of 10, 25, 50, and 100 s. Table 2 shows the calculated standard deviations for both the azimuth and elevation angles.

The daily pattern of σ_θ and σ_ϕ was examined, and the result is shown in Figures 7-10, 6-10 February 1977. In general, σ_θ and σ_ϕ increase with the time of day. They are at a maximum in the afternoon and fall to a minimum both in the early morning and in the evening.

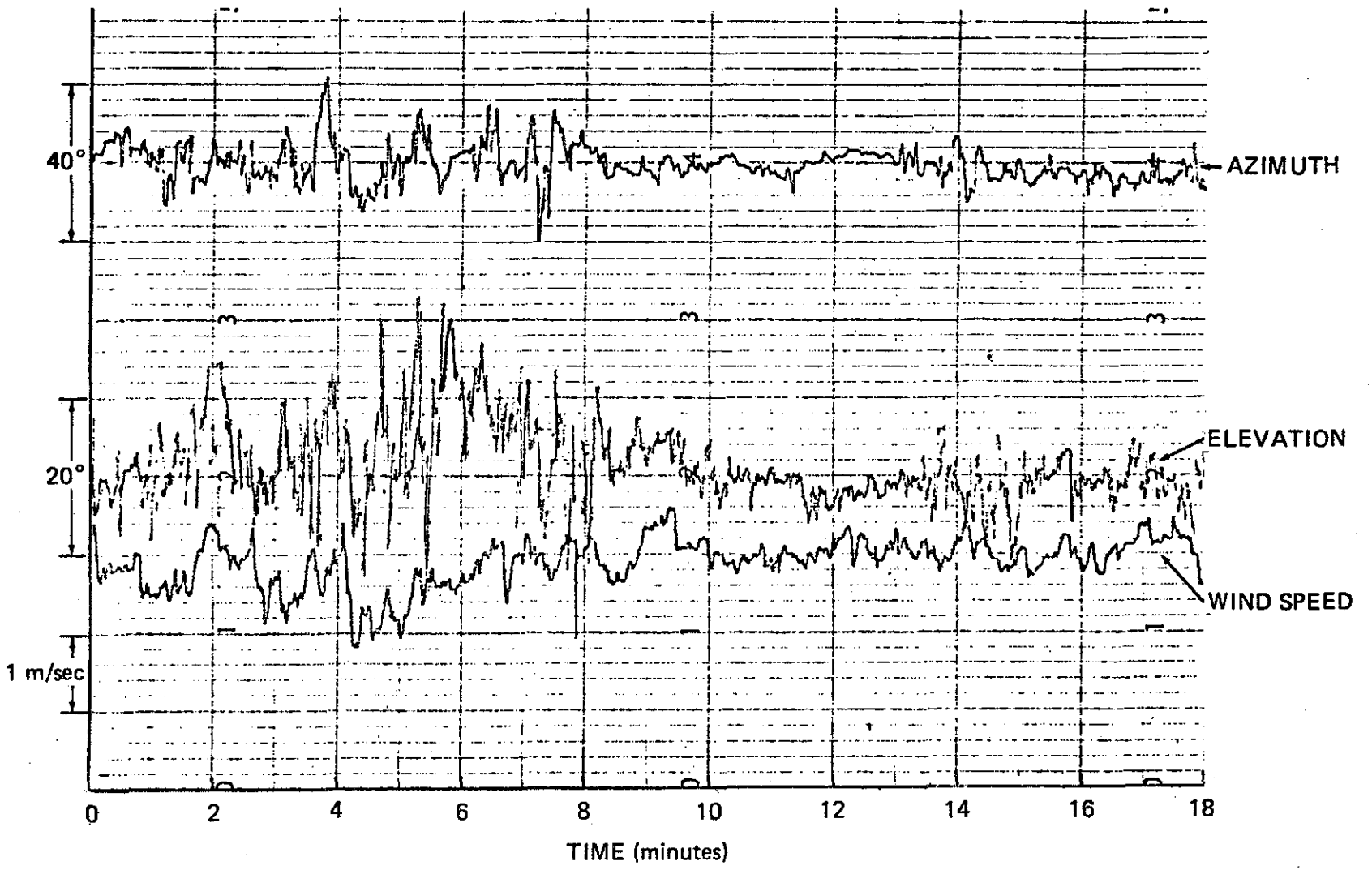

Figure 6. Sample of the bivane record for 18 min periods on 3 February 1977 at the Lower Syncrude Site.

Table 2. Standard deviations of bivane data (in degrees) and running means of 5, 10, 25, 50, and 100 s.

Date	Time	Data	Smoothing Time (Seconds)				
			5	10	25	50	100
05/02/77	1030	AZIMUTH	3.59	3.29	2.75	2.25	1.81
05/02/77	1030	ELEVATION	4.66	4.11	3.08	2.38	1.66
05/02/77	1140	AZIMUTH	2.14	2.04	1.79	1.52	1.36
05/02/77	1140	ELEVATION	2.17	1.96	1.58	1.18	0.83
05/02/77	1240	AZIMUTH	2.27	2.17	1.96	1.72	1.44
05/02/77	1240	ELEVATION	2.33	2.02	1.66	1.37	1.02
05/02/77	1615	AZIMUTH	1.76	1.63	1.39	1.19	0.99
05/02/77	1615	ELEVATION	2.53	2.22	1.68	1.30	0.96
06/02/77	0800	AZIMUTH	2.91	2.82	2.63	2.38	1.95
06/02/77	0800	ELEVATION	1.58	1.45	1.25	1.06	0.88
06/02/77	0900	AZIMUTH	2.30	2.24	2.09	1.89	1.61
06/02/77	0900	ELEVATION	1.53	1.49	1.41	1.29	1.16
06/02/77	1000	AZIMUTH	5.81	5.74	5.60	5.48	5.32
06/02/77	1000	ELEVATION	2.92	2.75	2.53	2.31	2.07
06/02/77	1100	AZIMUTH	2.57	2.55	2.47	2.37	2.23
06/02/77	1100	ELEVATION	1.65	1.58	1.49	1.38	1.19
06/02/77	1136	AZIMUTH	8.25	8.11	7.89	7.69	7.38
06/02/77	1136	ELEVATION	2.87	2.46	1.97	1.66	1.37
06/02/77	1300	AZIMUTH	7.91	7.45	6.90	6.36	5.34
06/02/77	1300	ELEVATION	3.19	2.67	2.00	1.53	1.10
06/02/77	1400	AZIMUTH	6.68	6.36	5.76	5.17	4.51
06/02/77	1400	ELEVATION	5.44	4.79	3.75	3.03	2.32
06/02/77	1500	AZIMUTH	4.28	3.97	3.43	2.99	2.34
06/02/77	1500	ELEVATION	4.01	3.28	2.56	1.82	1.34
06/02/77	1600	AZIMUTH	4.63	4.32	3.76	3.27	2.54
06/02/77	1600	ELEVATION	2.78	2.29	1.68	1.29	1.06

continued ...

Table 2. Continued.

Date	Time	Data	Smoothing Time (Seconds) 5	10	25	50	100
07/02/77	0920	AZIMUTH	3.89	3.77	3.59	3.49	3.41
07/02/77	0920	ELEVATION	1.16	0.95	0.73	0.57	0.46
07/02/77	1020	AZIMUTH	1.46	1.44	1.41	1.38	1.29
07/02/77	1020	ELEVATION	0.48	0.46	0.42	0.38	0.33
07/02/77	1100	AZIMUTH	3.72	3.66	3.57	3.46	3.27
07/02/77	1100	ELEVATION	1.28	1.14	0.95	0.80	0.61
07/02/77	1140	AZIMUTH	3.04	2.94	2.72	2.45	2.10
07/02/77	1140	ELEVATION	1.96	1.85	1.64	1.48	1.20
07/02/77	1300	AZIMUTH	7.52	6.90	5.34	4.24	3.36
07/02/77	1300	ELEVATION	5.32	4.39	2.97	2.31	1.73
07/02/77	1400	AZIMUTH	9.42	8.71	7.20	5.69	4.57
07/02/77	1400	ELEVATION	6.03	5.16	3.67	2.55	1.97
07/02/77	1435	AZIMUTH	7.71	6.87	5.27	3.86	2.62
07/02/77	1435	ELEVATION	5.84	5.06	3.70	2.75	2.19
08/02/77	0800	AZIMUTH	4.37	4.14	3.74	3.46	3.18
08/02/77	0800	ELEVATION	2.88	2.39	1.64	1.29	0.98
08/02/77	1000	AZIMUTH	8.32	8.17	7.88	7.55	7.12
08/02/77	1000	ELEVATION	2.40	1.96	1.44	1.09	0.76
08/02/77	1100	AZIMUTH	12.35	11.95	10.97	10.00	8.97
08/02/77	1100	ELEVATION	6.57	5.85	4.76	3.81	2.75
08/02/77	1200	AZIMUTH	4.82	4.77	4.64	4.35	3.80
08/02/77	1200	ELEVATION	1.29	1.14	0.94	0.80	0.66
08/02/77	1300	AZIMUTH	3.39	3.15	2.84	2.64	2.25
08/02/77	1300	ELEVATION	2.11	1.76	1.35	1.10	0.85
10/02/77	0720	AZIMUTH	5.68	5.31	4.66	4.28	4.04
10/02/77	0720	ELEVATION	3.06	2.59	1.87	1.57	1.38
10/02/77	0800	AZIMUTH	4.79	4.58	4.34	4.17	3.86
10/02/77	0800	ELEVATION	2.38	2.00	1.58	1.33	1.15
10/02/77	0900	AZIMUTH	2.95	2.81	2.56	2.24	1.84
10/02/77	0900	ELEVATION	2.05	1.74	1.36	1.10	0.81

continued ...

Table 2. Concluded.

Date	Time	Data	Smoothing Time (Seconds) 5	10	25	50	100
10/02/77	1000	AZIMUTH	2.00	1.91	1.74	1.49	1.19
10/02/77	1000	ELEVATION	1.50	1.36	1.21	1.07	0.92
10/02/77	1100	AZIMUTH	5.44	5.34	5.08	4.64	3.87
10/02/77	1100	ELEVATION	4.12	3.96	3.67	3.37	2.98
10/02/77	1200	AZIMUTH	6.52	6.25	5.63	4.66	3.13
10/02/77	1200	ELEVATION	5.57	5.25	4.48	3.73	3.14
10/02/77	1300	AZIMUTH	2.80	2.71	2.52	2.31	1.98
10/02/77	1300	ELEVATION	2.31	2.03	1.57	1.19	0.92
10/02/77	1400	AZIMUTH	4.52	4.36	3.92	3.27	2.53
10/02/77	1400	ELEVATION	4.46	4.11	3.40	2.86	2.30
10/02/77	1500	AZIMUTH	2.27	2.26	2.22	2.15	2.01
10/02/77	1500	ELEVATION	2.78	2.74	2.65	2.55	2.38
10/02/77	1600	AZIMUTH	7.93	7,91	7.84	7.71	7.48
10/02/77	1600	ELEVATION	2.43	2.34	2.13	1.86	1.71
12/02/77	0745	AZIMUTH	4.27	4.20	4.06	3.89	3.68
12/02/77	0745	ELEVATION	3.14	2.88	2.41	2.11	1.86
12/02/77	0810	AZIMUTH	7.38	7.25	6.94	6.63	6.16
12/02/77	0810	ELEVATION	5.21	4.16	3.62	3.29	2.80
12/02/77	0910	AZIMUTH	8.41	8.41	8.39	8.37	8.36
12/02/77	0910	ELEVATION	1.60	1.53	1.40	1.24	1.08

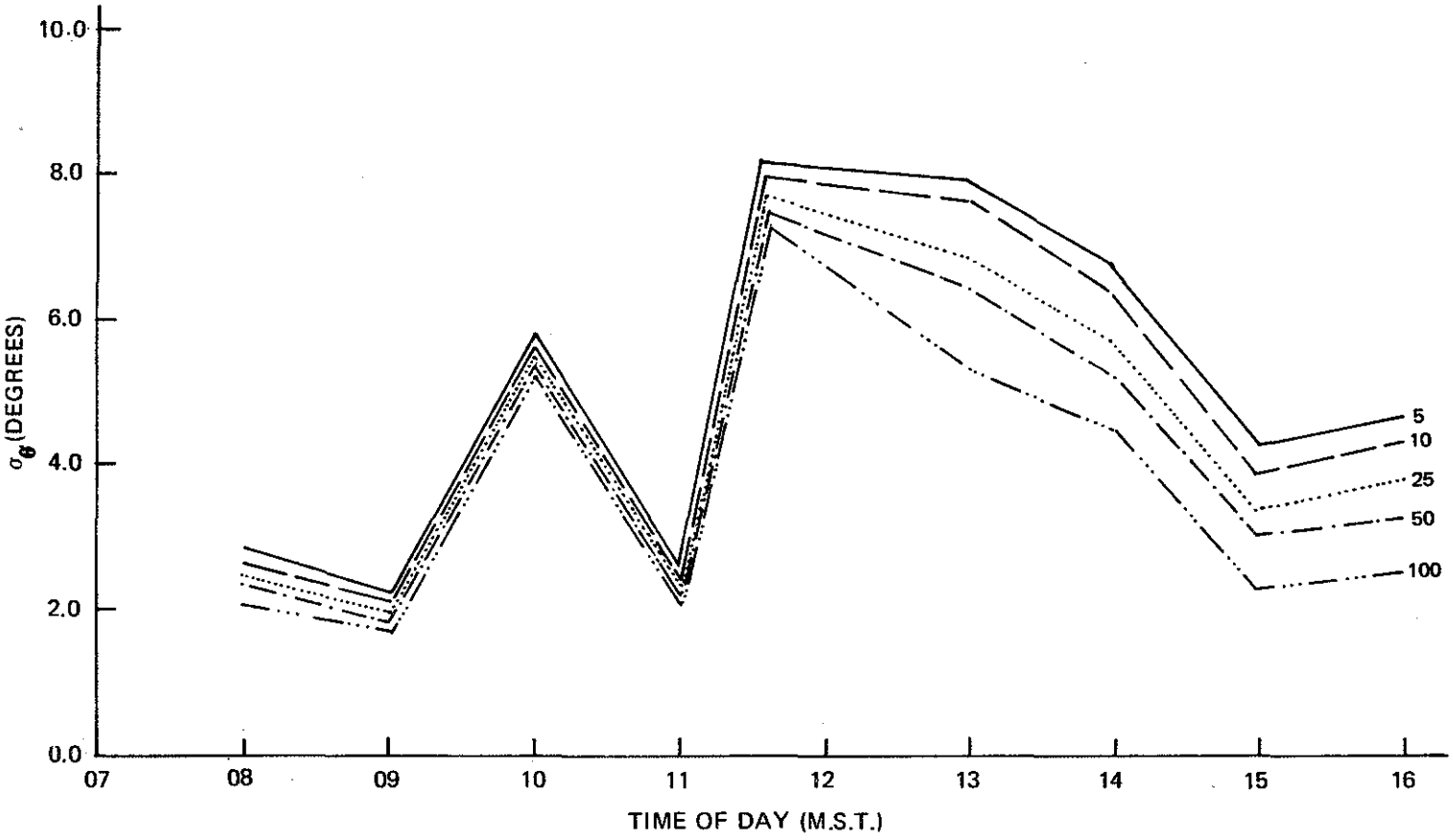

Figure 7. Variation of standard deviation of elevation angle with the time of day for 6 February 1977.

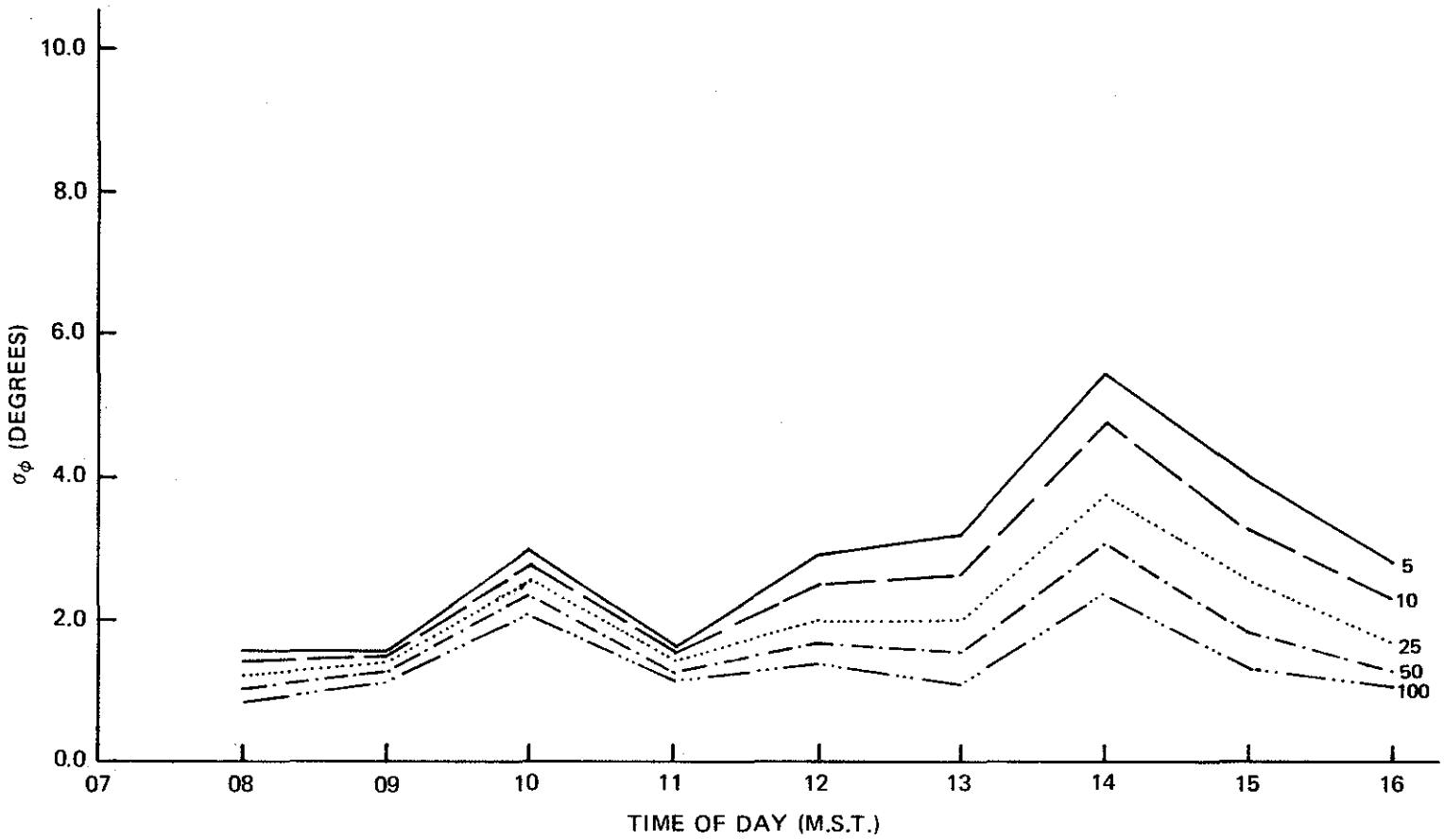

Figure 8. Variations of standard deviation of azimuth angle with the time of day for 6 February 1977.

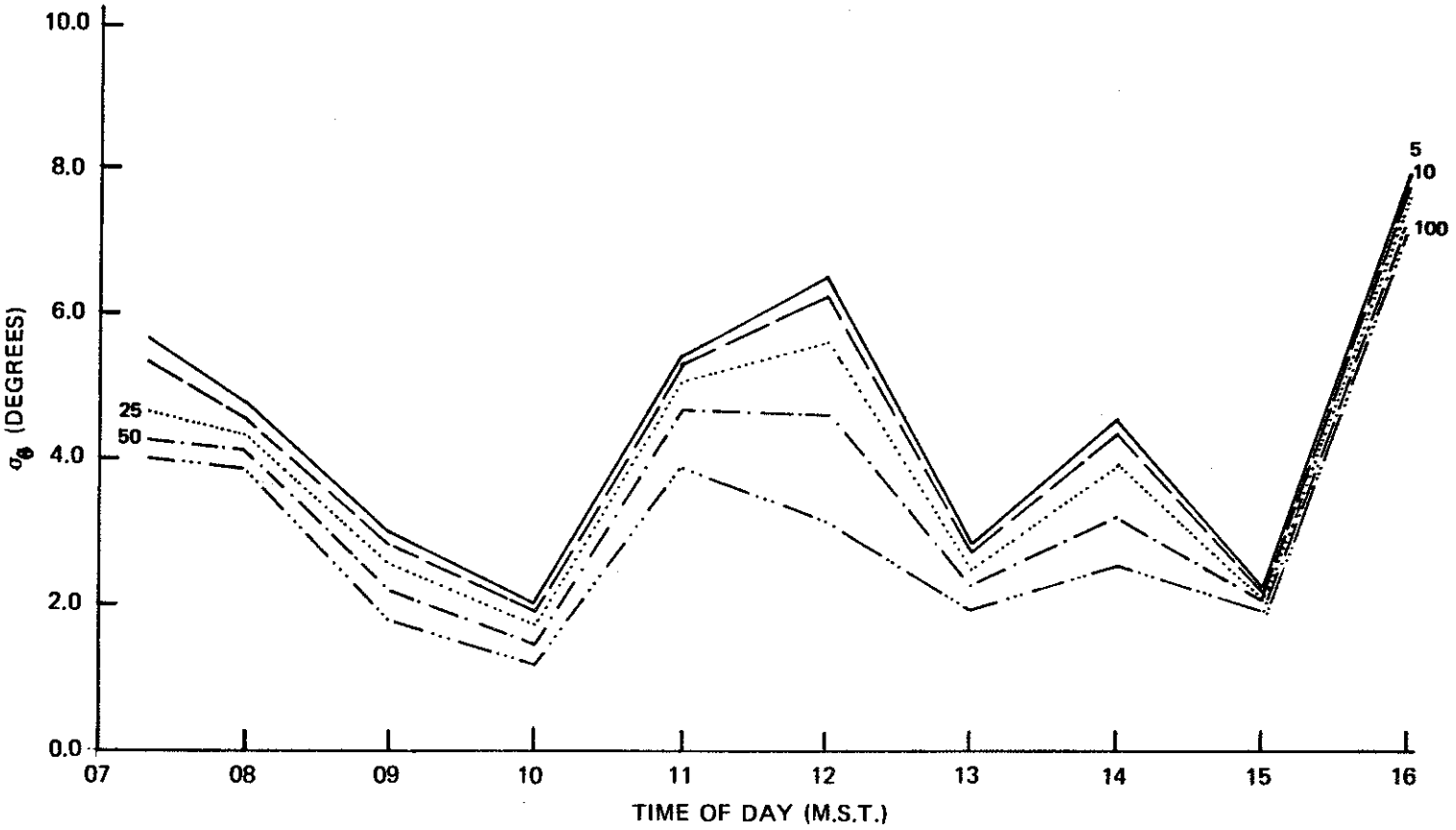

Figure 9. Variation of standard deviation of the elevation angle with the time of day for 10 February 1977.

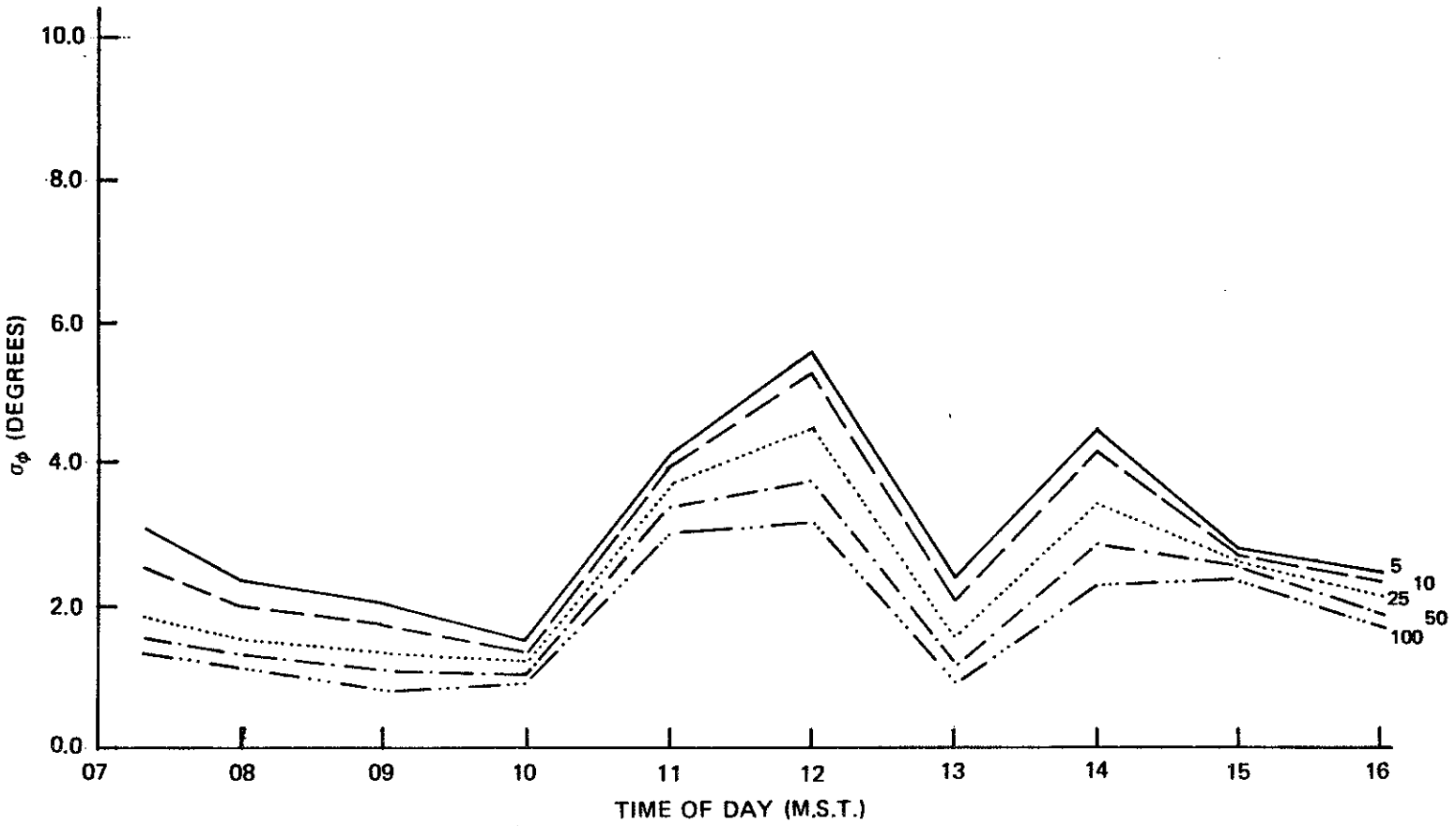

Figure 10. Variation of standard deviation of the azimuth angle with the time of day for 10 February 1977.

On 10 February, σ_θ at 1600 (Figure 9) increased to a value greater than 6. A strong destabilization of the atmospheric conditions occurred in the afternoon. A frontal inversion returned during that time as the occluded front passed.

The wind was calm. Measurements by the M/S indicated that the wind speed was less than 2 $m \cdot s^{-1}$ at the bivane level. One suspects, then, that the increase in the value of σ_θ at that time was due to the increase in turbulent intensity along the vertical induced by the local changes in the topography.

In order to examine the effect of changes of wind speed on the magnitude of both σ_θ and σ_ϕ, median values of σ were grouped according to wind speed (Table 3). Although the number of observations is too small to draw firm conclusions, it appears that both σ_θ and σ_ϕ decrease with increasing wind speed for all smoothing times. The increase is more evident with σ_θ than with σ_ϕ. One concludes that an increase in wind speed, which in turn supresses thermal turbulence during the day, deceases wind standard deviations along the vertical.

The bivane data described above were used to determine the dispersion parameters σ_y and σ_z. The basis working theories for determining σ_y and σ_z were discussed by Pasquill (1974, 1975). The parameters σ_y and σ_z have been derived by applying one of the following theories:

1. gradient transfer theory,
2. similarity theory, or
3. statistical theory.

No one of these theories has yet been conclusively demonstrated to be universally applicable. Statistical theory, however, has been applied extensively and offers the most promising solution to determine σ_y and σ_z. This type of analysis has been adopted in this report.

Table 3. Median values of $\sigma\theta$ and $\sigma\phi$ for different wind classes and different smoothing times.

Wind Speed Class ($m.s^{-1}$)	Number of Observations	$\sigma\phi$ (Elevation) (degrees) Smoothing Time (seconds)					$\sigma\phi$ (Azimuth) (degrees) Smoothing Times (seconds)				
		5	10	25	50	100	5	10	25	50	100
$o \leq u < 2.5$	6	3.62	3.42	3.02	2.70	2.34	7.22	7.08	6.73	6.18	5.30
$2.5 \leq u < 5$	16	2.87	2.42	1.75	1.45	1.17	4.80	4.68	4.49	4.22	3.83
$5 \leq u < 7.5$	15	2.17	1.96	1.64	1.29	1.02	3.39	3.15	2.75	2.45	2.10

It has been suggested that the diffusive spread of a plume from a continuous elevated point source, in a homogeneous field of turbulence, can be predicted by the following relation (Hay and Pasquill 1959):

$$\sigma_y,\ \sigma_z = \left[\sigma_\phi,\ \theta\right]\ \tau, S^{x-} \qquad (1)$$

where x is the downwind distance, τ denotes the sampling time, and S is a running average time over which the data were sampled to obtain Eulerian time wind statistics equivalent to Lagrangian statistics. S is given as:

$$S = \frac{x}{\beta \bar{U}} \qquad (2)$$

where $\bar{U}$ is the average wind speed and β is the Lagrangian-Eulerian time scale. Hay and Pasquill (1959) indicated that the value of β ranged from 1.1 to 8.5. Recently, however, Pasquill (1974) suggested that β is related to the turbulent intensity (i) by the following relation:

$$\beta i = \text{Constant} = 0.44 \qquad (3)$$

There is a limit for the averaging time S that can be applied, and this depends on the length of the record. In order to examine this relationship, variations of the wind direction variance σ^2 with S are plotted and are shown in Figure 11. It will be noted that there is a slow decrease of variance from S = 5 to S = 100 s. For S > 100 the variance decreases rapidly to near zero. This is probably due to the end-of-record effect.

For this study, the averaging time S = 5 s was short enough to allow a 20 min record of bivane data to be used.

To examine the applicability of Eq (1) to the AOSERP study area, the standard deviation of wind direction, using running means as indicated previously, was compared with the observed σ of the plume along the vertical. Values of σ_z were obtained from plume rise measurements (Section 4). No attempt was made to compare σ_y

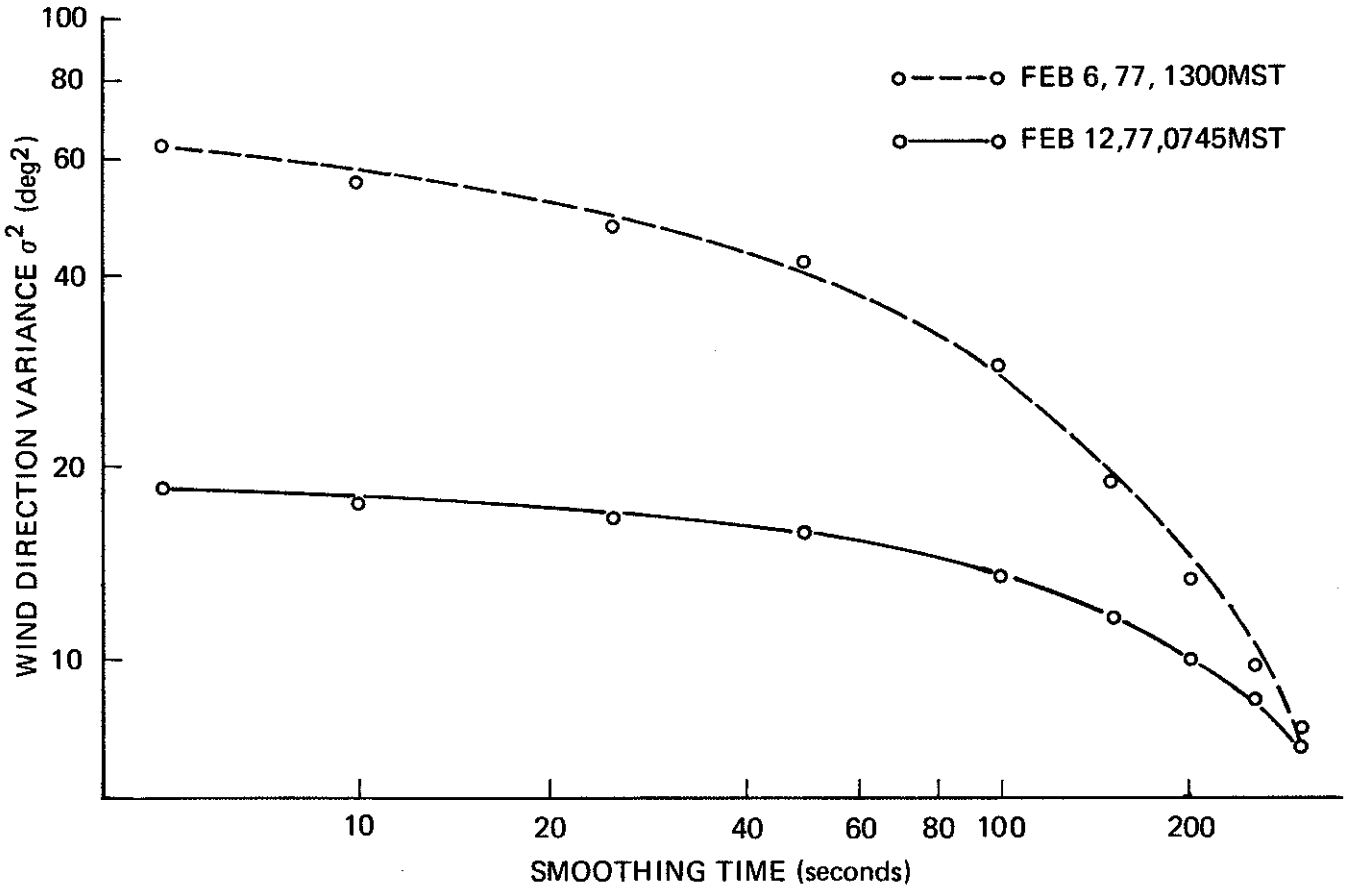

Figure 11. Variations of the wind direction variance with smoothing time for two days.

to this model because of the limited number of observations of σ_y. The result of the comparison is shown in Figure 12. It can be seen from the scatter of the points that Eq (1) underestimates the spread of the plume at various downwind distances.

The disagreement of the observed data with the theoretical model described by Eq (1) could be due to buoyancy-induced initial growth of the plume, which indicates that extrapolation of these theoretical models to the AOSERP study area must be done cautiously.

σ_θ is approximately equal to $\sigma_w/\bar{U}$ where σ_w is the standard deviation of the vertical wind. In turn, σ_w is proportional to the friction velocity. Consequently, σ_θ is strongly dependent on the topography surrounding the bivane tower. It is expected, then, that sites with different topography will give different values of σ_z. Furthermore, the spectrum of turbulence may differ from one location to another, and since the diffusion of the plume depends on this parameter, one expects that the bivane data may not describe the plume's σ when the plume is at a different location and level.

3.2.3 Tethersonde Measurements

The February 1977 tethersonde (T/S) field study had one primary objective: to compare profiles taken at the Lower Syncrude Site with those at the Syncrude Mine Site to ascertain whether those features observed above the valley during stable conditions were characteristic of the surrounding plains area. Figure 13 shows the T/S at the Syncrude Mine Site and Figure 14 a detailed picture of the T/S package.

It was recognized initially that this objective would have been most completely fulfilled if two systems were flown simultaneously at both sites; however, from a previous study, it was felt that the boundary layer above the valley was predictable under stable conditions, and therefore, the study was carried out at two separate experiments, one at each site. Also, M/S flights at Lower Syncrude and/or Syncrude Mine Site carried out during T/S operations could be used to supplement this data set.

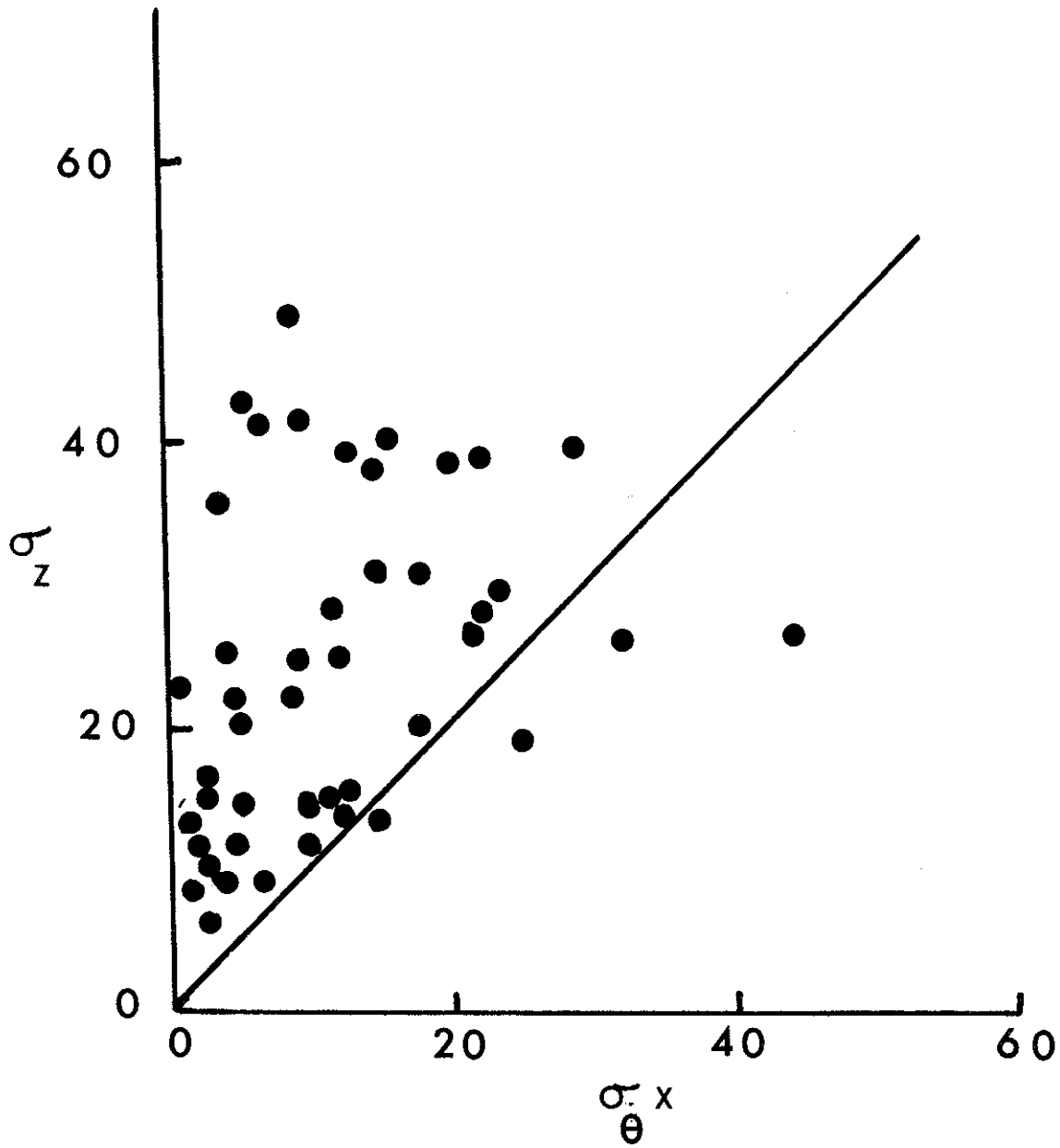

Figure 12. Comparison of predicted versus observed vertical dispersion coefficient using Eq (1). Solid line represents perfect agreement.

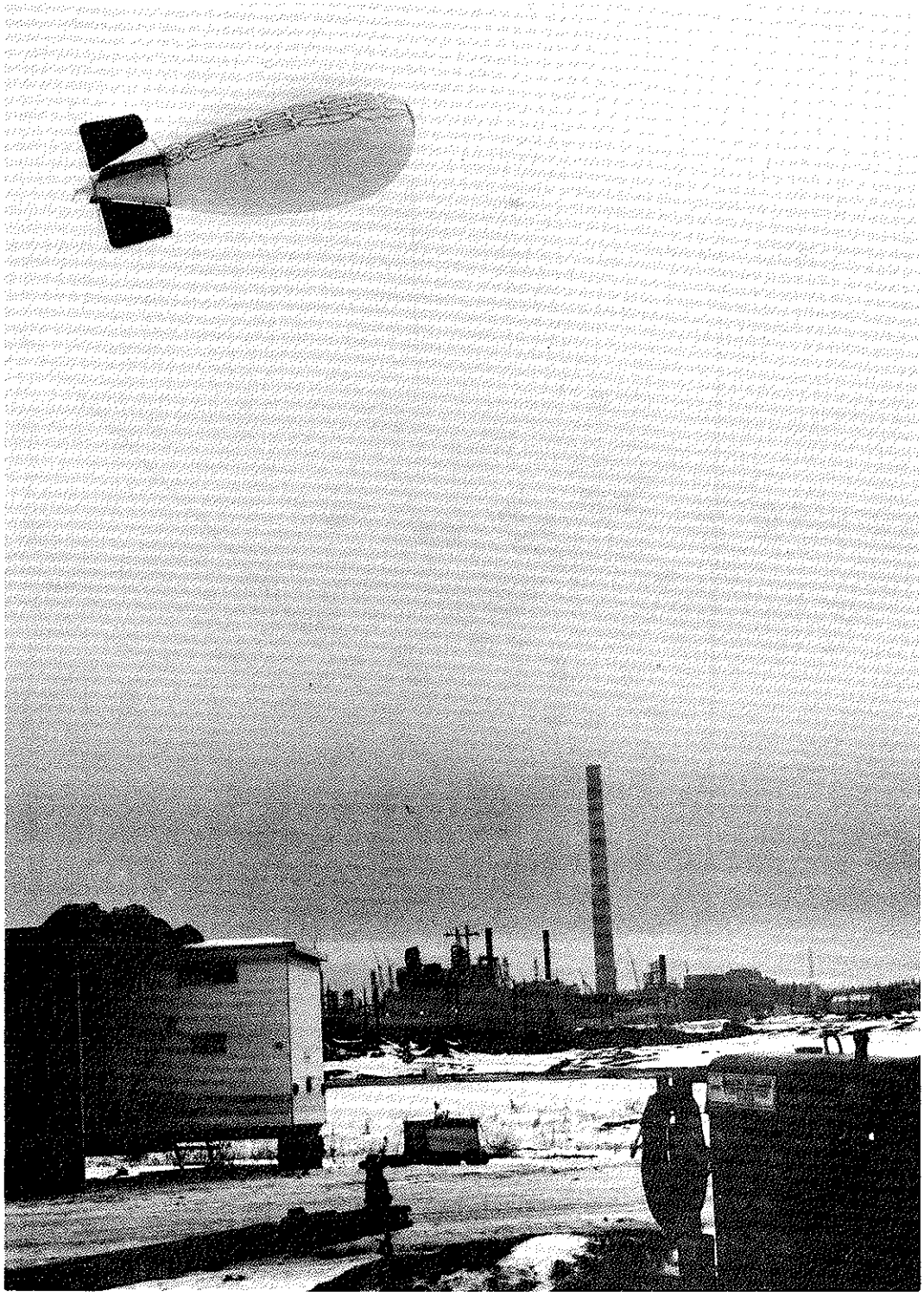

Figure 13. Tethersonde at the Syncrude Mine Site, February 1977.

Figure 14. Detailed photograph of the tethersonde package that was was used in this study, February 1977.

The instrument used was the same as the one employed in the March 1976 field study (Fanaki 1978). The profile mode was flown the majority of the time, with data collection taking place at the Lower Syncrude Site from 4 February through to 1303 on 8 February and from 1510 on 8 February until 11 February 1977 at the Syncrude Mine Site. The profile data available from these periods are in a separate file (see Descriptive Summary). The profiles are presented with ambient temperatures (^{o}C), virtual potential temperature (^{o}C), relative humidity (%), total horizontal wind speed ($m \cdot s^{-1}$), and wind direction (^{o}magnetic North) being plotted as a function of height above ground level (AGL).

As in the previous report (Fanaki 1978), the height of the valley walls is indicated on the right-hand graph. Flow down the valley is associated with flow at 124^{o} magnetic, while flow up the valley would be from 304^{o} magnetic.

3.2.3.1 Discussion of data. Data from 4 and 5 February indicated weak surface inversions to lapse conditions with little significant detail in the wind field. On 5 February, a small maximum in the wind field was observed to closely track the base of the elevated inversion above 350 m AGL. During the evening of 6 February, a strong surface inversion was observed through and above the valley. Within this surface inversion, a strong inversion of 8^{o} over a few metres can be identified with the top of the river valley. Associated with this strong inversion was flow down the valley, while aloft the flow was effectively across the valley leading to an intermediate veer layer. During the day, the warm air mass above the valley tended towards lapse, while the cold air remained trapped within the valley, leading to a $15^{o}C$ inversion at the top of the valley. It is worth noting that with this strong inversion the moist valley air was trapped in a thin layer at the inversion interface (06/02/77-1143, 1343). By 1343, the two regimes were totally decoupled, so that flow direction changed by nearly 150^{o} over a matter of 10-20 m. Increased turbulence was observed at this interface. As the day progressed, the warmer air began to erode into the colder valley flow, although complete mixing never occurred during the observation period (06/02/77-1613).

During this data period, one simultaneous run of the T/S at Lower Syncrude and at the Syncrude Mine Site was carried out to compare the wind directions above the valley and on the plains area. The results are presented in Figure 15. At both sites, the directional shift is associated with the top of the surface-based inversion. It is worth noting that the winds observed by the M/S near the surface align with the valley direction.

On 7 February, a situation similar to that on 6 February prevailed, with a warm air mass flowing over the colder valley air mass, leading to a strong surface-based inversion. As previously observed, the valley winds were decoupled from flow aloft. Again, the flux of moist air from the valley was retarded by the strong inversion between the two regimes, causing a moist layer to join at the top of the valley. By 1355 the warmer air mass had eroded better than half-way down into the valley until at 1520 the warm air was felt to impinge on the valley floor.

Again, simultaneous flights were carried out at the Mine Site and Lower Syncrude (Figure 16-21). In Figure 16, data are presented for simultaneous M/S and T/S flights at Lower Syncrude. The general features of the two sets of profiles are quite similar, both showing the top of the surface inversion near 300 m and the associated wind shift from valley flow to flow aloft. The winds, although similar at lower heights, tend to be different by at least 20% above 300 m. Some of the differences may be due to the variability associated with stable conditions as well as with the different sampling techniques.

Comparison with the M/S Syncrude Mines Site data (Figures 17, 18, 20, and 21) indicates that the wind shift persists through the surface inversion at both locations until at least 1100.

Data sets (Figures 22-26) are plotted for 8 February, where not only a surface inversion but an inversion aloft were apparent. Associated with the inversion aloft was a local wind maximum. Agreement between M/S and T/S data (Figures 22 and 25)

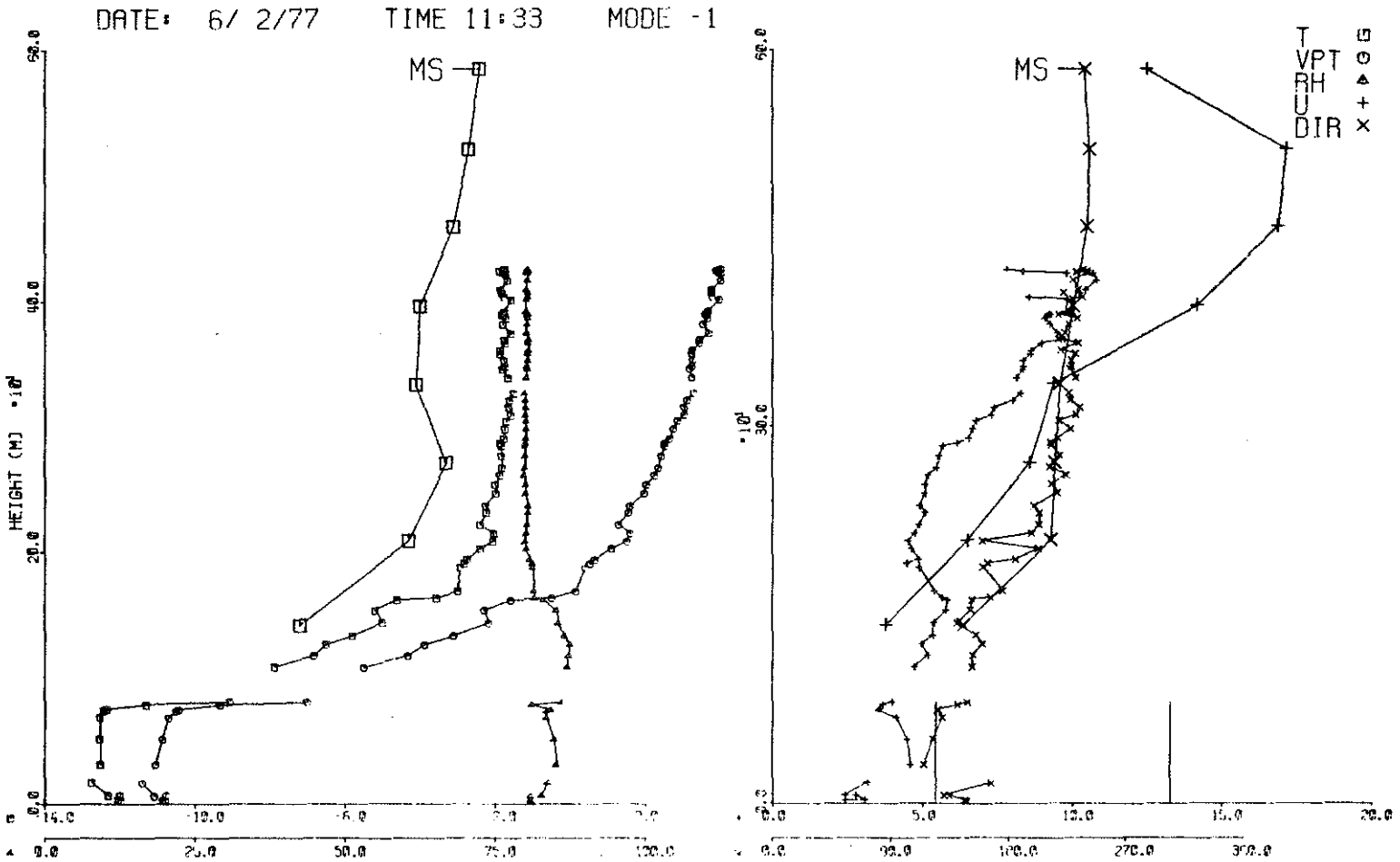

Figure 15. Minisonde and tethersonde profiles for 6 February 1977, 11:33.

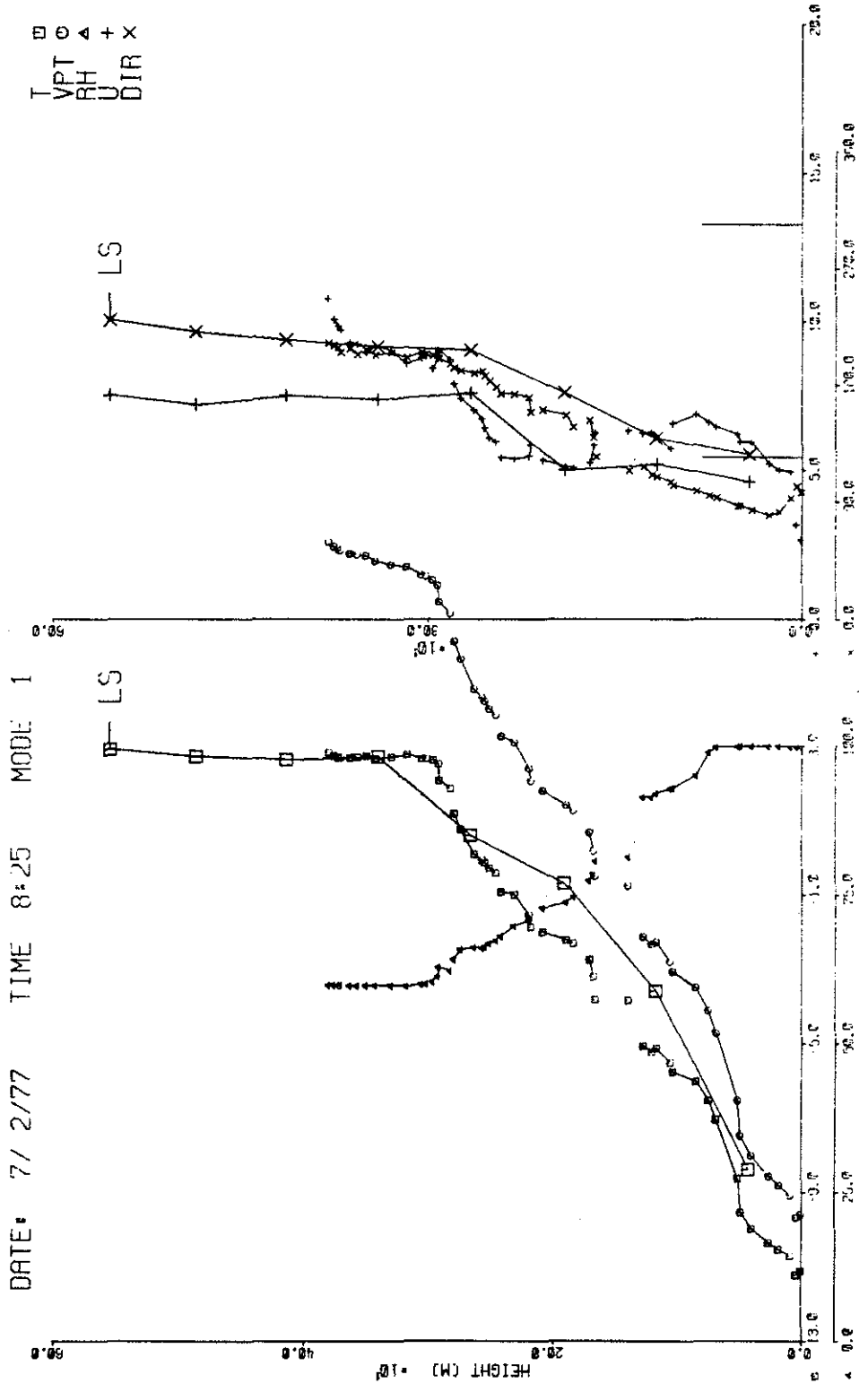

Figure 16. Tethersonde and minisonde inter-comparison for 2 February 1977.

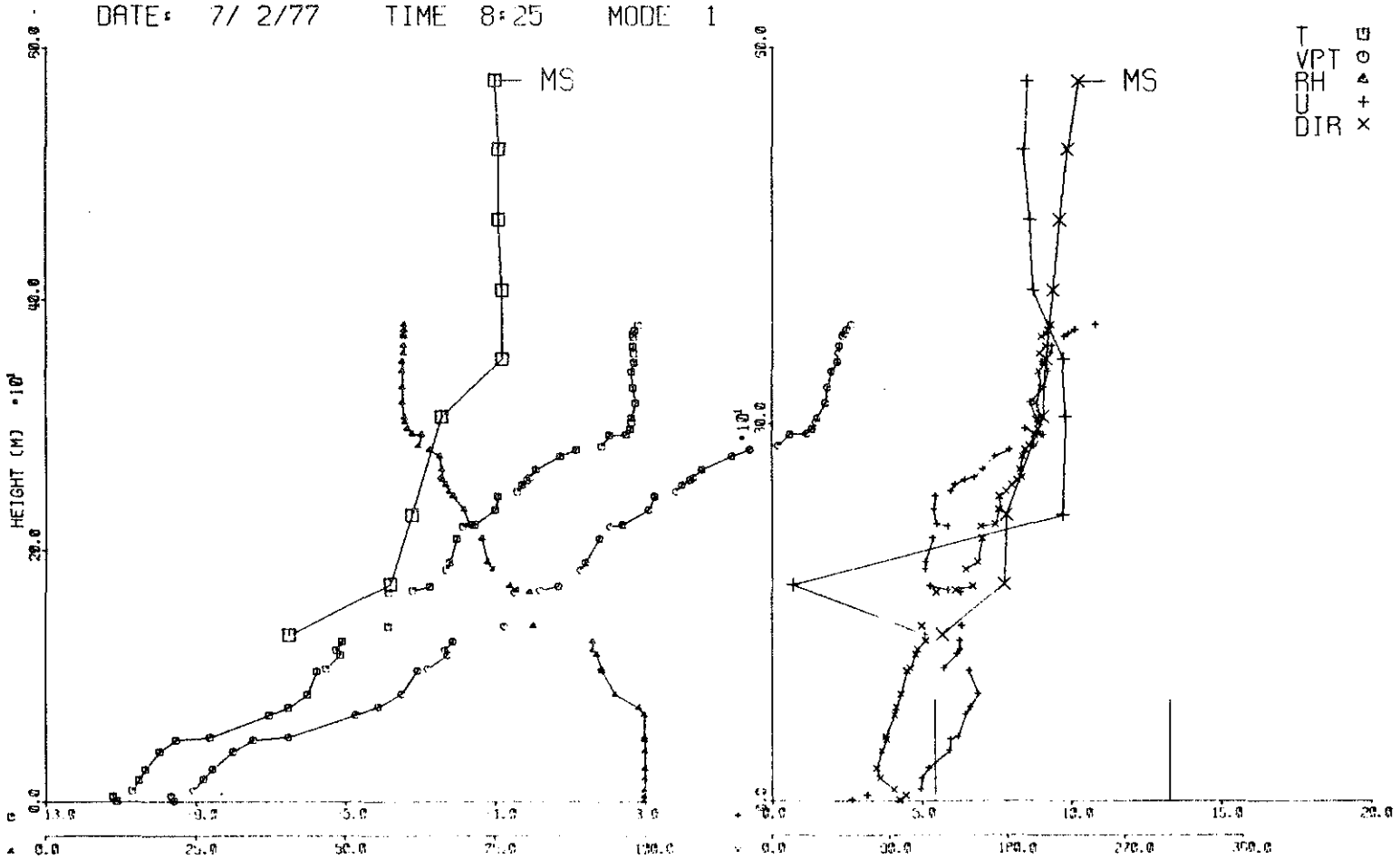

Figure 17. Tethersonde and minisonde profiles for 7 February 1977, 08:25.

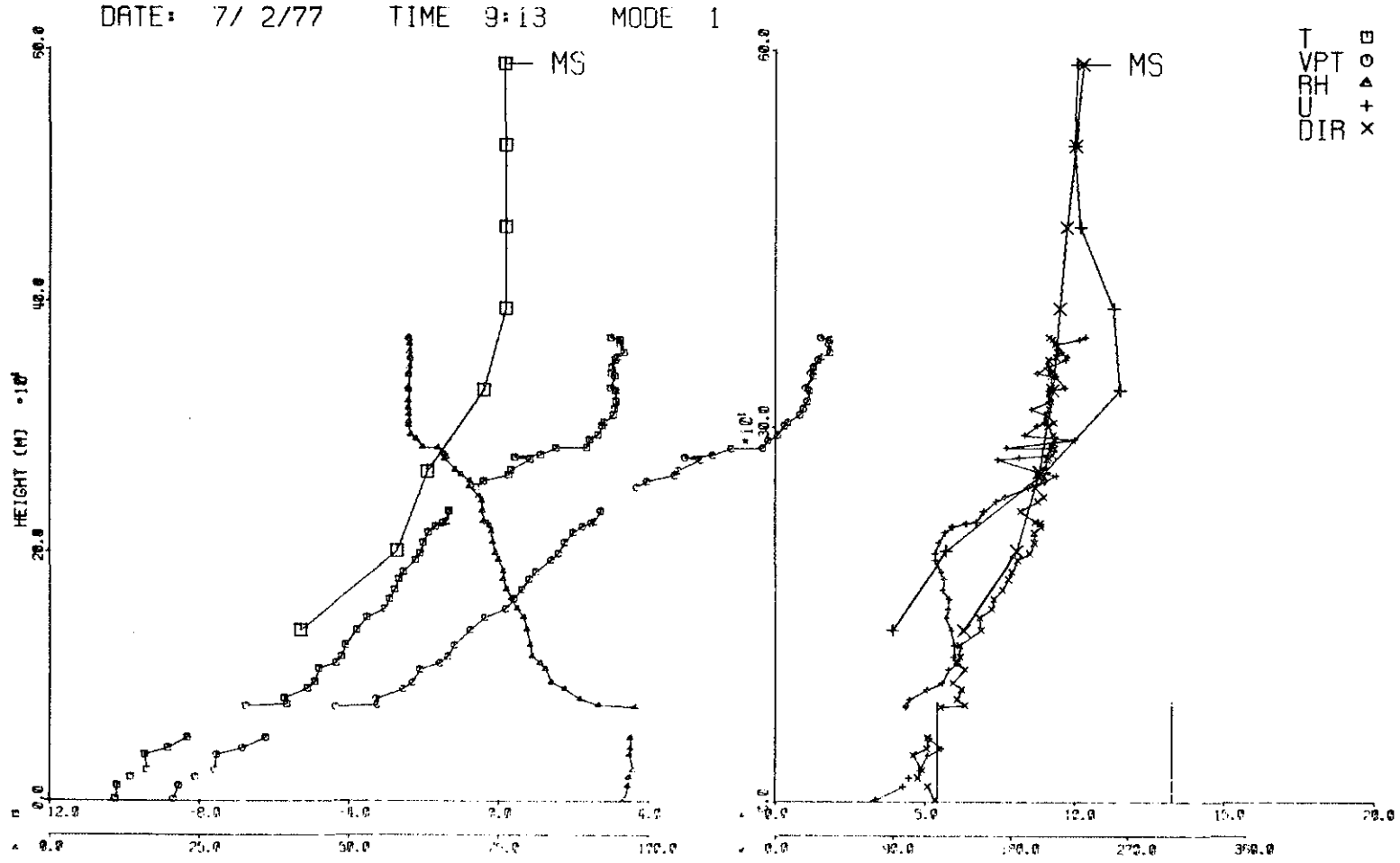

Figure 18. Tethersonde and minisonde profiles for 7 February 1977, 09:13.

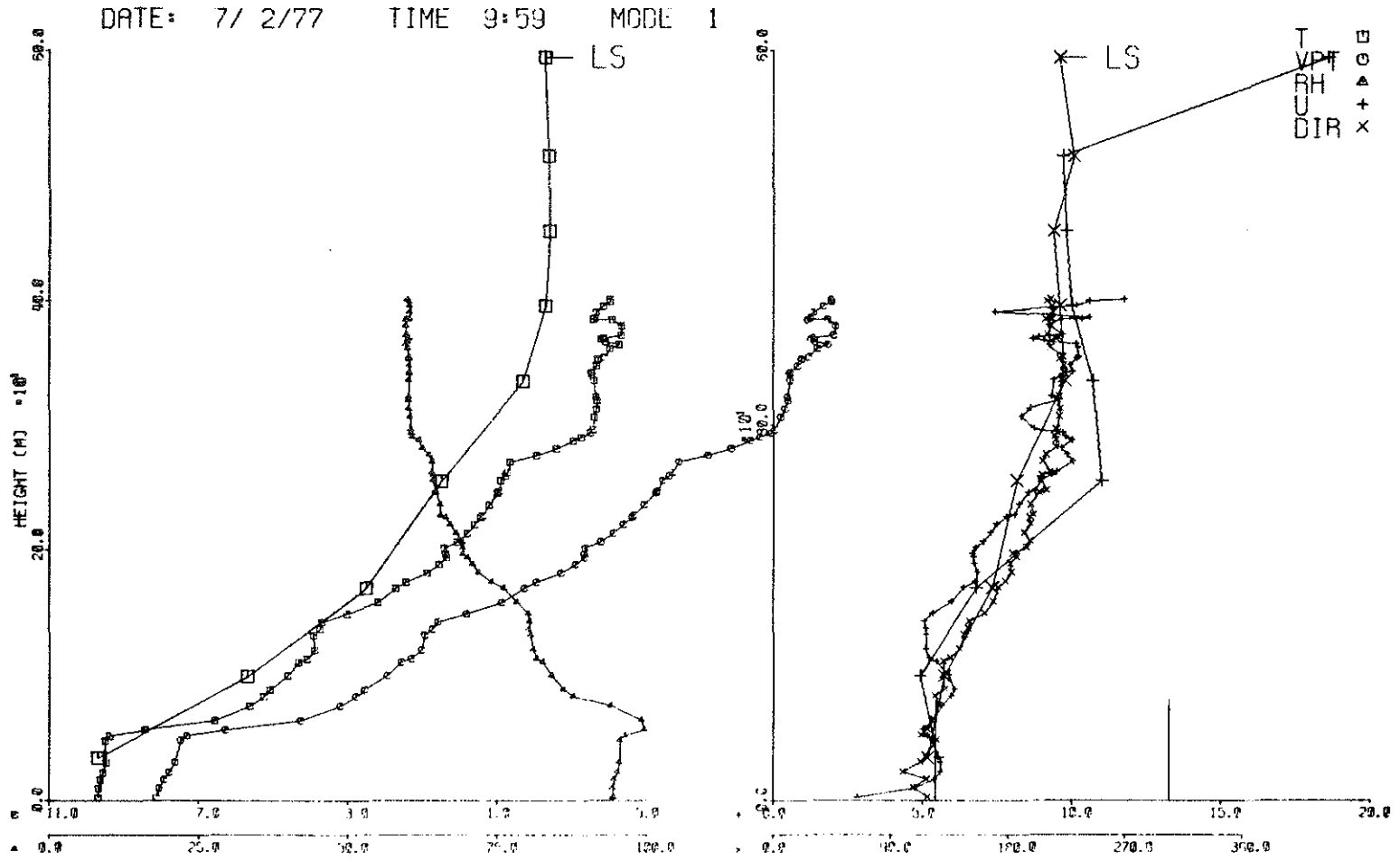

Figure 19. Minisonde and tethersonde inter-comparison for 7 February 1977, 09:59.

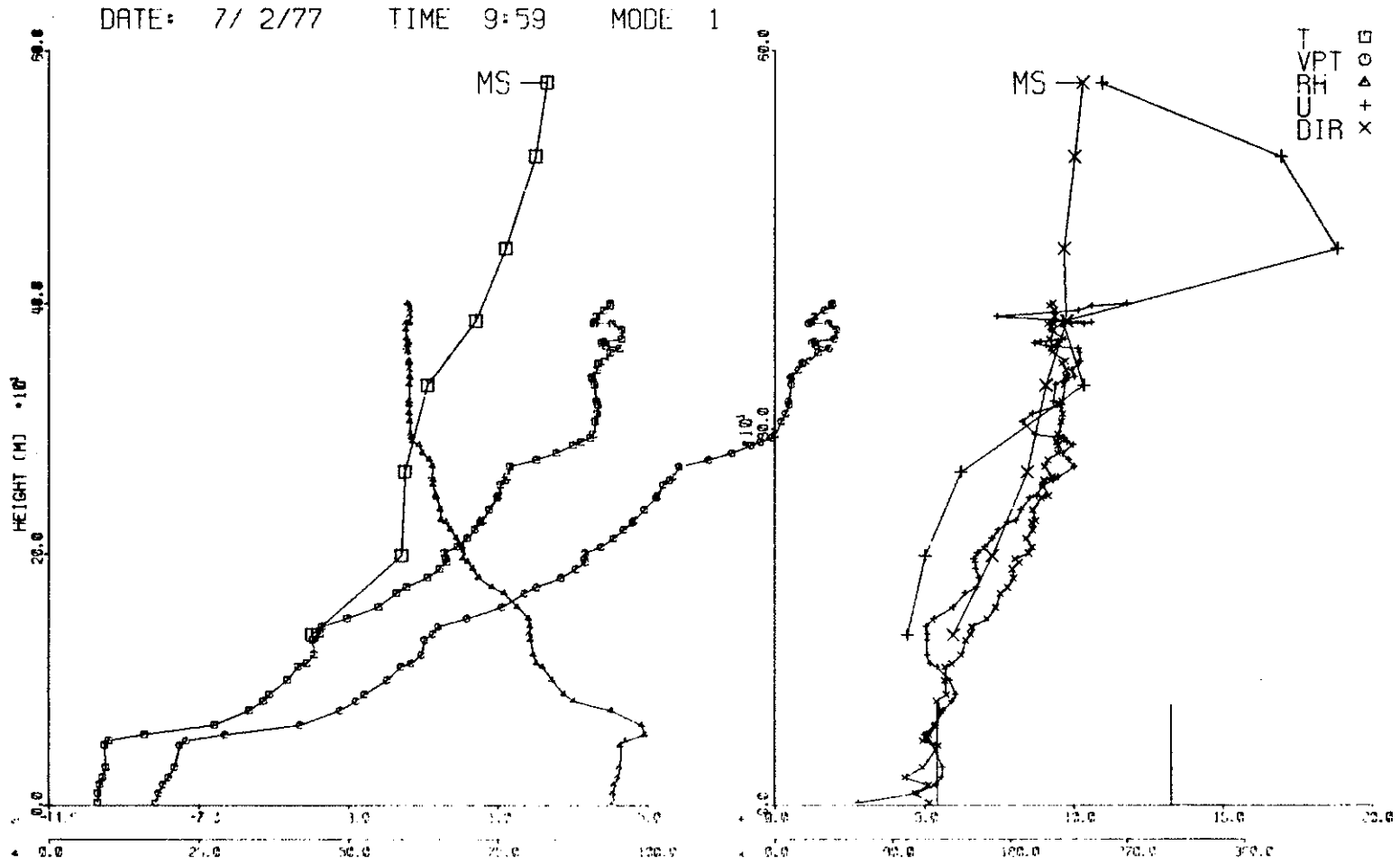

Figure 20. Tethersonde and minisonde profiles for 7 February 1977, 09:59.

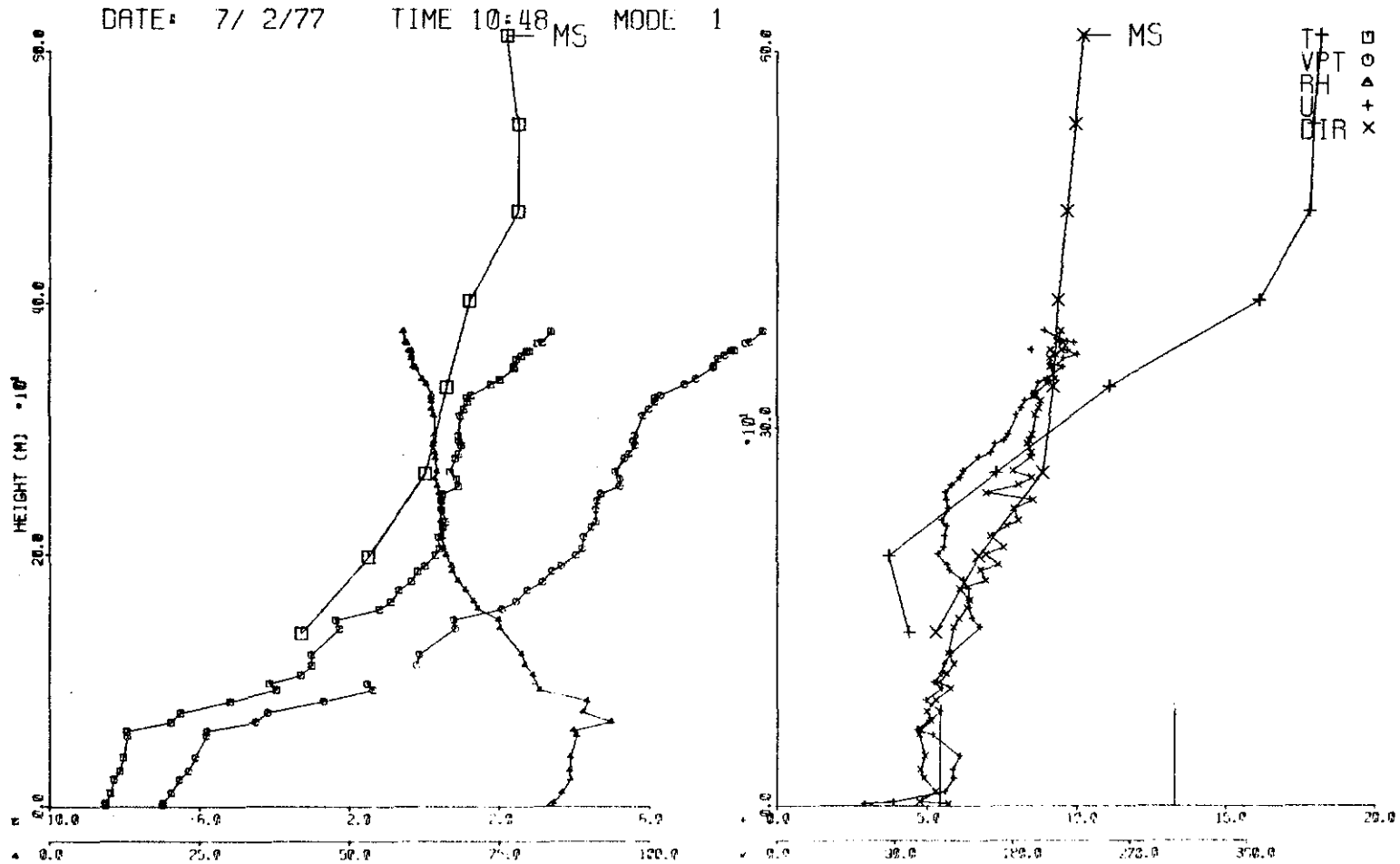

Figure 21. Tethersonde and minisonde profiles for 7 February 1977, 10:48.

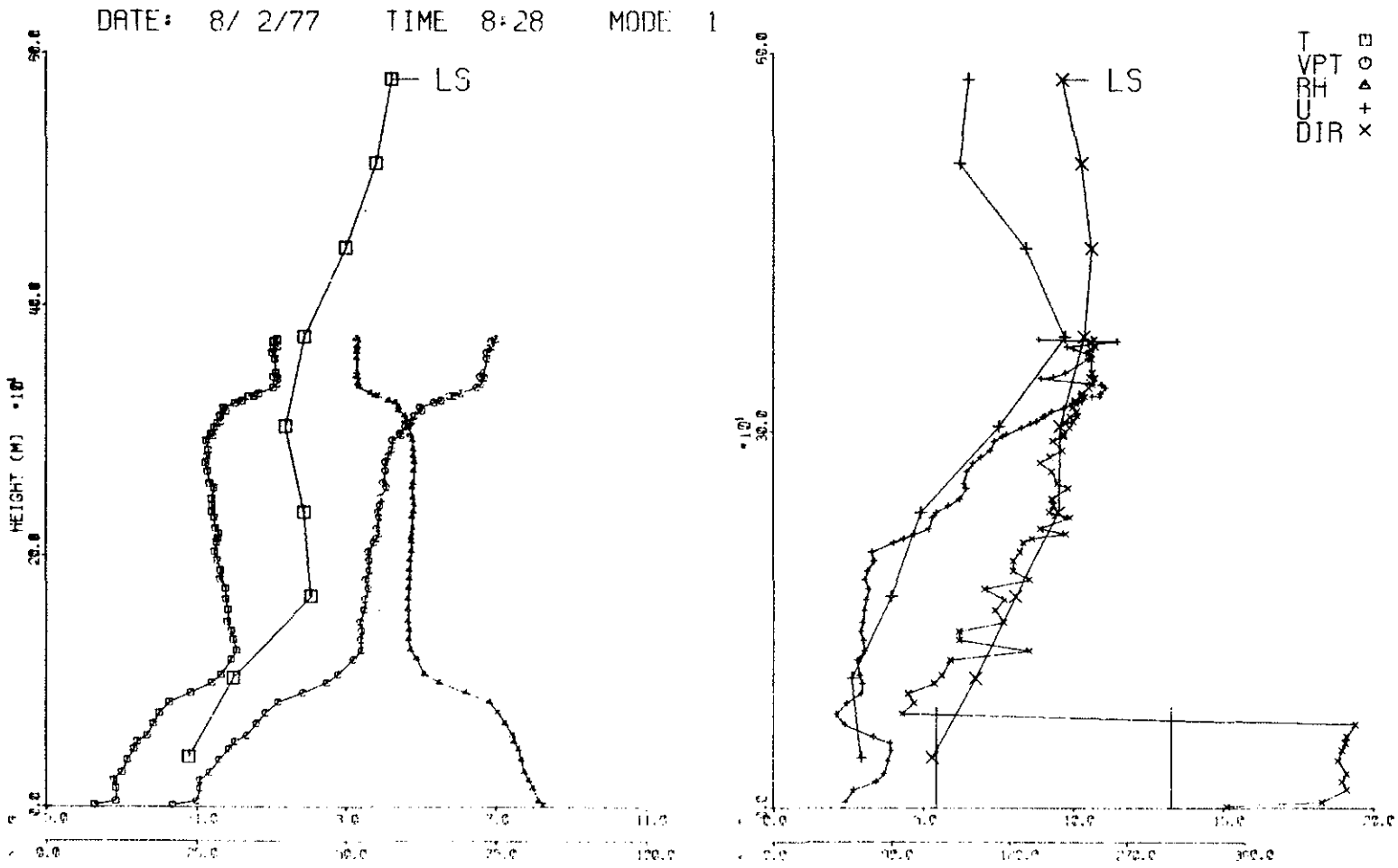

Figure 22. Minisonde and tethersonde inter-comparison for 8 February 1977, 08:28.

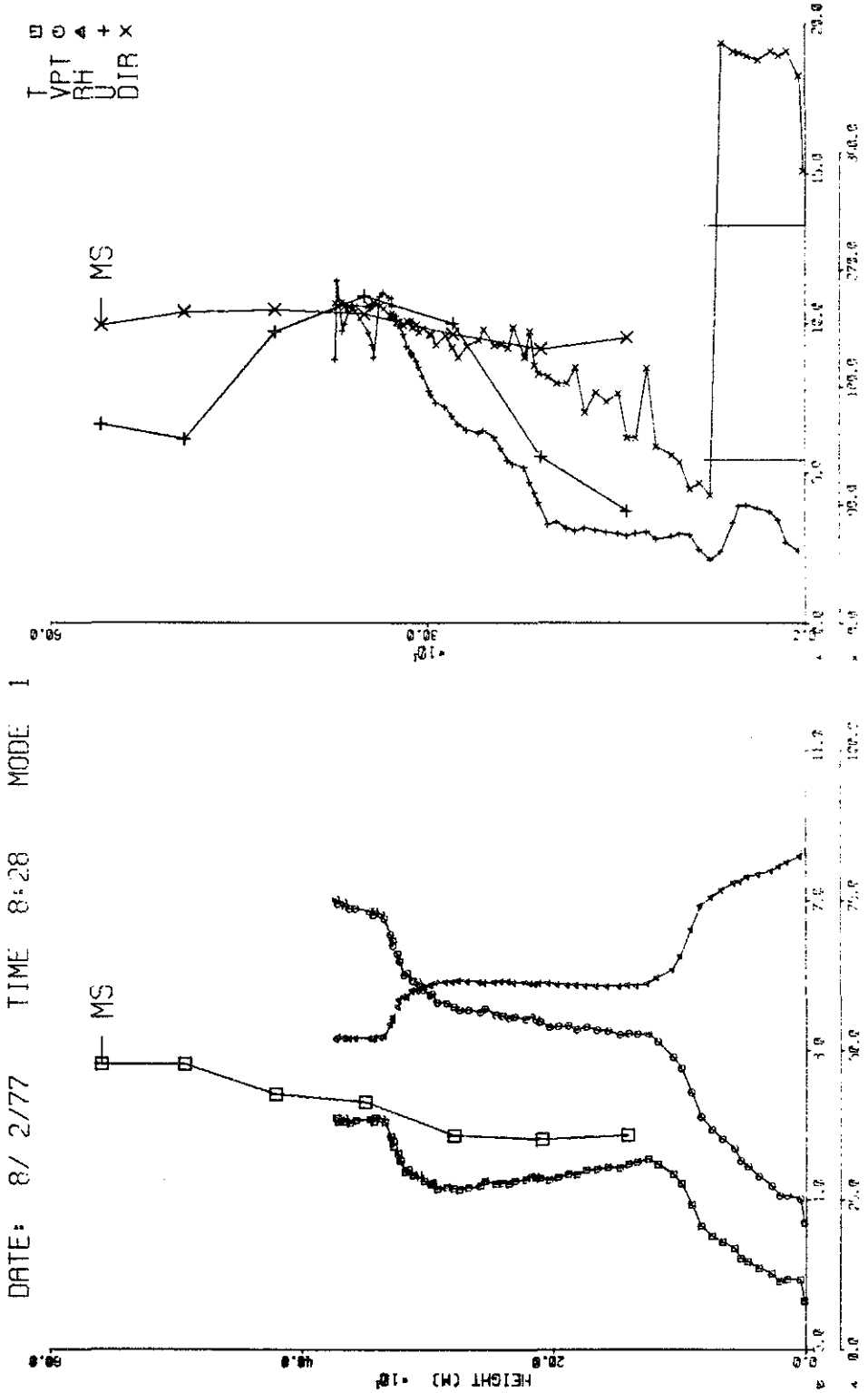

Figure 23. Tethersonde and minisonde profiles for 8 February 1977, 08:28.

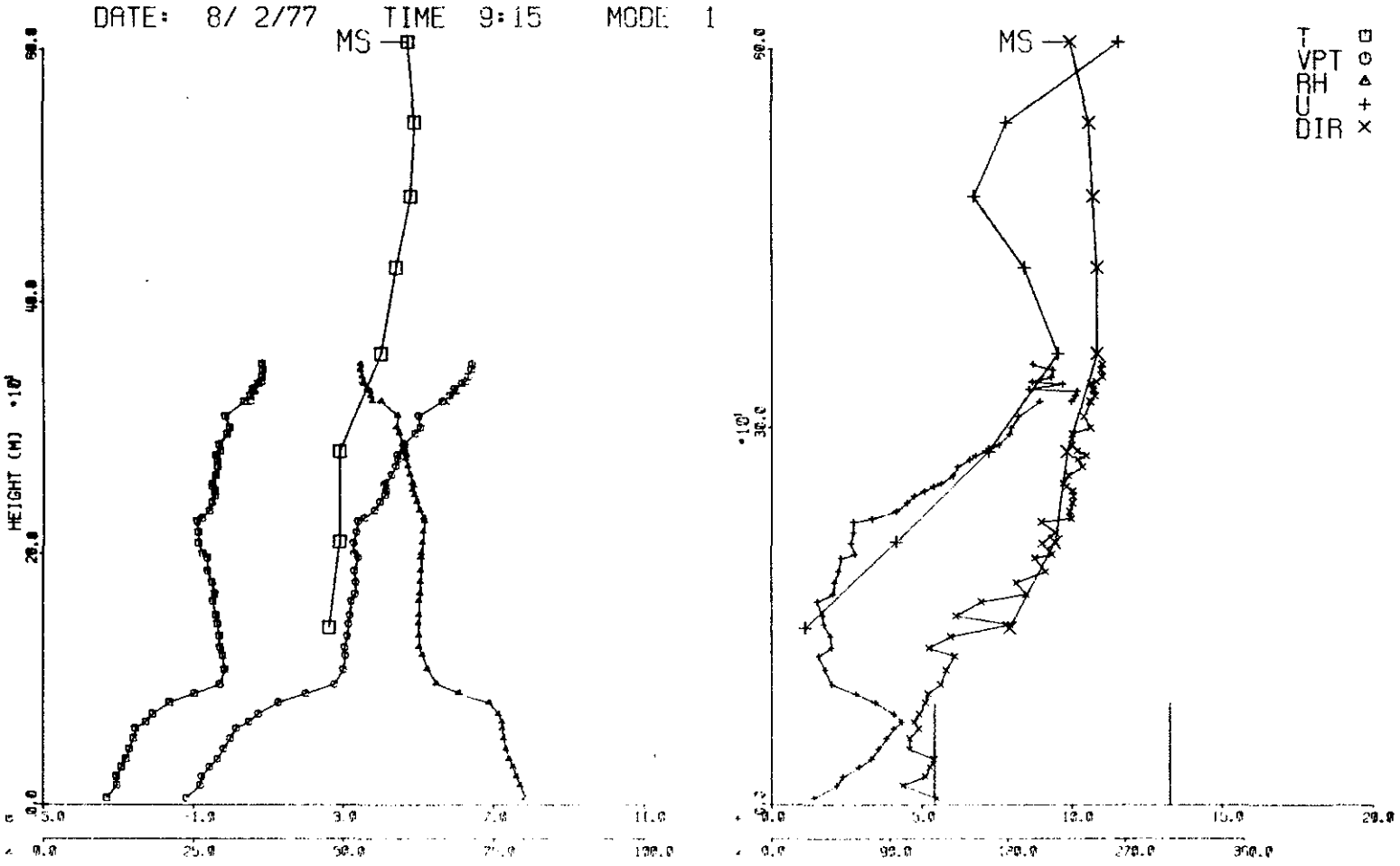

Figure 24. Tethersonde and minisonde profiles for 8 February 1977, 09:15.

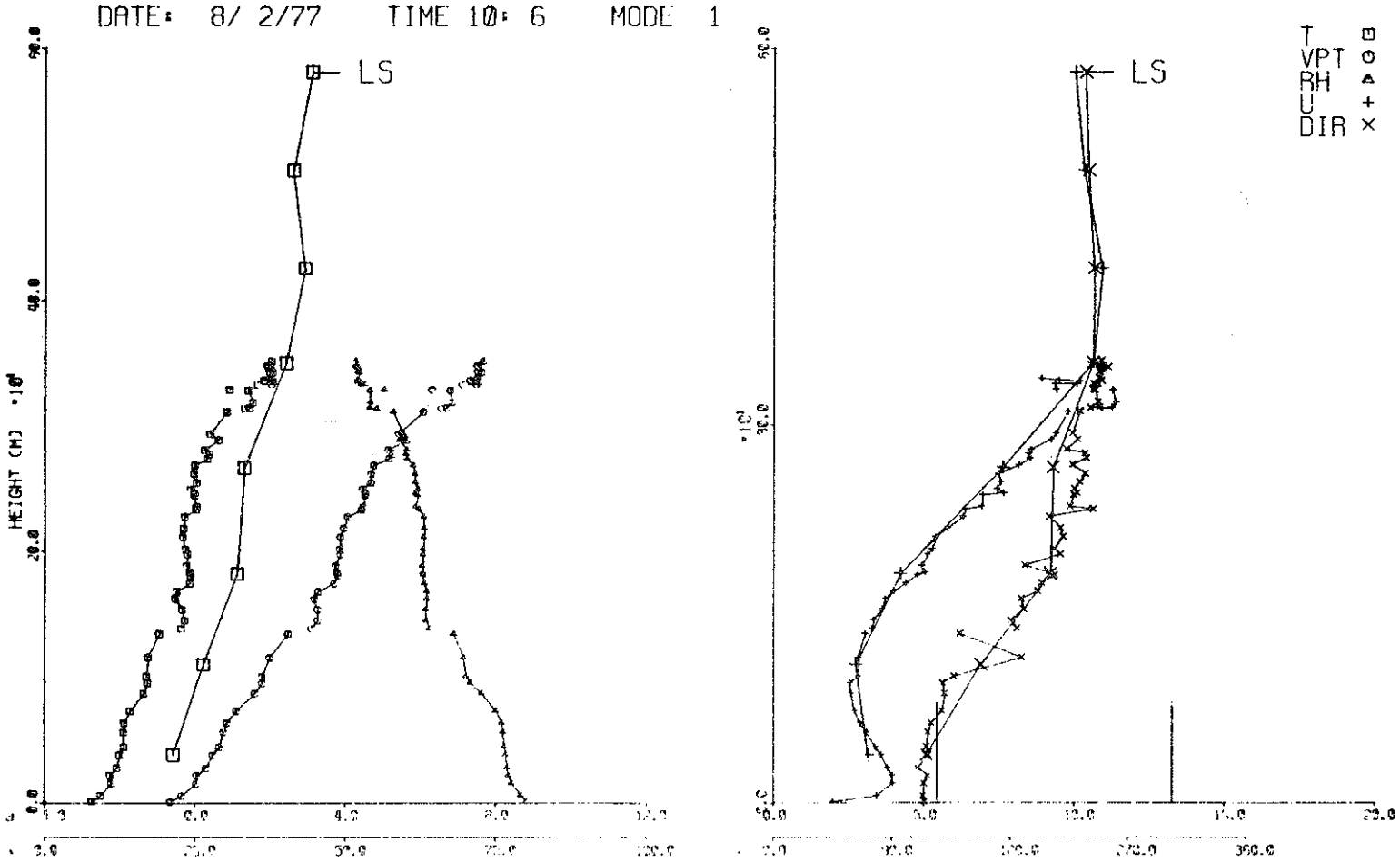

Figure 25. Minisonde and tethersonde inter-comparison for 8 February 1977, 10:06.

is good, comparison of M/S and T/S data (Figures 23, 25, and 26) again shows the wind shift, this time associated with the layer below the upper inversion. (Note: 08/02/77, 0828 has a 360° offset in wind direction at surface due to plot program.)

At 1315, the T/S was moved to the Mine Site; profiling commenced at 1510. Comparison of the 1303 and 1510 profiles shows good agreement between the two sets of data when the M/S data have been adjusted for the 100 m difference in height between the two locations.

On 9 February, a surface inversion again existed; however, the upper winds were from the southeast and flow was down the valley. Coupled to the top of this inversion was a local wind maximum that tended to oscillate with the inversion top.

A comparison of M/S and T/S wind-speed profiles (Figure 27) indicates that the integration height for the M/S (i.e., time between readings) is such that the maximum measured with the M/S is approximately 60% of that measured with the T/S. The M/S profile from the Lower Syncrude (Figure 28) indicates that the direction of the winds in the valley is down-valley.

During lapse conditions on 10 and 11 February, the wind direction at the Mine Site was cross-valley from surface up. Comparison of profiles with the Lower Syncrude M/S (Figures 29 and 30) indicates that at 1000 on 10 February, an inversion was observed above the valley, with an associated wind shift in the valley direction. By 1349, the T/S data indicate near lapse conditions with continuous cross-valley flow above the site, while the M/S, with a weak inversion aloft, indicates that the winds are still tending towards valley-directed flow within the valley.

3.2.4 Acoustic Sounder Measurements

A study of the temperature structure of the lower atmospheric boundary layer at the AOSERP study area was made using two acoustic sounders. Both sounders were vertically pointing types with the characteristics described in Table 4 and were operated

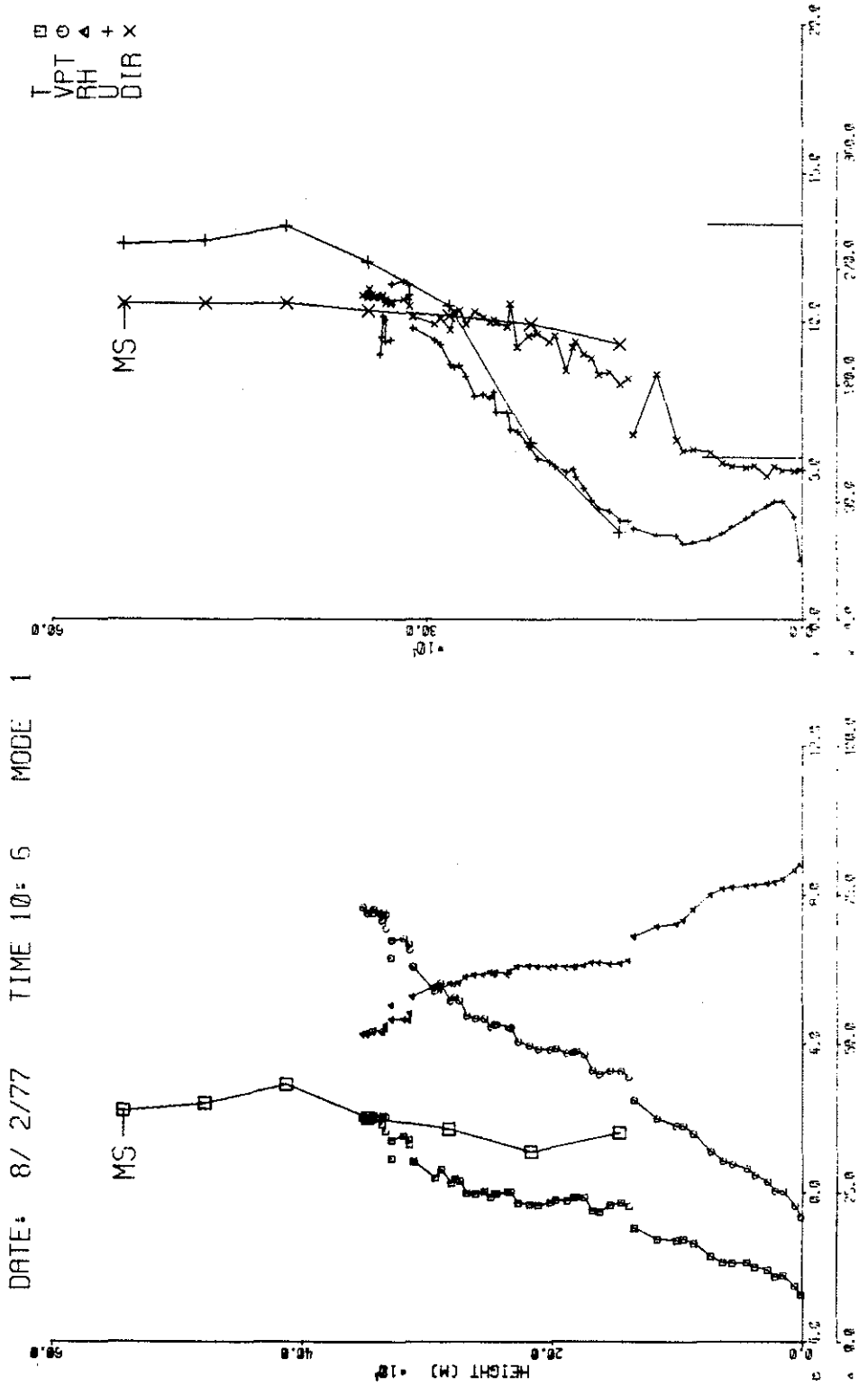

Figure 26. Tethersonde and minisonde profiles for 8 February 1977, 10:06.

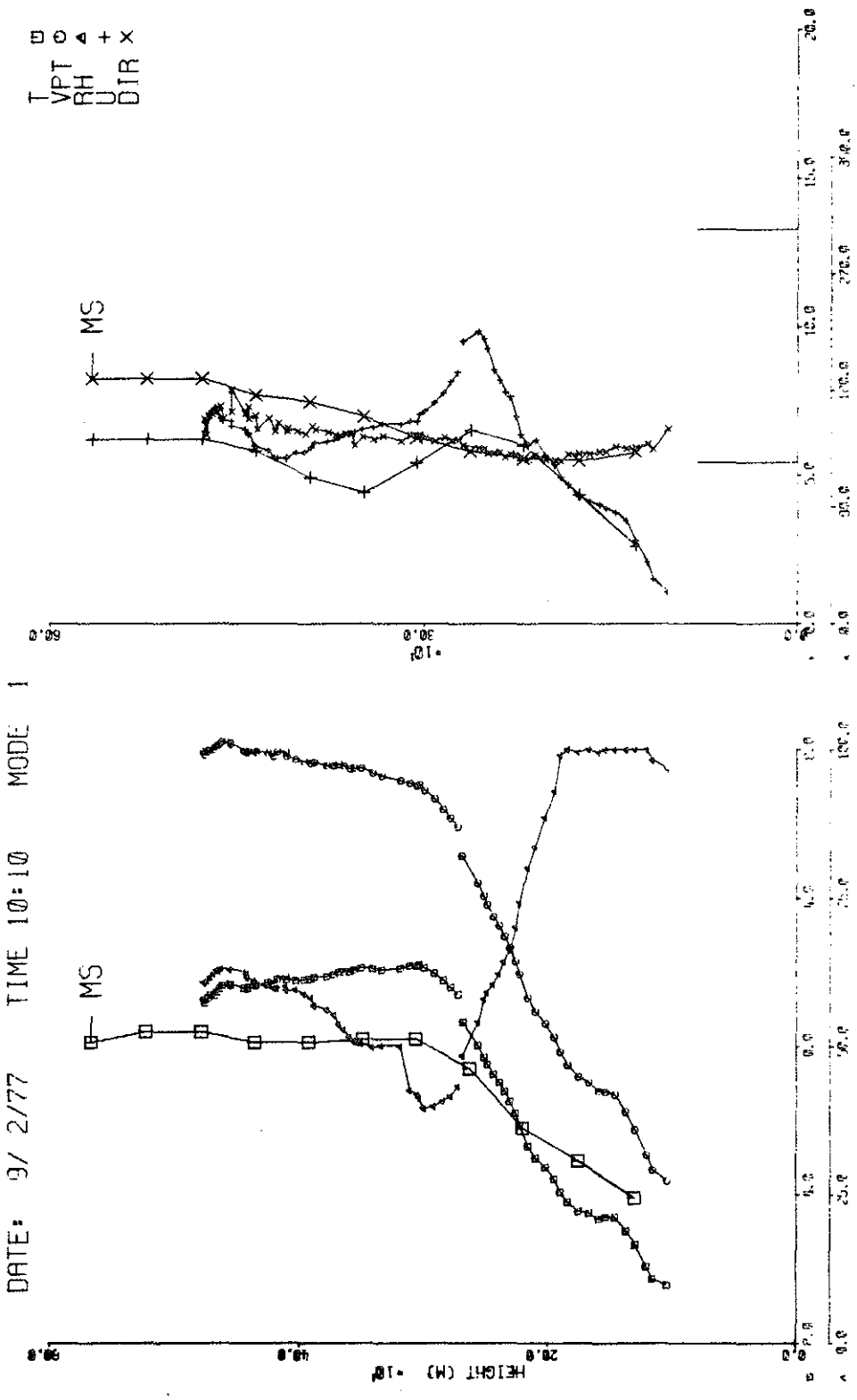

Figure 27. Minisonde and tethersonde inter-comparison for 9 February 1977, 10:10.

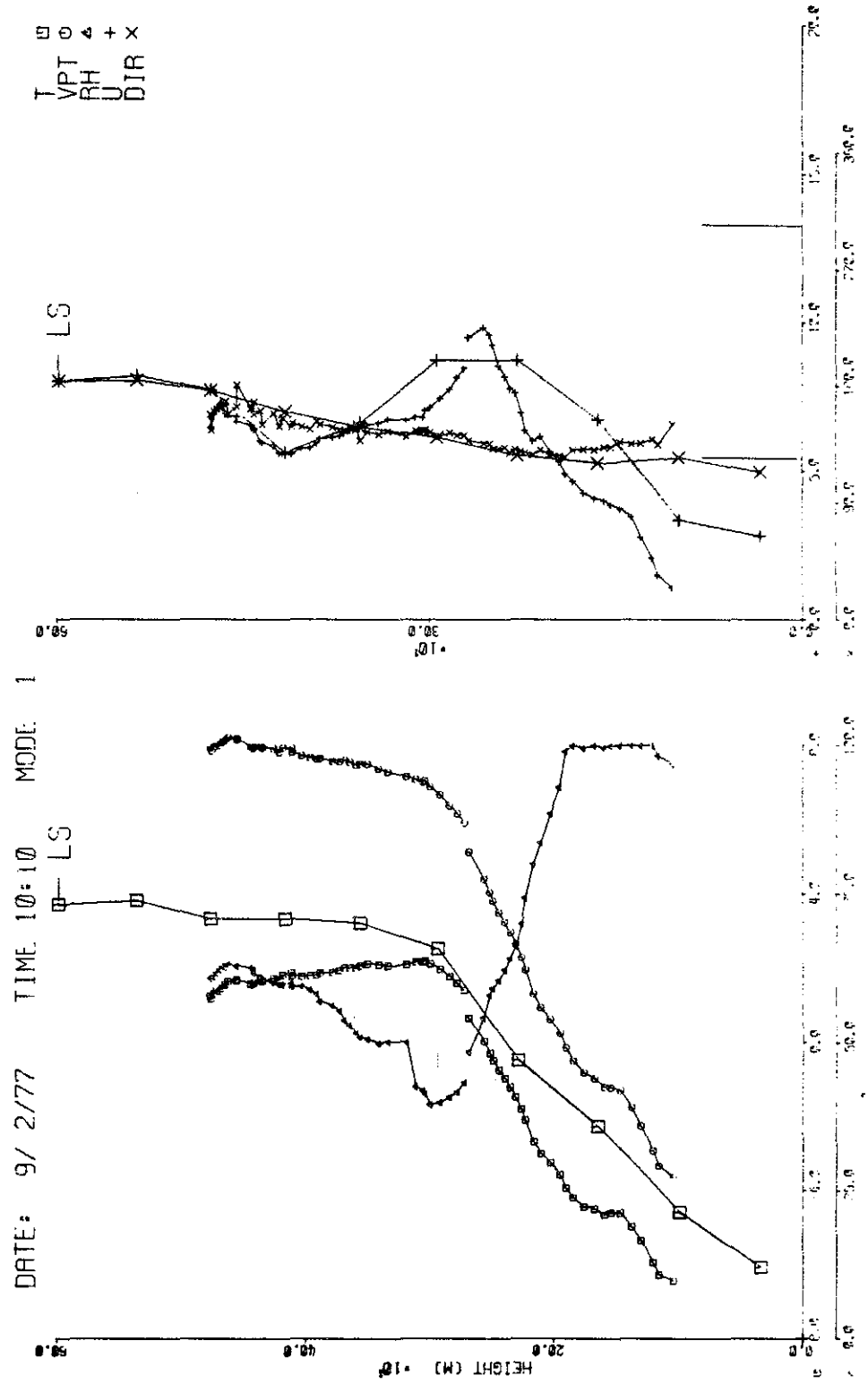

Figure 28. Tethersonde and minisonde profiles for 9 February 1977, 10:10.

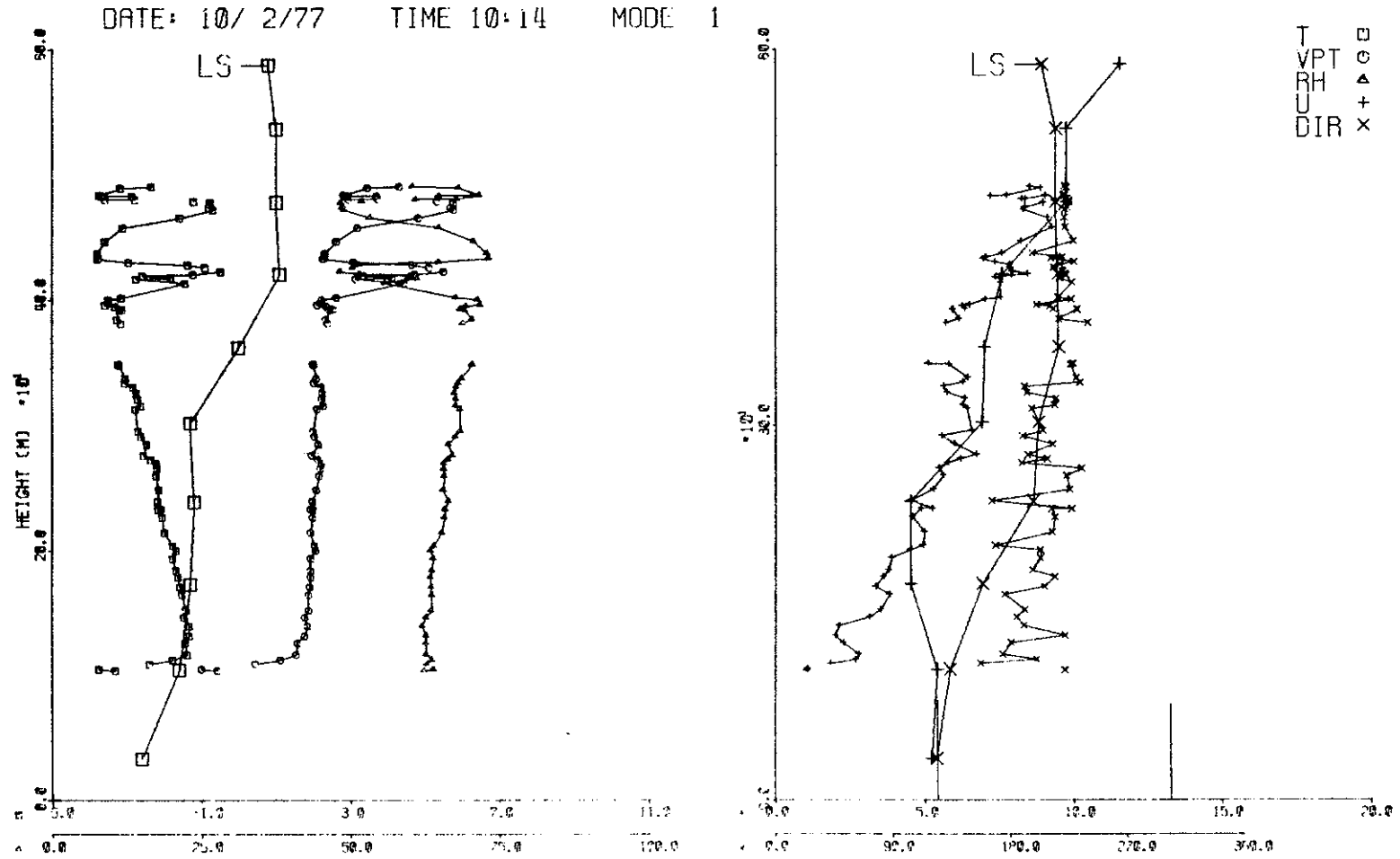

Figure 29. Tethersonde and minisonde profiles for 10 February 1977, 10:14.

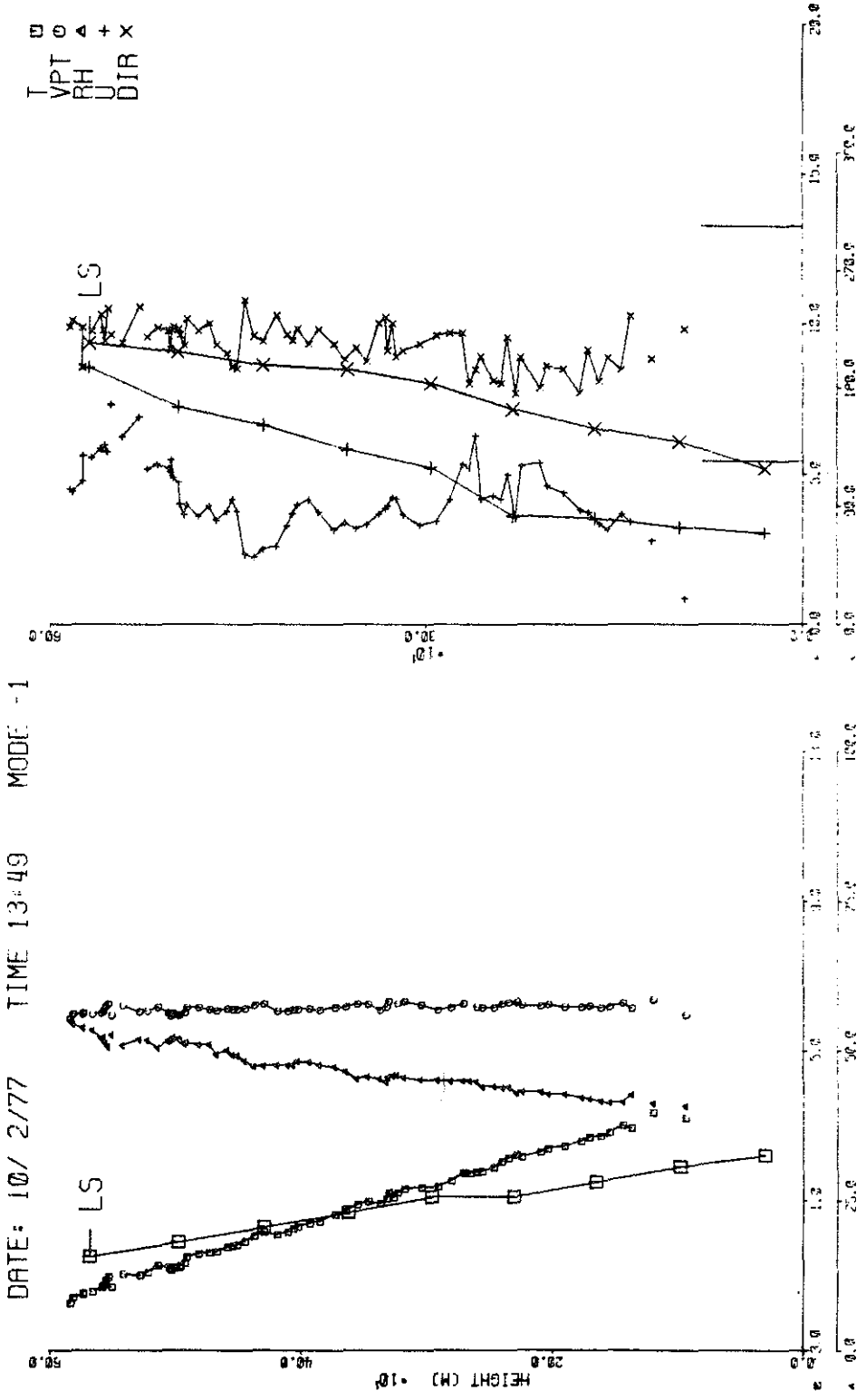

Figure 30. Tethersonde and minisonde profiles for 10 February 1977, 13:49.

Table 4. Characteristics of the aerovironment acoustic sounder Model No. 300 used in the AOSERP study area.

Parameter	Magnitude
Pulse Frequency	1600 Hz
Pulse Duration	100 $m \cdot s^{-1}$
Pulse Repetition Rate	1/7 s
Range	1000 m
Power Input	140 W

simultaneously. One sounder was located at Mildred Lake Airstrip and the second was placed at the Lower Syncrude Site (Figure 3).

A detailed description of the basics of acoustic sounding and its application was given in Kerman and Turner (1978) and will not be repeated here. Briefly, within the 1000 m range, the sounder will monitor fluctuations in temperature equal to one-half the sounder wave length (15 cm). Fluctuations in temperature below 50 m cannot be sensed by the sounder. Reflections of sound waves within the horn and from the surrounding terrain sensed by the side lobes of the acoustic antenna mask the signal return in that range. The output from the sounder is recorded in tracer form that displays these fluctuations as a function of time and height. A selected sample of the data will be shown later (Figure 31). In order to reduce the background and wind-generated noise, both sounder antennas were shielded by bales of hay that acted as an acoustically absorbing barrier. There was no noise problem at the Lower Syncrude Site. However, the second location was somewhat noisy during certain hours of the day when aircraft used the runway. Other sources of noise were motor vehicles occasionally passing close to the sounder. The noise was temporary and did not hinder the interpretation of the records.

The majority of the data from both locations shows turbulent, thin layers often associated with the presence of inversion layers. Figure 31 shows a facsimile recording for the sounder echo obtained at Mildred Lake on 12 February 1977 between 0530 and 1130 and between 1330 and 1730 on the same day. During the early morning hours, inversion layers were developed to the 600 m level. Between 0800 and 1000 these inversion layers dropped from the 600 m level to the 200 m level. Later in the day (1300-1730) the height of the sounder echo increased during the period of the run. Both sounder echoes were characterized by a wavy structure, indicating a vertical oscillation in the height of the echoes.

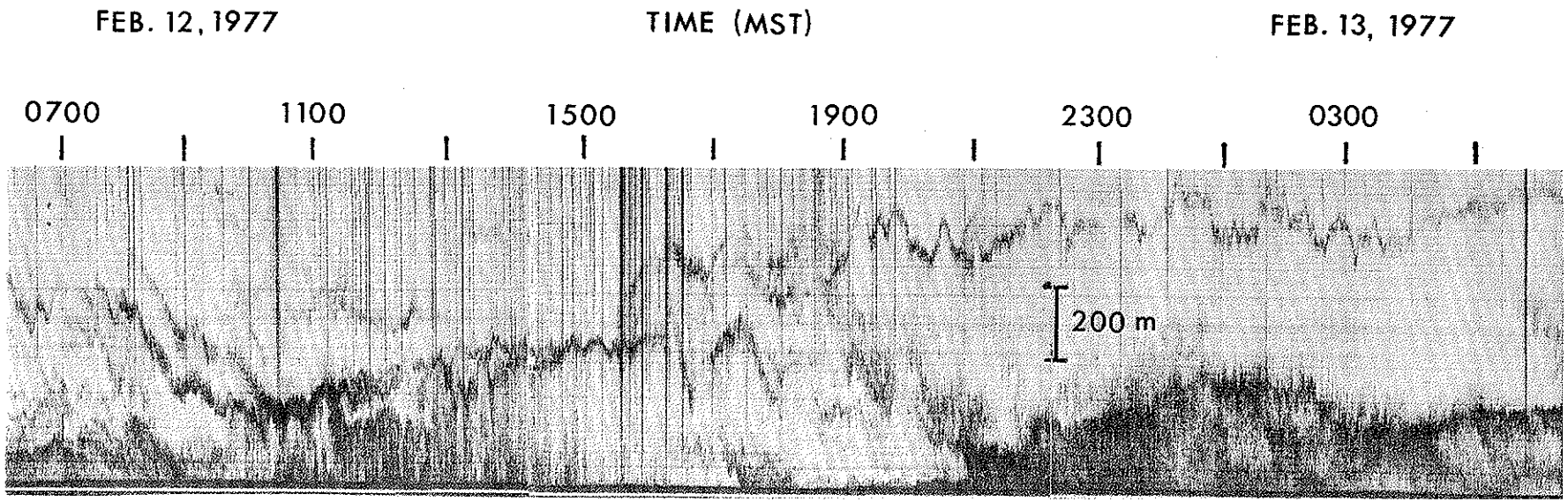

Figure 31. Variation of height of elevated inversion layers at Mildred Lake, 12-13 February 1977.

The same general features were observed at the Lower Syncrude Site. On that day the inversion layers persisted all night and into the early hours of the morning (Figure 32). During the early hours of the morning (0530, 12 February), heating of the underlying surface increased the convective activities, which dissipated the inversion layer at the 900 m level and formed a second one at a lower level. The sounder echo is characterized by a wavy structure. The increased thermal activities that are described by the dark band in Figure 32 may be attributed to the mixing by the surface wind at midnight. The mixing occurred to an elevation of about 400 m. Some wave characteristics are superimposed on the mixing layer, denoting wind shears aloft.

The height and the formation of inversion layers are controlled by the amount of heating from the underlying surface and the wind shear. Consequently, inversion layers are characterized by thermal and mechanical turbulent structures that are detected by the acoustic sounder. It is expected, then, that the top of the inversion layer will coincide with that of the dark band on the sounder record (see, e.g., Hicks et al. 1977).

To determine whether the return of the sounder signal is related to the actual temperature inversion, we compared the sounder records from the Syncrude Site with the sonde temperature profiles from M/S and T/S observations. A sample of this analysis is shown in Figures 33 and 34. In this analysis the inversion layer top as recorded by the sounder was determined and plotted against the inversion height as given by the sonde's profile (Figure 35). No attempt was made to calculate the error arising in the acoustic sounder data. Fifteen cases of observation, taken over a period of 6 days, were compared. Although the number of observations is too small to make concrete conclusions, the trend indicates a good agreement, as indicated by the solid line. The results show, however, that the height measured by the sonde profile is larger than that obtained from the acoustic record by 15%. Similar conclusions were reached by Wyckoff et al. (1973).

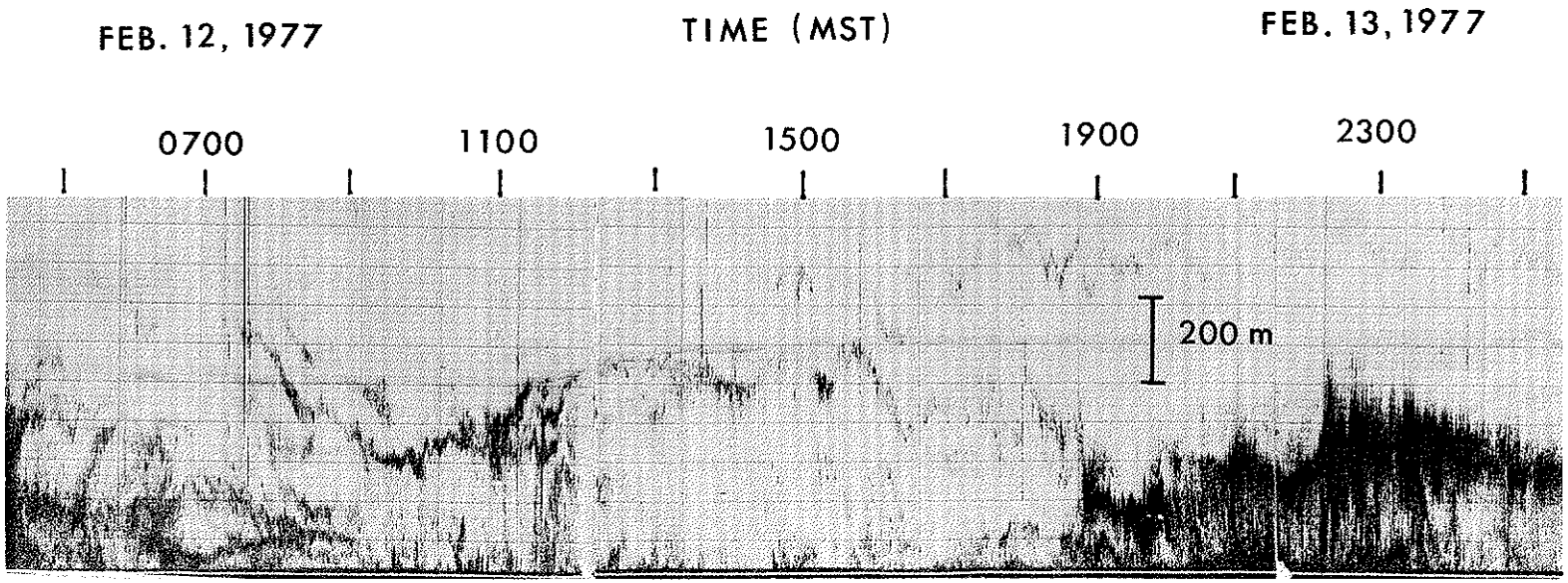

Figure 32. Variation of height of elevated inversion layers at Lower Syncrude Site, 12-13 February 1977.

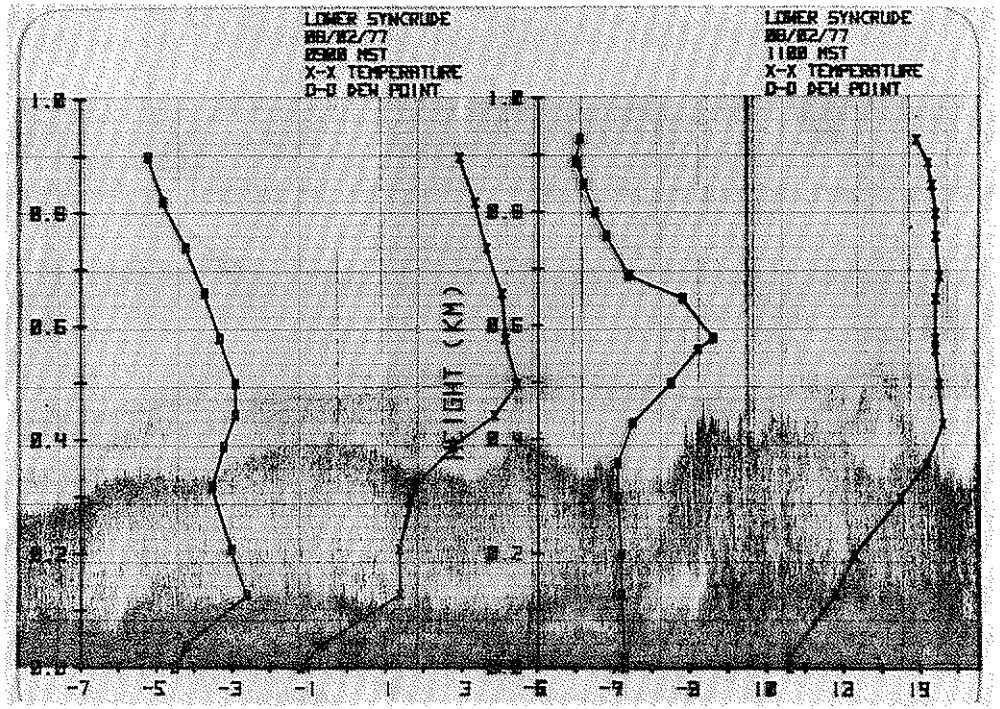

TEMPERATURE (^{o}C)

Figure 33. Comparison between the top of inversion layer and temperature profile at Lower Syncrude for 8 February 1977 at 0900 MST.

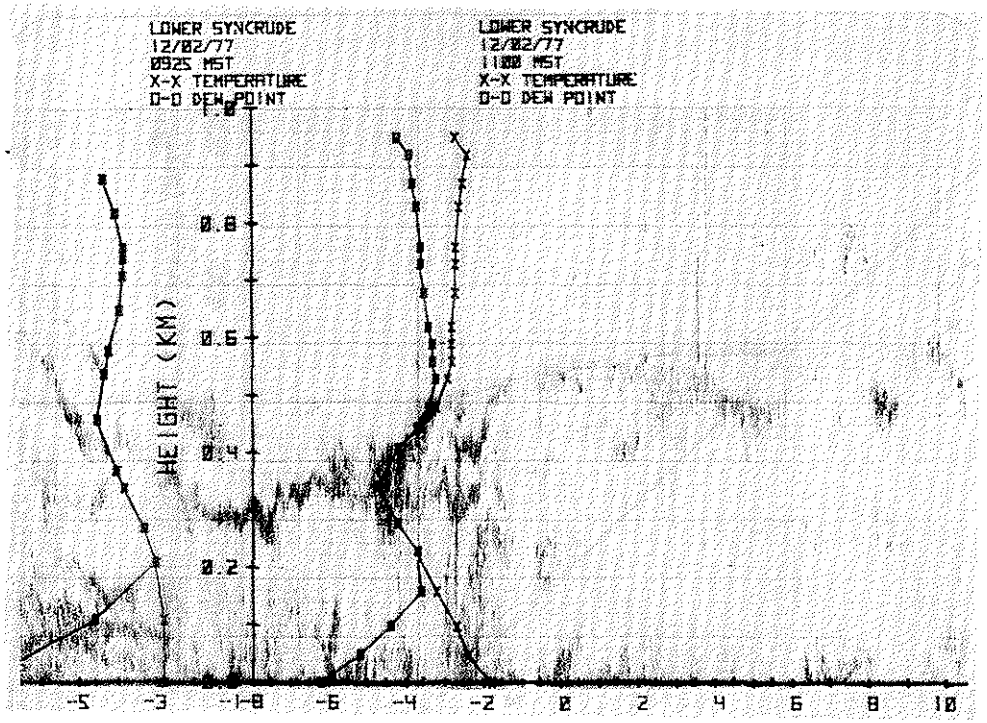

Figure 34. Comparison between the top of an elevated inversion layer and temperature profile at Lower Syncrude for 12 February 1977 at 1100 MST.

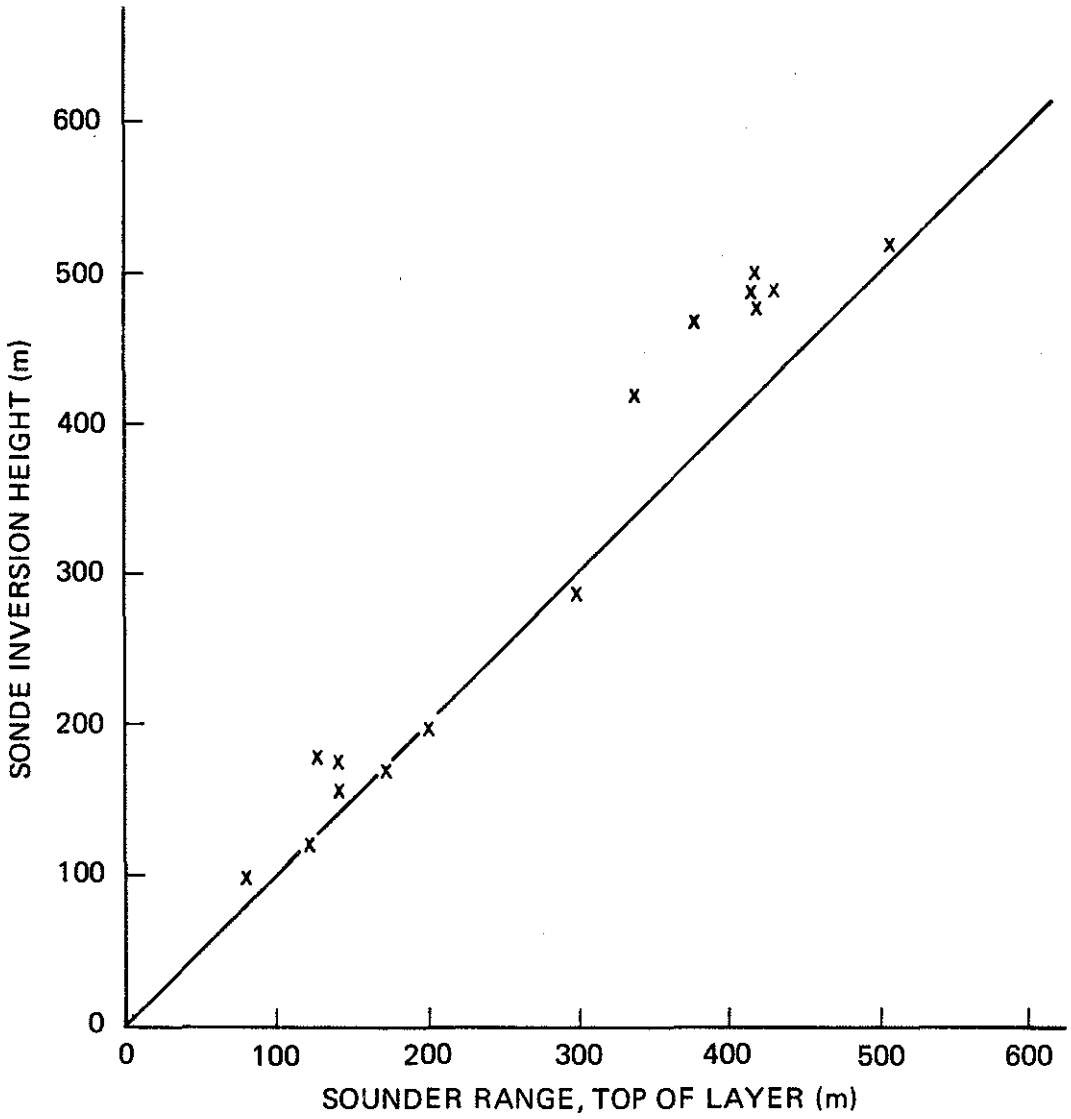

Figure 35. Comparison of predicted inversion height using sonde profiles versus observed using acoustic sounder.

The reasonable agreement discussed above suggests that the sounder may be used successfully to measure inversion heights in the AOSERP study area.

The sounder data obtained from the two locations, although agreeing in general, had a few differences, especially at the lower 300 m. Since the two sounders are at different elevations, both sounders recorded different heights for the same turbulent atmospheric structure (Figure 36). The data from the Lower Syncrude sounders showed a large number of inversion layers in the lowest 200 m (Figure 37). The intensity of the sounder echo at the Syncrude Site appears to be more dense than the one at Mildred Lake (Figure 38). This indicates either that mixing caused by wind is more pronounced at the latter site or that there is a slight difference in equipment intensity. The former reason is believed to be the case in this study, for care was taken to keep the intensity of the two sounders the same at all times.

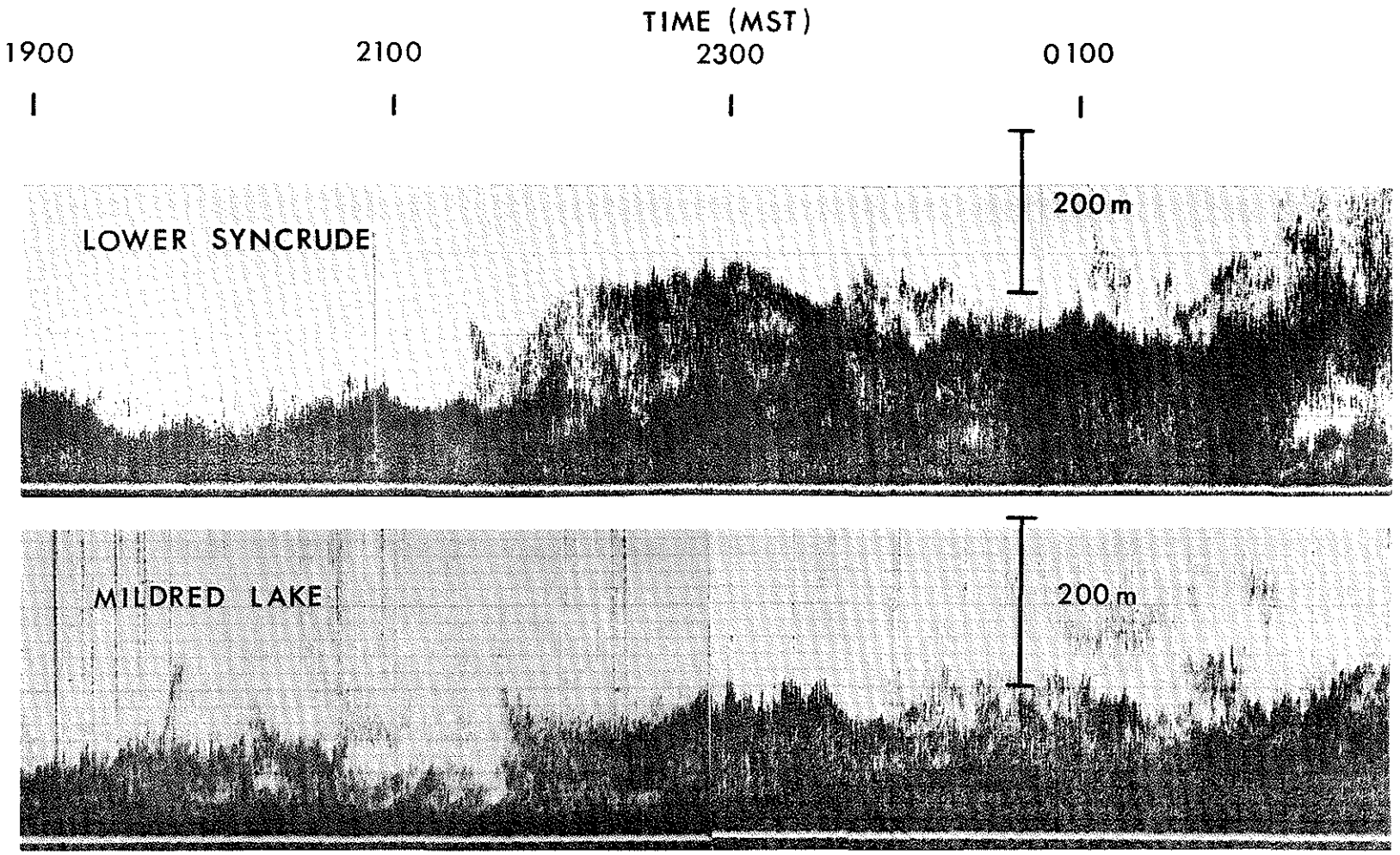

Figure 36. Comparison betwee two sounders' echoes at two different locations, 11 February 1977.

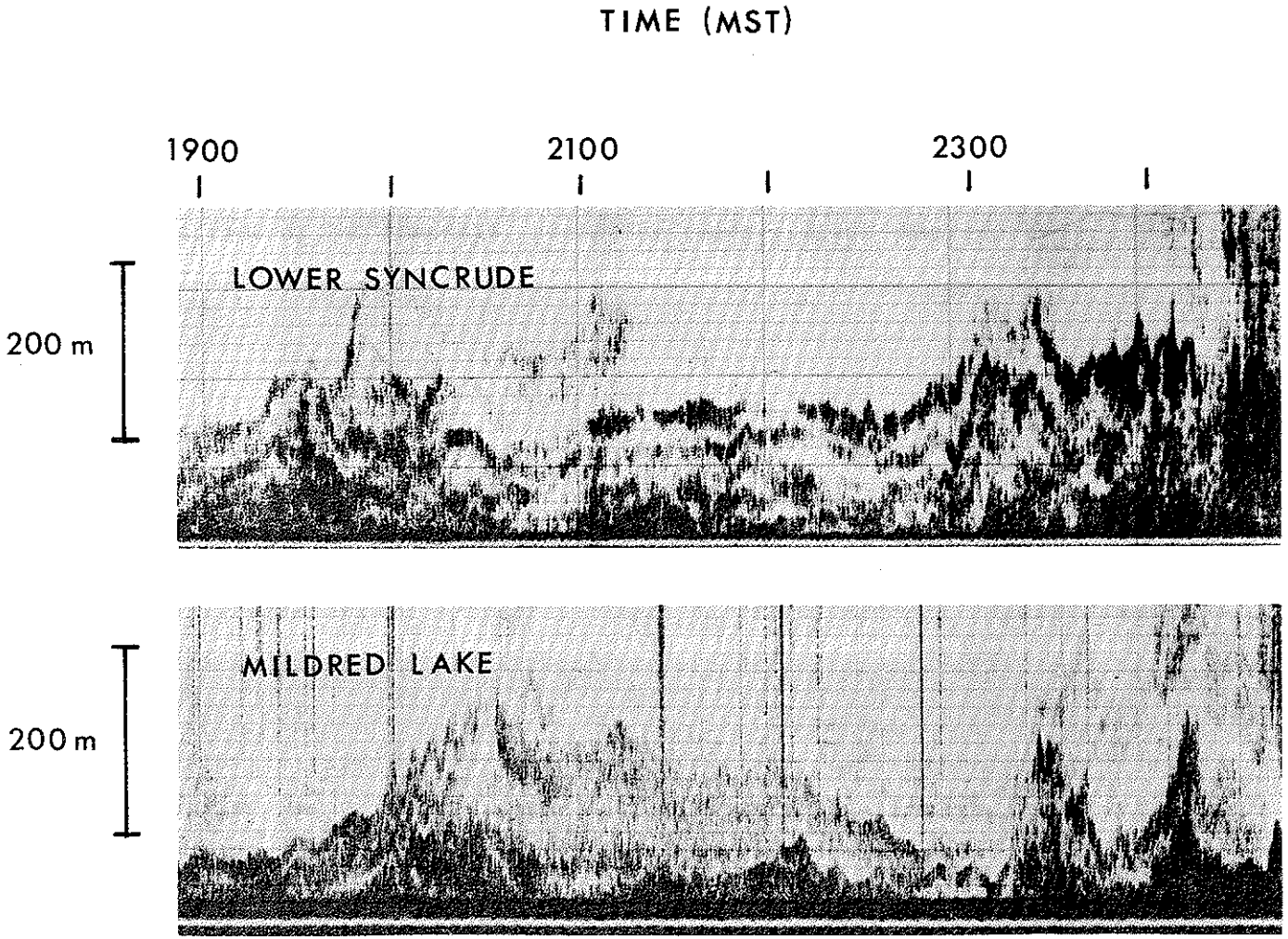

Figure 37. Comparison of two sounders' echoes at different locations, 10 February 1977.

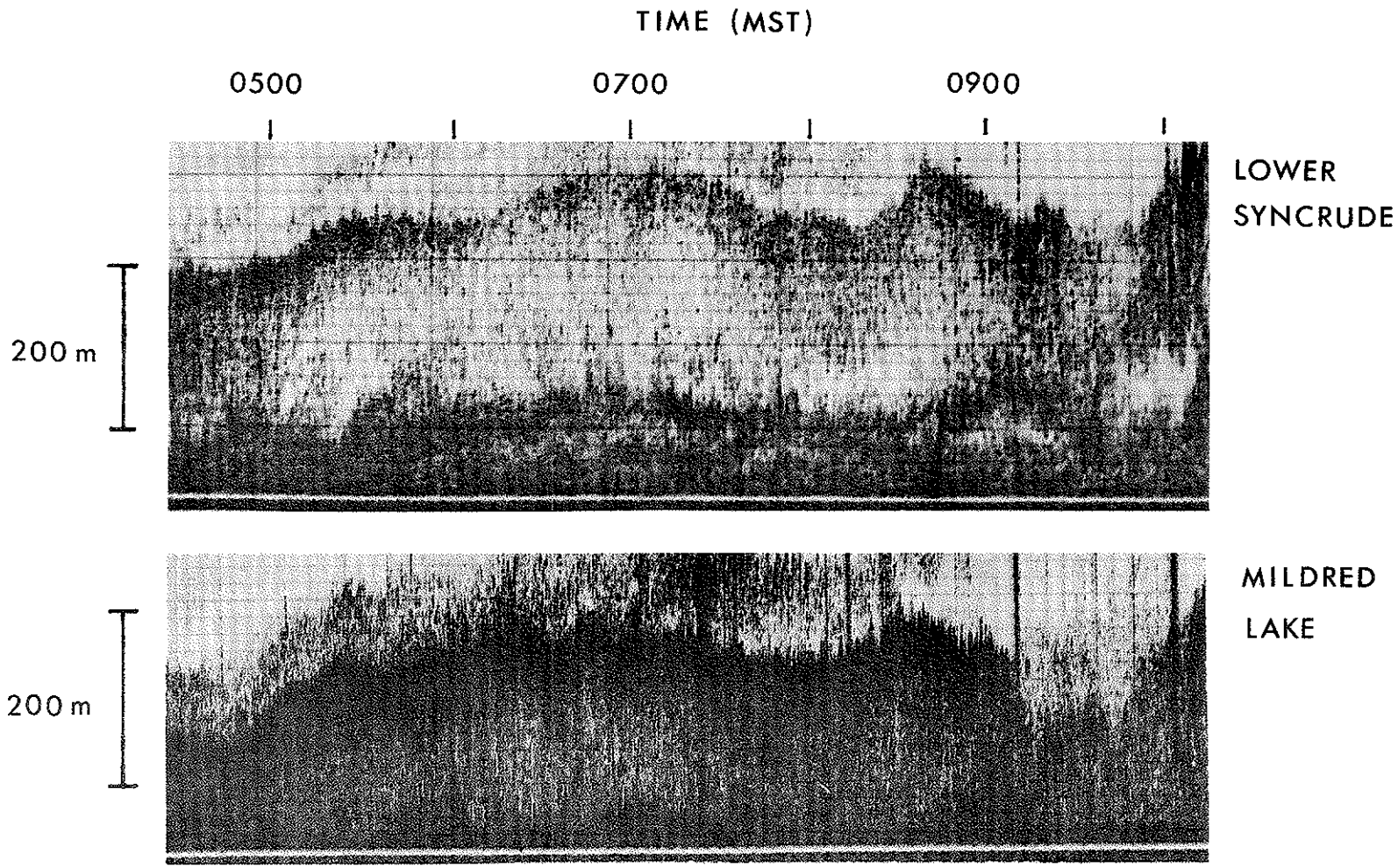

Figure 38. Comparison of two sounders' echoes at two different locations.

4. PLUME RISE STUDY

4.1 PLUME RISE MEASUREMENTS

The rise of the smoke plume from the power plant stack at GCOS was measured during the period 3-12 February 1977. The experimental technique employed in the study was the same as the one described in detail in the March AOSERP study (Fanaki 1978). A photograph of the equipment used in this study is shown in Figure 39.

The previous program of plume rise computation was extended by the transfer of the data after analysis into a form of plume traces. Figure 40 shows the plume "time-mean" path (dotted line) as a function of height and horizontal downwind distance. The program was also modified to store the plume rise data on tape for future use.

The predictive capability of the plume rise formulas, namely, Briggs (1969, 1971, 1972), TVA 1971 and 1972 (Montgomery et al. 1971, 1972), Holland (1953), CONCAWE (Brummage 1968), and Moses and Carson (1967), described in the previous AOSERP report, was examined using the data from this study as well as those from the March study. This was done by comparing the observed plume rise with the predictive value; the results are shown in Figures 41-46. Meteorological measurements were obtained from the M/S observations made at the Lower Syncrude Site.

These figures confirm the conclusions described earlier (Fanaki 1978). The new data points did not reduce the scatter of the data in the figures. It appears that none of the models is a good predictor for the observed rise of the plume, at least for the winter season. Again Briggs's, TVA 1972, and Moses and Carson's formulas underpredict the rise of the plume, while the Holland and CONCAWE formulas overpredict. The Briggs and Holland formulas appear to predict the rise of the plume better than the others.

Figure 39. Camera set up and associated equipments used in field study.

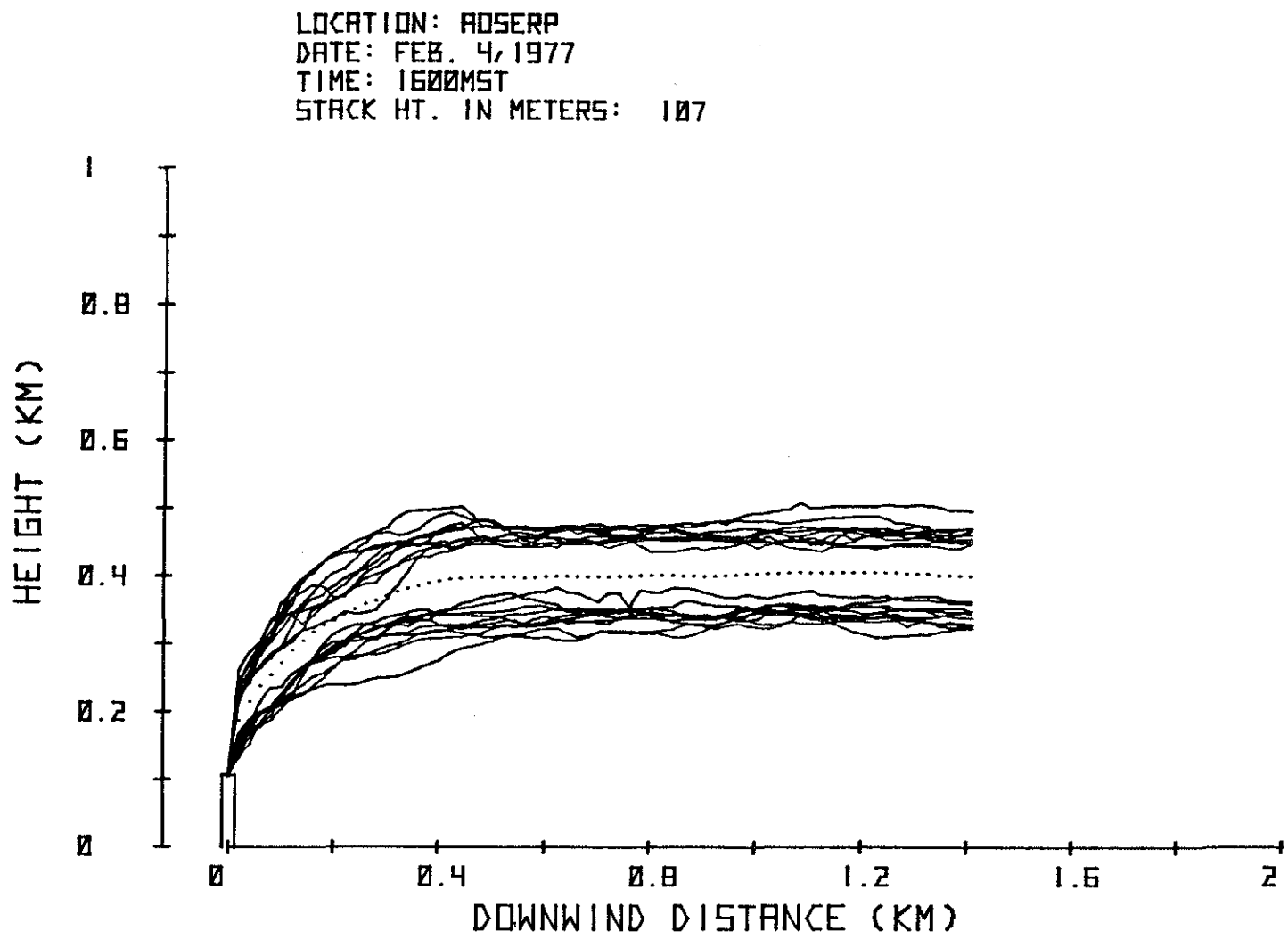

Figure 40. Computer trace of the power house stack plume as a function of height and downwind distance.

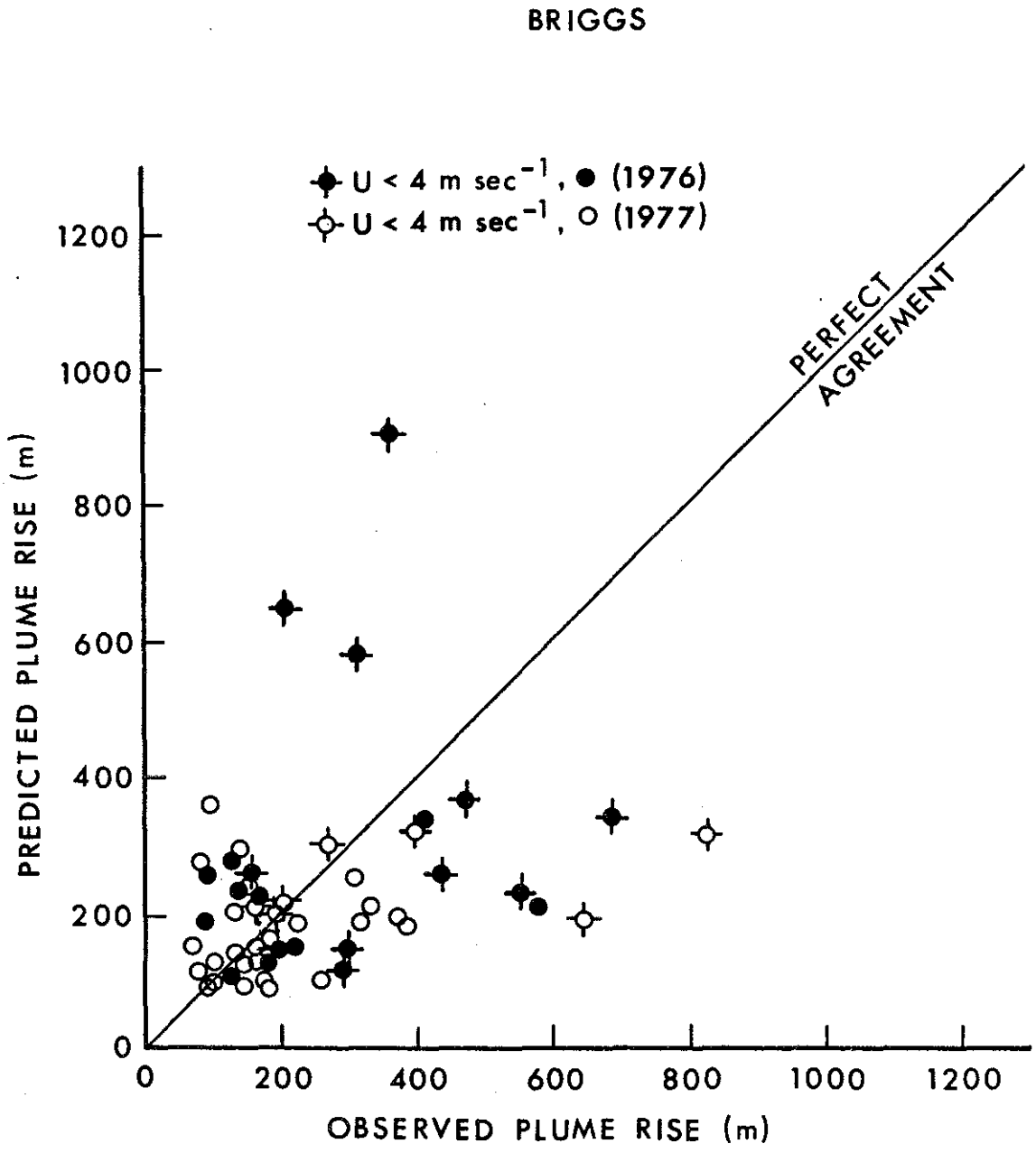

Figure 41. Comparison of predicted versus observed plume rise using Brigg's model. Solid line represents perfect agreement.

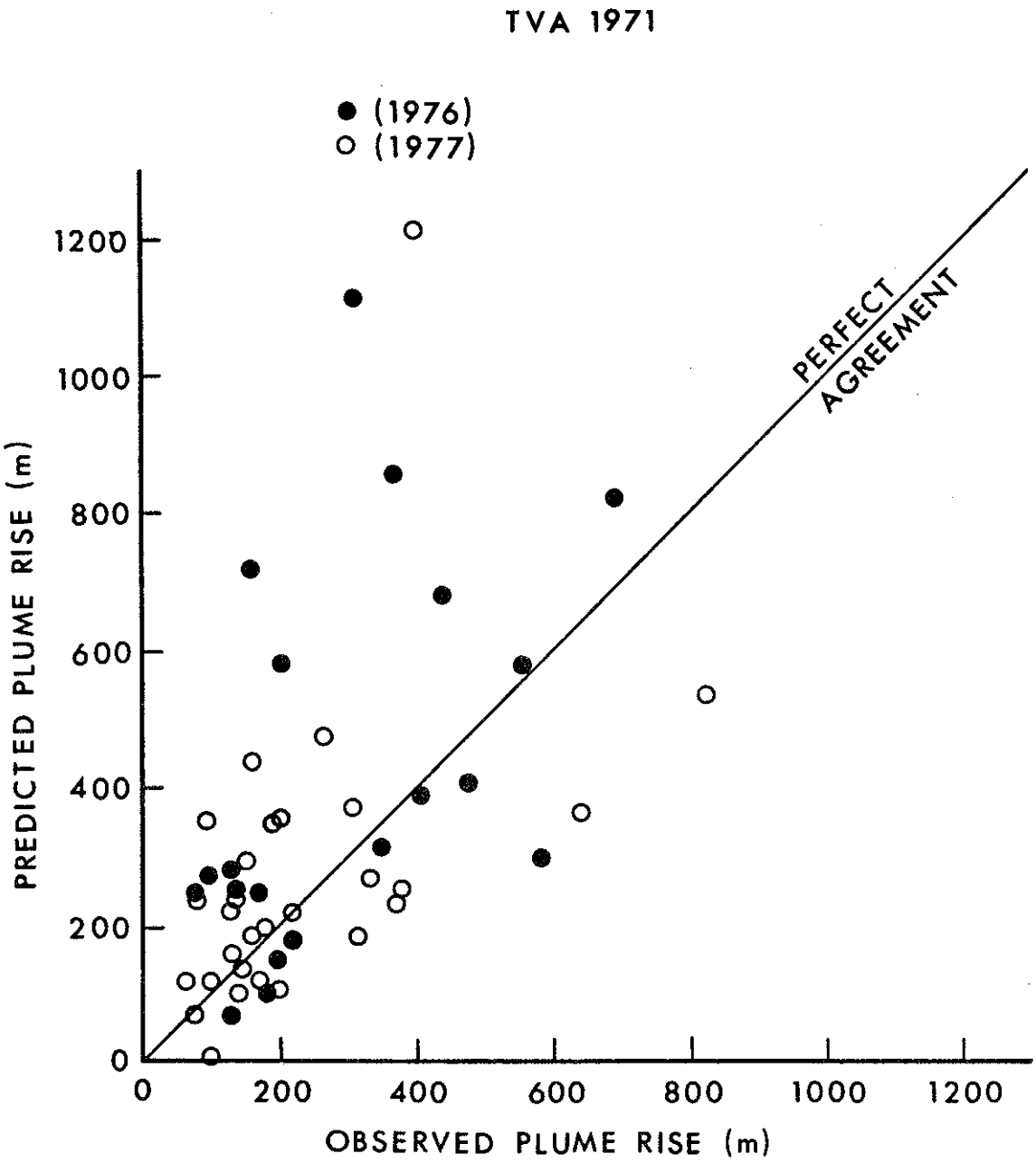

Figure 42. Comparison of predicted versus observed plume rise using TVA 1971 model. Solid line represents perfect agreement.

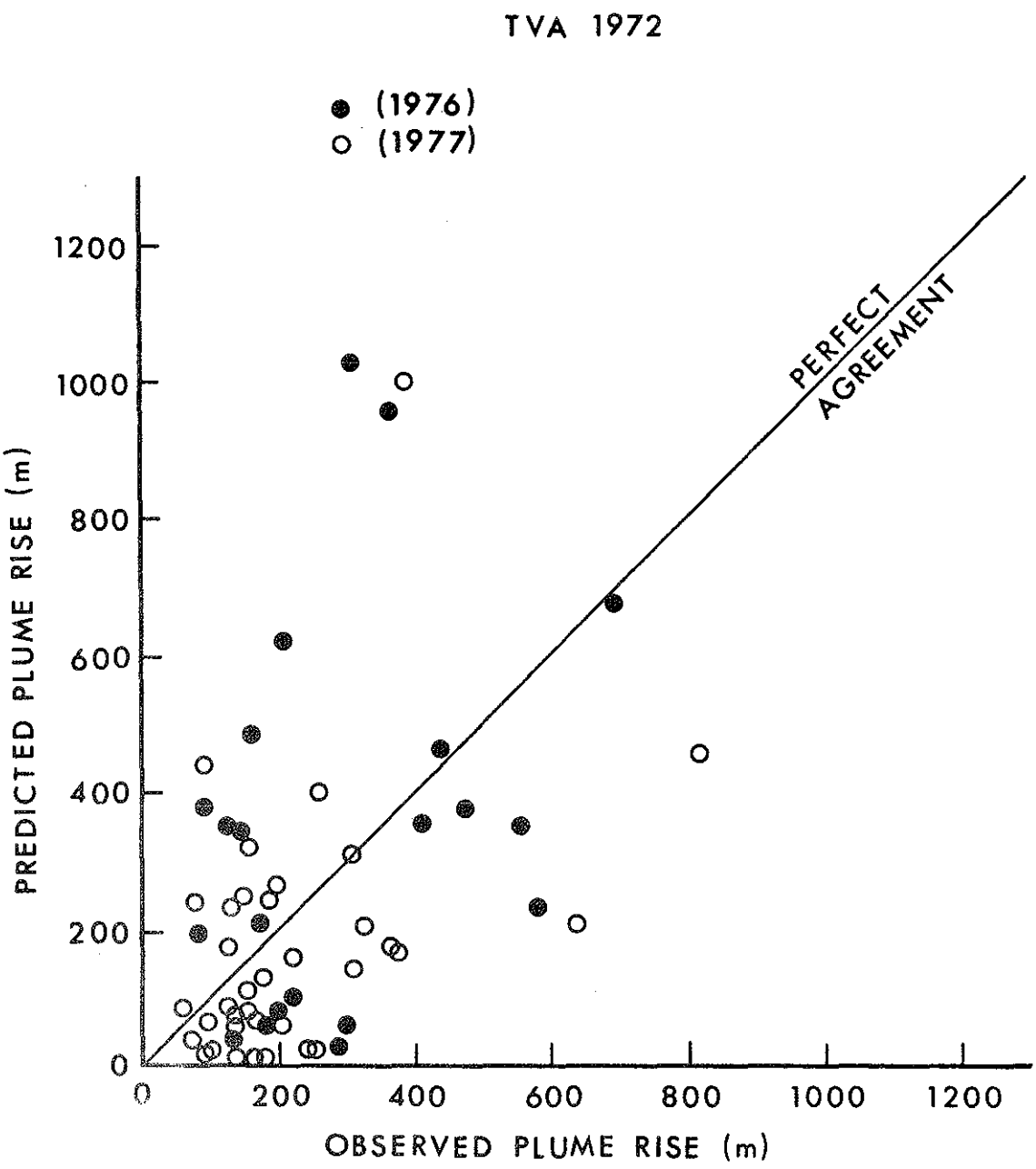

Figure 43. Comparison of predicted versus observed plume rise using TVA 1972 model. Solid line represents perfect agreement.

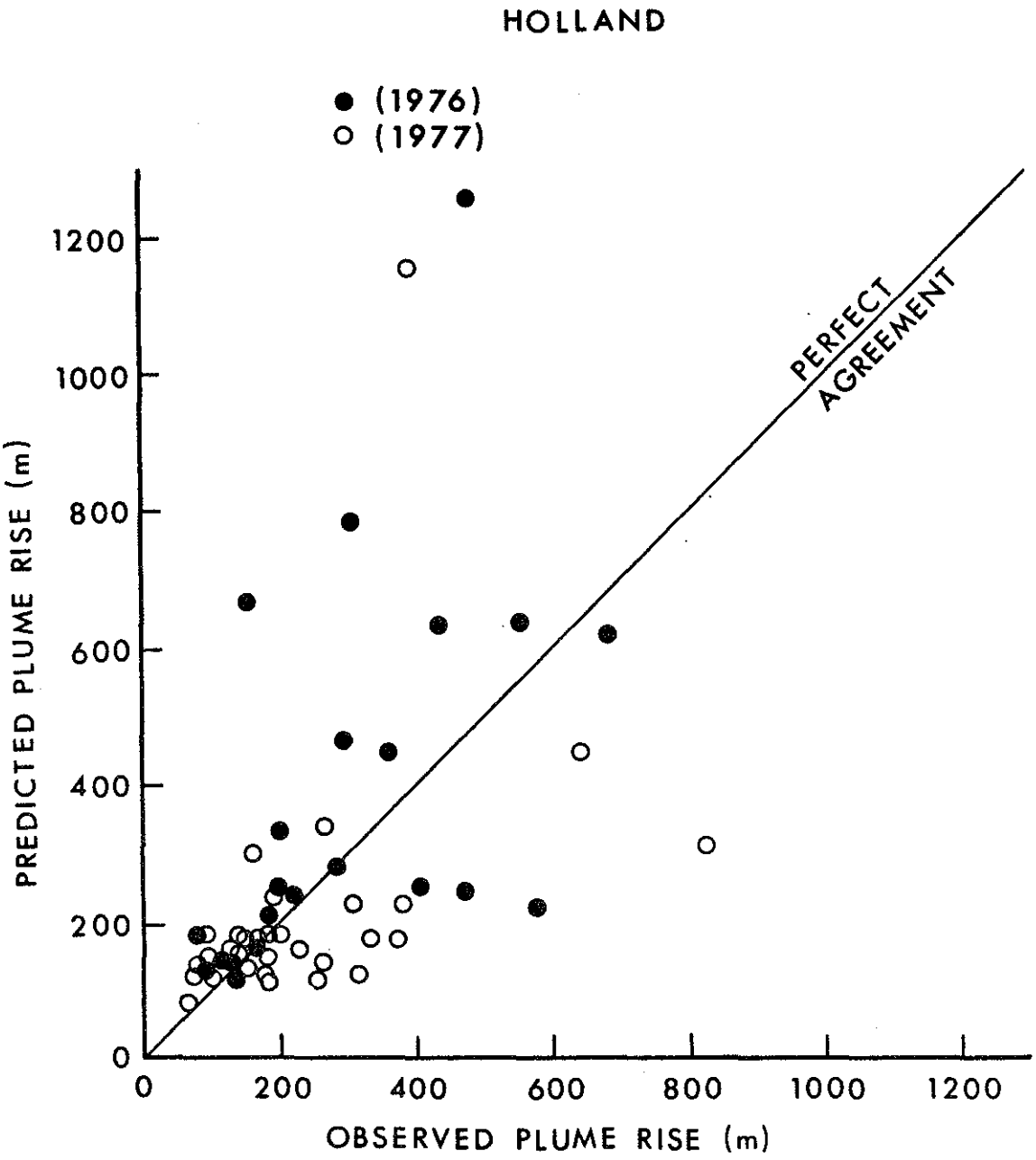

Figure 44. Comparison of predicted versus observed plume rise using Holland's model. Solid line represents perfect agreement.

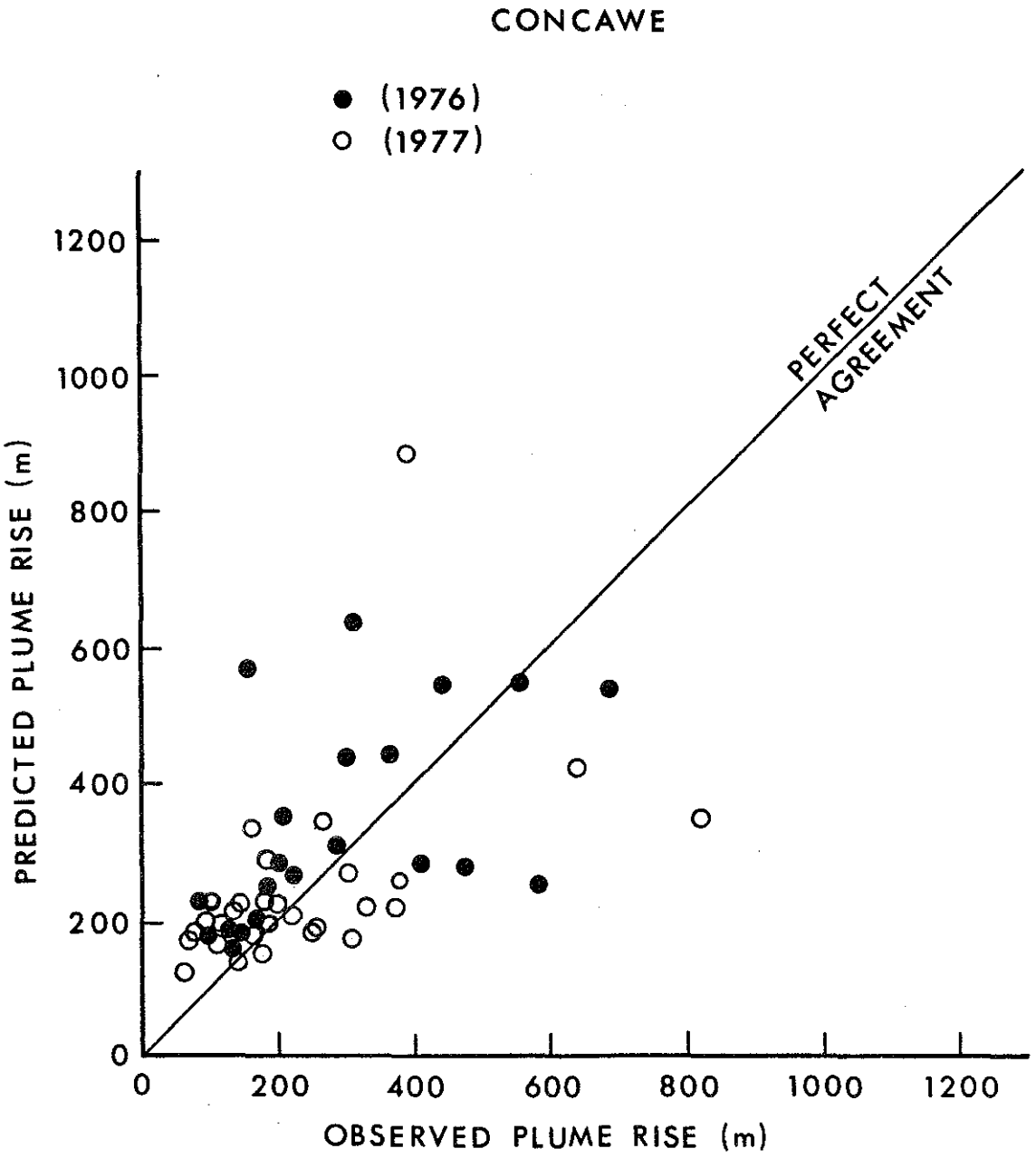

Figure 45. Comparison of predicted versus observed plume rise using Concawe's model. Solid line represents perfect agreement.

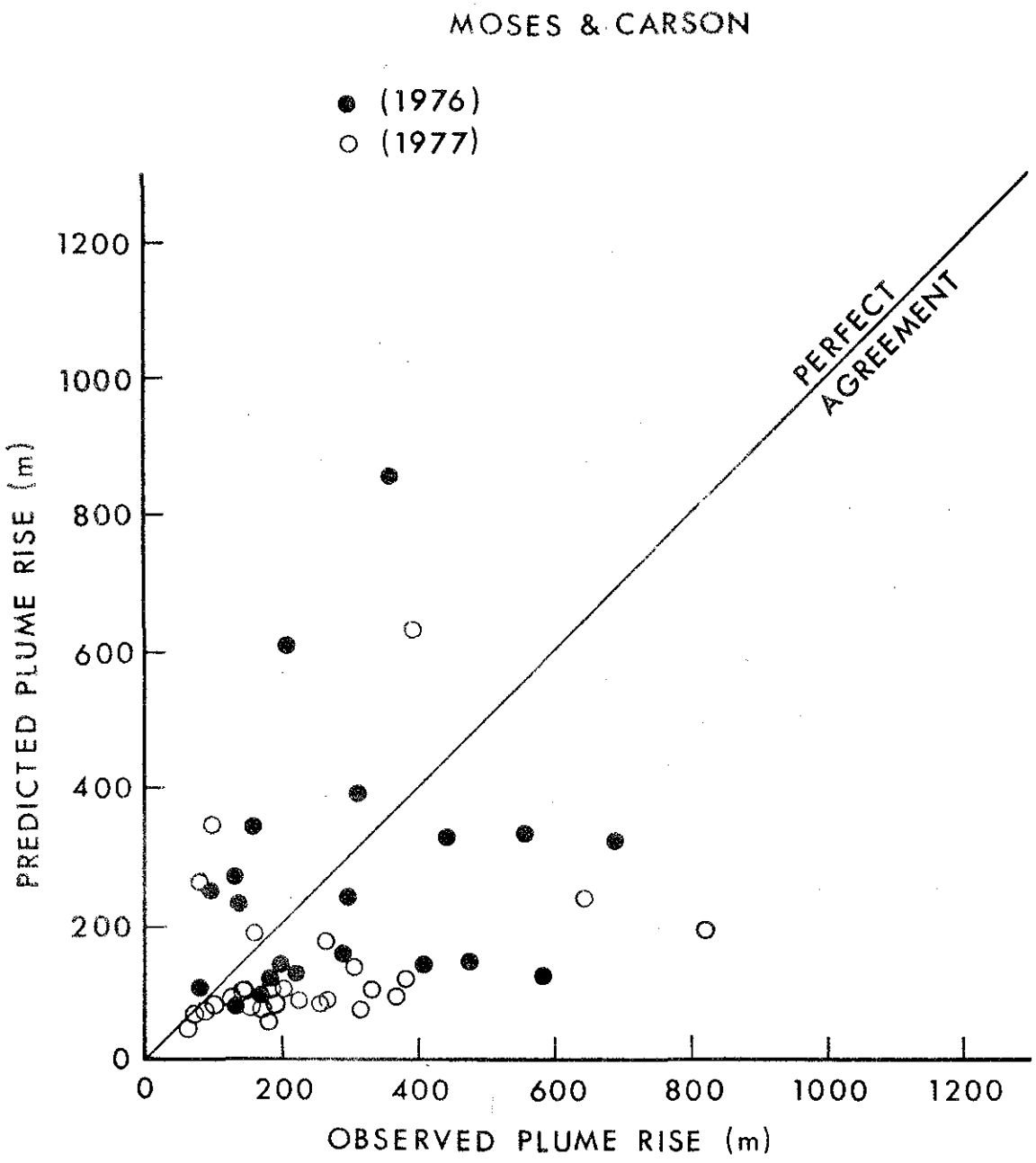

Figure 46. Comparison of predicted versus observed plume rise using Moses and Carson's model. Solid line represents perfect agreement.

Some interesting observations of the plume's behaviour were recorded in this study. Two cases were chosen in which the meteorological conditions were typical of the area during the winter season.

The first case is an example of the behaviour of the plume under inversion and calm conditions. This phenomenon occurs frequently, especially during the early morning hours. Figures 47 and 48 show profiles of wind speed, wind direction, and temperature for 4 February at two different times of the day at the Lower Syncrude Site. On that day the atmosphere was stable, with an isothermal temperature profile to a height of about 850 m MSL, the base of the inversion layer. The magnitude of the inversion layer (the difference in temperature between the top and the base of the inversion) reached a value of about 17°C over a layer of thickness 250 m. Surface wind direction veered from northerly to southeasterly flow below the inversion layer. The wind speed varied from 1 to 4 $m \cdot s^{-1}$. The inversion layer persisted until later in the day, when the inversion base dropped 100 m and its magnitude decreased to 14°C. Wind direction remained nearly westerly.

On that day the plume rose vertically to the inversion base, where it was trapped. The plume's outlines appear to be deeper than one might expect for a trapped plume (Figure 49).

In his studies on the predictions of the rise of plumes (Δh), Briggs (1975) indicated that:

$$\Delta h = 1.6\ F^{1/3}\ \frac{(X^{2/3})}{U} \qquad (4)$$

where F is the buoyancy flux. Briggs (1975) suggested also that the restricted rise of a bent-over plume due to stable stratified conditions is given by:

$$\Delta h = C\left(\frac{F}{US}\right)^{1/3} \qquad (5)$$

where S is a stability parameter and C is a constant. The value of C ranges from 1.8 to 3.1, with C = 2.5 being the recommended value.

Equation (4) was written in a nondimensional form to apply to our case:

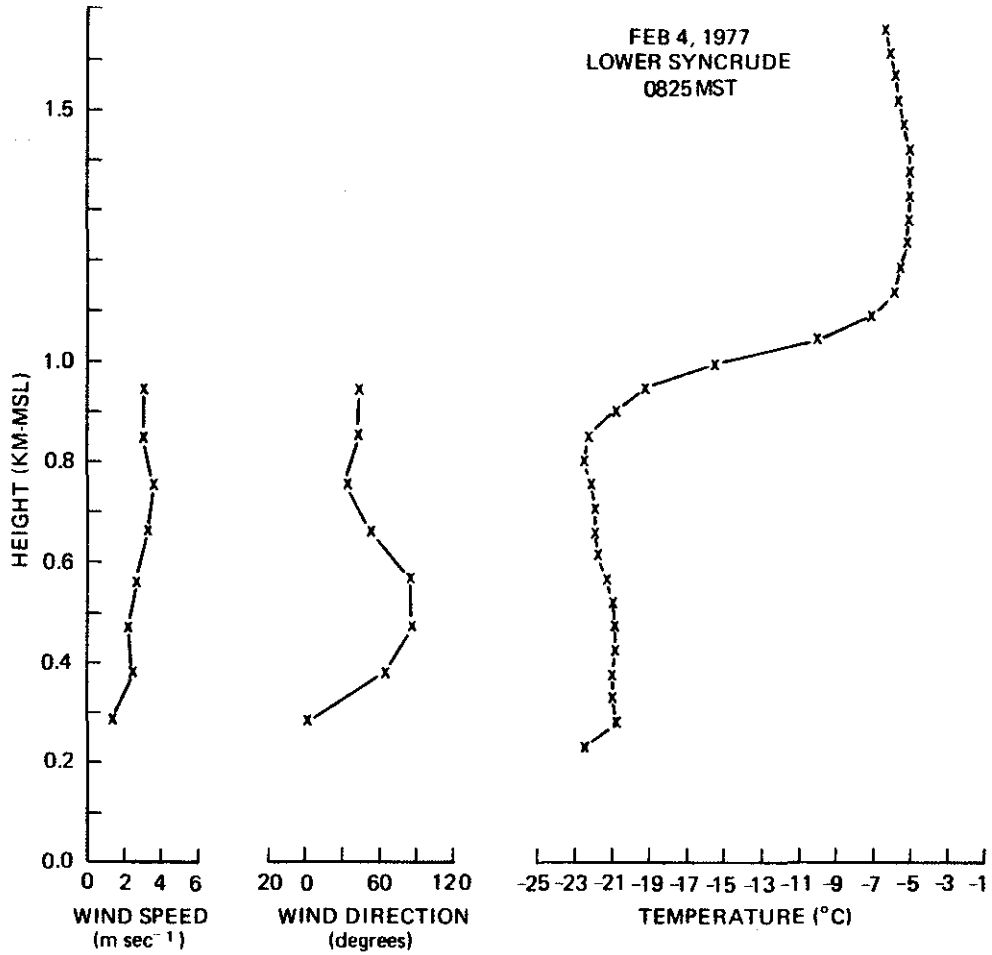

Figure 47. Wind and temperature profiles for 4 February 1977 at Lower Syncrude at 08:25.

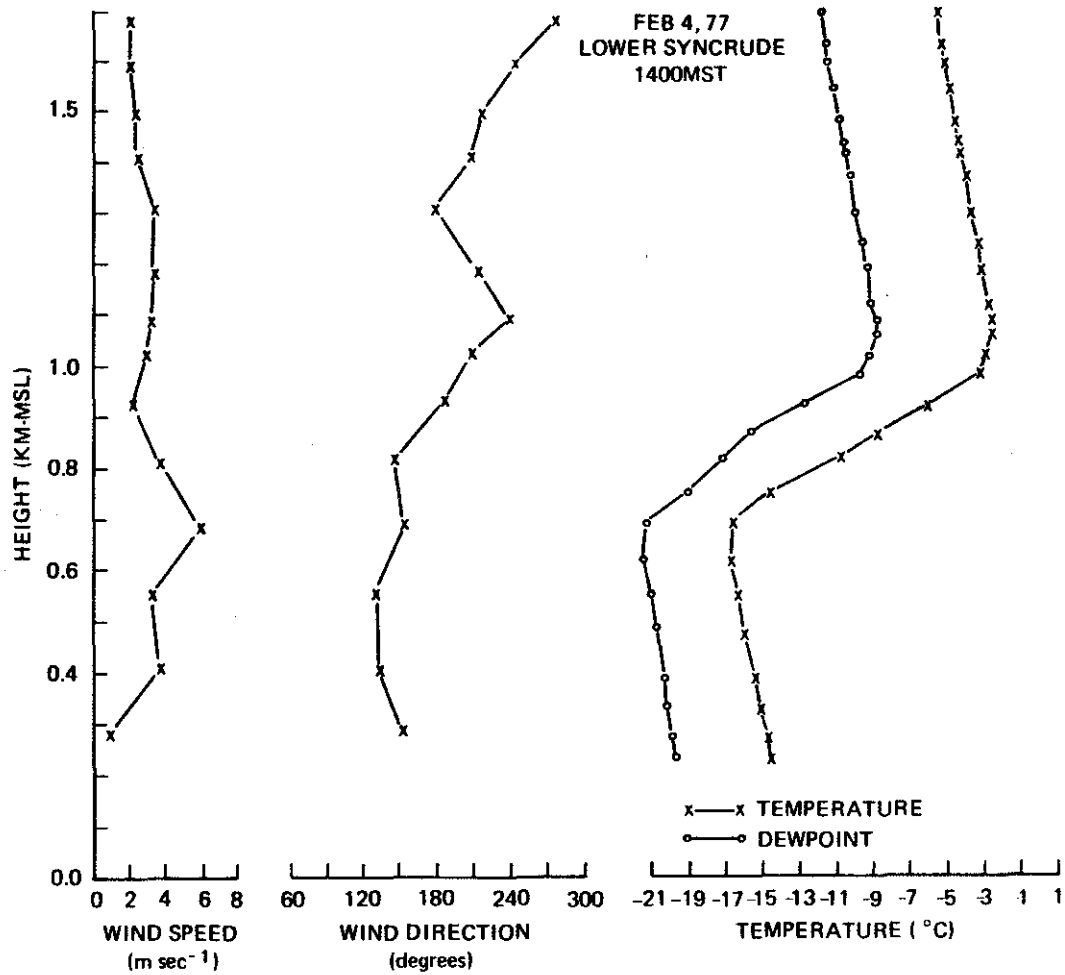

Figure 48. Wind and temperature profiles for 4 February 1977 at Lower Syncrude at 1400.

Figure 49. GCOS plumes during rising under inversion conditions.

$$\frac{\Delta h}{L} = 1.6 \left(\frac{x}{L}\right)^{2/3} \qquad (6)$$

Here, L is a scaling length equal to $\frac{F}{U^3}$.

The observed rise of the plume was plotted against downwind distance in a nondimensional form as shown in Figure 50. The figure also includes the theoretical model described by Eq (6). For this case study, the model underestimates the actual rise of the GCOS plume. The observed limit for the plume elevation was also compared with Eq (5). The data agree well with the theoretical model.

The foregoing analysis describes data from only one case study. There is a need for Briggs' model to be investigated furbher. This will be done later when the data from all three field studies will be used.

On some occasions during inversion conditions, the plumes from the GCOS plant were able to penetrate and continue to rise. Figure 51 shows the refinery flare and the power plant plumes penetrating an inversion layer. Plumes from the lower sources, however, were trapped by the inversion layer. At a later time the inversion layer was lifted to a higher level and capped all the GCOS plumes (Figure 52).

The second case shows the plume under wind shear conditions. The flow in this case is skewed where wind speed and direction change with elevation. As an example, Figure 53 shows the profiles of wind speed and direction under such conditions. The wind speed varies from 4 to 10 $m \cdot s^{-1}$ within the lower 300 m layer of the atmosphere. A change of 90° in direction within this layer also occurs. A plume from a continuous point source under such conditions changes its velocity components as it rises, causing its center line to curve with downwind distance. Figure 54 shows the two plumes from the flare stack and the power house stack under similar shear conditions; close to the ground, both plumes travel southeasterly,

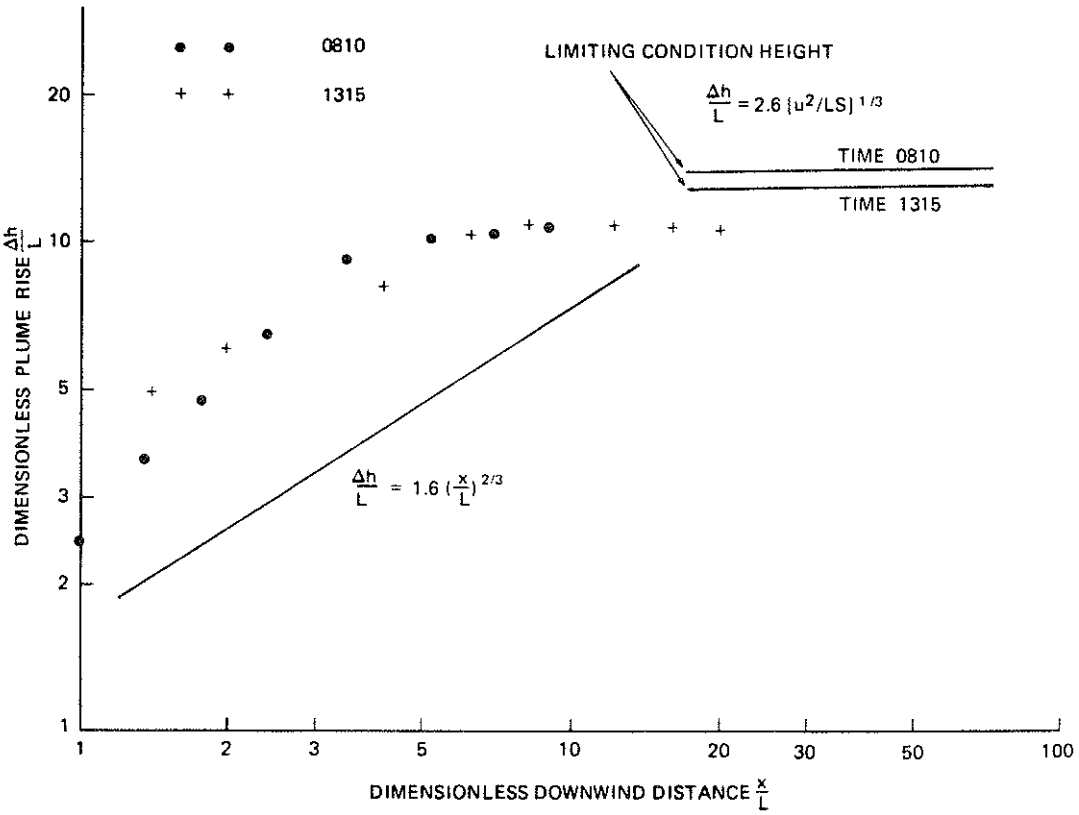

Figure 50. Comparison of predicted versus observed plume rise under limited mixing conditions. The solid line represents Eq (6).

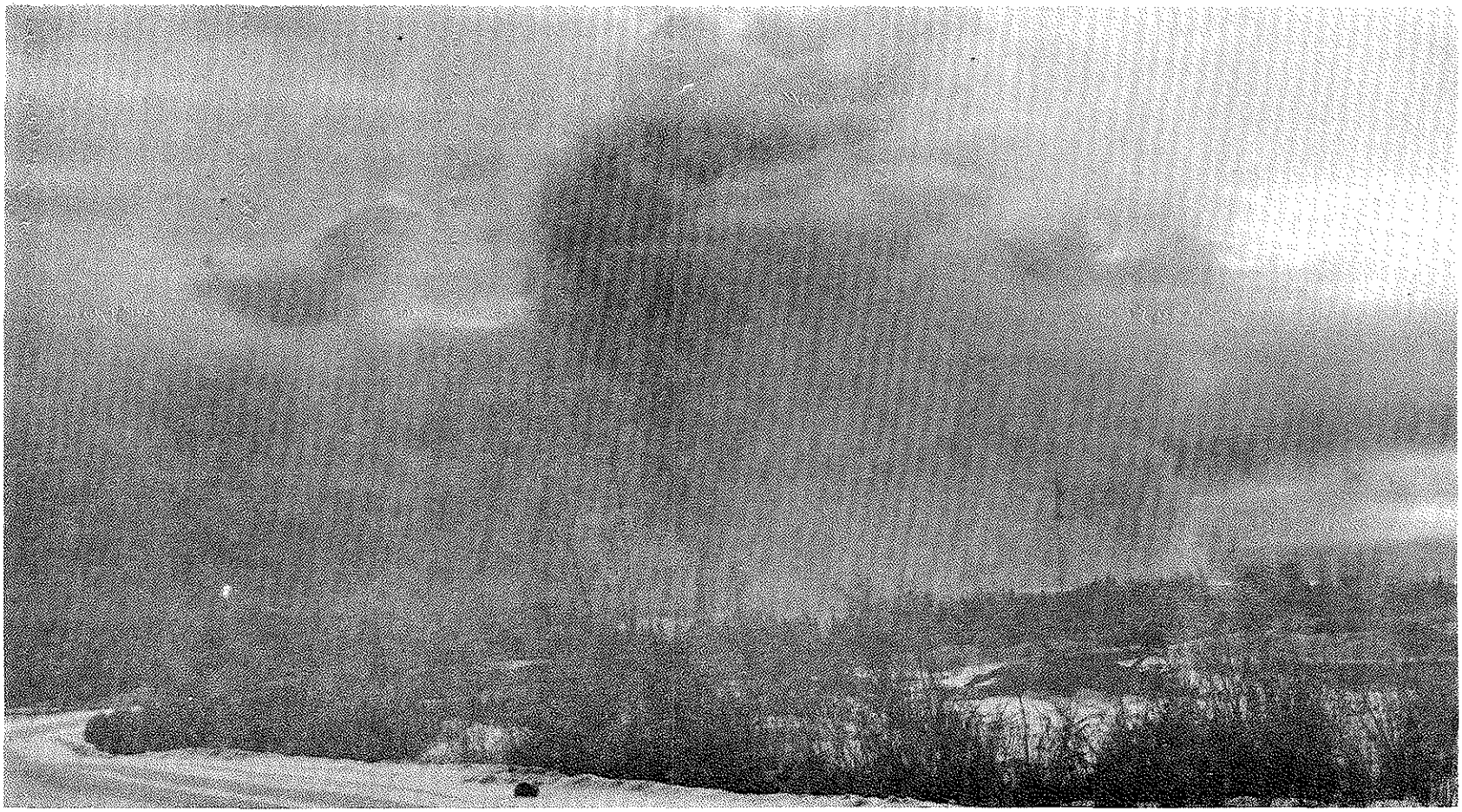

Figure 51. Photograph of the penetration of the inversion layer by the flare and power house plumes.

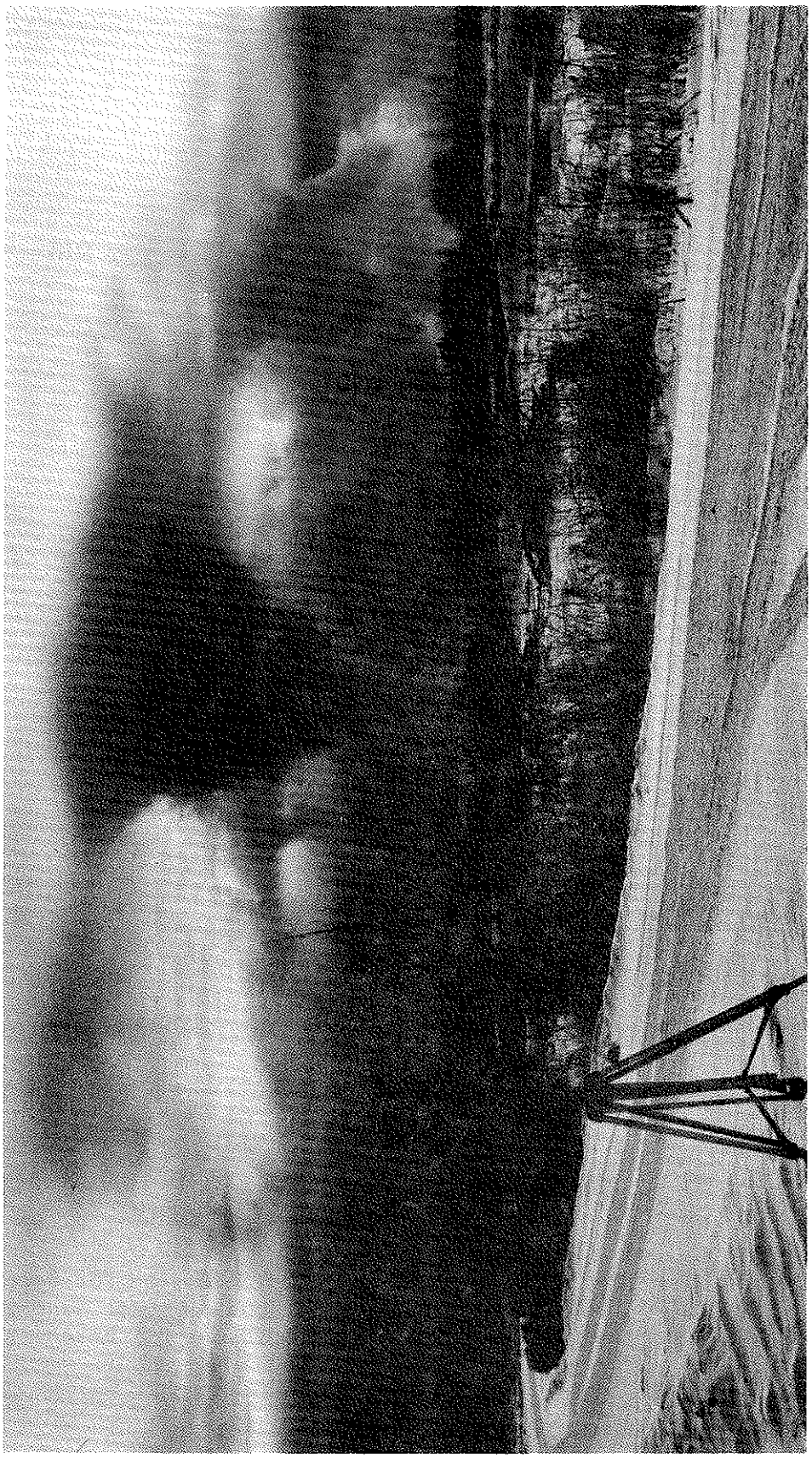

Figure 52. GCOS plumes capped by the inversion layer.

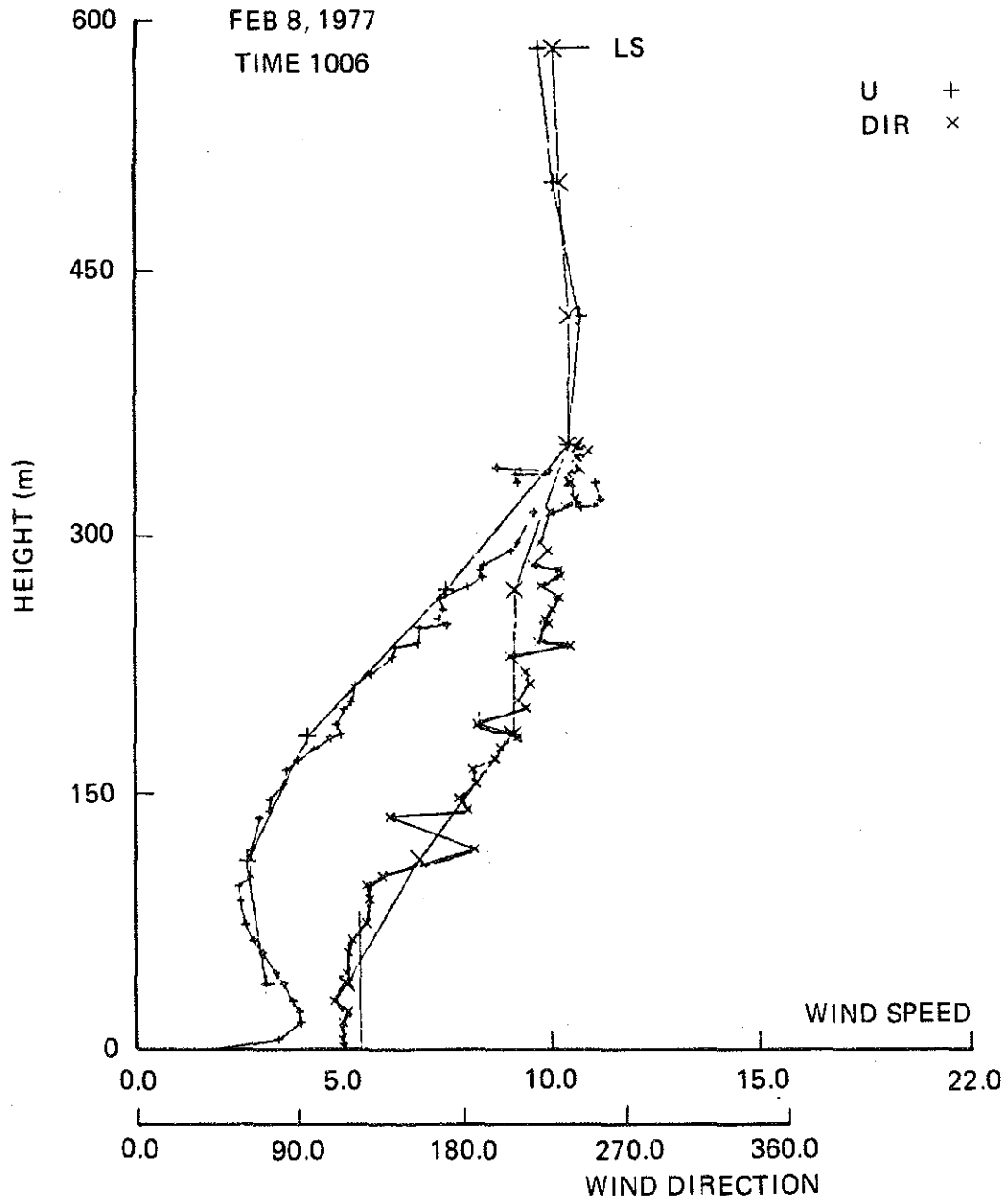

Figure 53. Profiles of wind speed and wind direction for 8 February 1977 from T/S and M/S observations at Lower Syncrude. The profiles with large crosses represent M/S observations.

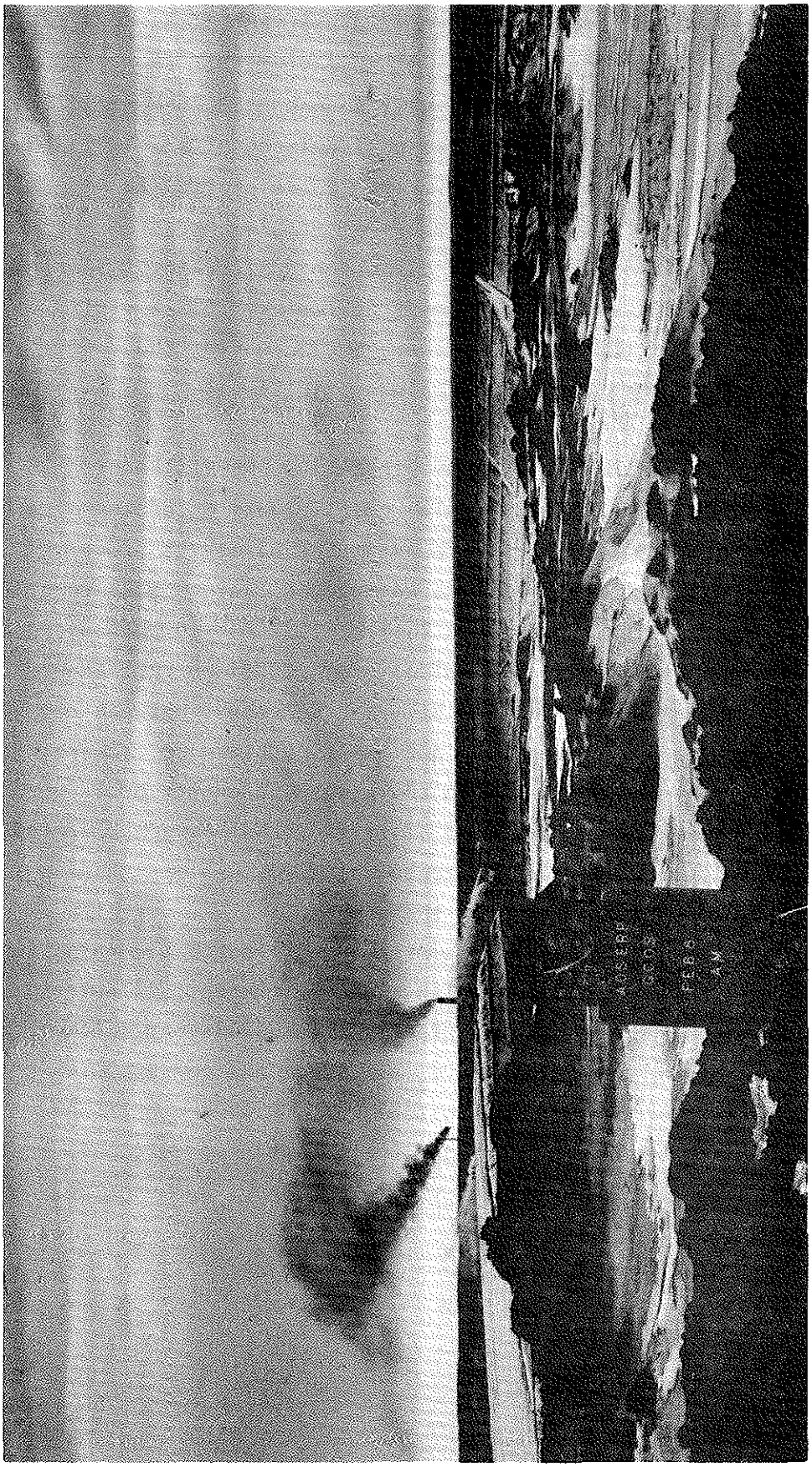

Figure 54. GCOS plumes under wind shear.

and at the 300 m level change their direction to southeasterly. Csanady (1973) and Pasquill (1974) suggested that the diffusion of a plume under shear conditions will be enhanced both along and across its axis. SO_2 concentration isopleths of the GCOS plumes as measured by the helicopter at 800 m are plotted in Figure 55. The isopleths reflect the increased plume growth due to the shear effects (Figure 53). The wind direction shear tends to deform the plume, which increases the plume's perimeter. Since mixing of the plume occurs arounds its perimeter, by increasing the perimeter one actually increases the rate of plume dilution.

4.2 MEASUREMENTS OF PLUME DISPERSION COEFFICIENTS

The vertical dispersion coefficients σ_z of the plume from the power plant stack were estimated using the procedure outlined in Fanaki (1978). The measured σ_z values as a function of downwind distance are given in Table 5. For comparison purposes the table includes also the values of σ_z obtained from the helicopter traverses (see Section 5). The agreement between the values of σ_z obtained by photography and those obtained by traversing the plume is reasonable. Although the two measurements of σ_z were made at two different downwind distances, they have a correlation coefficient of 0.65. No horizontal plume growth was evident between 0.8 km and 20 km from the source.

The estimated values of σ_z were grouped according to stability and were compared with those of the Pasquill-Gifford dispersion parameters (Turner 1967) (Figure 56). As in the previous study in March, the values of σ_z are large and compare with the Pasquill-Gifford values for unstable and neutral conditions. Similar to the March study, there is no apparent relationship between the observed σ_z and the predicted values.

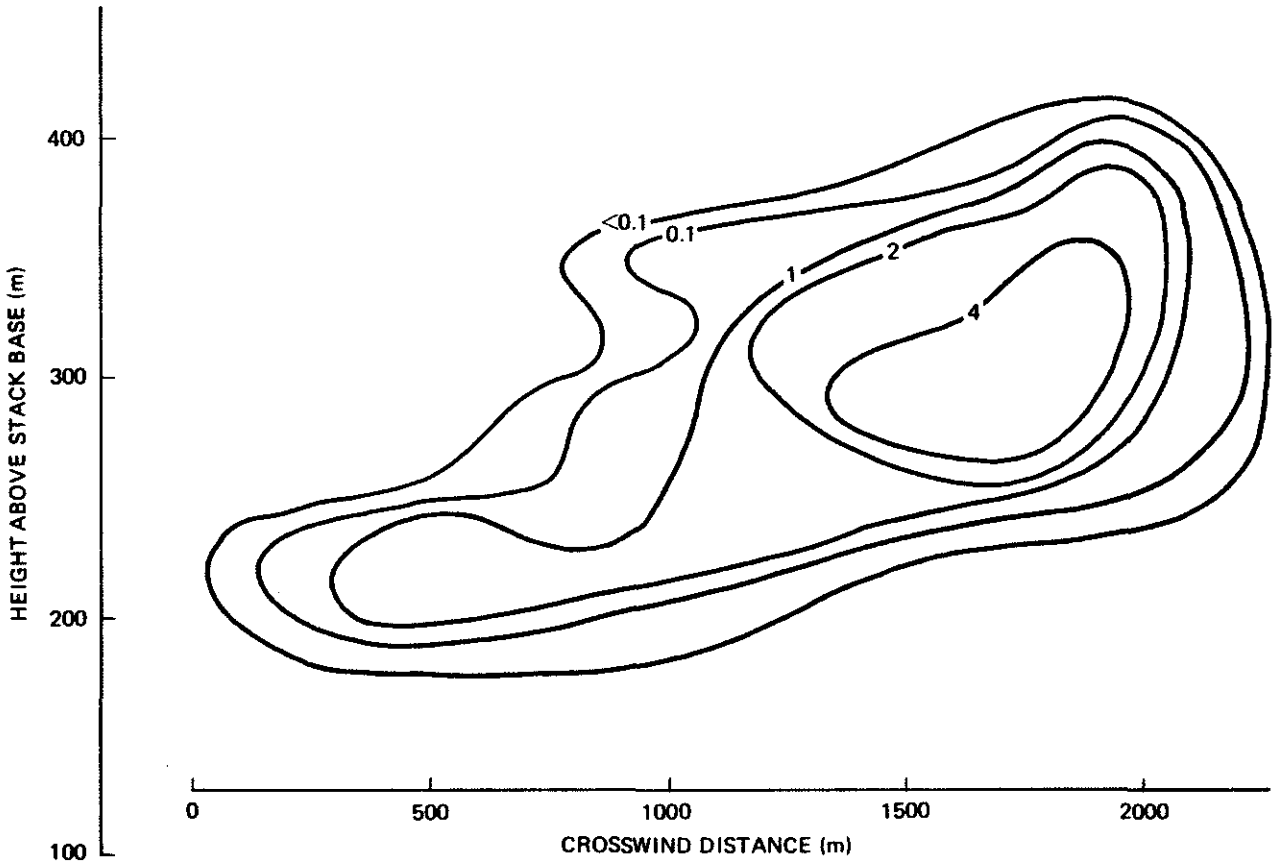

Figure 55. Isopleths of SO_2 concentration (ppm) across the GCOS plumes at 800 m downwind distance from the source.

Table 5. Plume standard deviation σ_z at different downwind distance.

Date	Time (MST)	Downwind Distance x(m) 100	200	300	400	500	600	700	800	900	1000	Helicopter Observation
3 Feb/77	1400	13	16	18	18			Δ				
	1620	17	40	54	62	62						
4 Feb/77	0810	11	28	54	87	89	86	86				
	1100	9	40	62	68	68						
	1315	25	44	44								
	1600	14	23	28	30	32	32					
5 Feb/77	0830	15	21	29	32	35	36	36				43(800)[a]
	1120	13	18	24	29	36	38	38				31 (30600)
	1330	9	15	22	27	29	31	31				
	1415	7	15	22	24	24						
	1600	7	13	16	31	34	36	40	40			
6 Feb/77	0940	9	18	24	27	29	29					
	1110	7	15	18	22	33	36	38	42	46	46	
	1330	14	18	27	33	36	36	40	42	42		66(800)

continued ...

Table 5. Continued.

Date	Time (MST)	Downwind Distance s(m)										Helicopter Observation
		100	200	300	400	500	600	700	800	900	1000	
6 Feb/77	1420	11	19	24	26	26	27	27				
7 Feb/77	0845	9	13	20	26	27	27					
	1015	11	20	22	24	24						
	1115	7	11	16	29	29						
	1415	7	13	18	20	22	22	24	24			
	1630	7	9	15	16	16	18	18				
8 Feb/77	0830	11	26	38	38	42	42					
	0930	11	24	38	46	47	47					
	1045	18	24	26	27	27						
10 Feb/77	0845	13	22	26	31	31	31	33	33			20(30400)
	0930	13	22	31	35	36	37	37				28(9700)
	1030	11	22	26	33	36	40	42	42			31(800)
	1100	9	18	26	36	45	51	55	55			
	1140	13	29	36	40	46	49	51	51			
	1445	7	18	27	31	33	33					
	1615	15	16	36	44	49	55	56	56	55	56	

continued ...

Table 5. Concluded.

Date	Time (MST)	Downwind Distance x(m)										Helicopter Observation
		100	200	300	400	500	600	700	800	900	1000	
11 Feb/77	1410	24	42	55	60	73	82	86	86			83(2000)
	1515	24	31	38	40	49	49	47	55			81(12000)
12 Feb/77	0900	11	20	22	26	27	31	31				

[a]Numbers in parentheses indicate the downwind distances at which the helicopter measurements were made.

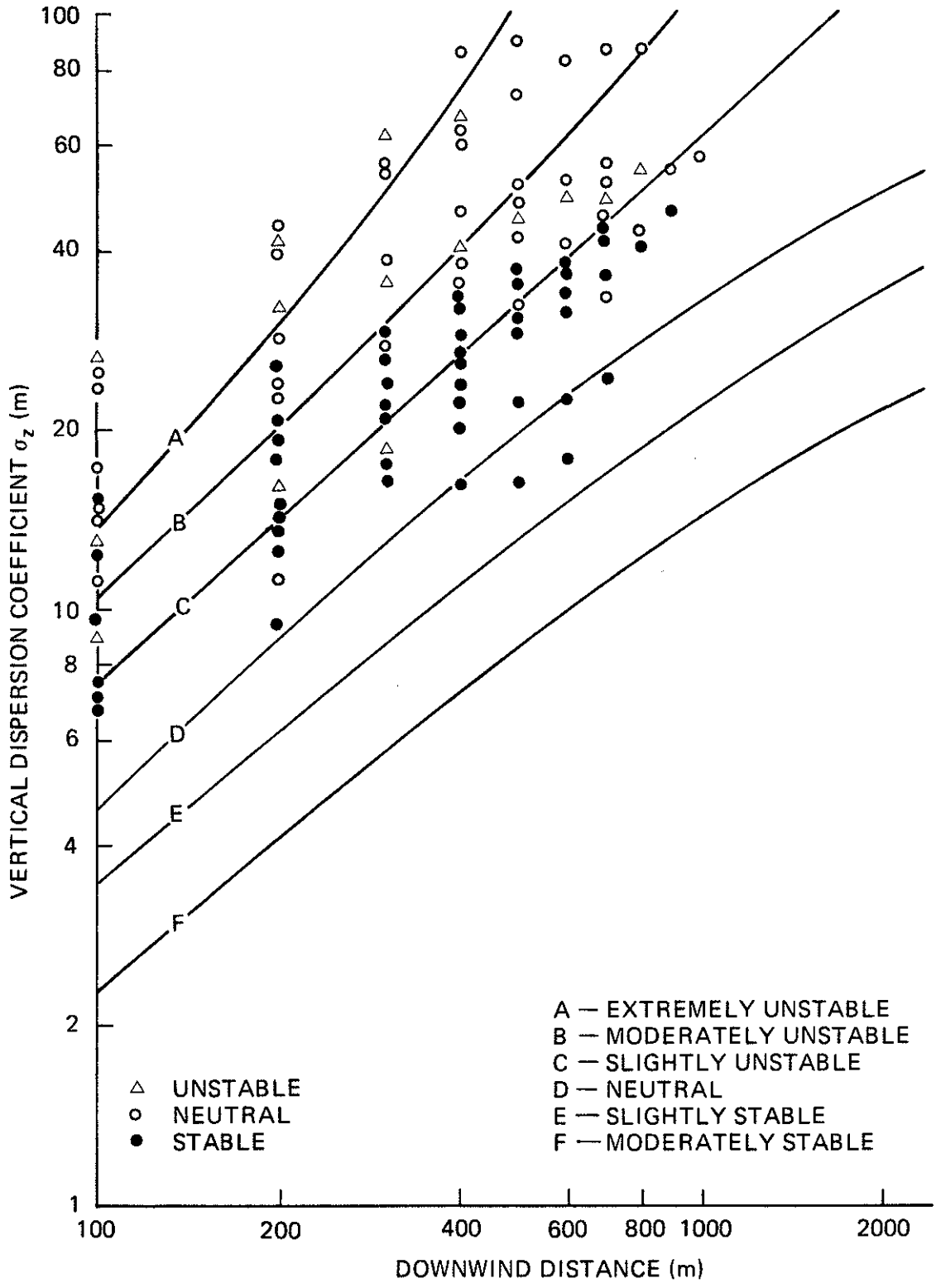

Figure 56. Comparison of observed vertical dispersion coefficient with Pasquill-Gifford predictions for the oil sands study, February 1977.

The few observed values of σ_y obtained by traversing the plume are also compared with the Pasquill-Gifford model (Figure 57). Although the number of observations is small, it is apparent that the observed σ_y does not agree with Pasquill-Gifford's predictions. The values are large for all observed stability categories. The results reflect increased horizontal plume growth due to the capping of the plume by elevated inversion layers. The effect of thermal stratification under stable conditions decreases the vertical scale of turbulence (Pasquill 1974 p. 60).

The observed values of σ were examined again using the TVA set of curves (Carpenter et al. 1971), and the result is shown in Figures 58 and 59. The curves appear to hold better for σ_z than for σ_y. The values of the observed σ_y are quite large and do not compare with the model at any stability. The relationship between the observed and predicted values of σ_z appears to hold better in this case than with the Pasquill-Gifford model.

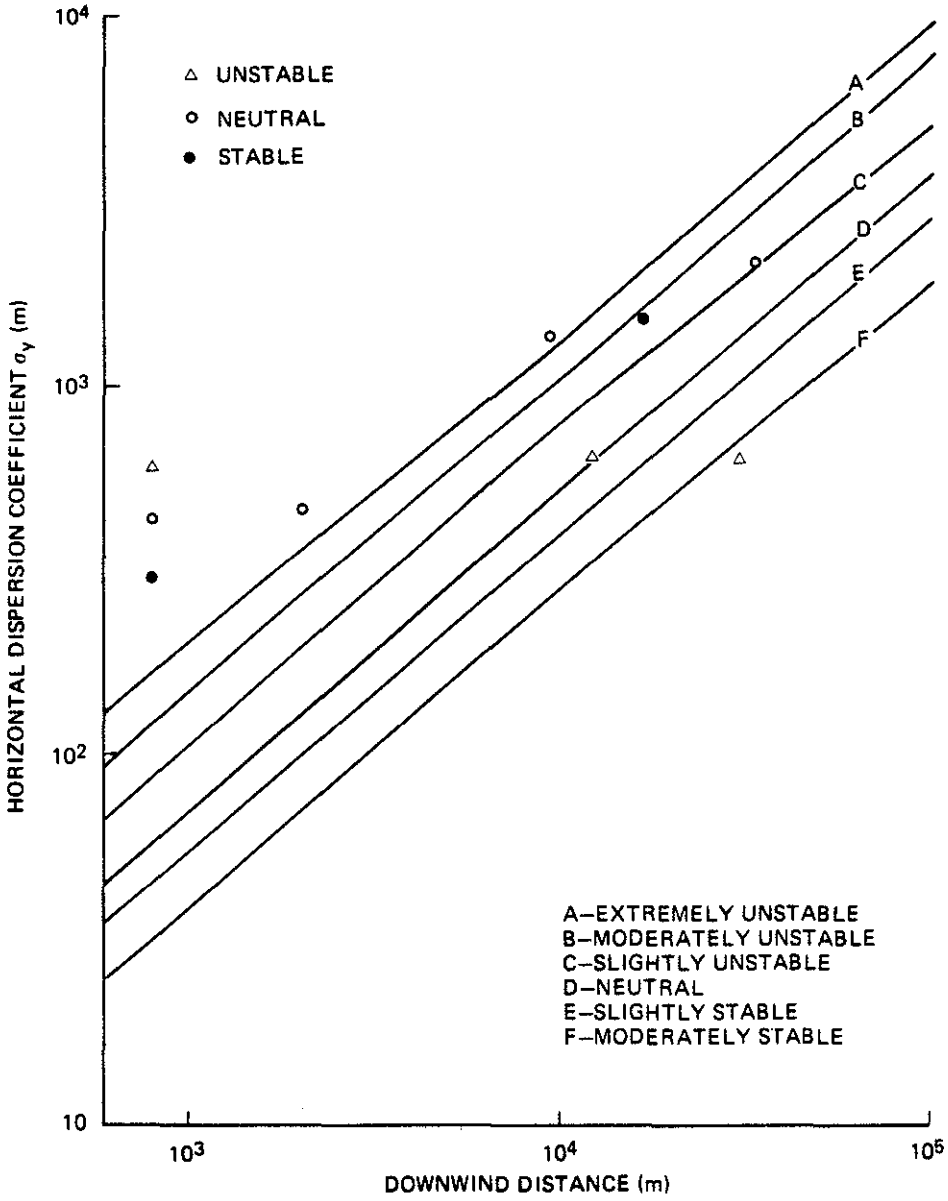

Figure 57. Comparison of observed horizontal dispersion coefficients with Pasquill-Gifford prediction for the AOSERP study, February 1977.

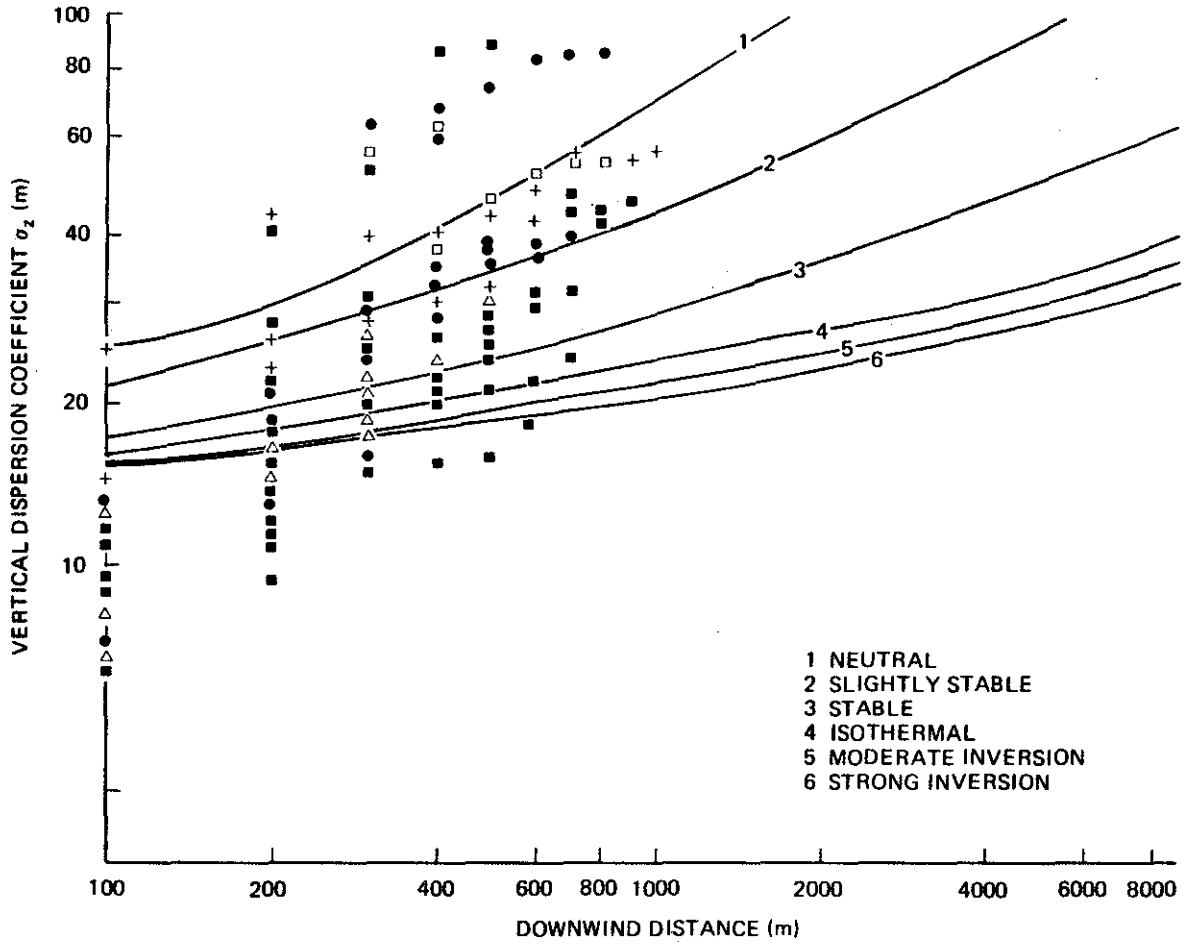

Figure 58. Comparison of observed vertical dispersion coefficients with TVA predictions for the AOSERP study, February 1977.

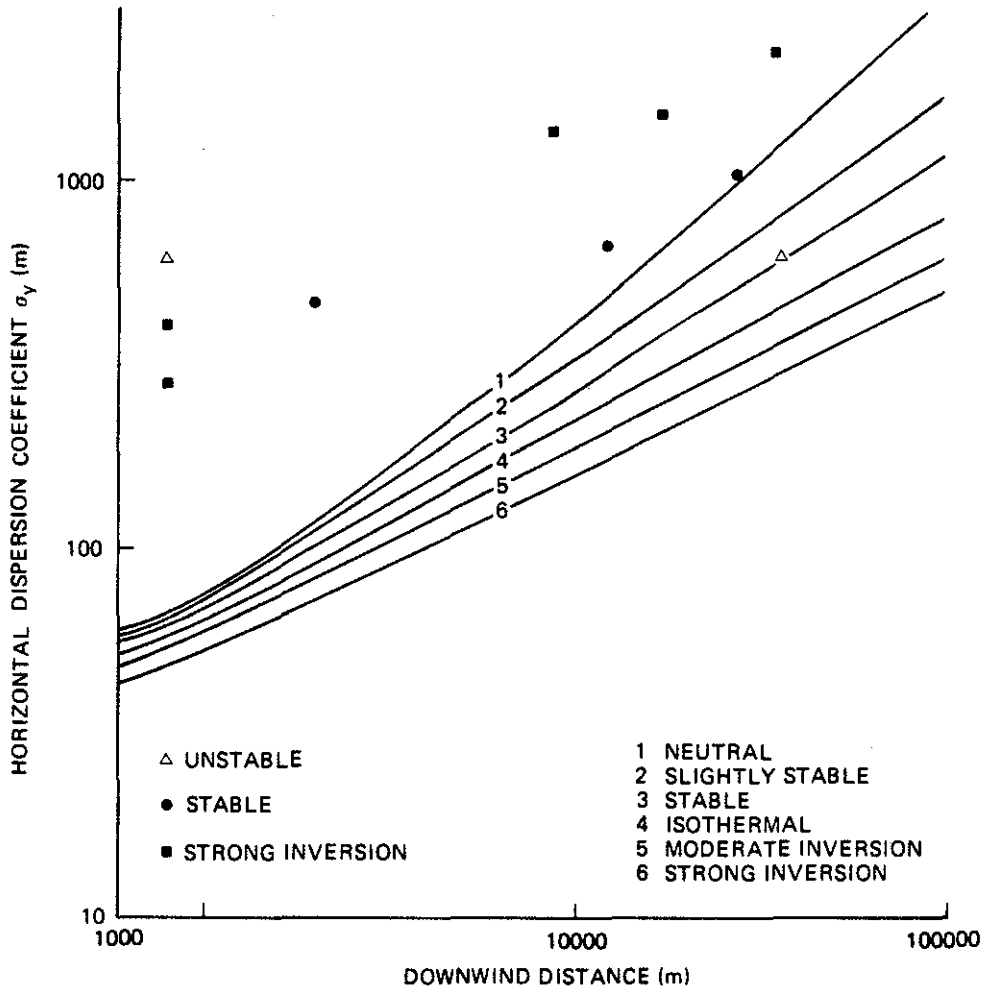

Figure 59. Comparison of observed horizontal dispersion coefficient wit TVA prediction for the AOSERP study, February 1977.

5. AREAL SURVEY OF GCOS PLUME

5.1 EXPERIMENTAL PROCEDURE

A Bell Jet Ranger helicopter was used in this survey of dispersion and oxidation of sulphur dioxide in the plume of the GCOS power plant. It was instrumented with a Sign X continuous sulphur dioxide analyser to determine dispersion rates, and two parallel filter packs to obtain sulphur dioxide oxidation data. Figure 60 shows the helicopter used in this study. Details of the sample intake are shown in Figure 61.

The Sign X analyser measures the change in electrical conductivity of deionized water due to the absorption of sulphur dioxide (as well as other gases and particulate matter constituents that can dissolve to form electrolytes in water) from the air sample. It has a sampling rate of about 2 $L \cdot min^{-1}$, and is one of the fastest-responding SO_2 analysers presently commercially available. The instrument used in this work had a "dead time" (time before a step change in concentration at the inlet is sensed by the instrument) of about 1.5 s and a time constant (time to rise to 63.2% of full scale) of 3.3 s. Its calibration was checked several times during the course of the field study using standard cylinders of SO_2 in nitrogen (0.70 and 3.5 ppm).

The filter pack method is described in detail in Section 8.2. Very briefly, the pack consisted of a modified Swinnex 47 mm filter holder which contained three filters: first, either a Whatman 40 (cellulose), Mitex (teflon), or Delbag (polystyrene) filter to collect particulate matter; and then, separated from the particulate filter, two chemically impregnated filters placed back-to-back, to trap the SO_2 in the same plume sample. Whatman 40 cellulose filters, treated with an aqueous solution of glycerol and potassium carbonate, were found to give a very high trapping efficiency. Figure 62 shows details of the type of pack used in this project.

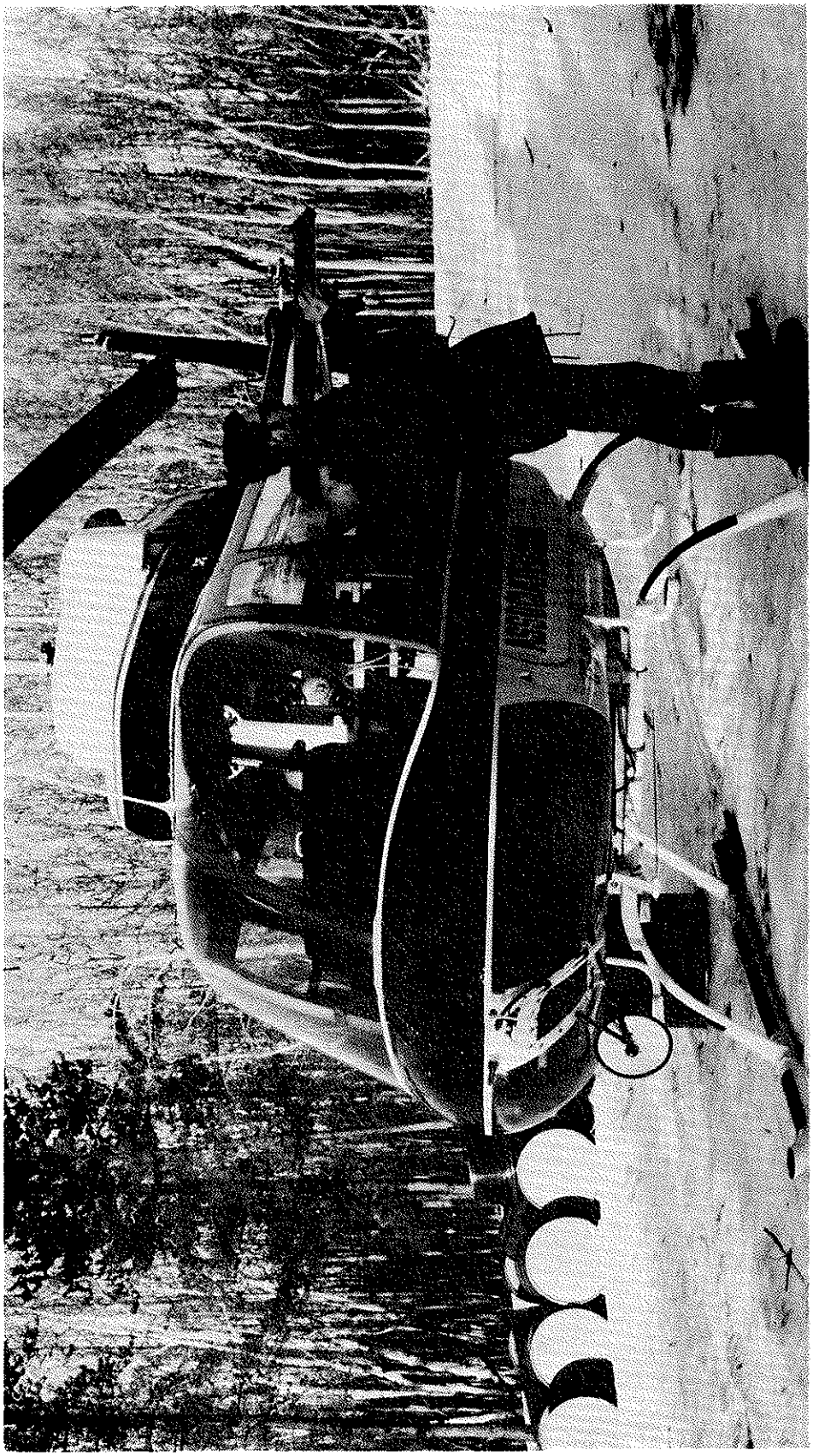

Figure 60. Photograph of the Bell Jet Ranger helicopter used in this study.

Figure 61. Details of the sample intake mounted on the helicopter.

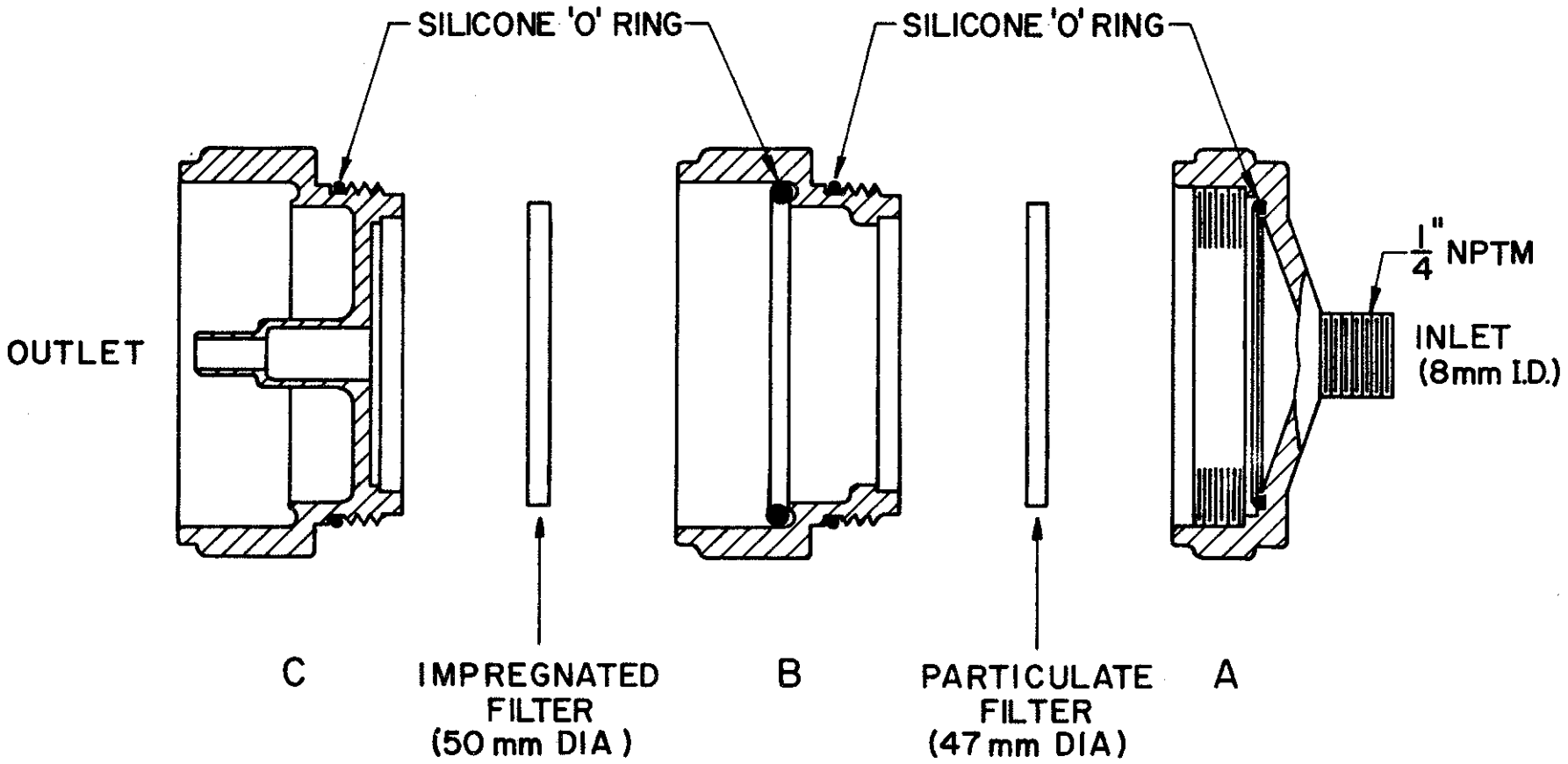

Figure 62. Dissassembled filter holder.

A schematic diagram of the equipment is given in Figure 63. The inlets to the Sign X analyser and filter pack sampling lines extended to about 30 cm beyond the nose of the helicopter, where they were well clear of any downwash effects from the rotor. The line to the Sign X was made of teflon (320 cm long, 0.24 cm i.d.), and was tapped from a short "tee" section to eliminate ram air effects. The sample line leading to each filter pack was also made of teflon (124 cm long, 0.95 cm i.d.), and was capped with a conical teflon tip that had been carefully machined to give approximately isokinetic sampling conditions at the helicopter air speed of $km \cdot h^{-1}$. Figure 64 shows details of the inlets to the Sign X and filter pack sample lines.

The line leading to the filter packs was almost straight, to minimize the possibility of particle loss due to impaction. The packs were attached to the line with a stainless steel Swagelok female connector. The sample was drawn over the filters at a rate of about 20 $L \cdot min^{-1}$ by means of two Duraire diaphragm pumps. The flow rate was measured downstream of the packs with calibrated Brooks rotameters and a Weksler absolute pressure gauge.

The output from the Sign X analyser was recorded on a Hewlett-Packard strip chart recorded. Power to the analyser, recorder, and vacuum pumps was supplied from the aircraft alternator via a 1 kW Topaz inverter.

The required number of filter packs were loaded with fresh filters prior to each flight and were stored in sealed plastic bags. At each sampling location, two packs were removed from their bags and attached to the sample line and vacuum pump. Sampling was usually carried out for about one-half hour by flying crosswind traverses across the plume at various altitudes. Group reference points were selected during the first traverse, and subsequently a mark was made on the Sign X chart each time the helicopter was over the reference points. The heading and altitude were also recorded for each pass.

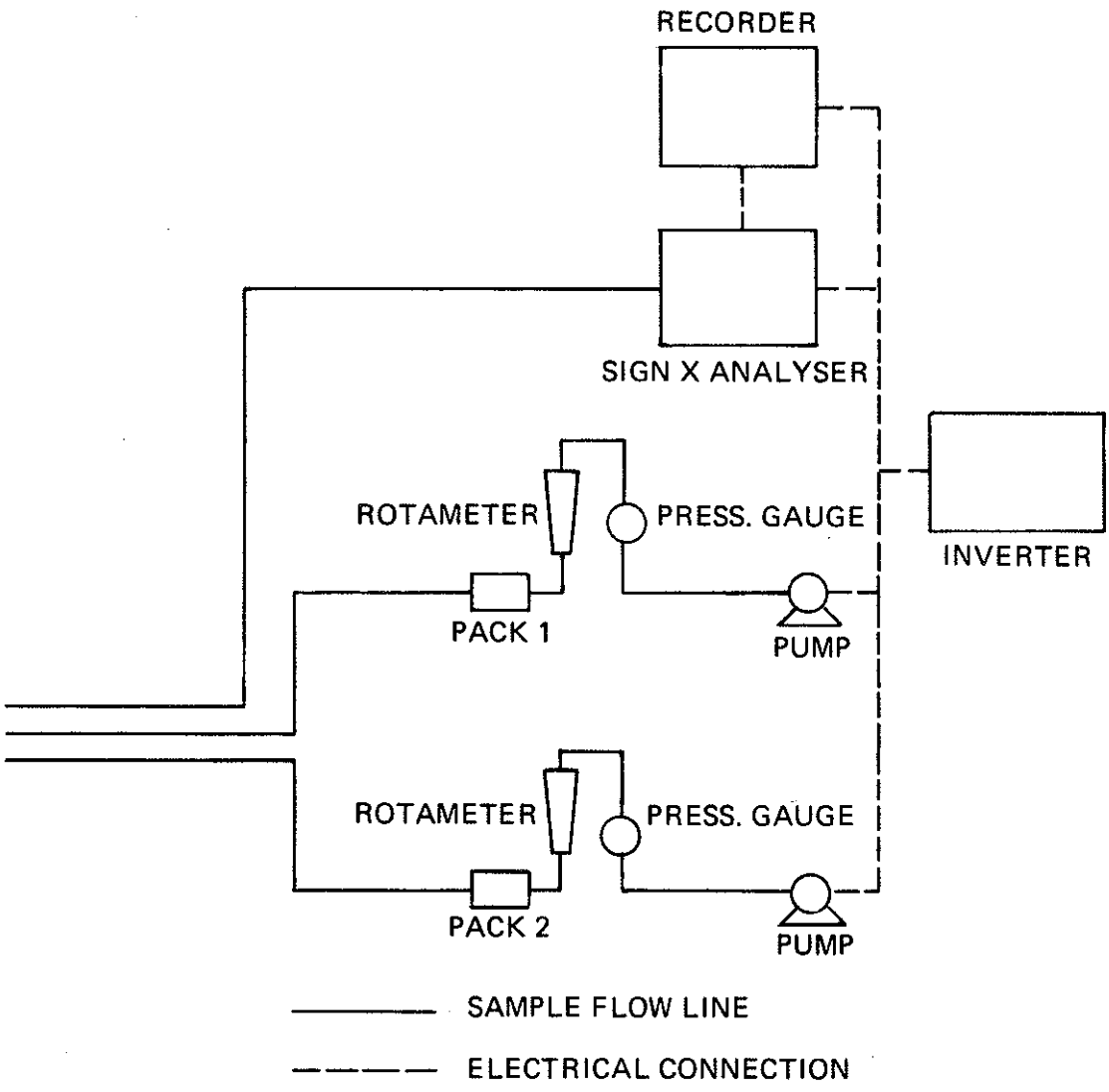

Figure 63. Schematic diagram of the equipment.

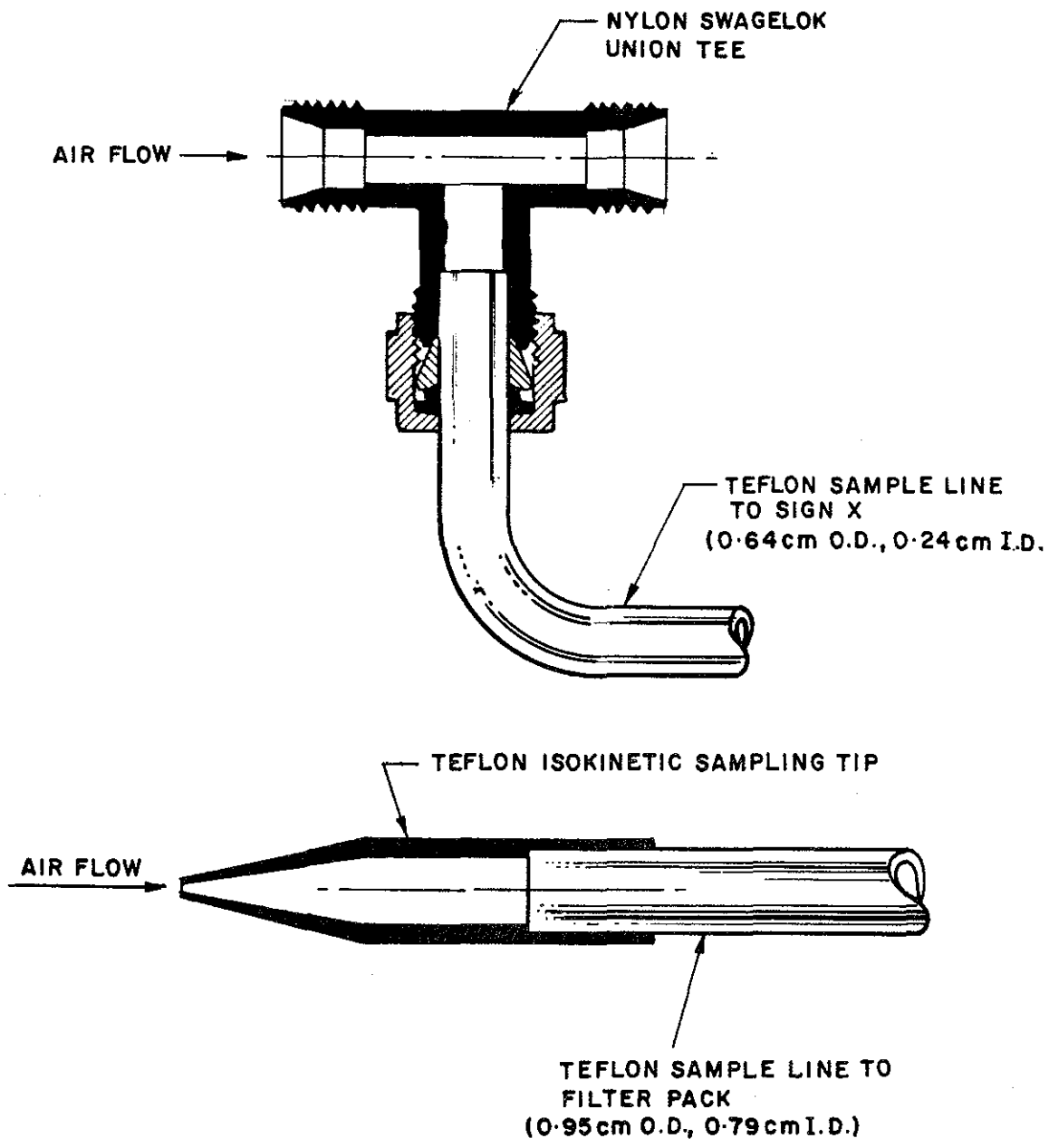

Figure 64. Inlets to Sign X and filter pack sampling lines.

Rotameter and pressure gauge readings in each of the filter pack sample lines were noted at the beginning and end of the sampling period. At the end of the sampling period, the filter packs were replaced in their respective plastic bags for subsequent unloading at the field station laboratory, and the zero reading on the Sign X analyser was checked by flying in clean air, well clear of the plume.

An attempt was made to sample the plume at two or three locations downwind of the chimney: one within about 1 km, another as far as possible (usually approximately 30 km), and the third at an intermediate location. Sometimes the plume was sampled initially near the chimney, while at other times the distant samples were collected first. On one occasion a "background" sample was collected over a half-hour period while flying clear of the plume. Occasionally special flights were carried out to collect samples close to the stack in order to obtain more information about the particulate matter in the GCOS power plant plume. These were subsequently analysed for total sulphates, sulphuric acid, and various metals (by neutron activation). On some of the flights, both of the parallel filter packs contained Whatman 40 particulate matter filters in order to check the reproducibility of the present sampling method. On other flights, one of the packs was loaded with a Whatman 40 filter (for total sulphate measurements), while the other contained either a Mitex or Delbag filter, both of which are inert to sulphuric acid, and thus suitable for studying concentrations of sulphuric acid aerosol downwind of the chimney.

After each flight, the Whatman 40 particulate filter, as well as the chemically impregnated filter papers, were removed from their filter packs, folded (exposed side inwards), and stored in sealed plastic bags. The Delbag and Mitex filter papers were placed in labelled petri dishes and stored over silica gel in a desiccator.

All chemical analyses were done at the Atmospheric Environment Service, Chemistry Division's laboratory, while the neutron activation analyses were carried out at the University of Toronto. Very briefly, the analysis for total sulphate and sulphuric acid on the particulate filters, and SO_2 on the impregnated filters, proceeded as follows.

The Whatman 40 particulate filters were extracted with 50 cm^3 of boiling deionized water and analyzed for total sulphate by the isotope dilution method of Klockow and Deazingen (1976). The Delbag filters were dissolved in 4 cm^3 of benzaldehyde, which is a specific solvent for sulphuric acid (Leahy et al. 1975). This benzaldehyde was then cleared of any other particulate matter on an ultracentrifuge and contacted with deionized water to extract the sulphuric acid. The water phase was analysed by the isotope dilution method. Blank determinations were carried out with every set of samples. The Mitex filters were analysed for total sulphate only because it proved very difficult to transfer the sulphuric acid into benzaldehyde from the surface of these filters with the equipment at our disposal.

The impregnated filters were extracted with 75 cm^3 of 0.03% hydrogen peroxide solution and analysed for SO_2 (as sulphate) by three methods: isotope dilution, Thorin (Persson 1966), and ion-exchange chromatography (Small et al. 1975). The three sets of determinations were generally in excellent agreement. Standards were prepared by soaking blank filter papers with a concentrated sodium sulphate solution and extracting them in exactly the same way as the samples.

5.2 SO_2 DISPERSION RESULTS

We report here only the results of flights where the plume was reasonably coherent at the intermediate and/or distant sampling locations as well as near the chimney. There were six such flights, for which details of the reference point locations

are given in Appendix 8.3. Sulphur dioxide concentrations are shown as a function of the altitude and crosswind distance from the reference points in Figures 76 to 91 in Appendix 8.3.

No attempt was made to correct the measured SO_2 concentration profiles for the analyser response delay (see, e.g., Larsen et al. 1965; Markowski 1975). For reactive gases such as SO_2, such corrections are, in any case, considered to be of questionable value under plume sampling conditions (Lusis 1976). Near the chimney, where concentrations are changing rapidly as a function of distance, some error could result in the SO_2 measurements due to analyser time lag. Farther afield, where concentration changes are less pronounced, such errors should be small.

It should be noted that, during many of the flights, it was very difficult to follow the plume more than a few kilometres downwind of the GCOS plant because of pronounced wind shear at plume height or because of fumigation conditions. Also the plume from the incinerator stack was often mixing with the power plant plume, under which conditions we were actually observing the effect of atmospheric dispersion and chemical reactions in both of these plumes together.

For Flights 3, 6, 11, and 14, dispersion coefficients were calculated from the data on Figures 76-91 by using the following Gaussian formulas for the plume corss-sectional area and width:

$$A = 2\Pi\sigma_y\sigma_z \ln\left(\frac{Q}{2\Pi\sigma_y\sigma_z CU}\right) \tag{7}$$

$$-\tfrac{1}{2}\left(\frac{y}{\sigma_y}\right)^2 = \ln\left[\frac{2\Pi\sigma_y\sigma_z CU}{Q}\right] \tag{8}$$

$$\sigma_z = \sigma_y\sigma_z / \sigma_y \tag{9}$$

where $C = SO_2$ concentration, $\mu g \cdot m^{-3}$

C = Plume cross-sectional area enclosed by concentration C isopleth, m^2

$Q = SO_2$ emission rate, $\mu g \cdot min^{-1}$

U = Wind speed at plume height, $m \cdot min^{-1}$

Y = One-half of plume width corresponding to concentration C, m

σ_y, σ_z = Horizontal and vertical dispersion coefficients, m

Average wind speeds at plume height were obtained from the M/S and radiosonde soundings, while SO_2 emission data were kindly supplied by Mr. Mark Strosher of Alberta Environment. The results of these calculations are shown in Table 6.

5.3 SO_2 OXIDATION RESULTS

An intercomparison of the amounts of particulate sulphate and SO_2 collected on parallel filter packs indicated that the reproducibility of the filter pack model is good for SO_2 (better than 15%), but much poorer for the particulate sulphate (about 30% or worse) (see Lusis and Phillips 1977). This is probably due to difficulties associated with the sampling of particulate matter rather than chemical analysis problems, and introduces a fairly large scatter in the experimental data.

Table 7 shows the concentration of sulphur (as total sulphate, sulphuric acid, and sulphur dioxide) determined at various points downwind of the chimney, together with the time of sampling and distance from the chimney. Also shown is the percentage of sulphur in the form of sulphate and sulphuric acid. The results in Table 7 are expressed in terms of concentration in order to show that, for these flights, contributions to plume sulphur from entrained ambient air should be very small (any such contributions were neglected in subsequent calculations), and to give the reader an idea of the reproducibility of the filter pack method for SO_2 and SO_4 determinations when two parallel

Table 6. Dispersion coefficients calculated from crosswind SO_2 plume profiles, February 1977.

Date	Time (MST)	Distance from Stack (km)	σ_y m	σ_z m
5 Feb/77	0840-0910	8.0	630	43
	0935-1000	30.6	650	31
6 Feb/77	1435-1455	0.8	290	66
	1525-1605	16.9	1500	91
10 Feb/77	1020-1030	0.8	440	31
	0950-1005	9.7	1400	28
	0830-0920	30.4	2200	20
11 Feb/77	1430-1450	2.0	470	83
	1500-1530	12.0	680	81
	1550-1600	28.8	1000	84

Table 7. Total sulphates, sulphuric acid, and sulphur dioxide found on the filter packs, GCOS plume study, February 1977.

Data	Time of Sampling (MST)	Distance from Stack (km)	µg S m^{-3} @			% of S as	
			$SO_4^=$	H_2SO_4	SO_2	$SO_4^=$	H_2SO_4
3 Feb/77	1435-1500	1.2	4.79	-	306	1.20	-
5 Feb/77	0820-0908	8.0	7.17	-	439	1.61	-
	0920-1015	30.6	1.99	-	136	1.45	-
	1427-1500	Approx. 1	1.73	-	247	0.70	-
			3.51	-	216	1.60	-
6 Feb/77	0815-0903	2.8	6.70	-	389	1.70	-
	0915-1014	26.4	2.50	-	81	2.99	-
	1016-1040	Background	0	-	4	-	-
	1435-1512	0.8	4.63	-	320	1.43	-
			3.96	-	337	1.16	-
	1525-1620	16.9	1.45	-	113	1.27	-
			1.70	-	119	1.41	-

continued ...

Table 7. Continued.

Date	Time of Sampling (MST)	Distance from Stack (km)	μg S m^{-3} σ_v			% of S as	
			$SO_4^=$	H_2SO_4	SO_2	$SO_4^=$	H_2SO_4
7 Feb/77	0935-1007	0.8	8.70	-	731	1.18	-
			9.70	-	647	1.48	-
	0825-0925	approx. 19	2.96	-	311	0.95	-
			4.73	-	277	1.67	-
	1425-1445	approx. 1	6.34	-	493	1.27	-
8 Feb/77	0940-1010	0.8	9.95	-	668	1.47	-
	0825-0925	33.8	2.06	-	163	1.25	-
9 Feb/77	0845-0930	28.8	4.64	-	91	4.86	-
10 Feb/77	1010-1030	0.8	8.43	-	587	1.41	
				5.61	598		0.93
	0930-1005	9.7	2.39		227	1.04	
				2.27	200		1.12
	0830-0920	30.4	1.89		118	1.58	-

continued ...

Table 7. Concluded.

Date	Time of Sampling (MST)	Distance from Stack (km)	μg S m^{-3} σ_v $SO_4^=$	H_2SO_4	SO_2	% of S as $SO_4^=$	H_2SO_4
				1.66	119	-	1.38
10 Feb/77	1600-1620	approx. 1		8.42	1028	-	0.81
11 Feb/77	0930-0940	1.2	6.65		509	1.29	
				7.00	508		1.36
	0847-0925	7.2	1.80		106	1.69	
				1.69	121		1.37
	1415-1450	2.0	2.91		205	1.39	
				2.22	222		0.99
	1500-1540	12.0	2.17		145	1.47	
				1.82	145		1.24
	1545-1630	28.8	1.88		156	1.19	
				1.45	157		0.91

σ_v at 1 atmosphere, 21°C.

packs were sampling the same air parcel (see above). These results should not be used for plume dilution rate or sulphur budget calculations, because the sampling pumps were not turned off while the helicopter was turning around outside the plume between passes, and the percentage of time spent outside the plume was not the same for all sampling locations; it was greater for passes near the stack than for those far downwind.

In Table 8, SO_2 oxidation rates are given for the various flights where sampling was done at several downwind locations. Also shown are the average wind speed, temperature, and relative humidity at plume height during the flights in question, as measured by radiosondes and/or M/S's. On flights where both filter packs were used to obtain total particulate sulphate concentrations, the average of two SO_2 and SO_4 concentrations were employed to calculate oxidation rates. A word of explanation is in order to clarify the meaning of the last two columns in this table. Consider the flight of 5 February, for example. During this flight, two samples were collected, at 8.0 and 30.6 km from the stack (Table 7). Since the average wind speed was 0.39 $km \cdot min^{-1}$, the plume ages corresponding to these two distances are 21 and 78 min, respectively. The percentage of sulphur in the form of sulphur was found to 1.61 and 1.45, respectively (Table 7). From these data the average conversion rate of sulphur from SO_2 to SO_4 can be calculated to be $-0.2\% \cdot h^{-1}$ during the plume age interval 21-78 min. The other values in Table 8 were obtained in a similar fashion.

Finally, Table 9 shows the results of the neutron activation analysis for samples collected in the GCOS plume near the power plant stack. Also shown is the weight of SO_2 trapped on the chemically impregnated filters from the same plume sample.

Table 8. Conversion rates of SO_2 to $SO_4^{=}$ and meteorological conditions at plume height, GCOS plume study, February 1977.

Date	Time (MST)	Ave. met. parameters at plume height			Plume age interval (min)	σ_v Ave. Conversion % h^{-1}
		Wind ($km.min^{-1}$)	Temp. (^oC)	r.h. (%)		
5 Feb/77	0820-1015	0.39	-13	89	21 - 78	-0.2
6 Feb/77	0815-1014	0.39	-2	93	7 - 68	1.3
	1435-1620	0.51	0	58	2- 33	0.1
7 Feb/77	0825-1007	0.54	0	83	1 - 35	-.04
8 Feb/77	0825-1010	0.48	3	60	2 - 70	-0.2
10 Feb/77	0830-1030	0.47	-1	82	2 - 21	-1.2
11 Feb/77	0847-0940	0.48	-3	90	3 - 15	2.4
	1415-1630	0.44	-3	75	5 - 27	0.2

σ_v Conversion of sulphur from SO_2 to SO_4

5.4 DISCUSSION OF EXPERIMENTAL RESULTS

The plume dispersion rate results are considered elsewhere in this report (see Section 4). We confine our present discussion to SO_2 oxidation rates and related considerations.

The results in Table 7 show that near the GCOS power plant chimney the percentage of sulphur in the plume in the form of sulphate varies between 0.7 and 1.5, with an average value of 1.3. About 80% of the particulate sulphur seems to be in the form of sulphuric acid. Within experimental scatter, the ratio of sulphuric acid to total sulphates in the particulate matter remains independent of the distance from the chimney. For distances up to 3.4 km from the stack, more than 95% of the plume sulphur is in the gaseous form.

During the February field study, there was very little oxidation of sulphur dioxide to particulate sulphates in the GCOS power plant plume, as can be seen from Table 7. Column 7 of that table shows as many positive as negative values of the oxidation rate, and one can conclude that, within experimental scatter of the data, the oxidation rate is essentially zero. This is a somewhat surprising result. Although the photochemical oxidation of SO_2 by homogeneous gas-phase processes is expected to be slow during the winter months at the northern latitude of the GCOS plant (see, for example, Bottenheim and Strausz 1977), the particulate loading of the emissions is relatively high, so that heterogeneous SO_2 oxidation mechanisms on particulate surfaces or in aerosols (Foster 1969; Freiberg 1974) could be important. The latter expectation was reinforced by the fact that an analysis of the fly ash collected at the GCOS plant during November and December of 1975 (Shelfentook 1978) showed appreciable amounts of the potential catalysts iron and vanadium to be present (about 5 and 2.5%, respectively, by weight). Freiberg (1974) has suggested that soluble iron, especially at low temperatures and high relative

humidities, can act as an effective catalyst for the oxidation of SO_2 to sulphates in aerosols. Lusis and Phillips (1977) have used Freiberg's chemical model for iron-catalysed SO_2 oxidation in aerosols to obtain the following expression for the conversion of SO_2 in a plume:

$$\frac{1}{f_2} - \frac{1}{f_1} = \frac{kQ_{Fe}\, Q_{SO_2}}{12\ (1-RH)^3\ (\pi U)^2} \int_{t_1}^{t_2} \frac{}{(\sigma_y\, \sigma_x)^2}$$

where f_1, f_2 = fraction of SO_2 remaining in the plume at the plume ages t_1, t_2 (min) respectively,

Q_{SO_2}, Q_{Fe} = emission rate of SO_2 and soluble iron (g mol·min^{-1}) respectively

RH = relative humidity at plume height

U = wind speed (m·min^{-1})

$\sigma_y \sigma_z$ = horizontal and vertical dispersion coefficients (m), respectively

k = a constant which is a function of rate, equilibrium, and Ostwald constants as well as the ambient ammonia concentration and the vapour pressure lowering coefficient of sulphuric acid. See Lusis and Phillips (1977) and Freiberg (1974) for a full discussion of the terms involved.

This expression was used to estimate oxidation rates that might be expected by an iron-catalysed mechanism in aerosols, for some of the experiments from the GCOS plume study of February 1977. Meteorological data and dispersion coefficients were taken from Tables 6 and 8. The data necessary for calculating k were taken from Freiberg (1974) and Lusis and Phillips (1977), with the exception of the NH_3 concentration. Here it was assumed that a value of 0.18×10^{-6} mol·m^{-2} would be more representative of wintertime conditions around the GCOS plant than the 0.6×10^{-6} previously used.

The former value has been given by Junge and Ryan (1958) as typical for fairly clean country air in the northeastern U.S.A., and by Georgii (1977) for Western Germany during the wintertime. The SO_2 emission rates used were those supplied by Mr. M. Strosher of Alberta Environment, while particulate emissions were assumed to be about one-fifth of the SO_2 emission. Following Freiberg (1976), it was assumed that about 8% of the emitted iron was soluble and catalytically active. The calculations indicated that the oxidation rate should be significant ($<2\% \cdot h^{-1}$) for flights carried out during low temperature and/or high relative humidity atmospheric conditions (such as those on 5 and 6 February). The reason for the absence of SO_2 oxidation in the plume of the GCOS plant is not clear. Several workers (Foster 1969; Newman et al. 1975; Freiberg 1976) have suggested that heterogeneous SO_2 oxidation mechanism is important in power plant plumes. Although our findings are far from conclusive, they seem to contradict this. In this connection, it is interesting to cite here one flight in particular. On the morning of 8 February, the plume was observed to be extremely dirty and brownish in colour, presumably due to some change in the power plant operation. A sample was collected about 34 km from the chimney right after sunrise, so that the air parcel, which had a plume age of slightly over 1 h, could not have been exposed to significant amounts of solar radiation. Although the particulate loading was so high that a dark stain was observed on the Whatman 40 filter papers, there was no apparent oxidation of SO_2 in the plume (see Table 8). On the other hand, data from other recent field studies of chimney plumes (Davis et al. 1974; Wilson et al. 1976) have pointed to the importance of photochemical homogeneous gas-phase reactions in SO_2 oxidation. Because of the low actinic irradiance during February at the location of the GCOS plant, oxidation rates by such processes would be expected to be slow; this is consistent with our observations. However, during

the summer months homogeneous reactions could become quite important (Bottenheim and Strausz 1977), and thus it will be very interesting to see what results the June 1977 field study yields.

Unfortunately, the particulate matter samples collected near the chimney were too small for accurate analysis of many of the elements by the neutron activation technique. As can be seen from Table 9, quantitative results were obtained only for Mn, Na, V, Al, Cl, K, and Cr. Of these seven metals, only V and Al were found in the particulate matter in amounts (column 7 of Table 9) significantly above the amounts in the filter blank (column 2). It is interesting to note that the ratio of V/Al in the plume particulate samples is 0.24, in close agreement with the value of 0.22 obtained from an anlysis of some fly ash samples collected during tests on an electrostatic precipitator at the plant in November and December 1975 (Shelfentook 1978). The ratio of the weights of Al and V to that of SO_2 was found to be 4.1×10^{-3} and 1×10^{-3}, respectively, from the plume samples (Table 9).

During the June 1977 field study, it is planned to collect considerably larger samples near the chimney to get quantitative data for more metals than was possible from the February study.

Table 9. Results of neutron activation analysis for heavy metals in particulate matter of the GCOS plume (all quantities in μg).

Heavy Metal	Blank Filter	Samples 1	2	3	4	Average (less blank)
SO_2 [σ]	-	506.000	544.000	494.000	522.000	517.000
Ti	<0.280	0.620	<0.430	<0.450	0.460	<0.620
Mg	<0.900	<1.800	<0.800	<1.500	<1.800	<1.800
Mn	0.032	0.068	0.056	0.460	0.051	0.024
Cu	<0.170	<0.360	<0.300	<0.340	<0.380	<0.380
Na	15.000	14.000	19.000	13.000	19.000	1.000
V	0.024	0.660	0.330	0.540	0.710	0.540
Al	0.470	3.610	1.990	2.100	2.650	2.120
Cl	20.000	23.000	23.000	22.000	28.000	4.000
Ca	<3.300	4.400	<4.400	<3.500	<4.300	<4.400
Si	<80.000	<120.000	110.000	<120.000	<120.000	<120.000
As		.....<0.015....				<0.015
K	5.300	7.900	5.900	7.200	5.100	1.200
Zn		.....<0.300....				<0.300
Cr	0.280	0.400	0.410	0.200	0.290	0.050
Ni		.....<2.000....				<2.000
Fe		.....<6.000....				<6.000
Sc		.....<1.000....				<1.000

[σ] Determined by isotope dilution model

6. CONCLUDING REMARKS AND RECOMMENDATIONS

Different aspects of air pollution studies have been discussed in this report. The studies illustrate the important role that meteorology, topography, and plume chemistry play in the dispersion of air pollutants.

Most of the results described in this report are the outcome of the February 1977 field study. Some of the results, however, incorporate those obtained during March of the previous year, for comparative reasons. Although during those two months the local weather conditions were abnormally warm, the program was successful and provided valuable information on the meteorology of the AOSERP study area and on the dispersion and chemistry of the GCOS plume.

For the majority of the experiments, surface inversion conditions were observed. During this condition, it was noted that:

1. The wind in the valley decoupled from the winds aloft with the flow aligning with the valley walls.
2. The winds at the Syncrude Mine Site showed a similar shifting of the surface winds to align along the valley direction. These results suggest that during stable conditions the flow through the surface inversion is strongly influenced by the broad topographical basin in which the Athabasca River is situated.

This implies that during stable conditions winds observed from towers situated within this inversion should show biases of wind direction along the valley direction. Wind roses plotted on a monthly basis should consequently indicate a high frequency of winds aligned along the valley (SE flow possibly predominating) during the stable winter months, which is not necessarily related to the winds aloft.

3. Two cases were observed where the colder basin air was trapped by warmer air aloft. During the day, a slow erosion of the upper interface proceeded with the strengthening of the inversion at the height of the valley wall. It appears that this inversion acts as a lid on moisture flux out of the valley so that a thin moist layer forms along the interface.
4. At the Syncrude Mine Site, local wind maxima up to twice the speed measured by the M/S were observed to track the top of the surface inversion.
5. During lapse conditions, the lower winds were nc longer decoupled from the flow aloft, suggesting that the topography had little influence on the wind field.
6. During neutral or unstable conditions (i.e., summer months), wind roses would be more representative of winds aloft, because the wind field is no longer affected by topographical effects.
7. Coupled with the results of the previous experiment (Fanaki 1978) it would appear that, under stable conditions, ground base emissions at the Syncrude Mine Site will tend to flow along the valley. Because the surface-based inversion at the Mine Site is effectively an elevated inversion at the GCOS plant, emissions from the latter stack would occur along the direction of the predominating wind field.
8. The rise of the GCOS plume is complicated by the frequent occurrence of inversion layers during the winter. Again, the Holland (1953) and Briggs (1972) formulas appear to predict the rise of the plume better than the other formulas examined in this study. It is felt, however, that other models e.g., Moore's (1974) and Csanady's (1965) should be applied later to examine their predictive capabilities, especially under stable conditions.

9. The model proposed by Briggs for stratified conditions underestimates the actual rise of the plume. However, Briggs's model predicts the maximum observed rise of the plume when it is capped by an inversion layer. As noted earlier, the formulas tested were not the Briggs formulas for two-layer or multilayer atmospheres (limited mixing). A test of these more refined formulations may provide the desired agreement between observations and predictions. Alternatively, one could re-examine the fundamental governing differential equations and devise a better method of predicting plume rise, for instance, by numerically integrating some simplified version.
10. The lack of agreement between the concurrent bivane measurements and σ_z of the plume using existing models indicates that care must be taken in applying the bivane results to the GCOS plume.
11. Most of the stability conditions covered in this study were stable, where frequent inversion layers occurred. The diffusion of the GCOS plume, under such conditions, is suppressed along the vertical. In such cases a bivane at a different location and at a different level may produce results that do not describe the dispersive characteristics of the plume.
12. The TVA model of σ_z appears to predict the observed plume dispersion coefficients better than the Pasquill-Gifford model. The reverse if true for σ_y.

Agreement between the sounder data and those obtained by the sondes is good. This implies that the sounder may be used successfully to measure inversion heights in the AOSERP study area. At least one M/S station should be used with the acoustic system for calibration purposes.

13. For winter conditions, SO_2 oxidation rates in the plume of the GCOS power plant are very low, in spite of the considerable potential for heterogeneous chemical processes. The results suggest that, for those conditions, oxidation of SO_2 can be neglected in mathematical models describing the GCOS emissions. However, this may not be wise for other times of the year, and further work is necessary, especially under summer atmospheric conditions.
14. To what extent the results described in this report apply to other sources in the AOSERP study area is not yet known. Further work with other sources in the area is certainly warranted.

7. REFERENCES CITED

Bottenheim, J.W., and O.P. Strausz. 1977. Review of pollutant transformation process relevant to the Alberta Oil Sands area. Prep. for the Alberta Oil Sands Environmental Research Program by the University of Alberta, Hydrocarbon Research Centre. AOSERP Report 25. 166 pp.

Briggs, G.A. 1969. Plume rise. AEC Critical Review Series TID-25075; National Technical Information Service. 81 pp.

Briggs, G.A. 1971. Some recent analyses of plume rise observations. Pages 1029-1032 in Proceedings, Second International Clean Air Congress. Academic Press.

Briggs, G.A. 1972. Discussion on chimney plumes in neutral and stable surroundings. Atmos. Environ. 6:507-510.

Briggs, G.A. 1975. Plume rise predictions. Lectures on air pollution and environmental impact analyses. Am. Meteorol. Soc. 59-104.

Brummage, K.G. 1968. The calculation of atmospheric dispersion from a stack. Atmos. Environ. 2:197.

Carpenter, S.B., T.L. Montgomery, J.M. Leavitt, W.C. Colbaugh, and F.W. Thomas. 1971. Principal plume dispersion models TVA Power Plants. J. Air Pollut. Control Assoc. 21:491-495.

Csanady, G.T. 1965. The buoyant motion within a hot gas plume in a horizontal wind. J. Fluid Mech. 22:225-238.

Csanady, G.T. 1973. Turbulent diffusion in the environment. Page 248 in Geophysics and Astrophysics Monographs. D. Reidel Publishing Company, Dordrecht-Holland.

Davis, D.D., G. Smith, and G. Glauber. 1974. Trace gas analysis of power plant plumes via aircraft measurements: O_3, NO_x, and SO_2 chemistry. Science 186:733-736.

Fanaki, F., compiler. 1978. Meteorology and air quality winter field studies in the AOSERP study area, March 1976. Prep. for the Alberta Oil Sands Environmental Research Program by Fisheries and Environment Canada, Atmospheric Environment Service. AOSERP Report 27. 249 pp.

Fanaki, F.H., J. Kovalick, and R. Froud. 1978. Plume rise. Pages 48-91 in Fanaki, F., compiler. Meteorology and air quality winter field study, March 1976. Prep. for the Alberta Oil Sands Environment Research Program by Fisheries and Environment Canada, Atmospheric Environment Service. AOSERP Report 27. 249 pp.

Foster, P.M. 1969. The oxidation of sulphur dioxide in power station plumes. Atmos. Environ. 3:157-175.

Freiberg, J. 1974. Effects of relative humidity and temperature on iron-catalysed oxidation of SO_2 in atmospheric aerosols. Environ. Sci. Technol. 8:731-734.

Freiberg, J. 1976. The iron catalysed oxidation of SO_2 to acid and sulphate mist in dispersing plumes. Atmos. Environ. 10:21-130.

Georgil, H.W. 1977. Spatial and temporal distribution of sulphur compounds. International Symposium on Sulphur in the Atmosphere, Dobrounik, Sept. 7-14.

Gifford, F.A. 1960. Some recent atmospheric dispersion observations. Nucl. Saf. (U.S.A.E.C., Oak Ridge, Tennessee) 1:56-62.

Hay, J.S., and F. Pasquill. 1959. Diffusion from a continuous source in relation to the spectrum of turbulence. Advances in Geophysics 6:346-365. F.N. Frankiel and P.S. Sheppard, eds. Academic Press Inc., New York.

Hicks, R.B., D. Smith, and T. Mathews. 1977. Preliminary results of atmospheric acoustic sounding at Calgary. J. Boundary-Layer Meteorol. 12(2):201-212.

Holland, J.Z. 1953. A meteorological survey of the Oak Ridge area. U.S. Atomic Energy Commission Report ORO-99, 554 pp.

Junge, C.E., and T.G. Ryan. 1958. Study of SO_2 oxidation in solution and its role in atmospheric chemistry. Q. J. R. Meteorol. Soc. 84:46-55.

Kerman, B.R., and H.E. Turner. 1978. An applicaton of acoustic sounding to the estimation of mixing depth and vertical plume spread in the Alberta Oil Sands area. Pages 22-47 in Fanaki, F., compiler Meteorology and air quality winter field study in the AOSERP study area, March 1976. Prep. for the Alberta Oil Sands Environmental Research Program by Fisheries and Environment Canada, Atmospheric Environment Service. AOSERP Report 27. 249 pp.

Klockow, D., and H. Denzinger. 1976. Determination of sulphate by sub-stoichiometric isotopic dilution analysis. European Monitoring Programme Manual for sampling and Chemical Analysis Procedures, Norwegian Institute for Air Research, P.O. Box 130, N-2001, Lillestrom, Norway.

Larsen, R.I., F.B. Benson, and G.A. Jutze. 1965. Improving the dynamic response of continuous air pollutant measurements with a computer. J. Air Pollut. Control Assoc. 15:19-22.

Leahy, D.R., R. Siegel, P. Klotz, and L. Newman. 1975. The separation and characterization of sulphate aerosol. Atmos. Environ. 9:219-229.

Lusis, M.A. 1976. The effect of sample humidity on the response characteristics of SO_2 and NO_x analyser system. Report ARQA el-76, Atmospheric Environment Service, Downsview, Ontario.

Lusis, M.A., and C.R. Phillips. 1977. The oxidation of SO_2 to sulphates in dispersing plumes. Atmos. Environ. 11:239-241.

Markowski, G.R. 1975. A useful method for transient response analysis and data correction applied to aircraft plume sampling. 68th Annu. Meet., Air Pollut. Control Assoc., Boston, June 15-20.

Montgomery, T.L., S.B. Carpenter, W.C. Colbaugh, and F.W. Thomas. 1971. Fullscale study of plume rise at large electric generating stations - Bull Run supplement. Air Quality Branch, Tennessee Valley Authority. Muscle Shoals, Ala. 58 pp.

Montgomery, T.L., S.B. Carpenter, W.C. Colbaugh, and F.W. Thomas. 1972. Results of recent TVA investigations of plume rise. J. Air Pollut. Control Assoc. 22:779-784.

Moore, D.J. 1974. A comparison of the trajectories of rising buoyant plumes with theoretical empirical models. Atmos. Environ. 8:441-457.

Moses, H., and J.E. Carson. 1967. Stack design parameters influencing plume rise. 60th Annu. Meet. Air Pollut. Contr. Assoc., Clevelant, Ohio. Pap. 67-84.

Munn, R.E. 1964. Turbulence statistics at Douglas Point. J. Appl. Meteorol. 3:771-779.

Newman, L., J. Forrest, and B. Manowitz. 1975. The application of an isotopic ratio technique to a study of the atmospheric oxidation of sulphur dioxide in the plume from a coal fired power plant. Atmos. Environ. 9:969-977.

Pasquill, F. 1974. Atmospheric diffusion, 2nd Ed. Ellis Horwood Ltd. 429 pp.

Pasquill, F. 1975. The dispersion of material in the atmospheric boundary layer--the basis for generalization. Lectures on Air Pollution and Environmental Impact Analysis, 1-34. Am. Meteorol. Soc.

Persson, G.A. 1966. Automatic colorimetric determination of concentrations of sulphate for measuring sulphur dioxide in ambient air. Air Water Pollut. Int. J. 10:845-852.

Shelfentook, W. 1978. An inventory system for atmospheric emissions in the AOSERP study area. Prep. for the Alberta Oil Sands Environmental Research Program by SNC Tottrup Ltd. AOSERP Report 29. 58 pp.

Small, H., T.S. Stevens, and W.C. Bauman. 1975. Novel ion exchange chromatographic method using conductometric detection. Anal. Chem. 47:1801-1809.

Turner, D.B. 1967. Workbook of atmospheric dispersion estimates. Public Health Service Publication 999-AP-26, U.S. Dep. of Health, Education, and Welfare. 84 pp.

Wilson, W.E., R.B. Husar, W.H. White, K.T. Whitby, and D.B. Kittleson. 1976. Chemical reactions in power plant plumes. Am. Chem. Soc. 171st Natl. Meet., New York, April 4-9.

Wyckoff, R.J., D.W. Beran, and F.F. Jr. Hall. 1973. A comparison of the low-level radiosonde and the acoustic echo sounder for monitoring atmospheric stability. J. Appl. Meteorol. 12:1196-1204.

8. APPENDICES

8.1 SYNOPTIC CONDITIONS

8.1.1 3 February 1977

A weak low linked with the quasi-stationary front had evolved over the AOSERP study area during early morning hours. As this low migrated southeast into southern Saskatchewan during the morning, a strong ridge gradually replaced it over the area (Figure 65).

Overbast weather returned during the morning with thick cumulus and altocumulus cloud cover. With displacement of the front south of the region by the high pressure ridge, skies began to clear rapidly, and by late afternoon stratocumulus cloud coverage had been reduced to one-tenth. A strong frontal inversion based at about 500 m developed at this time. Visibility extended to 15 nautical miles throughout the day.

Winds were westerly at 4-6 $m.s^{-1}$ during morning hours, but veered to northwesterly at 2-4 $m.s^{-1}$ after passage of the cold front.

8.1.2 4 February 1977

The ridge had intensified while spreading over northern Alberta and Saskatchewan. The quasi-stationary front had been displaced about 500 km southwest of Fort McMurray by early morning (Figure 66).

Relatively cold air mass returned to the AOSERP study area. Low stratocumulus, which gradually covered most of the sky by early morning, brought continuous, light, snowflurry activity. The deep, elevated frontal inversion continued to exist throughout the day with base about 600 m above ground. Mostly sunny afternoon skies gave way to high altocumulus clouds covering nine-tenths of the sky. Visibility remained very good.

Winds were calm throughout the morning hours but picked up from the southwest at 0.5-1.0 $m.s^{-1}$ by late afternoon.

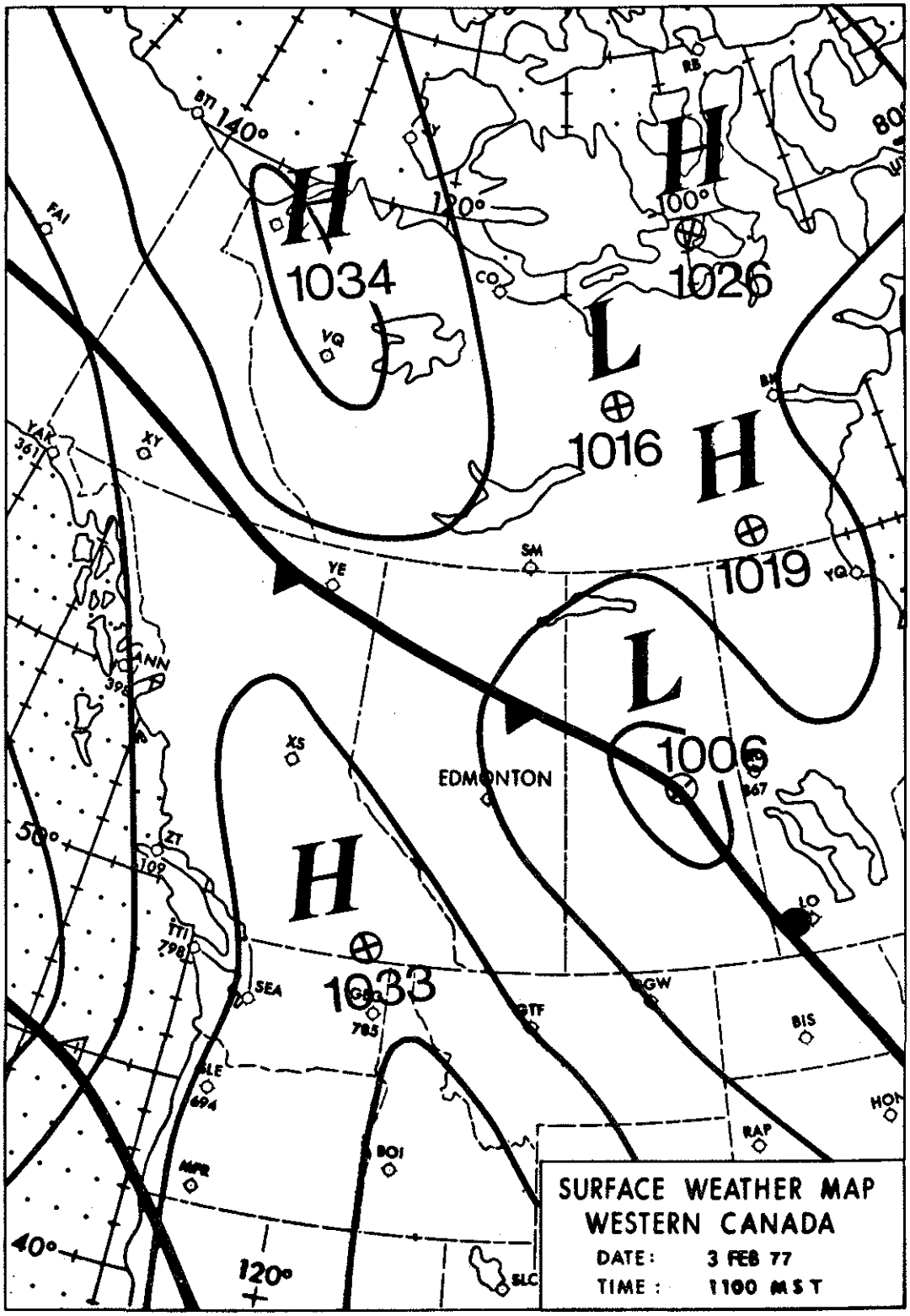

Figure 65. Surface pressure contours for 3 February 1977, 1100 MST.

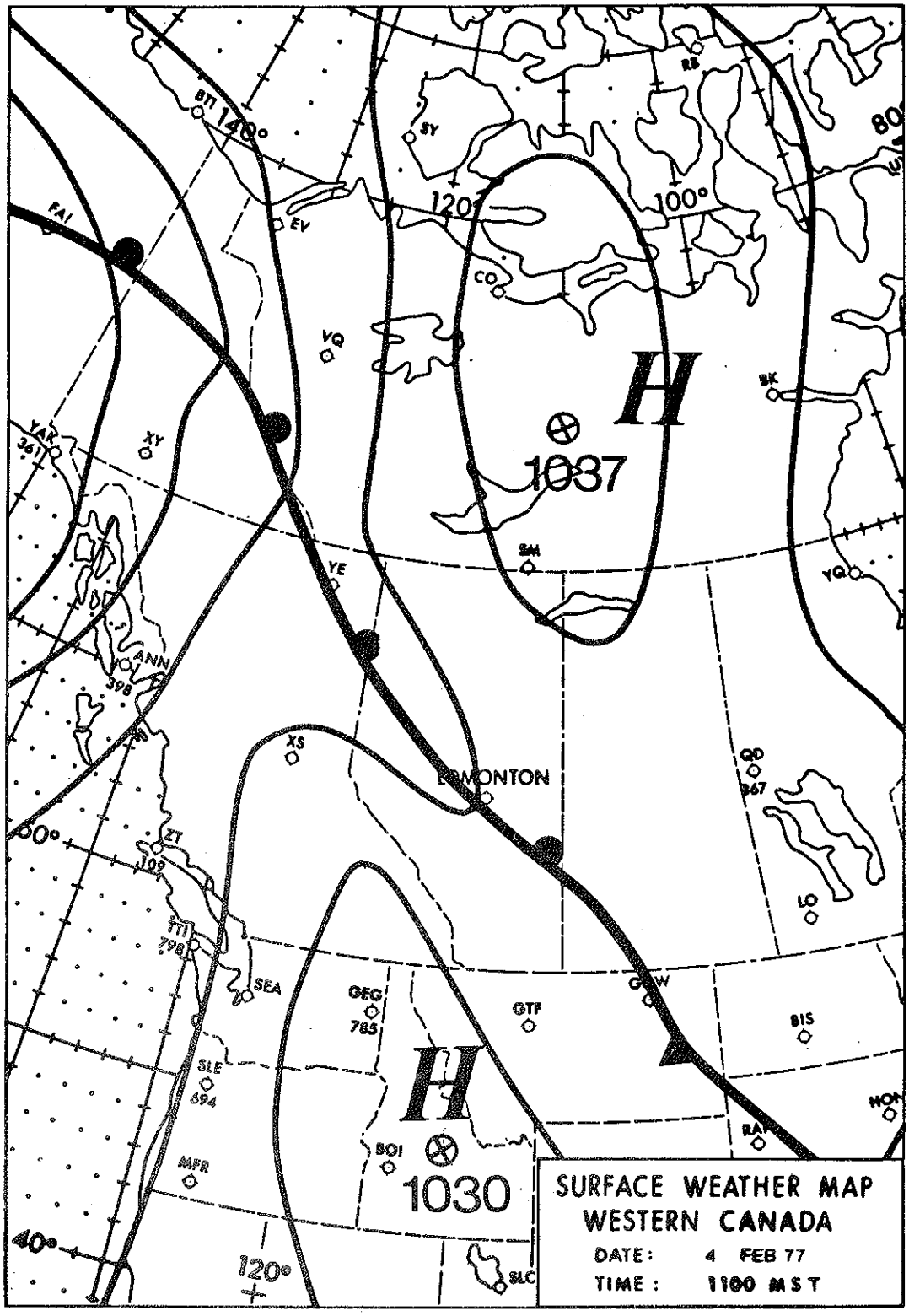

Figure 66. Surface pressure contours for 4 February 1977, 1100 MST.

8.1.3 5 February 1977

The high-pressure ridge over the AOSERP study area had weakened slightly while spreading further eastward. The quasi-stationary frontal system over central Alberta remained parallel to the Rocky Mountains during the morning. By afternoon the front's axis had shifted slightly, causing it to be north-south oriented and still 600 km southwest of the study area (Figure 67).

Partly cloudly weather with low stratocumulus clouds and stable lapse rate conditions continued to prevail throughout the day. Altocumulus cloud cover became more extensive around noon, but skies cleared rapidly during the afternoon. Retreat of the warm front of the quasi-stationary system back towards the study area weakened the deep frontal inversion late in the afternoon. Visibility remained very good.

Winds were from the southeast at 1-2 $m \cdot s^{-1}$ under anti-cyclone ciruclation during the morning but became calm as the warm front approached.

8.1.4 6 February 1977

The ridge intensified farther over the southern Prairies. The elongated quasi-stationary front remained north-south oriented about 100 km west of the AOSERP study area during the morning. By late afternoon this front was directly over the Lower Syncrude Site, and a weak trough developed over Lake Athabasca (Figure 68).

Clear weather with slightly stable lapse rate conditions continued to dominate the AOSERP study area through morning and early afternoon hours. As the quasi-stationary front retreated northeastward, the portion approaching the study area--a warm front aloft--reduced the elevated frontal inversion to ground level. As the warm front passed through the area during late morning and afternoon hours, the weak frontal inversion gradually subsided and weakened under rapidly clearing skies. Visibility remained very good.

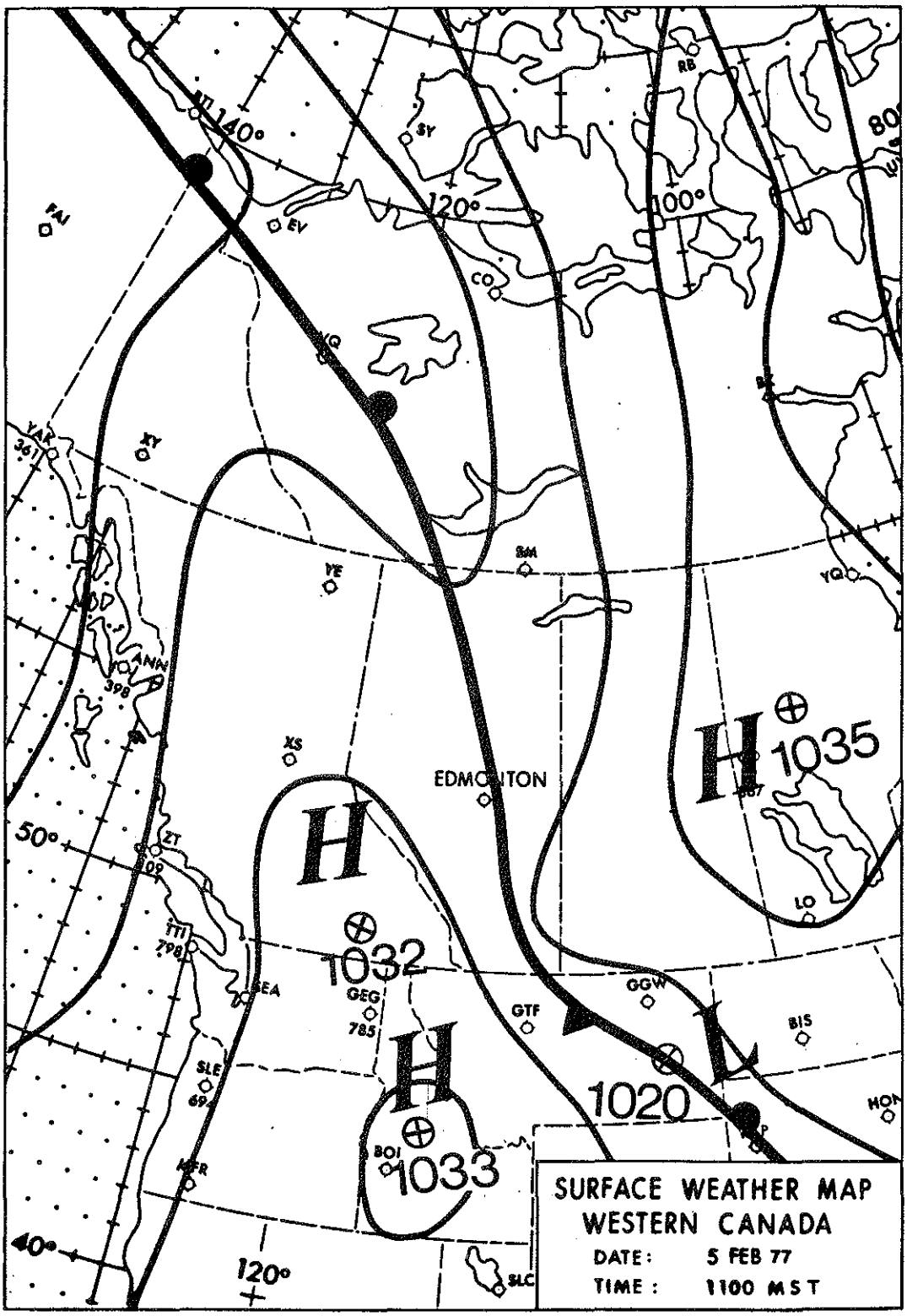

Figure 67. Surface pressure contours for 5 February 1977, 1100 MST.

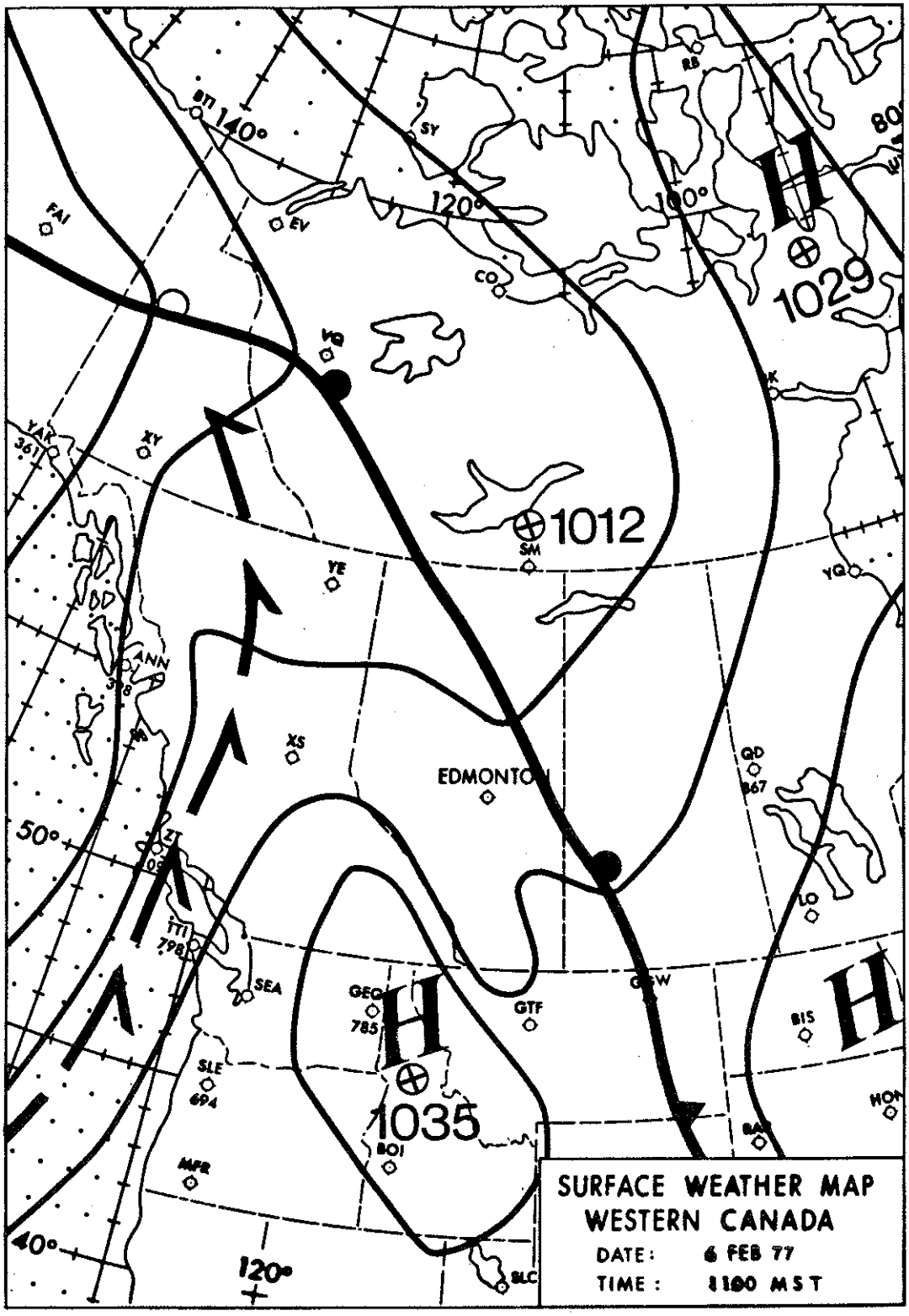

Figure 68. Surface pressure contours for 6 February 1977, 1100 MST.

Winds were calm before passage of the warm front but picked up from the west at 2-4 $m \cdot s^{-1}$ by afternoon.

8.1.5 7 February 1977

The high-pressure ridge strengthened further over Manitoba and the northern trough passed through Saskatchewan coupled to the frontal system. An occluded front linked to a low off the British Columbia coast also linked up with a developing upstream trough over Lake Athabasca. By late afternoon this occlusion had passed east of the AOSERP study area (Figure 69).

Remnants of the frontal inversion resulting from the front maintained clear, stable conditions until early afternoon. The occlusion brought increasing altocumulus cloud cover at this time, but by late afternoon clearing skies resulted in destabilization. Visibility remained very good.

Winds were calm until early afternoon, when they picked up to 6-8 $m \cdot s^{-1}$ from the west. Midafternoon freezing levels rose to a height of about 3000 m above ground.

8.1.6 8 February 1977

The quasi-stationary front immediately north of the AOSERP study area continued to dominate weather patterns in the area. A strong ridge had developed over southern British Columbia ahead of another occluded low disturbance off the coast (Figure 70).

Cloudy, stable conditions due to the frontal inversion remained throughout the morning hours. As altocumulus and stratocumulus clouds broke up in the early afternoon, rapid destabilization led to surface heating. Visibility continued to be very good.

Winds were calm in the early morning but picked up from the west at 2-4 $m \cdot s^{-1}$ by late morning before becoming calm again by midafternoon. Midday freezing level heights fell to about 2500 m.

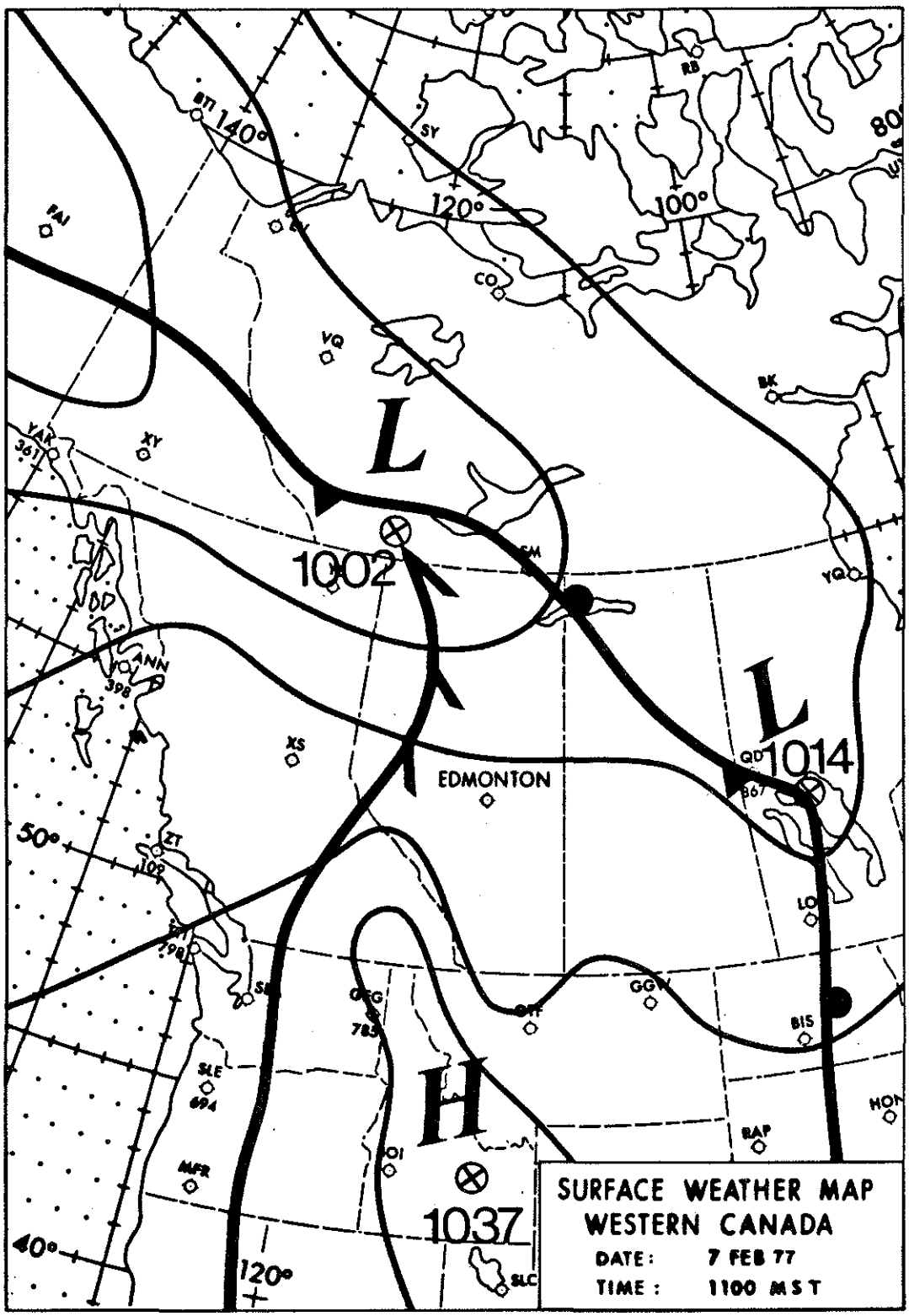

Figure 69. Surface pressure contours for 7 February 1977, 1100 MST.

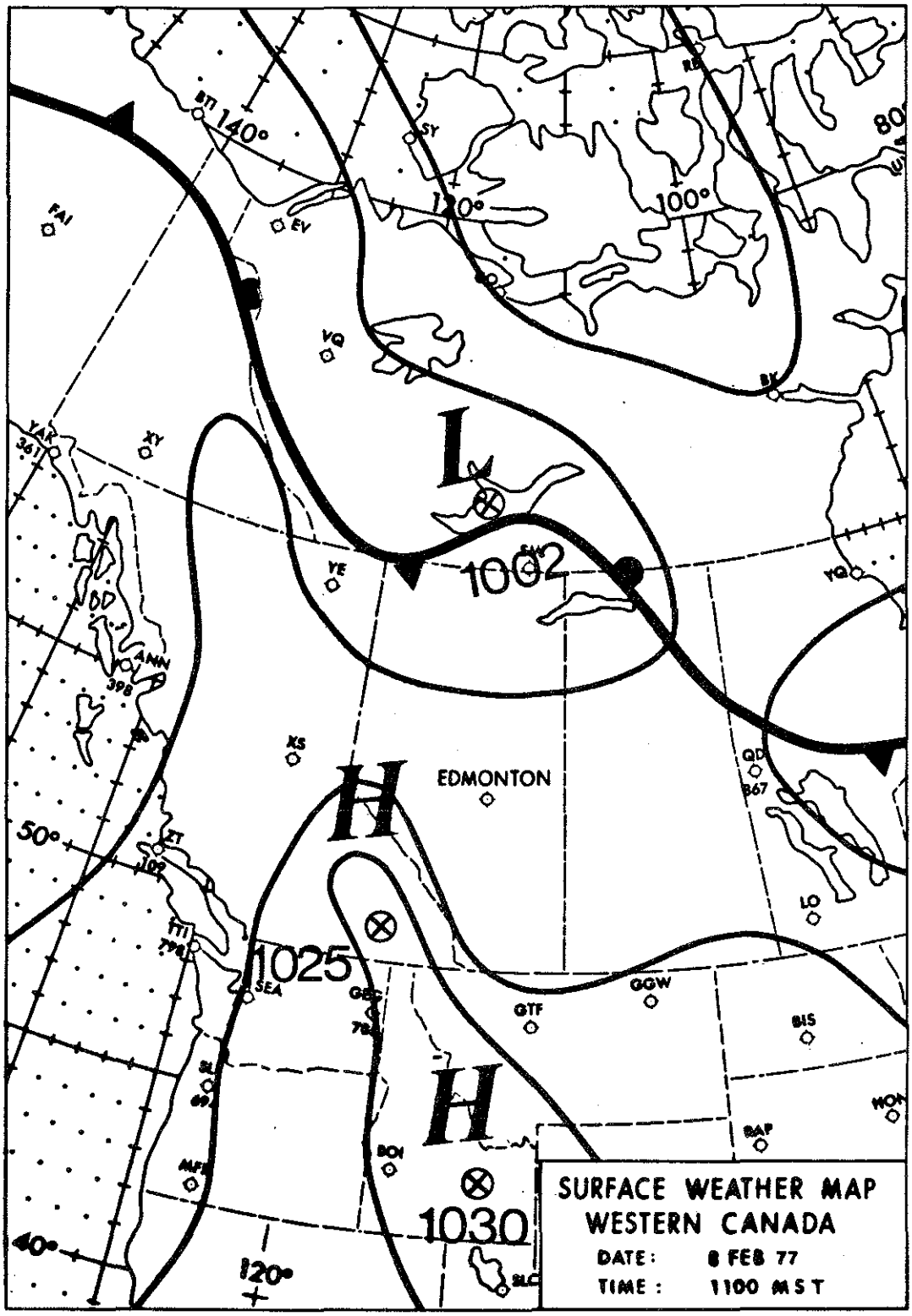

Figure 70. Surface pressure contours for 8 February 1977, 1100 MST.

8.1.7 9 February 1977

The frontal networks remained almost unchanged from those patterns prevailing over the previous few days. The trough formerly over Lake Athabasca had moved along the quasi-stationary front to Lake Winnipeg. The coastal occlusion had moved inland and, coupled with the frontal network, generated another closed low disturbance over the AOSERP study area (Figure 71). Partly cloudy weather with mild stable lapse conditions due to the frontal inversion returned during the morning. Passage of the occluded front of the coastal disturbance maintained extensive stratocumulus cloud cover until midafternoon, when clearing skies again brought rapid destabilization. Visibility remained very good.

Winds were from the west-southwest at 2-4 $m \cdot s^{-1}$ during the morning, but became calm by afternoon.

8.1.8 10 February 1977

The low disturbance over the AOSERP study area had moved along the quasi-stationary front to Lake Winnipeg. Another closed low and occluded front pushed into southern British Columbia during the morning and by late afternoon had linked up with the low. A strong high-pressure ridge developed over Utah and Montana (Figure 72).

Partly cloudy, stable weather with a surface frontal inversion persisted throughout the morning for another day. Strong early afternoon destabilization occurred with the breakup of altocumulus and altostratus cloud cover. A shallow frontal inversion returned in late afternoon as the cold frond receded southeast over the AOSERP study area. Visibility remained the same.

Winds were calm throughout morning and afternoon hours, except around noon when they were from the west at 2-4 $m \cdot s^{-1}$. The freezing level briefly rose to about 2500 m above ground during midafternoon.

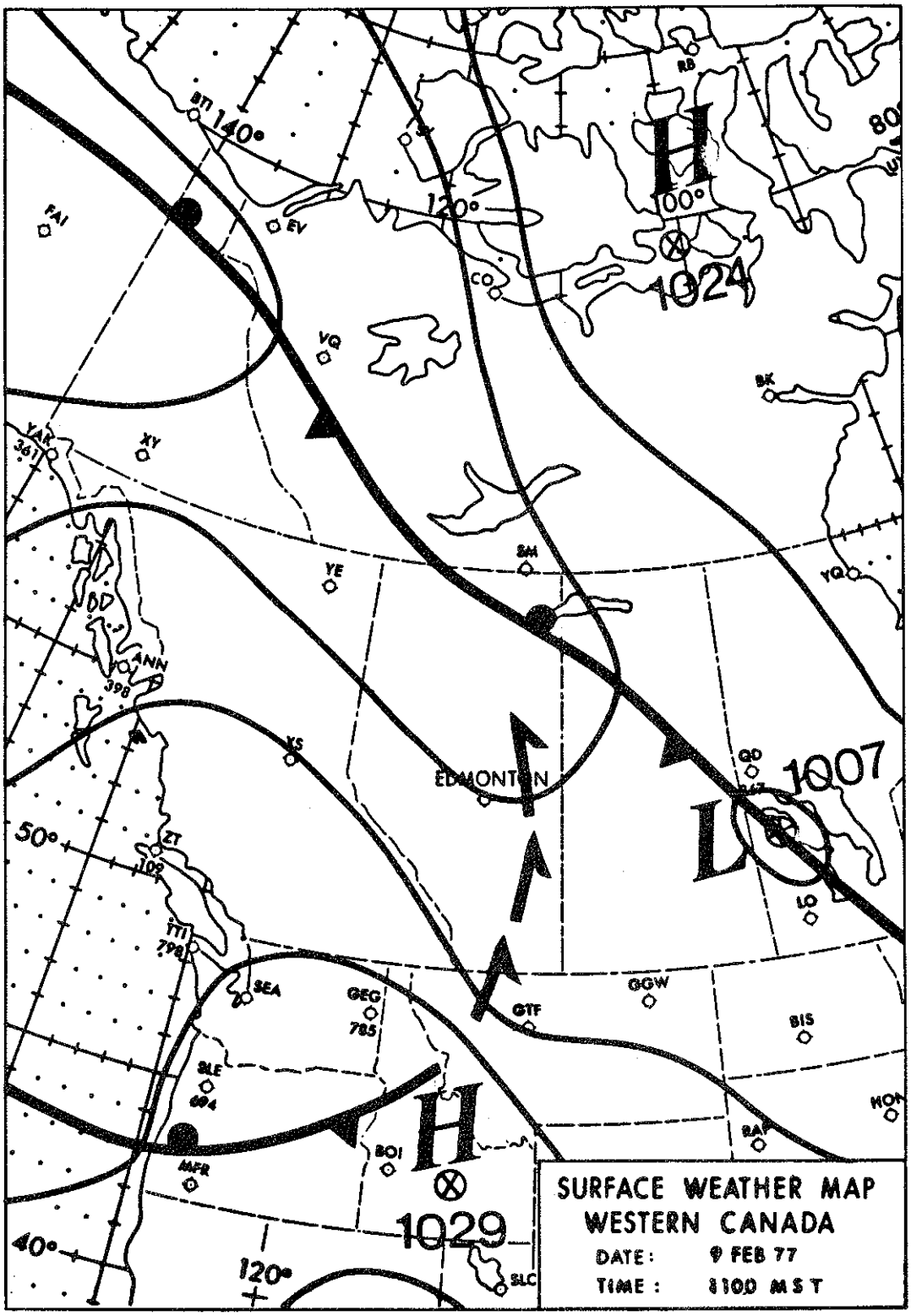

Figure 71. Surface pressure contours for 9 February 1977, 1100 MST.

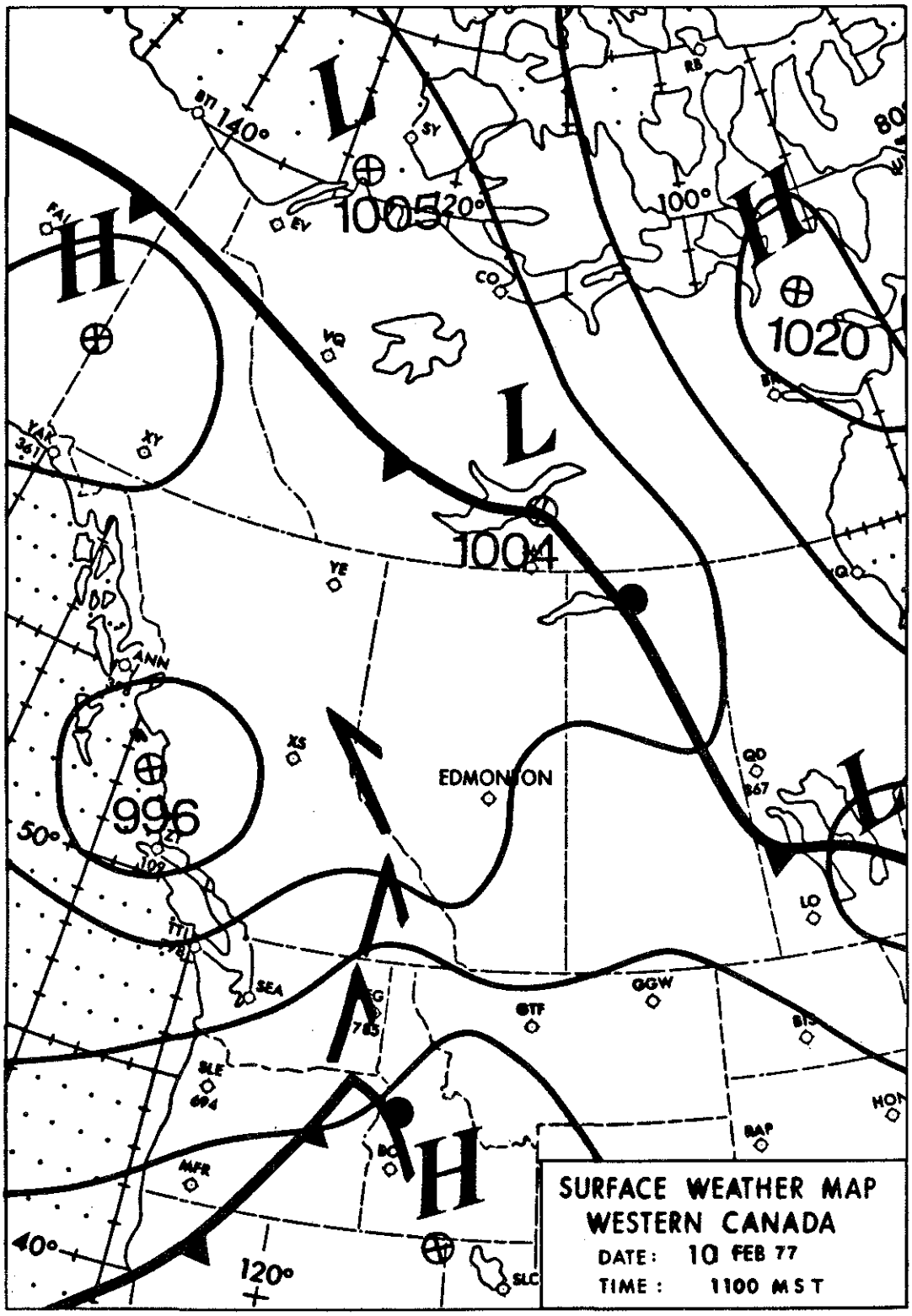

Figure 72. Surface pressure contours for 10 February 1977, 1100 MST.

8.1.9 11 February 1977

The occluded low progressed rapidly across the Prairies during the morning and afternoon hours. The quasi-stationary front had pushed south of the AOSERP study area overnight and remained there until midafternoon when it receded north of the area (Figure 73).

Mild, unstable lapse conditions prevailed in the study area for most of the morning and afternoon. Low stratocumulus and stratusfractus cloudsbrought overcast conditions, during morning and afternoon hours that retarded destabilization. Visibility remained very good.

Winds were from the northwest at 2-4 $m \cdot s^{-1}$ during early morning hours, but backed around to the west-northwest at 6-8 $m \cdot s^{-1}$ by noon. Westerly winds at 2-4 $m \cdot s^{-1}$ persisted for the rest of the day. The freezing level had fallen to a midafternoon maximum of 1 km.

8.1.10 12 February 1977

The closed low had migrated to the Upper Great Lakes while another weak Aleutian low disturbance moved along the quasi-stationary front from the Yukon. A second intense Pacific occluded low evolved off the northern coast of British Columbia. By late afternoon, this low's frontal system was over southern British Columbia, and the occluded front extended to the Yukon (Figure 74).

Mild, unstable, almost isothermal lapse conditions prevailed thorughout morning and afternoon hours. Again the proximity of the stationary front immediately north of the AOSERP study area in late morning and afternoon hours caused an elevated inversion based at about 400 m leading to localized stability. Skies were gradually nine-tenths covered by stratocumulus throughout the day; visibility remained about the same as yesterday.

Winds were calm throughout the day, and the freezing level had fallen to ground level.

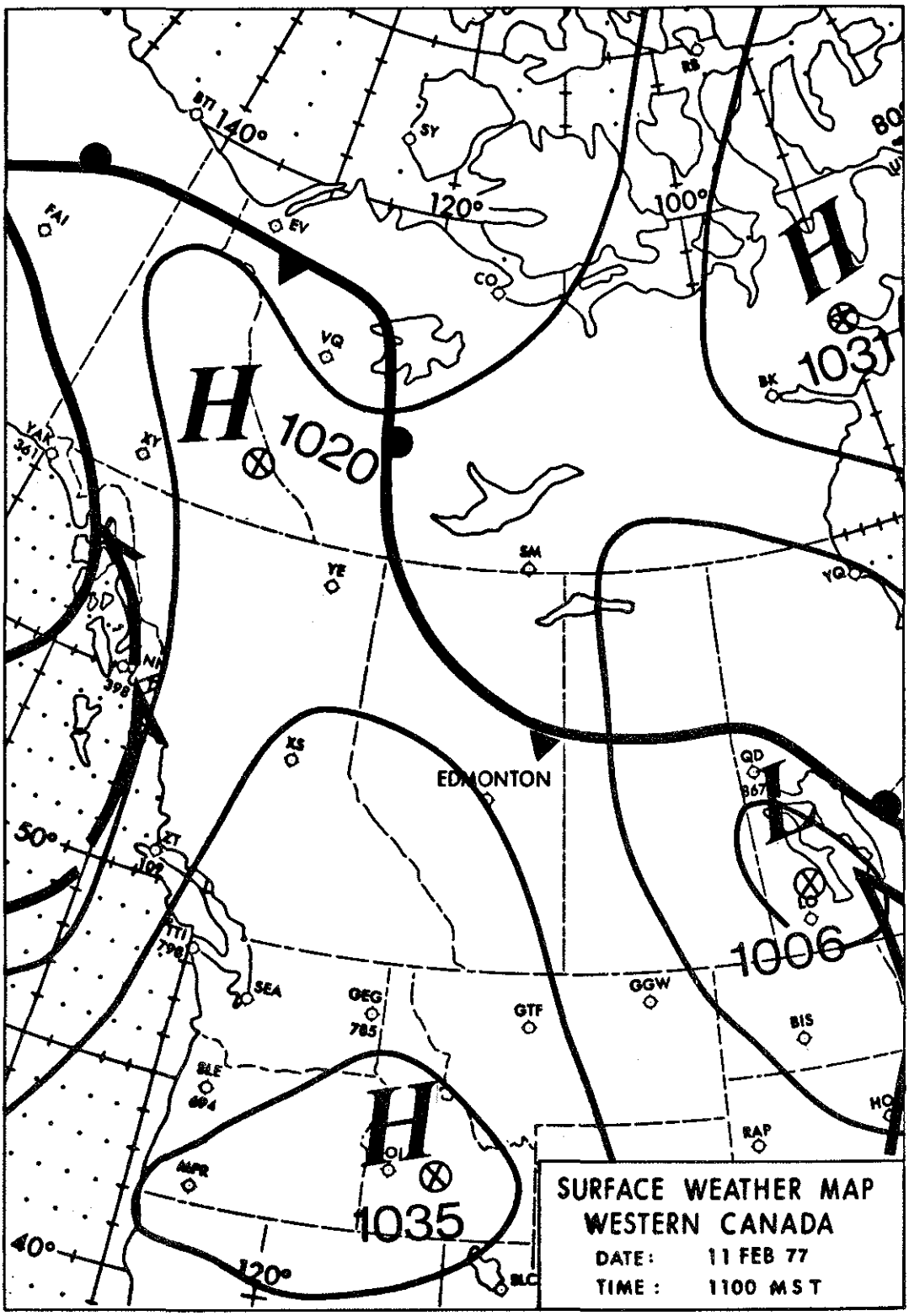

Figure 73. Surface pressure contours for 11 February 1977, 1100 MST.

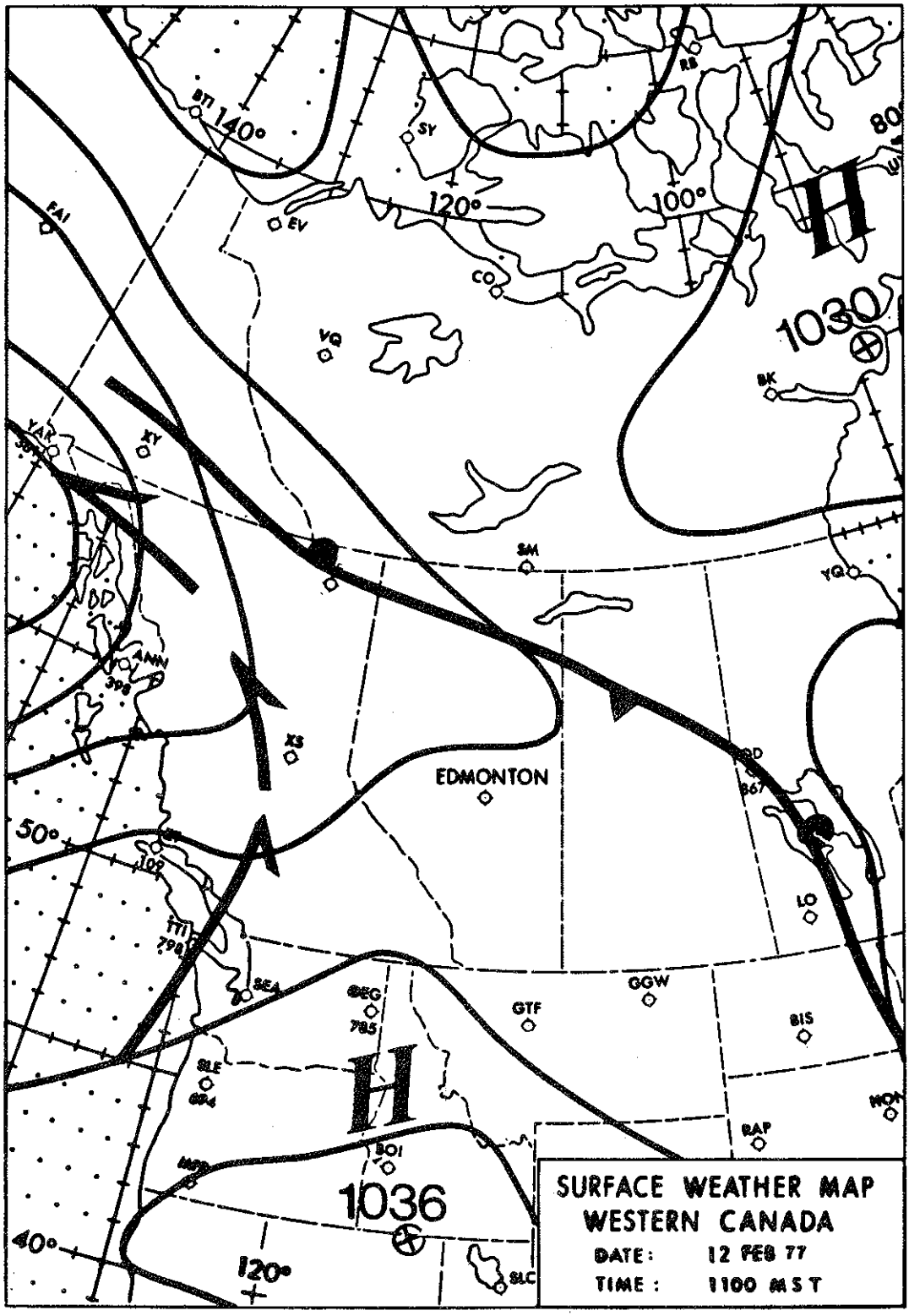

Figure 74. Surface pressure contours for 12 February 1977, 1100 MST.

8.2 DEVELOPMENT AND TESTING OF A FILTER PACK FOR SIMULTANEOUS SAMPLING OF GASEOUS AND PARTICULATE SULPHUR COMPOUNDS IN THE ATMOSPHERE (M.A. LUSIS, L.A. BARRIE, H.A. WIEBE, AND K.G. ANLAUF)

8.2.1 Introduction

Growing concern over the long-range transport of sulphur dioxide and sulphates in North America and Europe (e.g., Altshuller 1976; Wilson et al. 1976; Smith and Jeffrey 1975) had led to intensive efforts in both studying regional flows of sulphur compounds and measuring their chemical transformation and removal rates in the atmosphere. Airborne instrument platforms have played an important role in these studies. Several investigations (Gartrell et al. 1963; Dennis et al. 1969; Stephens and McCaldin 1971; Newman et al. 1975; Lusis and Wiebe 1976; Whitby et al. 1976) have determined SO_2 oxidation and depletion rates in the plumes of strong point sources such as power plants or smelters, using both helicopter and fixed-wing aircraft. Others have used airborne systems over larger space scales. Here one can mention the MISST (Midwest Interstate Sulfur Transport and Transformation Study) studies on the St. Louis urban plume (Husar et al. 1976) and the work of Smith and Jeffrey (1975) on airborne transport of sulphur dioxide from the U.K.

This section describes the development and testing of a filter pack method for sampling sulphur dioxide and aerosols which can be used for aircraft studies of plumes from power plants and other types of chimneys, as well as air masses on a regional scale. Particulate matter is retained on a prefilter, while the gaseous sulphur dioxide is trapped on chemically impregnated filters. In several respects, the method is similar to that of Johnson and Atkins (1975). After considering various techniques used by other investigators, the present method was chosen because:

1. Sulphur dioxide and its oxidation products (sulphates and sulphuric acid can be measured in the same air volume, thus giving directly the proportions of

particulate and gaseous sulphur (this is of particular advantage in cases wehre there are sharp concentration gradients, as in plumes);

2. The equipment is relatively simple, compact, and rugged, and therefore well suited for aircraft sampling. For the same reasons, it is capable of being used on the ground by relatively inexperienced personnel (e.g., in a regional sampling network); and
3. The cumulative nature of the technique is of advantage in studies of regional air masses where the sulphur dioxide concentration is often below the detection limits of continuous SO_2 analysers.

The following sections describe in detail the filter pack, and laboratory and field studies carried out to test its performance.

8.2.2 Description of the Equipment

8.2.2.1 Filter-Pack Design. The filter-pack was constructed by modifying a commercial filter holder (Millipore, Swinnex 47 mm) made of polypropylene. A detailed diagram of the 6 x 8 cm holder is shown in Figures 62 and 75. The front section (A) was modified from its original form by enlarging the inlet to 8 mm in diameter and by removing the structural supports on the inside face to leave a smooth surface. Section (B) consists of the back-half of a Swinnex holder with its outlet spout removed and a silicone O-ring (3.5 mm thick, 50 mm o.d.) inserted to ensure an air-tight seal of the second filter. The base section (C) is an unmodified back-half of a Swinnex holder.

8.3.2.2 Filters and Filter Preparation. Two types of filters were used to separate particulates from the air stream, Whatman 40 cellulose and Delbag polystyrene filters. Both have a high

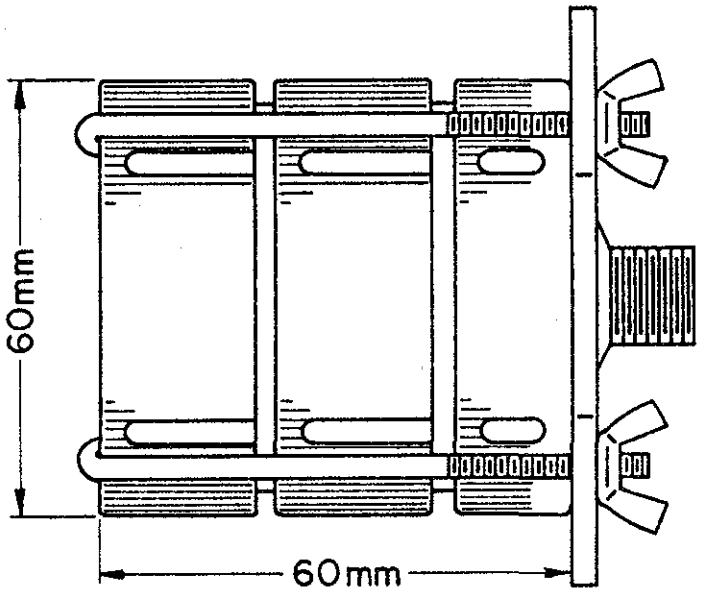

Figure 75. Assembled filter holder.

particle-collection efficiency (Johnson and Atkins 1975: Air Sampling Instruments 1972) and do not absorb SO_2 (see laboratory test results in Section 8.2.2; Lazrus et al. 1971; and Johnson and Atkins 1975). Whatman 40 filters were used in measurements of total-sulphur content of particulates since they have a low sulphur blank and are easily extracted with water. To determine the sulphuric acid content of particulate matter, polystyrene filters were used in conjunction with a benzaldehyde extraction technique (Leahy et al. 1975). Polystyrene filters do not neutralize sulphuric acid and are readily soluble in benzaldehyde. Glass fiber filters were avoided since they react with SO_2 to form sulphates (Tanner and Newman 1976; and Witz and MacPhee 1977).

The use of impregnated filters to collect SO_2 is by no means new. Several types of impregnants have been proposed and tested (Huygen 1963; Pate et al. 1963; Chamberland et al. 1973; and Axelrod and Hansen 1975). We chose the combinations of triethanolamone (TAE)-potassium hydroxide (KOH) and glycerol-potassium carbonate (K_2CO_3), for our sampling since they have been tested in the field (Forrest and Newman 1973; and Johnson and Atkins 1975) as well as in the laboratory (Huygen 1963). Whatman 41 filters were prepared by soaking 15 x 30 cm sheets in an aqueous solution of the impregnate (either 10% W/W TEA-20% W/W KOH or 10% glycerol-25% W/V K_2CO_3), squeezing them out on a glass plate with a buna rubber roller and then drying them in an oven at 100°C for 5 min. Forty-seven millimetre discs were cut from the impregnated sheets with a stainless-steel punch, sealed in a plastic bag, and stored in a desiccator.

It was found that both impregnants trapped SO_2 efficiently (Section 8.2.2). However, glycerol-K_2CO_3 interfered less with the sulphur analysis and was, therefore, chosen for atmospheric sampling.

8.2.2.3 Sampling, Extraction, and Analysis. Filters were loaded into filter packs with stainless-steel forceps in an SO_2-free atmosphere. Prior to use each unit was stored in a plastic bag. In both laboratory and field tests, the sampling set-up was essentially the same (Figure 76). Air was drawn at a rate of 20-30 L/min through 214 cm of teflon tubing (9.5 mm diameter), the filter pack, and a flow meter by a Cole-Parmer pump.

After sampling, Whatman 40 and 41 papers were removed from the filter-pack and sealed in plastic bags. Delbag particulate filters were put in petri dishes and stored in a desiccator. Extraction and analysis of the filters were carried out within one day in laboratory tests and within two weeks for field tests. A check on the handling procedure was periodically made by analysing filters that had been mounted as if to sample but that had not been exposed.

Total particulate sulphur was extracted from Whatman 40 filters by placed them in 50 to 100 mL of hot ($80^{\circ}C$) deionised water for several minutes. Sulphuric acid was removed from Delbag filters by dissolving them in 4 mL of benzaldehyde, centrifuging 1.5 mL of the solution at 200 G for 10 min to remove particulates, and then extracting the sulphuric acid from benzaldehyde by shaking 0.5 mL with 1 mL of deionised water for another one hour. Impregnated Whatman 41 filters were extracted with 50 to 100 mL of 0.03% H_2O_2 in water at room temperature.

Three different sulphur analysis techniques were used to determine the concentration of sulphur in the filter extracts. They were:

1. An isotope dilution technique developed by Klockow et al. (1974). Detection limit 0.01 ppm-S with 1 mL of solution;
2. An ion-exchange chromatographic technique (Dionexion exchange chromatograph). Detection limit 0.03 ppm-S with 1.5 mL of solution; and

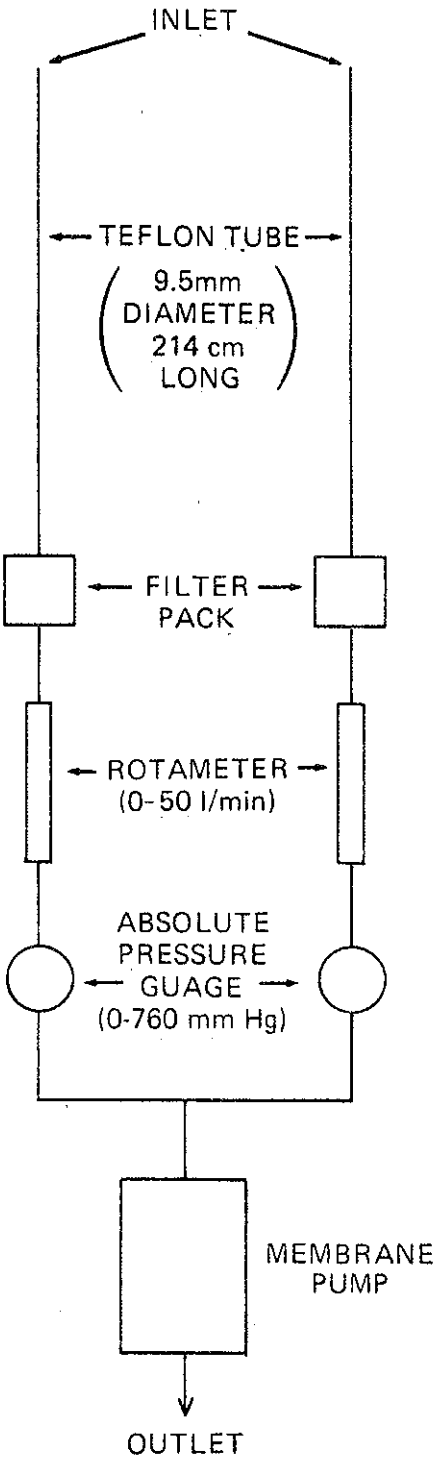

Figure 76. Sampling arrangement.

3. The spectrophotometric barium perchlorate-thorin method. Detection limit 0.1 ppm-S with 2 mL sample.

Simultaneous analysis by the above three methods of 57 extracts of glycerol-K_2CO_3 impregnated filters agreed within 10%.

8.2.3 System Calibration and Performance in the Laboratory

Laboratory tests were carried out on the filter pack system using a large mylar bag (2 m^3 volume), filled with room air containing traces of SO_2 (20-3000 ppbv), and a sulphur gas-chromatograph (Tracor 270HA). The latter was calibrated with standard SO_2-air mixtures prepared by passing clean air at a known flow rate over a thermostated permeation tube whose SO_2-loss rate had been accurately measured by weighing (error ± 2%).

During calibration tests, the filter pack system (Figure 76) and chromatograph were connected to a glass manifold (Figure 77) through which air from the mylar bag was drawn.

8.2.3.1 SO_2-Uptake by Whatman 40 Prefilters and Filterpack Walls. SO_2-uptake by the filter holder itself was measured for SO_2-concentrations from 20 to 200 ppbv. Differences between concentrations upstream and downstream of a filter holder containing no filters were determined with the gas chromatograph. Care was taken to correct for pressure differences between upstream and downstream sampling ports. For all four filterpacks tested, SO_2 wall-loss was less than 5%.

The same tests carried out with Whatman 40 prefilters in place indicated no detectable uptake by the cellulose fibres. Chemical analysis of the filters after exposing them to several hundred micrograms of SO_2-S confirmed this result (Table 10). Less than 0.1% removal of SO_2 from the airstream occurred. Johnson and Atkins (1975) reported similar findings.

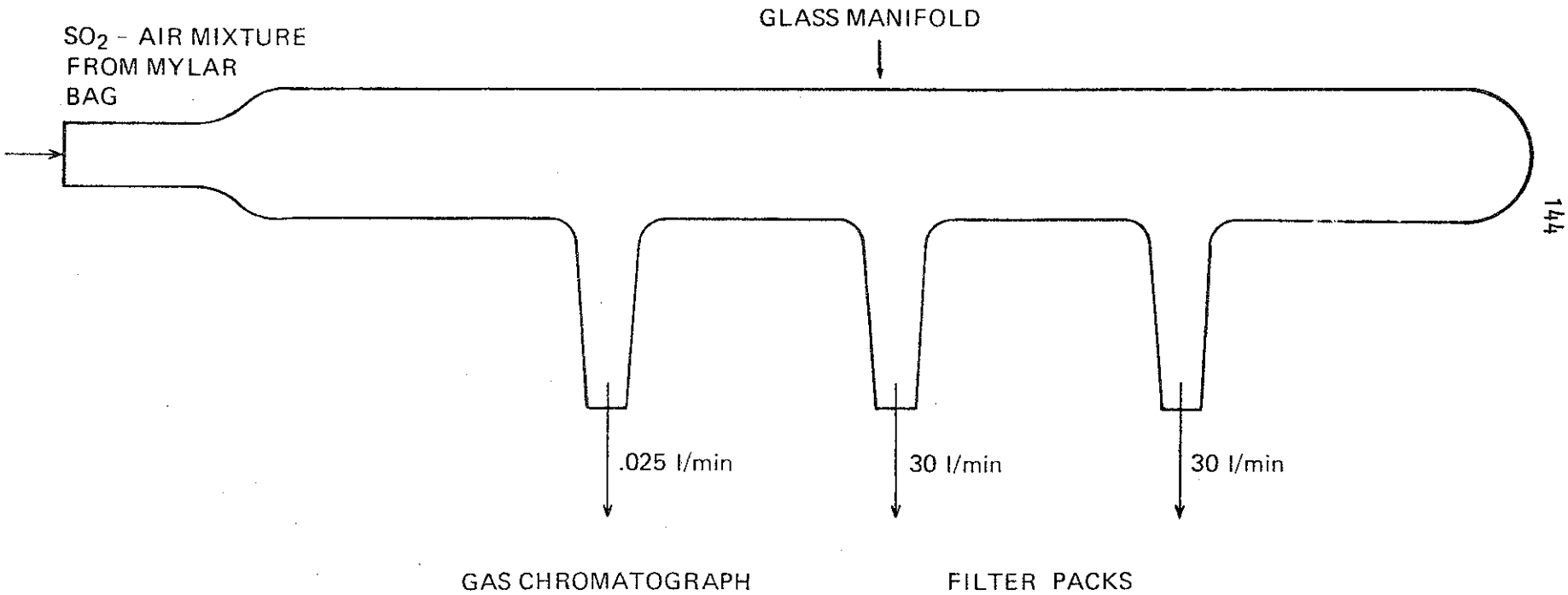

Figure 77. Interface between mylar bag and sampling arrangement.

Table 10. SO_2-removal by Whatman 40 cellulose filters at 25°C, ~30% RH, and 200 ppbv SO_2.

SO_2 Passed Through (µgS)	SO_2-S Removed (µgS)	SO_2-S Removed %
100	0.05	0.05
200	0.20	0.10
750	0.30	0.04

8.2.3.2 Trapping Efficiency of Impregnated Filters. Tests similar to those described above were conducted with impregnated filters (glycerol-K_2CO_3) in place to determine their SO_2-collection efficiency as a function of time and loading. Two atmospheres were sampled to test the effects of relative humidity (R.H.) Both contained 600 ppbv SO_2 and were sampled at a rate of 22 L/min. However, one atmosphere had an R.H. of 30%, the other was much drier with an R.H. of less than 8% (very dry air is encountered when cold outside air is warmed before reaching the filter pack inside; e.g., in aircraft sampling). A dewpoint hygrometer (Cambridge Instruments) and a calibrated thermometer were used to measure R.H.

Experiments carried out in duplicate yielded similar results (Figure 78). At 30% R.H., the collection efficiency of a single impregnated filter was greater than 95% for a sampling time of 100 min and a sulphur loading of 2000 µg-S. The filter's performance deteriorated, however, when the humidity was lowered below 8%. Fifty percent breakthrough occurred after 50 min and 900 µg-S loading. Huygen (1963) observed similar humidity effects.

Two impregnated filters back-to-back were tested at a low R.H. (dashed curve, Figure 78) as a possible remedy to the severe sampling problem caused by low humidities. With two filters collection efficiencies were greater than 95% up to 70 min and 1300 µg-S loading. This result was confirmed by field tests (Section 8.2.4.2) in which two filters were used. Sulphur on the second filter was less than 15% of that on the first. The reason for such behaviour is not clear. In any case, when dry air (RH<30%) is expected double filters should be used.

8.2.3.3 Comparison With a Calibrated Gas Chromatograph. Before embarking on extensive field sampling programs, an intercomparison on the filter pack technique with another method was carried out. Seven atmospheres containing SO_2 concentrations between 20 and 2000 ppb

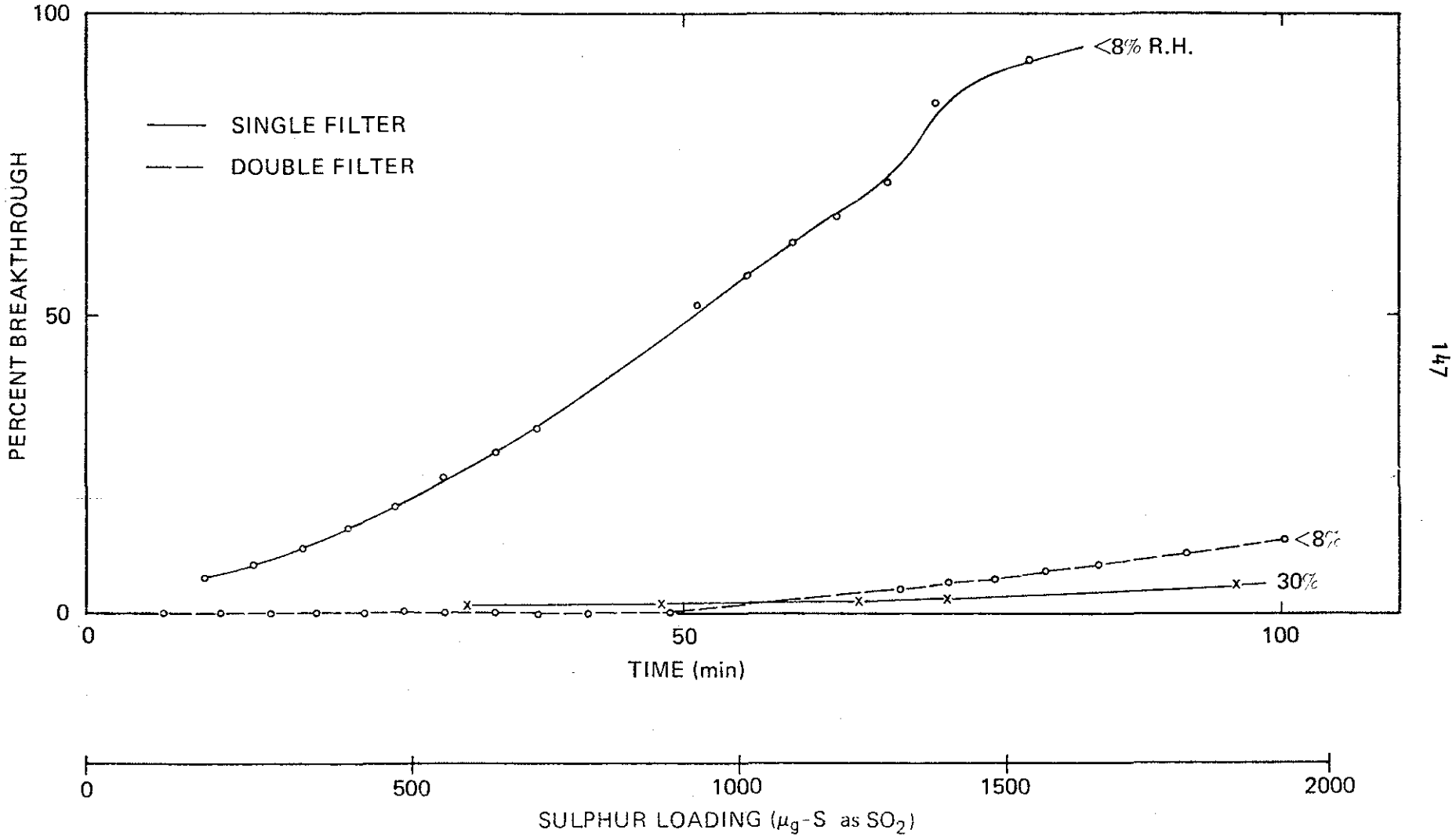

Figure 78. SO_2 capture by impregnated filters (K_2CO_3-glycerol) as a function of time, loading, and relative humidity.

were sampled with two filter packs and a gas chromatograph. SO_2 concentrations were intercompared. Agreement between the two methods was good. For seven concentrations, differences between filter packs ranged from 1.8 to 11% and averaged 4.9%. Agreement between the filter packs and chromatograph over a concentration range of two orders of magnitude was better than 10% (Figure 79). Similar verification of the impregnated filter technique during field tests using bubblers has been reported by Johnson and Atkins (1975).

8.2.4 Field Tests of the Method

During February 1977, a two-week helicopter sampling program was carried out to determine the rate of sulphur dioxide oxidation in the plume of the power plant chimney at the Great Canadian Oil Sands crude oil extraction and upgrading complex near Fort McMurray, Alberta. This afforded an opportunity to test the filter pack technique under field conditions. These tests are reported below.

8.2.4.1 Procedure. The sampling installation was in many respects similar to that described in Section 8.2.2.3. The air sample was drawn at a rate of about 20 L/min^{-1} over two parallel filter packs by means of diaphragm pumps. The sample line leading to each filter pack was made of teflon (9.5 mm diameter, 214 cm long). It extended to about 30 cm beyond the nose of the aircraft where it was well clear of any downwash effects from the rotor, and was capped with a conical teflon tip which had been carefully machined to give approximately isokinetic sampling conditions. The sample line was almost straight between the inlet and the filter packs. A calibrated Brooks rotameter and an absolute pressure gauge were inserted between each filter pack and the vacuum pump. Provision was made for temperature measurement of the air stream. This permitted measurement of sample flow rates over the filter to an accuracy of about 5%.

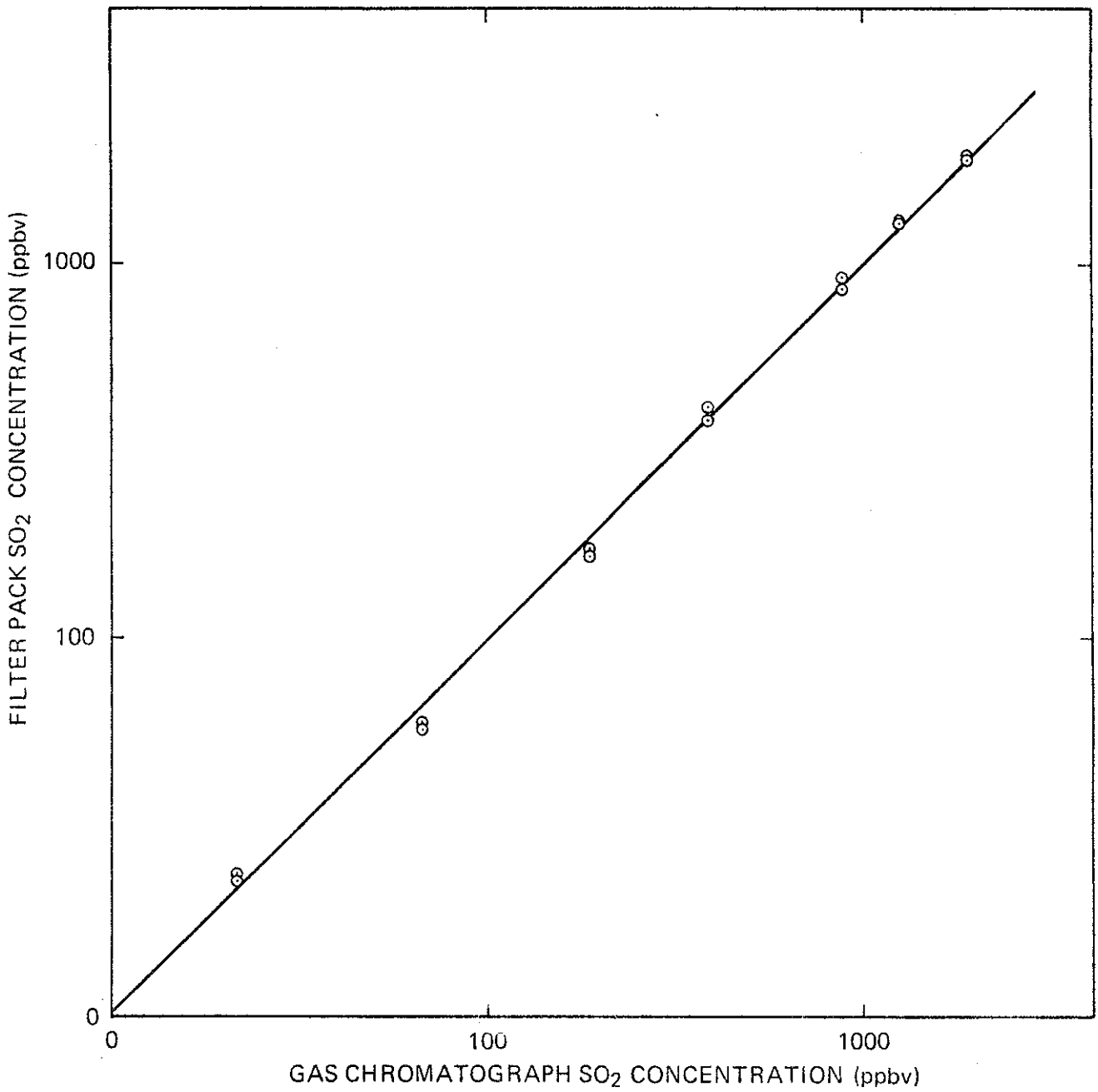

Figure 79. Intercomparison of filter pack sampling technique with gas chromatographic measurements (solid line is 1:1).

Two chemically impregnated filters, placed back-to-back, were used in this study in order to check the efficiency of SO_2 collection under field conditions. After each flight the filters were folded so that the upstream paper faced inwards, and were stored in the same sealed plastic bag. On some flights one of the two filter packs contained a Whatman 40 paper to collect particulates, while the other had either a Delbag microsorban or Mitex filter (for H_2SO_4 analysis). On other flights, both packs had Whatman 40 particulate filters in them.

The instrument package also contained a continuous Sign X sulphur dioxide analyser, which measures the increase in electrical conductivity when SO_2 in the air sample is dissolved in deionised water. The sample to this analyser was tapped from a short "T" section which was located beside the inlets to the filter packs (this was done to eliminate the "ram" air effects). It was then conducted through a 320 cm long, 0.24 cm i.d. teflon sample line to the analyser at a rate of about 2 L/min^{-1}. The analyser was calibrated several times during the program with two standard cylinders of SO_2 in nitrogen, containing 0.70 and 3.50 ppm SO_2.

Figure 64 shows a detailed view of the inlets to the Sign X and filter pack sampling lines.

8.2.4.2 Results.

8.2.4.2.1 Retention of SO_2 on the Impregnated Filters. During these flights the relative humidity at plume height varied between 50 and 100%, while the temperature range was +6 to-15°C.

The percentage of sulphur dioxide trapped on the upstream impregnated filter was determined by analysing upstream and downstream filters separately. It must be pointed out that part of the sulphur dioxide found on the downstream filter may have been transferred to it from the upstream filter through physical contact, since

both filters were stored together in the same plastic bag. Therefore, the present results probably make the filter pack technique look worse than it actually is with respect to trapping efficiency.

In every case it was found that more than 85% of the SO_2 was removed by the upstream impregnated filter. On the average, 98% of all the sulphur dioxide captured was on the upstream filter, indicating almost complete trapping of SO_2 from the sample by the two impregnated filters in series.

8.2.4.2.2 Comparison of SO_2 Trapped on Parallel Filter Packs. An indication of the reproducibility of the present SO_2 trapping technique may be obtained by comparing the amounts collected on filter packs sampling plume air in parallel (Figure 80). There is generally very good agreement between sulphur dioxide collected on filter packs operating in parallel. The reproducibility of the present method is SO_2 is better than about 15%.

8.2.4.2.3 Comparison of Sign X Analyser and Filter Pack Results. In Section 8.2.3.3 we presented the results of a laboratory comparison of the filter pack and a carefully calibrated tracor sulphur gas analyser. In this section we consider a comparison of the pack with the Sign X analyser, under the rather more adverse field study conditions.

The average SO_2 concentration at a given sampling location was obtained from the Sign X strip chart record by integration. This average concentration was then multiplied by the filter pack sampling rate, to obtain the amount of SO_2 which should have been collected on the filter pack (according to the Sign X analyser).

Figure 81 compares the amount of sulphur (as SO_2) expected from the Sign X data with that actually collected by the filter pack. The comparison is not nearly as good as in the case of the laboratory experiments (see Figure 79). About 70% of the points agree to with 30%. The filter pack results tend to be higher than

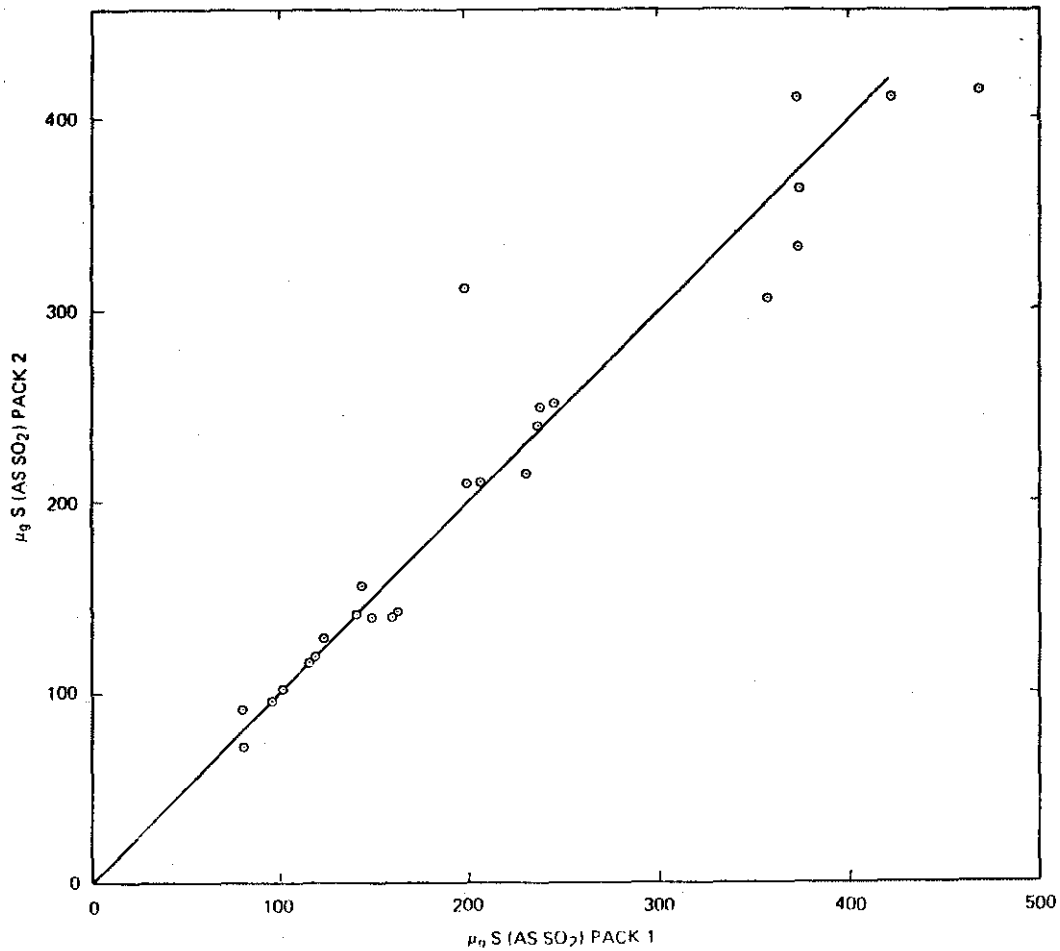

Figure 80. Intercomparison of filter packs; SO_2 collected on impregnated papers at 20 L/min^{-1} (21^0C, 1 atm).

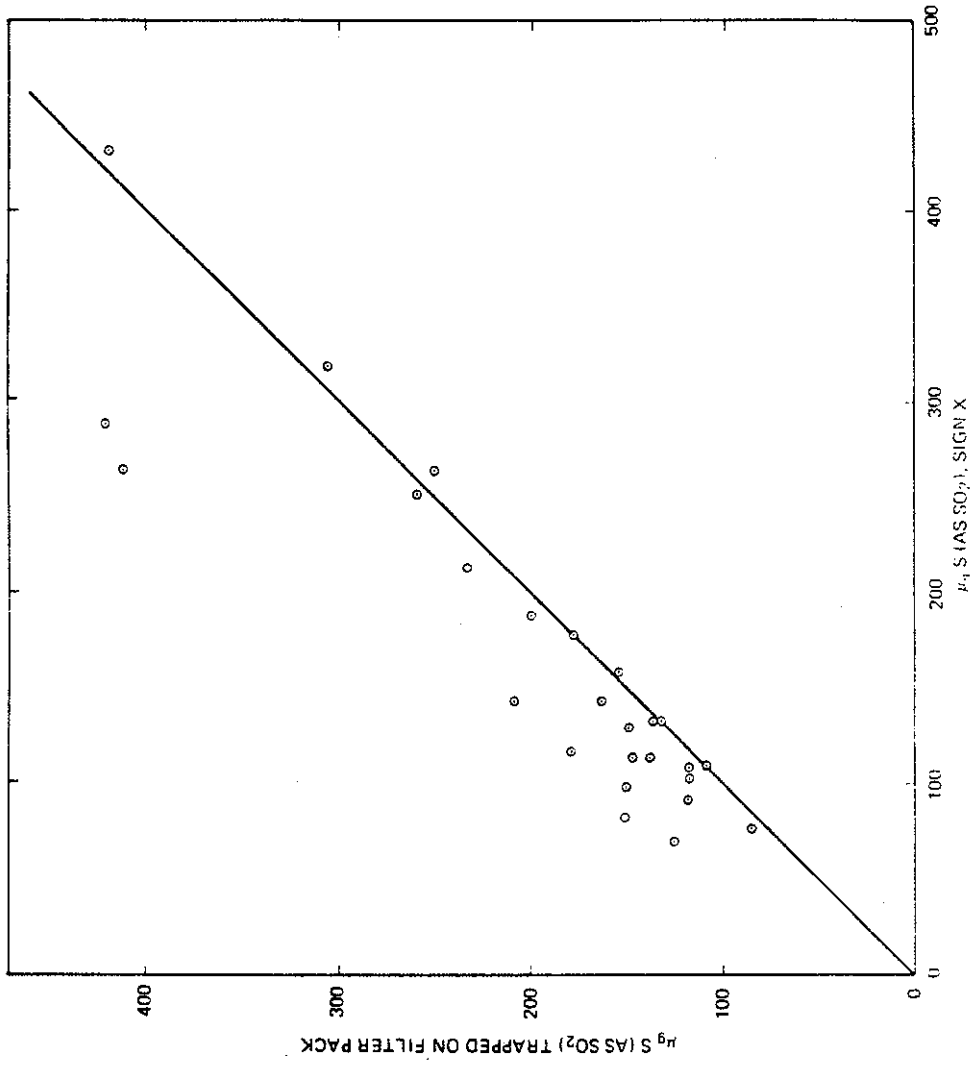

Figure 81. Comparison of Sign X analyser and filter pack.

the Sign X results, especially for small-sized samples (i.e., less than 50 µg sulphur). In several cases the filter pack results are about 50% higher than the Sign X results. The reason for this discrepancy is not clear. Errors in the analyser calibration may be partly responsible. (The concentration of SO_2 in the standard gas cylinders used for calibration of the Sign X was checked about 3 months prior to the field study.) Another possibility could be destruction of SO_2 on sample lines. Even teflon sample lines show evidence of interactions with reactive gases such as SO_2 when exposed to short "bursts" of concentration, as for instance when traversing a plume with an aircraft (e.g., Lusis 1976). In this connection, it is interesting to mention a comparison of SO_2 concentrations obtained with two different analysers during a plume sampling study carried out by the Electric Power Research Institute (1976). Parallel measurements disagreed by as much as 50%. These results are mentioned to emphasise the problems encountered in sampling of sulphur dioxide under field conditions, where sample lines can accumulate moisture and potentially reactive particulate matter. In the present case, we are inclined to suspect the Sign X analyser results rather than the filter pack results, because of the good agreement between filter packs operating in parallel (see Section 8.2.4.2.2).

8.2.4.3.4 Comparison of Sulphates Trapped on Parallel Filter Packs. In several flights, both of the filter packs contained Whatman 40 particulate filters in order to compare total sulphate concentrations obtained in the same plume volume. In other cases, the Mitex (teflon) filter in one pack was analysed for total sulphate and the amount collected was compared to that simultaneously obtained with a Whatman 40 particulate filter in the other pack.

Figure 82 compares the amount of sulphur collected as particulate on two parallel packs (corrected to a standard sampling rate of 20 L/min^{-1} at 21°C and 1 atmosphere).

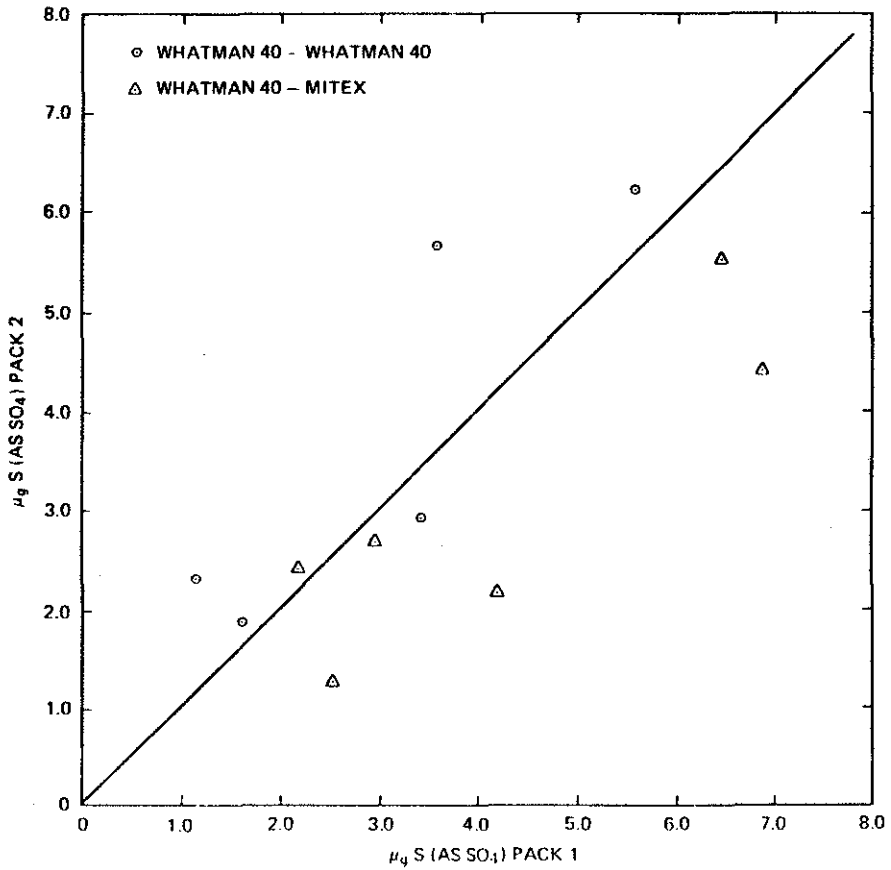

Figure 82. Intercomparison of filter packs for particulate sulphate at 20 L/min^{-1} (21°C, 1 atm).

A comparison of Figures 82 and 80 shows much poorer agreement between filter packs for particulate sulphur than for gaseous sulphur. In the former case, only about half of the results agree to within 30%, the discrepancies in some cases being as high as 50%. It is improbable that these results are due to errors in the chemical analysis of the particulate samples because generally duplicate analyses were in good agreement (better than 15%). Rather, they are thought to be due to sampling problems. As mentioned in Section 8.2.4.1 considerable care was taken when designing the sample lines: provision was made for isokinetic sampling conditions, only teflon lines were used upstream of the filter pack, and the residence time for the samples in the line was less than 0.5 s. Nevertheless, halfway through the study a faint deposit of particulate matter was noticed near the tip of the sampling probes, indicating some wall deposition, possibly due to electrostatic effects. This is probably the major source of error in sulphur dioxide oxidation studies with the equipment described in this report. A major improvement would be too mount the filter pack outside of the aircraft, with no sample lines upstream of it.

8.2.5 Summary and Recommendations

A method was described for the simultaneous determination of sulphur dioxide and sulphates in air samples. Sulphates are collected on a Whatman 40 or Delbag pre-filter, while SO_2 is trapped on Whatman 41 paper impregnated with a K_2CO_3-glycerol solution. These filters are placed in a modified, 47 mm Swinnex filter holder, which is convenient to handle and can be loaded and unloaded in the laboratory away from any sources of contamination that might occur in the field. Laboratory tests indicated excellent trapping properties of the impregnated filters, and very good agreement with SO_2 concentrations measured by a carefully calibrated sulphur gas-chromatograph. Field tests confirmed the laboratory findings on SO_2 trapping efficiency of the filters and suggested that the

reproducibility of the present method for SO_2 is about 15% or better. Although agreement with the Sign X analyser used in the field test was not nearly as good as with the laboratory chromatograph, we suggest that the problems are largely associated with the analyser rather than the filter pack.

The present filter pack method has been tested primarily with a view to aircraft studies of SO_2 transformation rates in plumes. Provided that a sensitive method is available for the analysis of the particulate sulphur (such as the isotope dilution technique), about 10 crosswind traverses through a typical power generating station plume at a sampling rate of 20-30 L/min^{-1} should yield a sufficiently large sample for accurate determination of the relative proportions of sulphates and SO_2 at that particular plume age. The filter pack may also be of value for ground-level monitoring of gaseous and particulate sulphur, at much lower concentration levels, though a correspondingly longer sampling time would be necessary.

It should be pointed out that the present technique shares the drawbacks common to all methods which involve filtration of air samples with subsequent analysis in the laboratory (e.g., Tanner and Newman 1976). Thus, there is a possibility of chemical reactions between gaseous constituents (such as NH_3 or SO_2) in the air sample and particulate matter deposited on the filter, or of interconversion from one chemical form of sulphur to another in the particulate matter itself during the collection-analysis interval. It is difficult to evaluate the error introduced by such factors. No doubt errors will depend on the composition of the gaseous and particulate matter at the particular locality of interest. The problem of conversion of SO_2 to sulphates by interaction with the filter material itself should be significant in the present method, because both Whatman 40 and Delbag papers are essentially inert to SO_2.

The main recommendations for improving the usefulness of the filter pack method proposed in this report are:

1. In field applications, double chemically impregnated filters should be used. In this way a high collection efficiency of SO_2 is ensured even at relative humidities significantly below 30% (see Section 8.2.3.2);
2. The sample line leading up to the filter pack should be as short as possible, and if possible should be eliminated entirely in order to minimize losses of particulate matter (see Section 8.2.4.2); and
3. If ambient air sampling is intended, the pack should be tested in parallel with several other methods to verify that the SO_2 collection efficiency is high over long sampling times (i.e., approximately one day), especially at the low temperatures encountered in Canada. We plan to carry out such tests in the future.

8.3 SO_2 CONCENTRATION MEASUREMENTS

This Appendix contains details of the reference points of sampling and sulphur dioxide concentrations as a function of the altitude and crosswind distance. The methodology is described in Section 5.

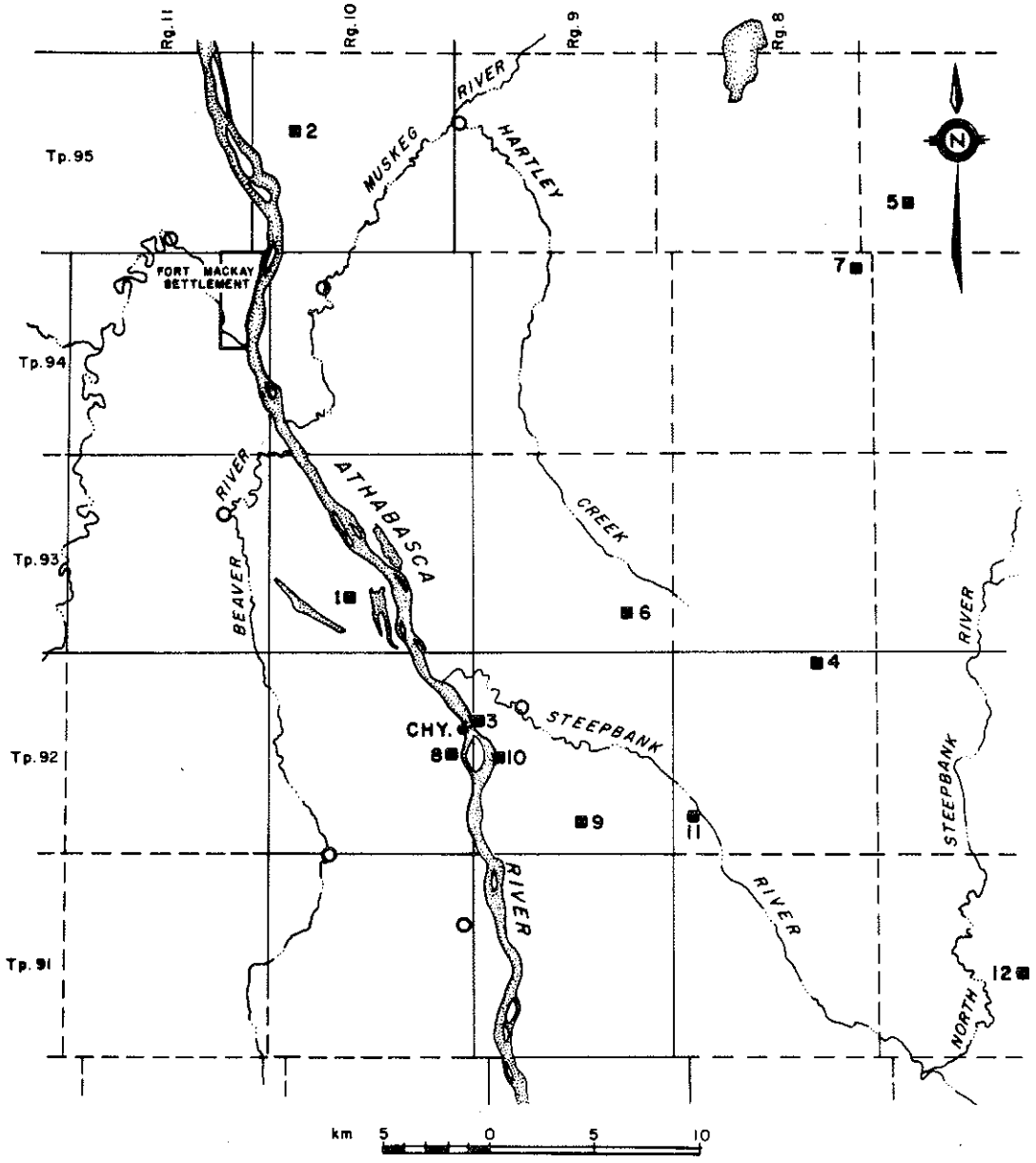

Figure 83. Locations of reference points for the February 1977 GCOS plume dispersion study.

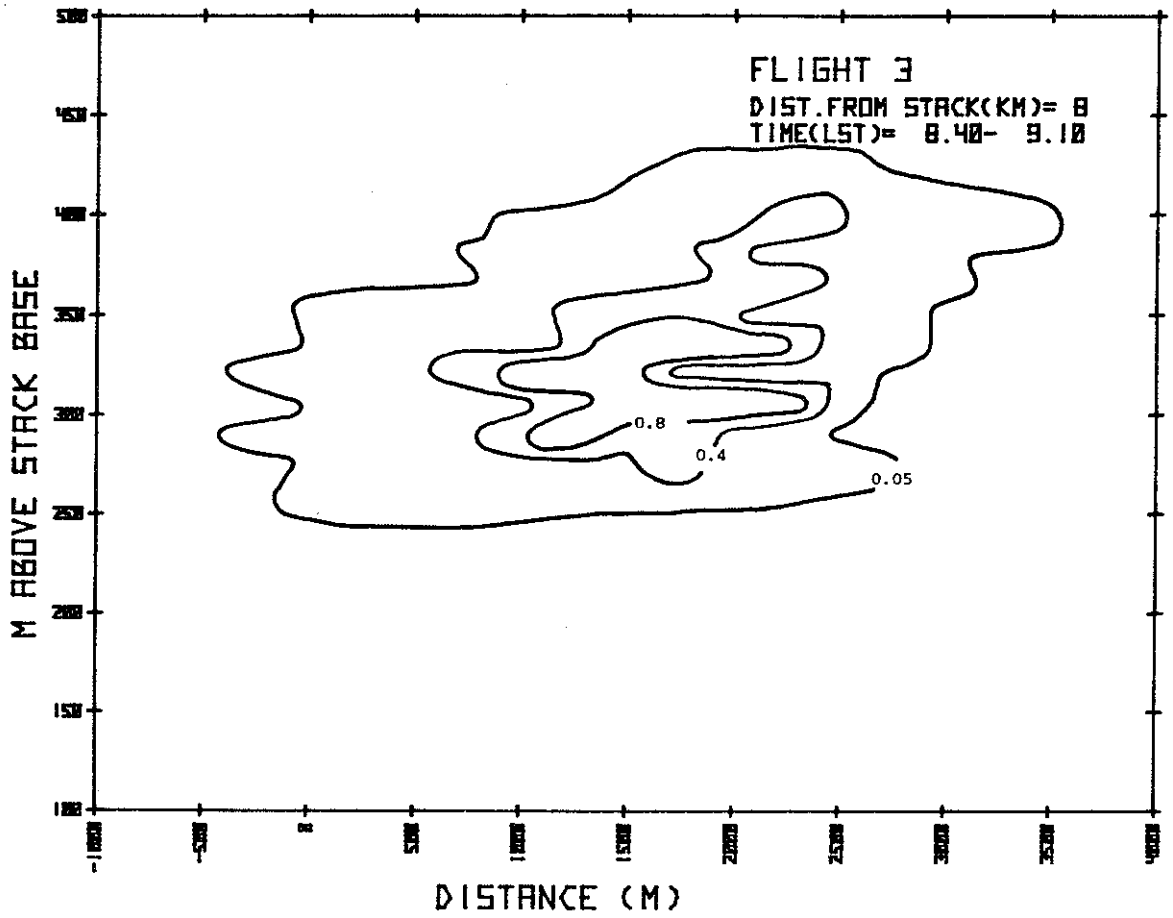

Figure 84. Concentrations (ppm) of SO_2 as a function of crosswind distance and height above the stack base, 5 February 1977.

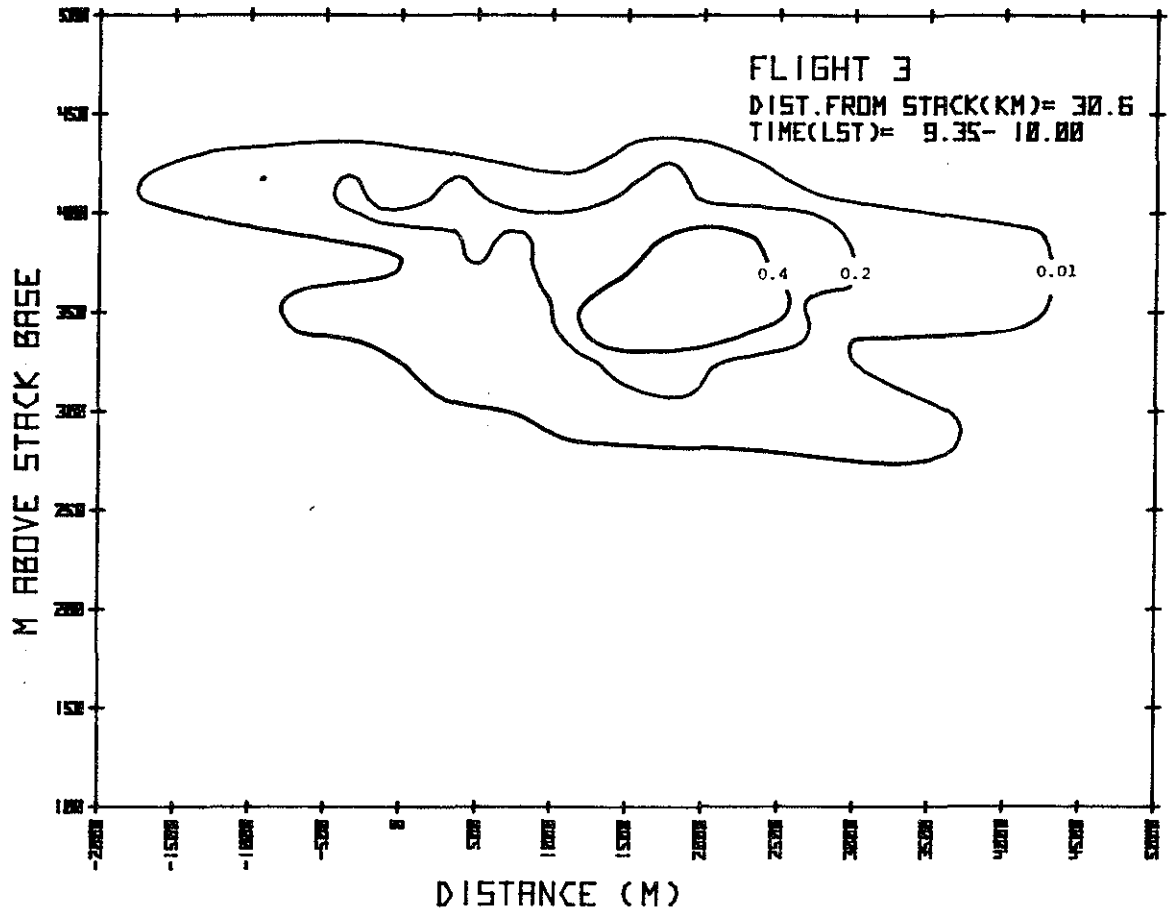

Figure 85. Concentrations (ppm) of SO_2 as a function of crosswind distance and height above the stack base, 5 February 1977.

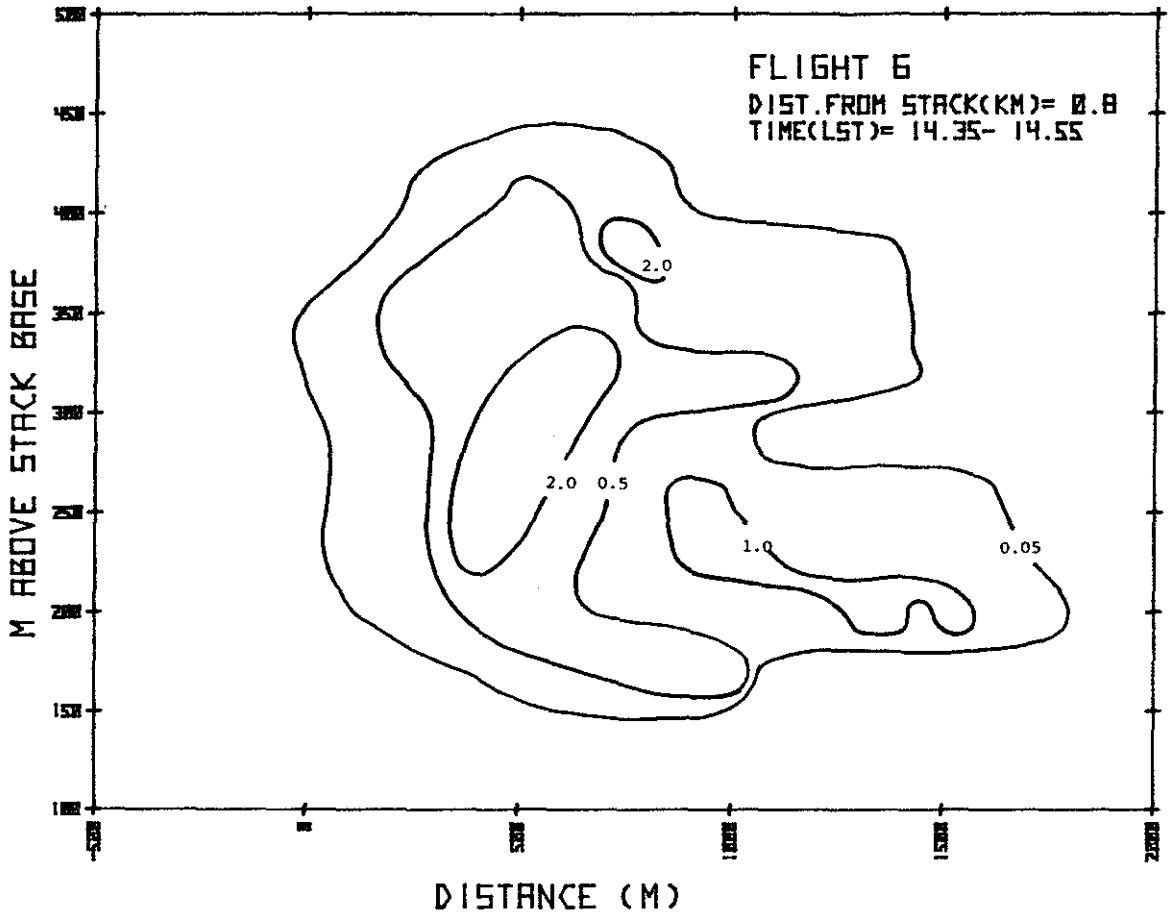

Figure 86. Concentrations (ppm) of SO_2 as a function of crosswind distance and height above the stack base, 6 February 1977.

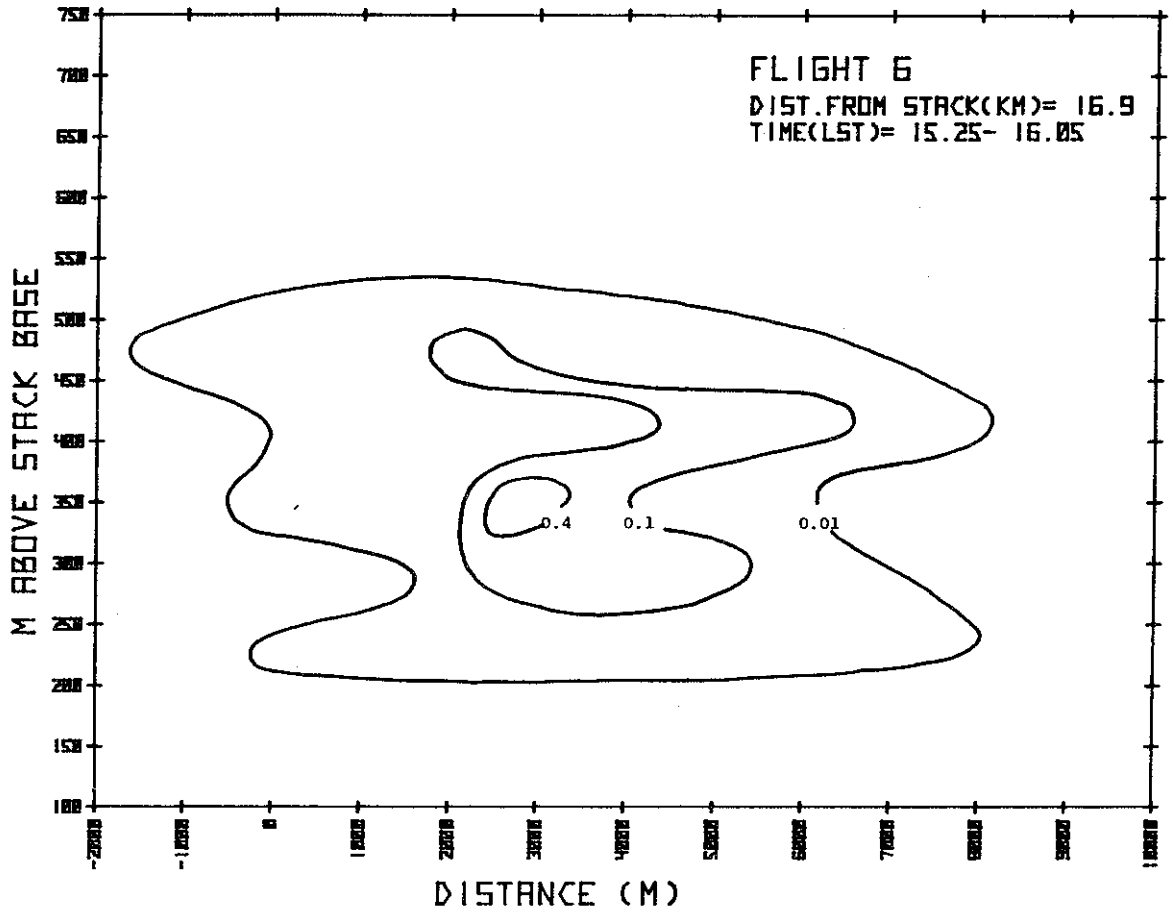

Figure 87. Concentrations (ppm) of SO_2 as a function of crosswind distance and height above the stack base, 6 February 1977.

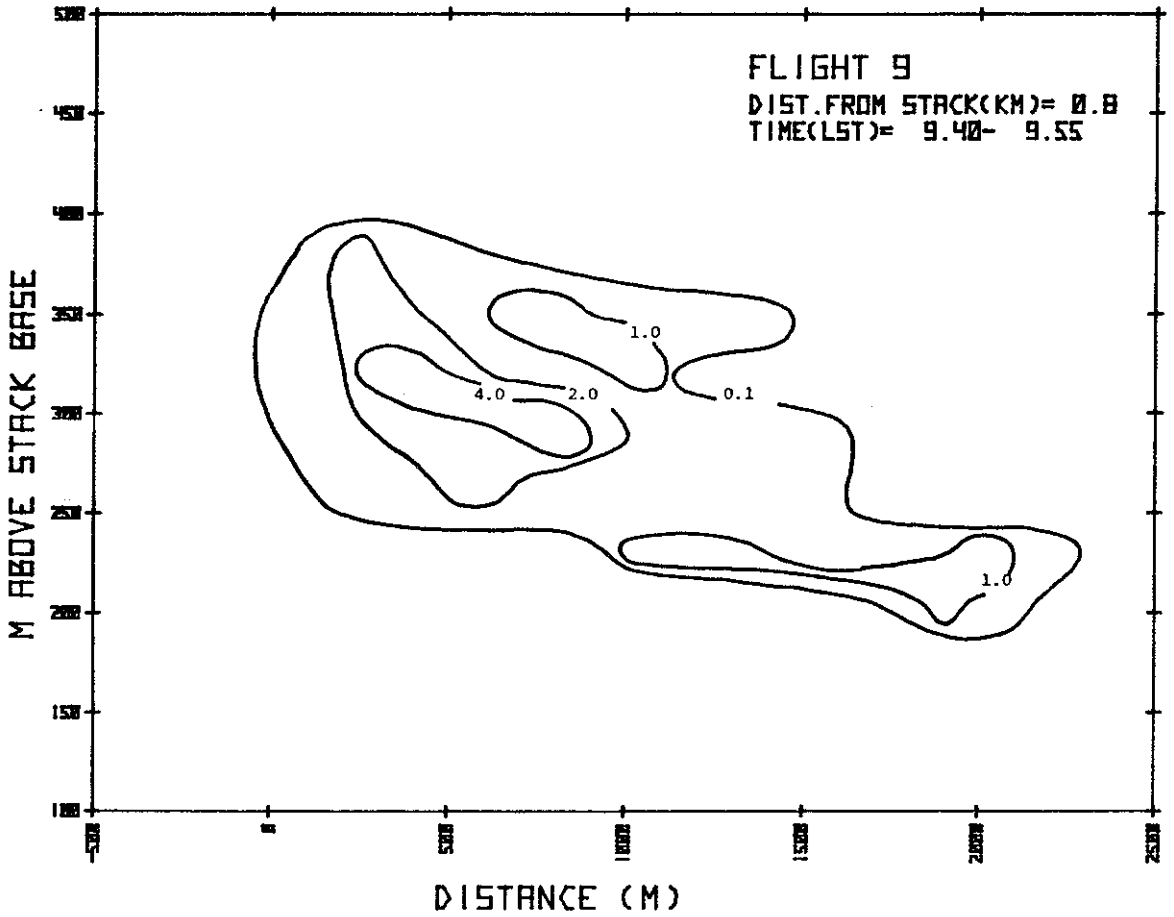

Figure 88. Concentrations (ppm) of SO_2 as a function of crosswind distance and height above the stack base, 10 February 1977.

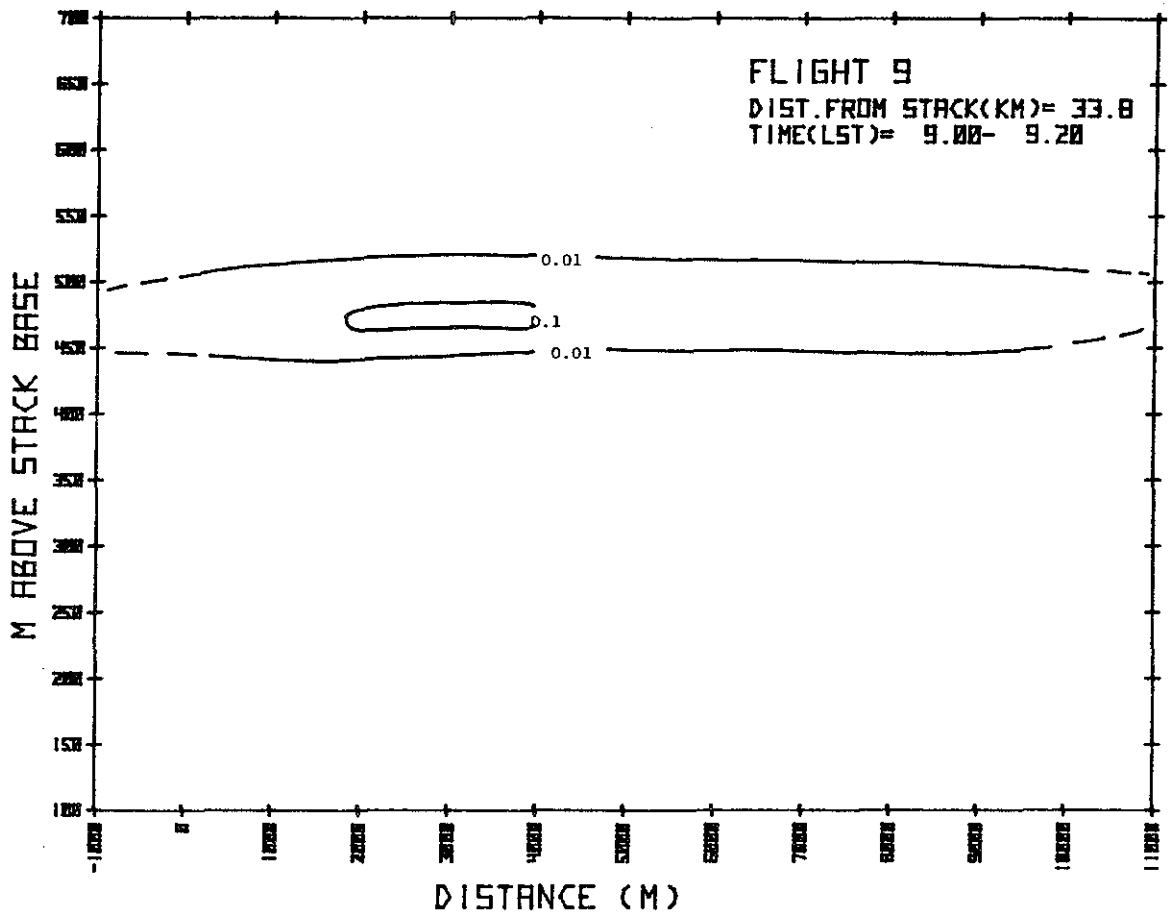

Figure 89. Concentrations (ppm) of SO_2 as a function of crosswind distance and height above the stack base, 10 February 1977.

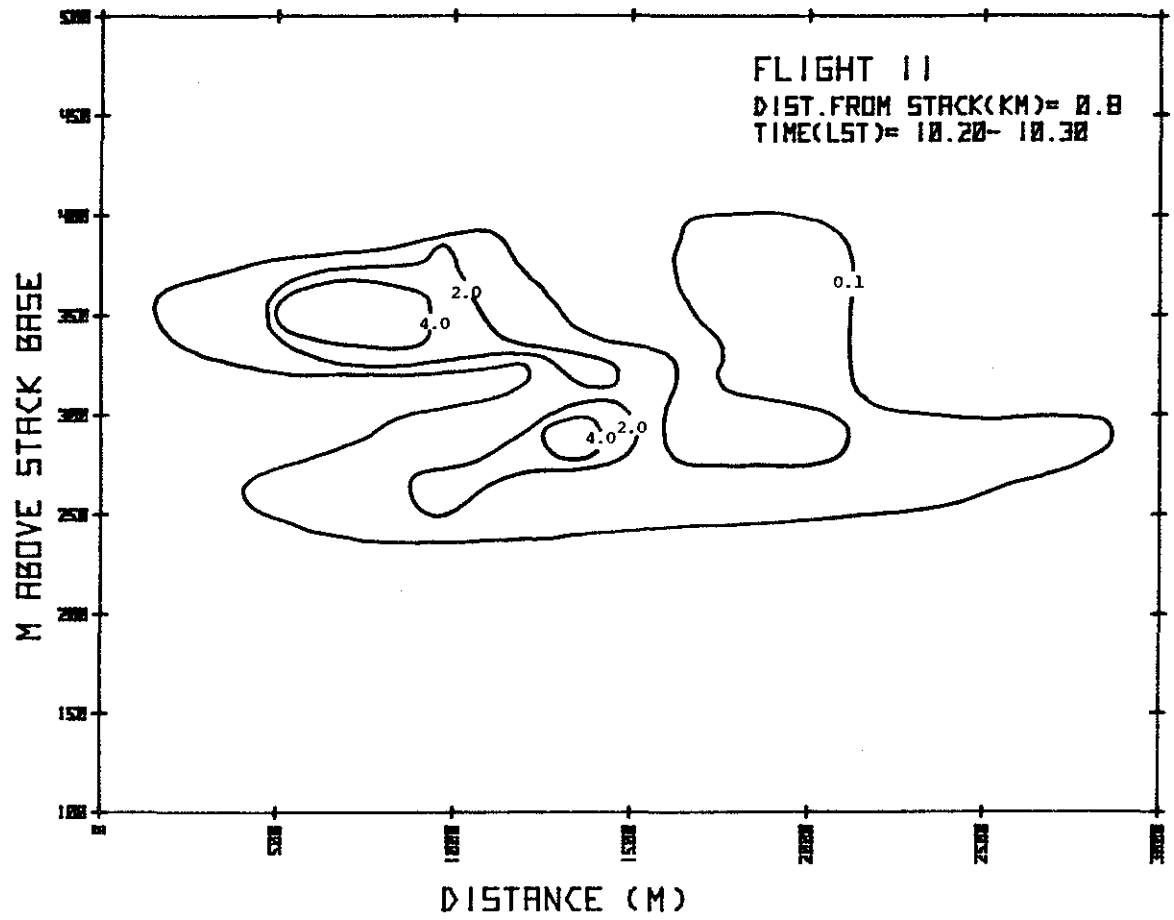

Figure 90. Concentrations (ppm) of SO_2 as a function of crosswind distance and height above the stack base, 10 February 1977.

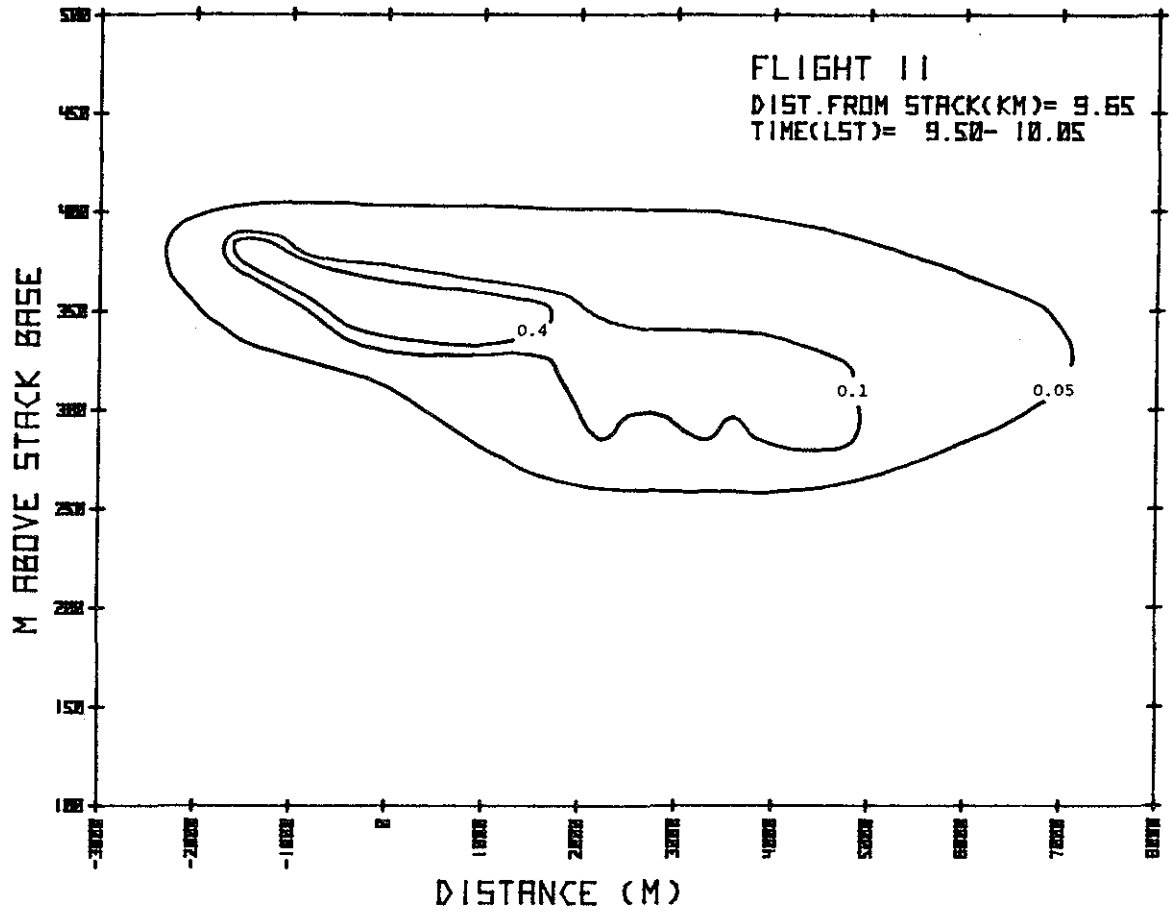

Figure 91. Concentrations (ppm) of SO_2 as a function of crosswind distance and height above the stack base, 10 February 1977.

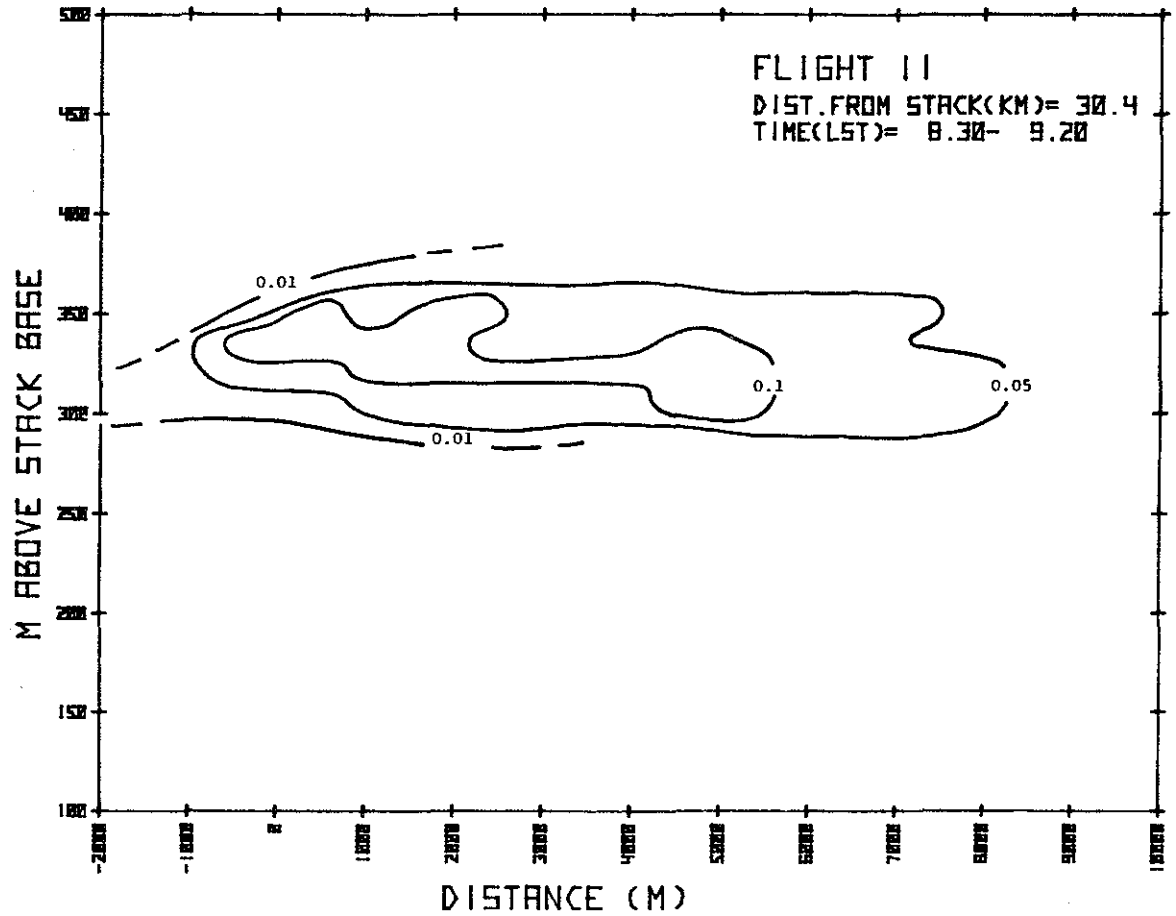

Figure 92. Concentrations (ppm) of SO_2 as a function of crosswind distance and height above the stack base, 10 February 1977.

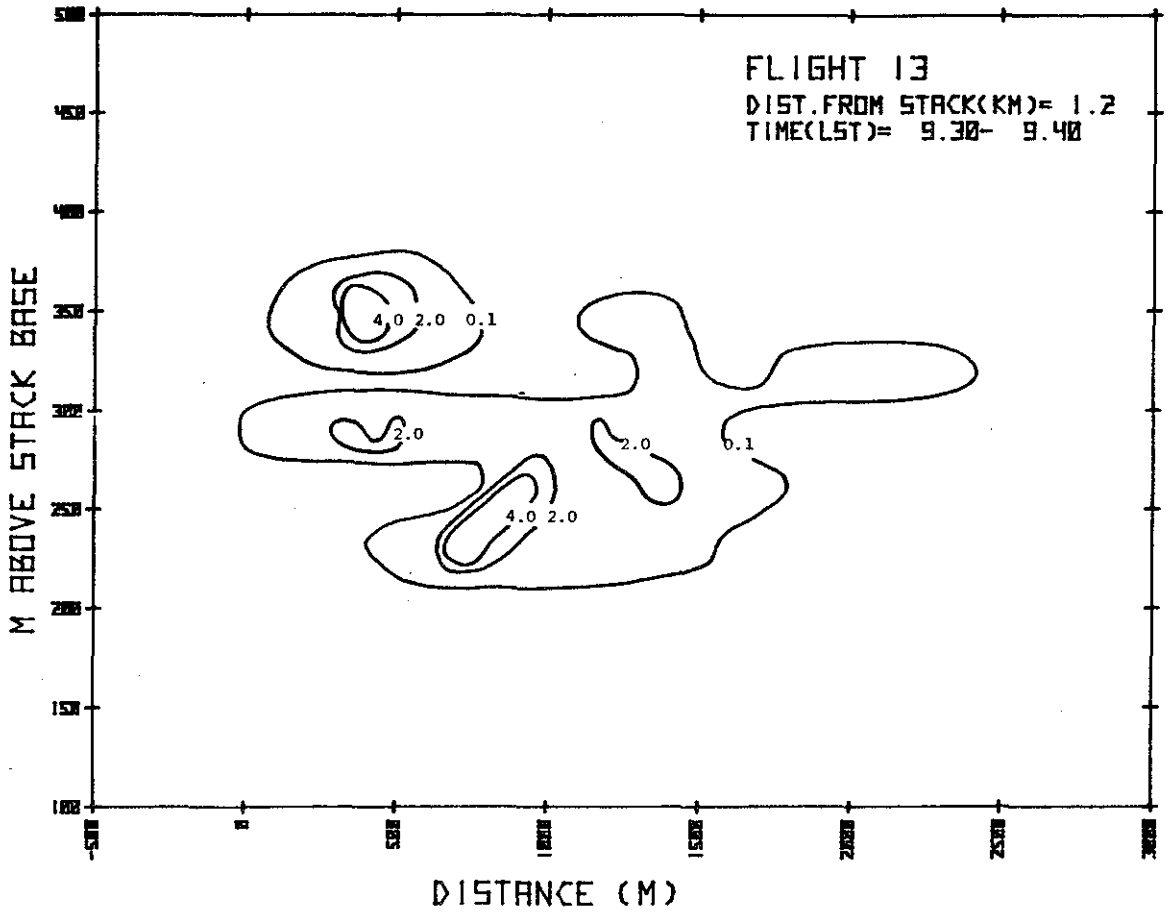

Figure 93. Concentrations (ppm) of SO_2 as a function of crosswind distance and height above the stack base, 11 February 1977.

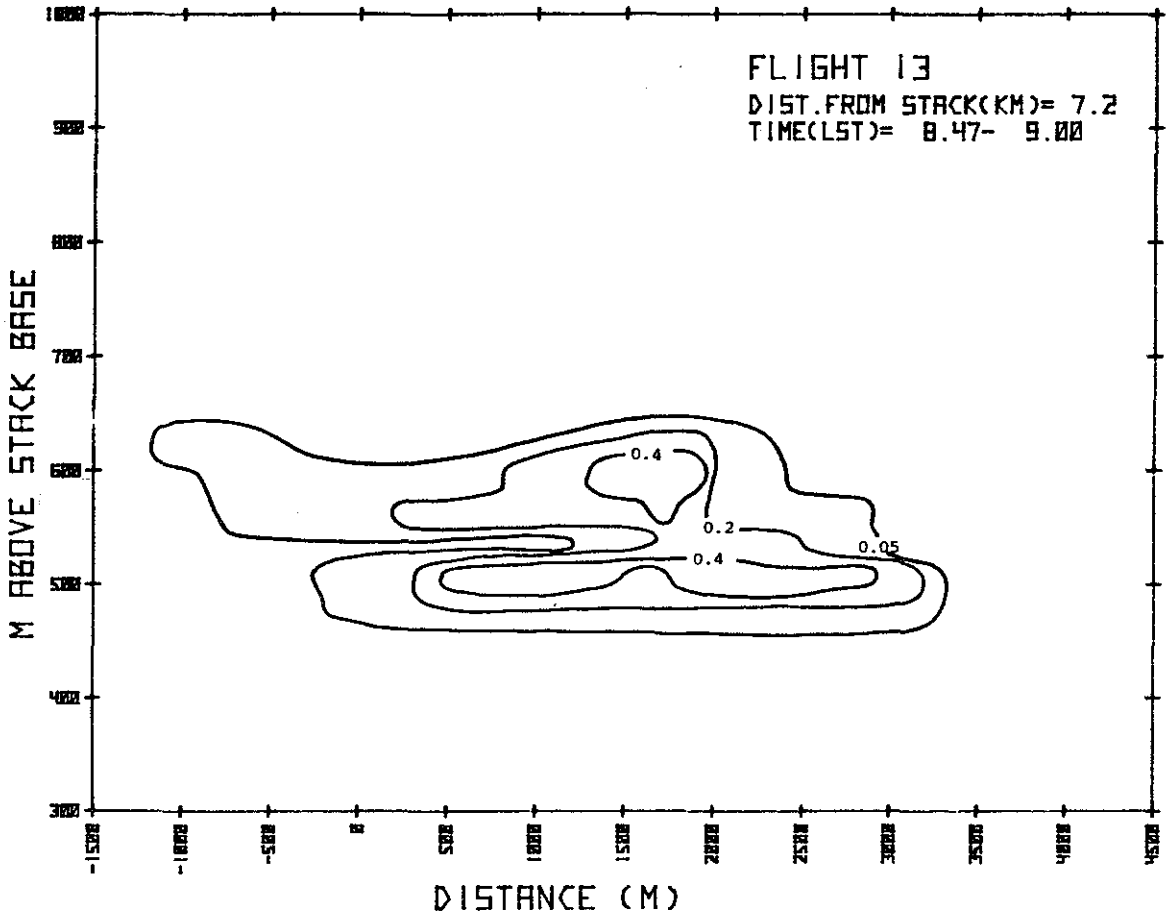

Figure 94. Concentrations (ppm) of SO_2 as a function of crosswind distance and height above the stack base, 11 February 1977.

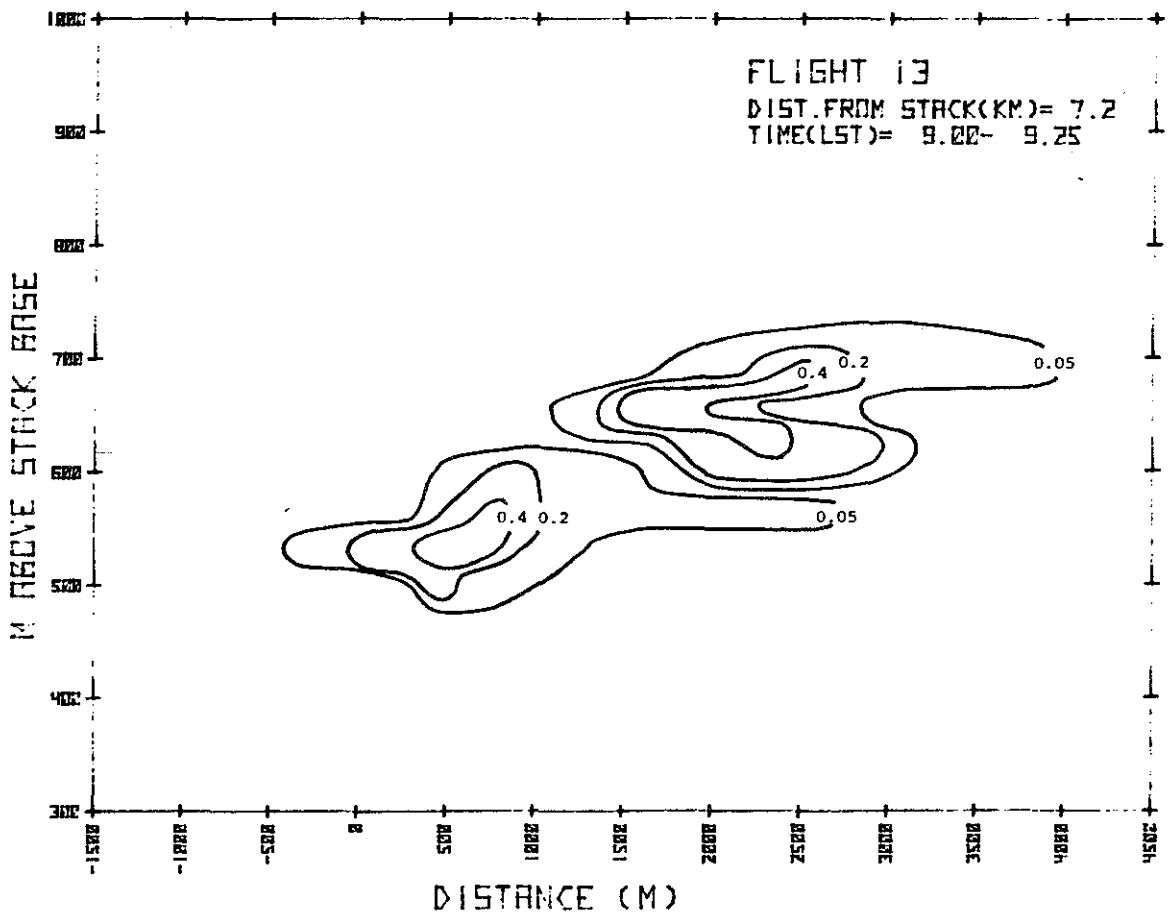

Figure 95. Concentrations (ppm) of SO_2 as a function of crosswind distance and height above the stack base, 11 February 1977.

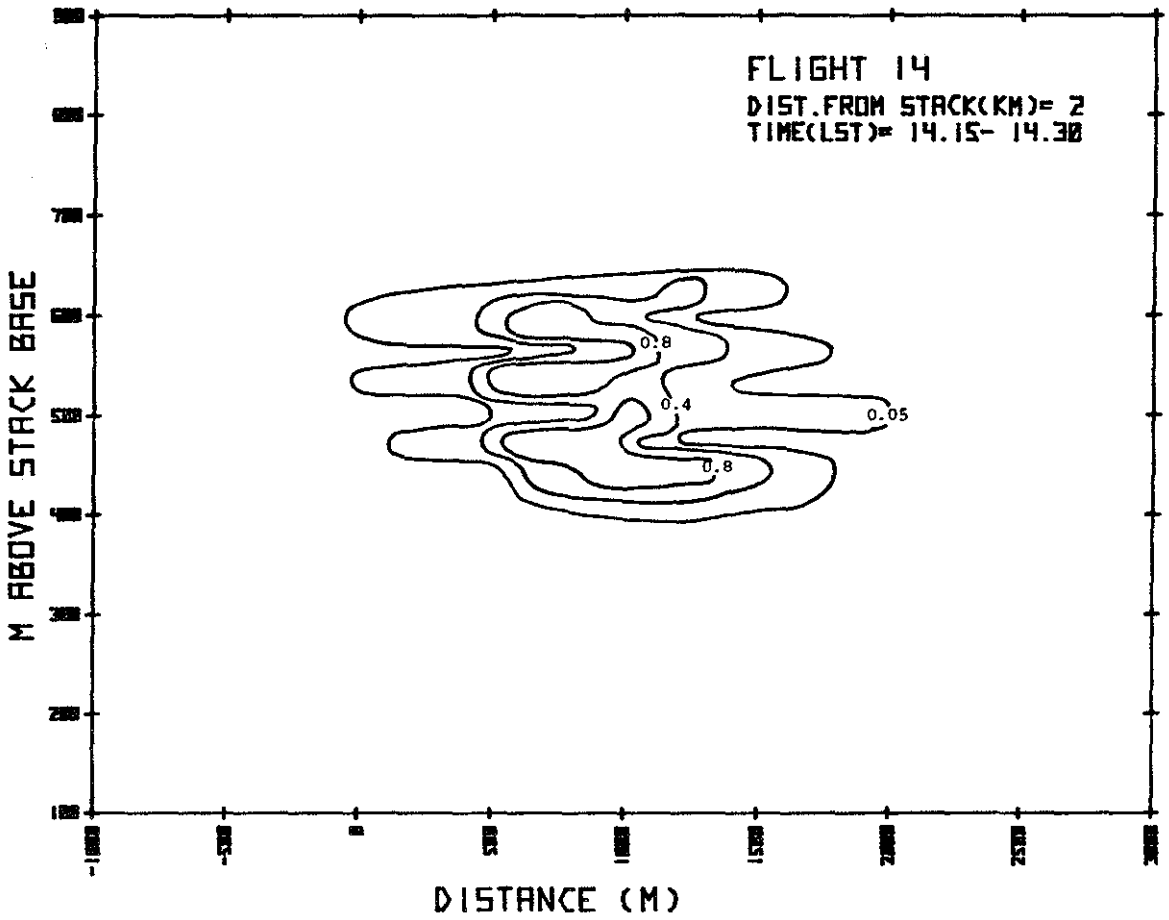

Figure 96. Concentrations (ppm) of SO_2 as a function of crosswind distance and height above the stack base, 11 February 1977.

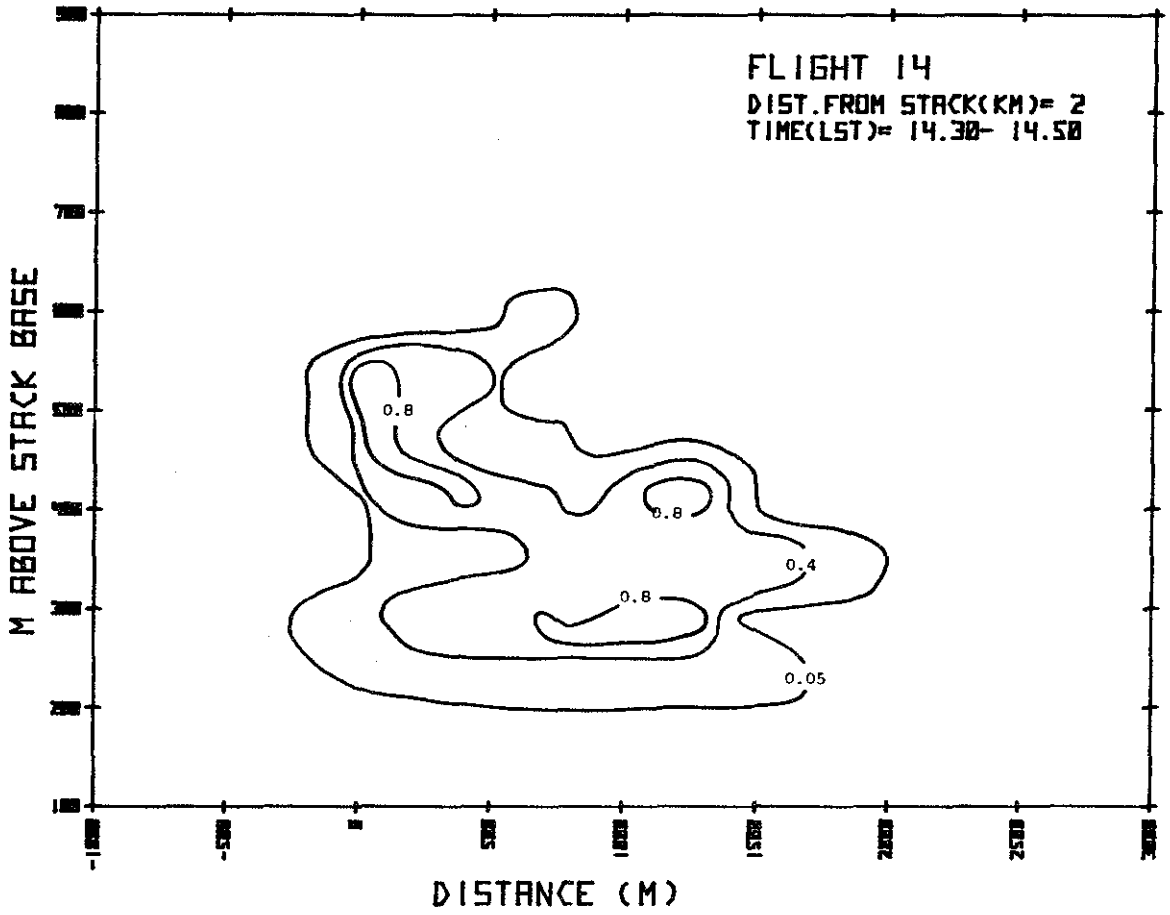

Figure 97. Concentrations (ppm) of SO_2 as a function of crosswind distance and height above the stack base, 11 February 1977.

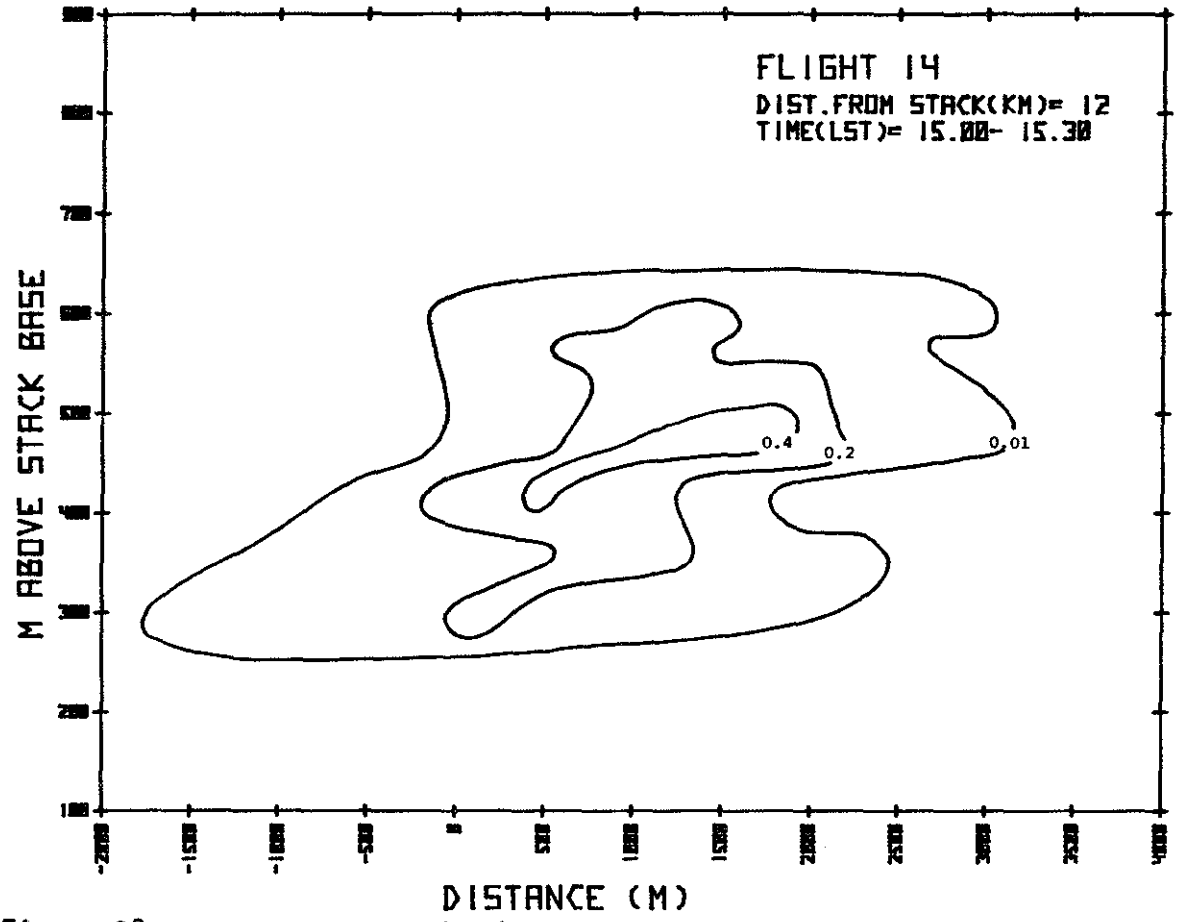

Figure 98. Concentrations (ppm) of SO_2 as a function of crosswind distance and height above the stack base, 11 February 1977.

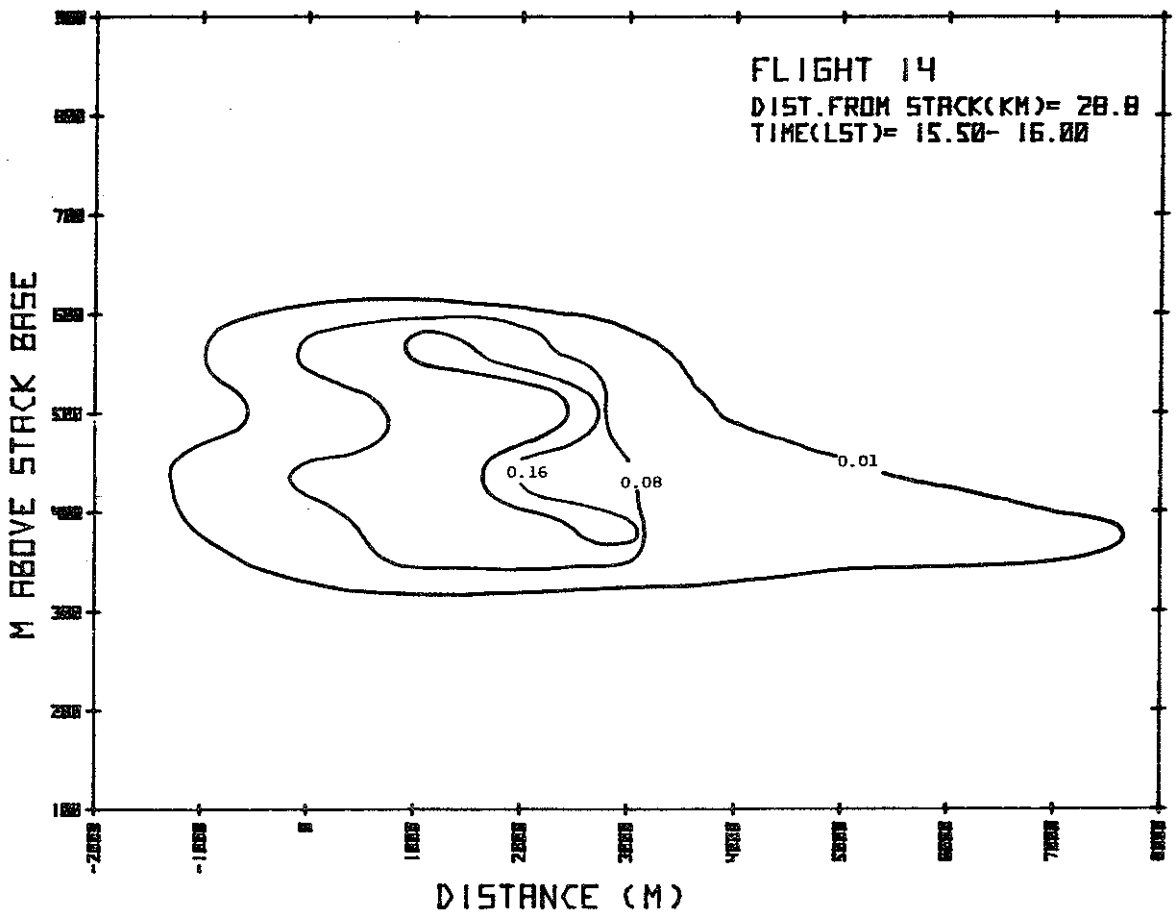

Figure 99. Concentrations (ppm) of SO_2 as a function of crosswind distance and height above the stack base, 11 February 1977.

8.4 REFERENCES CITED

Air Sampling Instruments, 4th Ed., American Conference of Governmental Industrial Hygeinists, P.O. Box 1937, Cincinnatti, Ohio (1972).

Altshuller, A.P. 1976. Regional transport and transformation of SO_2 to sulfates in the U.S. J. Air Pollut. Control Assoc. 26:318-424.

Axebrod, H., and S.G. Hansen. 1975. Filter sampling method for atmospheric sulfur dioxide at background concentrations. Anal. Chem. 47:2460-2462.

Chamberland, A.M., P. Bourbon, and R. Malbosc. 1973. Collection of atmospheric sulfur dioxide on impregnated fiberglass filters and colorimetric measurement. Internat. J. Environ. Anal. Chem. 2:303-311.

Dennis, R., C.E. Billings, F.A. Record, P. Warneck, and M.L. Arin. 1969. Measurements of sulfur dioxide losses from stack plumes. 62nd Meeting of the Air Pollut. Control Assoc., New York.

Electric Power Research Institute. 1976. Determination of the feasibility of ozone formation in power plant plumes. Report EPRI EA-307.

Forrest, J., and L. Newman. 1973. Sampling and analysis of atmospheric sulfur compounds for isotope ratio studies. Atmos. Environ. 7:561-673.

Gartrell, F.E., F.W. Thomas, and S.B. Carpenter. 1963. Atmospheric oxidation of SO_2 in coal-burning power plant plumes. J. Amer. Ind. Hyg. Assoc. 24:113-120.

Husar, R.B., J.D. Husar, N.V. Gillani, S.B. Fuller, W.H. White, J.A. Anderson, W.M. Vaughan, and W.E. Wilson. 1976. Pollutant flow rate measurement in large plumes. 171st National Meeting of the Amer. Chem. Soc., New York.

Huygen, C. 1963. The sampling of sulfur dioxide in air with impregnated filter paper. Anal. Chim. Acta. 28:349-360.

Johnson, D.A., and D.H.F. Atkins. 1975. An airborne system for the sampling and analysis of sulfur dioxide and atmospheric aerosols. Atmos. Environ. 9:825-829.

Klocknow, D., and H. Denzinger. 1976. Determination of sulfate by substoichiometric isotopic dilution analysis. European Monitoring Programme Manual for Sampling and Chemical Analysis Procedures, Norwegian Institute for Air Research, P.O. Box 130, N-2001, Lillestrom, Norway.

Lazrus, A.L., B. Ganrud, and B.D. Cadle. 1971. Chemical composition of air filtration samples of the stratospheric sulfate layer. J. Geophys. Res. 76:8083-8088.

Leahy, D.R., R. Siegel, P. Klotz, and L. Newman. 1975. The separation and characterization of sulfate aerosol. Atmos. Environ. 9:219-

Lusis, M.A. 1976. The effect of sample humidity on the response characteristics of SO_2 and NO_x analyser systems. Report ARQA 31-76, Atmospheric Chemistry Division, Atmospheric Environment Service, Downsview, Ontario.

Lusis, M.A., and H.A. Wiebe. 1976. The rate of oxidation of sulfur dioxide in the plume of a nickel smelter stack. Atmos. Environ. 10:793-798.

Newman, L., Forrest, J., and B. Manowitz. 1975. The application of an isotopic ratio technique to a study of atmospheric oxidation of sulfur dioxide in the plume from an oil-fired power plant. Atmos. Environ. 9:959-968.

Pate, J.B., J.P. Lodge, and M.P. Neary. 1963. The use of impregnated filters to collect traces of gases in the atmosphere. Anal. Chim. Acta. 28:341-348.

Persson, G.A. 1966. Automatic colorimetric determination of concentrations of sulfate for measuring sulfur dioxide in ambient air. Air and Water Pollut. Int. J. 10:845-852.

Small, H., T.S. Stevens, and W.C. Bauman. 1975. Novel ion exchange chromatographic method using conductometric detection. Anal. Chem. 47:1801-1809.

Smith, F.B., and G.H. Jeffrey. 1975. Airborne transport of sulfur dioxide from the U.S. Atmos. Environ. 9:643-659.

Stephens, N.T., and R.O. McCaldin. 1971. Attenuation of power station plumes as determined by instrumented aircraft. Environ. Sci. Technol. 5:615-621.

Tanner, R.L., and L. Newman. 1976. The analysis of airborne sulfate. J. Air. Poll. Cont. Assoc. 27:737-747.

Whitby, K.T., B.K. Cantrell, R.B. Husar., N.V. Gillani, J.A. Anderson, D.L. Blumenthal, and W.E. Wilson. 1976. Aerosol formation in a coal-fired power plant plume. 171st National Meeting of the Amer. Chem. Soc., New York.

Wilson, W.E., R.J. Charlson, R.B. Husar, K.T. Whiby, and D. Blumenthal. 1976. Sulfates in the atmosphere. 69th Amer. Meeting of the Air Pollut. Control Assoc., Portland, Maine.

Witz, S., and R.D. MacPhee. 1977. Effect of different types of glass filters on total suspended particulates and their chemical composition. J. Air Poll. Control. Assoc. 27:239-241.

9. AOSERP RESEARCH REPORTS

1.		AOSERP First Annual Report, 1975
2.	AF 4.1.1	Walleye and Goldeye Fisheries Investigations in the Peace-Athabasca Delta--1975
3.	HE 1.1.1	Structure of a Traditional Baseline Data System
4.	VE 2.2	A Preliminary Vegetation Survey of the Alberta Oil Sands Environmental Research Program Study Area
5.	HY 3.1	The Evaluation of Wastewaters from an Oil Sand Extraction Plant
6.		Housing for the North--The Stackwall System
7.	AF 3.1.1	A Synopsis of the Physical and Biological Limnology and Fisheries Programs within the Alberta Oil Sands Area
8.	AF 1.2.1	The Impact of Saline Waters upon Freshwater Biota (A Literature Review and Bibliography)
9.	ME 3.3	Preliminary Investigations into the Magnitude of Fog Occurrence and Associated Problems in the Oil Sands Area
10.	HE 2.1	Development of a Research Design Related to Archaeological Studies in the Athabasca Oil Sands Area
11.	AF 2.2.1	Life Cycles of Some Common Aquatic Insects of the Athabasca River, Alberta
12.	ME 1.7	Very High Resolution Meteorological Satellite Study of Oil Sands Weather: "a Feasibility Study"
13.	ME 2.3.1	Plume Dispersion Measurements from an Oil Sands Extraction Plant, March 1976
15.	ME 3.4	A Climatology of Low Level Air Trajectories in the Alberta Oil Sands Area
16.	ME 1.6	The Feasibility of a Weather Radar near Fort McMurray, Alberta
17.	AF 2.1.1	A Survey of Baseline Levels of Contaminants in Aquatic Biota of the AOSERP Study Area
18.	HY 1.1	Interim Compilation of Stream Gauging Data to December 1976 for the Alberta Oil Sands Environmental Research Program
19.	ME 4.1	Calculations of Annual Averaged Sulphur Dioxide Concentrations at Ground Level in the AOSERP Study Area
20.	HY 3.1.1	Characterization of Organic Constituents in Waters and Wastewaters of the Athabasca Oil Sands Mining Area

21.		AOSERP Second Annual Report, 1976-77
22.	HE 2.3	Maximization of Technical Training and Involvement of Area Manpower
23.	AF 1.1.2	Acute Lethality of Mine Depressurization Water on Trout Perch and Rainbow Trout
24.	ME 4.2.1	Air System Winter Field Study in the AOSERP Study Area, February 1977
25.	ME 3.5.1	Review of Pollutant Transformation Processes Relevant to the Alberta Oil Sands Area
26.	AF 4.5.1	Interim Report on an Intensive Study of the Fish Fauna of the Muskeg River Watershed of Northeastern Alberta
27.	ME 1.5.1	Meteorology and Air Quality Winter Field Study in the AOSERP Study Area, March 1976
28.	VE 2.1	Interim Report on a Soils Inventory in the Athabasca Oil Sands Area
29.	ME 2.2	An Inventory System for Atmospheric Emissions in the AOSERP Study Area
30.	ME 2.1	Ambient Air Quality in the AOSERP Study Area, 1977
31.	VE 2.3	Ecological Habitat Mapping of the AOSERP Study Area: Phase I
32.		AOSERP Third Annual Report, 1977-78
33.	TF 1.2	Relationships Between Habitats, Forages, and Carrying Capacity of Moose Range in northern Alberta. Part I: Moose Preferences for Habitat Strata and Forages.
34.	HY 2.4	Heavy Metals in Bottom Sediments of the Mainstem Athabasca River System in the AOSERP Study Area
35.	AF 4.9.1	The Effects of Sedimentation on the Aquatic Biota
36.	AF 4.8.1	Fall Fisheries Investigations in the Athabasca and Clearwater Rivers Upstream of Fort McMurray: Volume I
37.	HE 2.2.2	Community Studies: Fort McMurray, Anzac, Fort MacKay
38.	VE 7.1.1	Techniques for the Control of Small Mammals: A Review
39.	ME 1.0	The Climatology of the Alberta Oil Sands Environmental Research Program Study Area
40.	VE 7.1	Interim Report on Reclamation for Afforestation by Suitable Native and Introduced Tree and Shrub Species
41.	AF 3.5.1	Acute and Chronic Toxicity of Vanadium to Fish
42.	TF 1.1.4	Analysis of Fish Production Records for Registered Traplines in the AOSERP Study Area, 1970-75
43.	TF 6.1	A Socioeconomic Evaluation of the Recreational Fish and Wildlife Resources in Alberta, with Particular Reference to the AOSERP Study Area. Volume I: Summary and Conclusions
44.	VE 3.1	Interim Report on Symptomology and Threshold Levels of Air Pollutant Injury to Vegetation, 1975 to 1978
45.	VE 3.3	Interim Report on Physiology and Mechanisms of Air-Borne Pollutant Injury to Vegetation, 1975 to 1978

46.	VE 3.4	Interim Report on Ecological Benchmarking and Biomonitoring for Detection of Air-Borne Pollutant
47.	TF 1.1.1	A Visibility Bias Model for Aerial Surveys of Moose on the AOSERP Study Area
48.	HG 1.1	Interim Report on a Hydrogeological Investigation of the Muskeg River Basin, Alberta
49.	WS 1.3.3	The Ecology of Macrobenthic Invertebrate Communities in Hartley Creek, Northeastern Alberta
50.	ME 3.6	Literature Review on Pollution Deposition Processes
51.	HY 1.3	Interim Compilation of 1976 Suspended Sediment Data in the AOSERP Study Area
52.	ME 2.3.2	Plume Dispersion Measurements from an Oil Sands Extraction Plant, June 1977
53.	HY 3.1.2	Baseline States of Organic Constituents in the Athabasca River System Upstream of Fort McMurray
54.	WS 2.3	A Preliminary Study of Chemical and Microbial Characteristics of the Athabasca River in the Athabasca Oil Sands Area of Northeastern Alberta.
55.	HY 2.6	Microbial Populations in the Athabasca River
56.	AF 3.2.1	The Acute Toxicity of Saline Groundwater and of Vanadium to Fish and Aquatic Invertebrates
57.	LS 2.3.1	Ecological Habitat Mapping of the AOSERP Study Area (Supplement): Phase I

These reports are not available upon request. For further information about availability and location of depositories, please contact:

Alberta Oil Sands Environmental Research Program
15th Floor, Oxbridge Place
9820 - 106 Street
Edmonton, Alberta T5K 2J6